Kinetic descriptions and asymptotic limits of thermonuclear plasmas

Etienne Lehman

RÉPUBLIQUE FRANÇAISE
Liberté Égalité Fraternité

Université de Toulouse

Doctorat de l'Université de Toulouse

préparé à l'Université Toulouse III - Paul Sabatier

Descriptions cinétiques et limites asymptotiques des plasmas de fusion thermonucléaire

---

Thèse présentée et soutenue, le 1 juillet 2024 par

Etienne LEHMAN

École doctorale
EDMITT - Ecole Doctorale Mathématiques, Informatique et Télécommunications de Toulouse

Spécialité
Mathématiques et Applications

Unité de recherche
IMT : Institut de Mathématiques de Toulouse

Thèse dirigée par
Claudia NEGULESCU

Composition du jury
M. Jean DOLBEAULT, Rapporteur, CNRS
M. Bruno DESPRÉS, Rapporteur, Sorbonne Université
M. Franck BOYER, Examinateur, Université Toulouse III - Paul Sabatier
M. Nicolas CROUSEILLES, Examinateur, INRIA
M. Maurizio OTTAVIANI, Examinateur, CEA Cadarache
Mme Claudia NEGULESCU, Directrice de thèse, Université Toulouse III - Paul Sabatier

À Nanou.

Stanley felt the cool breeze upon his skin, the feeling of liberation, the immense possibility of the new path before him. This was exactly the way, right now, that things were meant to happen. And Stanley was happy.

The Narrator
in *The Stanley Parable.*

Remerciements

Il me serait impossible de soutenir aujourd'hui cette thèse de doctorat sans le soutien d'une myriade de personne. Prenons alors le temps de les remercier.

Mes premières pensées vont naturellement à Claudia, dont l'humour au quotidien, le soutien scientifique et les relectures exigeantes m'ont tant appris. Merci pour tout, je suis fier du travail accompli avec toi. Je tiens également à remercier chaleureusement Bruno Després et Jean Dolbeault pour leur intérêt, ainsi que pour avoir rapporté le présent manuscrit. Merci également à Nicolas Crouseilles, Maurizio Ottaviani, ainsi que Franck Boyer d'avoir complété mon jury, et de l'intérêt porté à mon travail.

Chacun de mes voyages à Munich durant cette thèse fut un plaisir, notamment en raison de l'accueil chaleureux de l'Institut Max Planck pour la physique des plasmas. Merci de leur accueil pour la Numkin et au quotidien. Je remercie tout particulièrement Stefan pour son temps, son flegme, ses qualités scientifiques, son accueil chaleureux. Je garde un excellent souvenir de notre collaboration, ainsi que mon intégration au projet STRUPHY.

Il me semble également nécessaire de remercier un certain nombre de personnes au sein des chercheurs et personnels BIATSS de l'Institut de Mathématiques de Toulouse. Tout d'abord merci à Franck Barthe et Franck Boyer pour leur dévouement à la direction du laboratoire. Je remercie massivement tous les enseignants avec qui j'ai eu le plaisir de collaborer durant ces années. C'est particulièrement le cas de Xavier et Mihai, ainsi que, dans une autre UE, Laurent : ce fut un plaisir de travailler avec vous. Je tiens tout particulièrement à remercier Fanny de m'avoir donné l'opportunité d'enseigner dans le cadre de la préparation à l'agrégation de Toulouse pendant ces trois ans. Merci également pour tous tes précieux conseils sur l'enseignement, la prépa, et cet étrange présentation au rectorat. Merci aux membres permanents, particulièrement Jean-François, Gregory, Judith, Jerôme, Mihai, Manon, Pascal, Pierre, Marie-Hélène pour votre engagement administratifs ainsi que les discussions que j'ai pu partager avec vous. Remercions finalement le pôle administratif, en particulier à Céline et Nicole pour votre soutien, votre bonne humeur au quotidien ainsi que votre investissement pour le laboratoire. Désolé par ailleurs à tous les personnels du pôle administratif que nous avons dérangé durant la pause midi ! Nous y reviendrons bien sûr plus tard.

Restons quelque temps dans le laboratoire, et remercions tout particulièrement sa plus grande source de vie : ses doctorants et ses post-doctorants, et notamment ceux que j'ai eu la joie de croiser/la tristesse de quitter tout au long de ces trois années riches en émotions. Comment ne pas commencer par les habitants éphémères des bureaux 301 et 302 du batiment 1R3 : Louis, Viviana et Diego, d'abord, qui étaient là tout au début. Louis, merci à toi et Anaëlle pour tous ces repas, chez vous, j'espère que vous allez bien. Viviana, félicitations pour ton poste, je suis beaucoup trop content pour toi ! ! Diego enfin, c'est vraiment bluffant la vitesse à laquelle tu as appris le Français ! ! J'espère que mon successeur saura apprécier la beauté

des simulations numériques qui apparaissent régulièrement sur ton écran d'ordinateur. Je te souhaite une très bonne continuation. Michèle ensuite, le soleil et la vie qui a jadis irradiée sur tout le laboratoire, qui a speedrun le postdoc pour juste décider d'être beaucoup trop stylée au CNRS. Merci Clément, que j'ai parfois le plaisir d'apercevoir sur l'écran d'une conversation zoom de mon voisin de bureau actuel ! Et parlant de celui-ci, merci à Paul pour ces instants de vie au laboratoire ! Merci de jouer le jeu quand je dis n'importe quoi, et d'être si bon public au quotidien. Merci à Loukman, pour ces brefs moments où nous nous croisions au bureau. Mention spéciale à Lucas, qui n'a jamais rechigné à détourner sa journée du cours prévu à cause d'une question stupide de ma part. Merci pour tout, j'espère que tout ira bien pour ton postdoc, même si je ne me souviens Padoue ce sera.

Comment parler de la vie au laboratoire sans parler de l'IMT Tarot Club (parfois appelé IMT Loto Club, en fonction du nombre de joueurs) ? Ce rendez-vous quotidien de la mauvaise foi. Derby au sommet tous les midis, aux multiples ligues, mais dont les GOATs resterons toujours Perla et Candice ! Merci à vous tous, membres passés et présents de l'IMT Tarot Club, pour tous ces chiens appelés, petits au bout, garde sans et autres coupes franches au roi appelé. Merci infiniment à Alexandre, Javi, Joachim, Perla, Maxime, Antho, Candice, Arnaud, Louis C. et Louis D., Corentin, Paola, Nicolas O., Ilenia, Elio, Boris, Niki, Elie, Joseph, Alejandro, Armand, Fanny, Fu-Hsuan, Laurens, Ronan, la mystérieuse R1, Léo, Florian et tant d'autres. Quel jeu de merde.

Ceux qui me connaissent bien connaissent mon affection pour le JDR, et à ce titre il me faut remercier mes deux MJs préférés, Élio et Alexandre, pour leurs qualités de conteurs. Remercions également mes confrères de jeux, Fanny, Sophia, Clément B., Pauline, Antho.

Ne vous en faites pas, je ne vais pas oublier l'IMT Running Club, je ne suis pas un chicken ! ! Que ce soit sous sa forme moins structurée des années précédentes (je garde un souvenir impérissable de ce dénivelé surprise à Rodez !), ou sous sa forme moderne, il me tient à cœur de remercier tous ses membres : merci à Alejandro, Javi, Maxime, Antho, Pauline, Joachim, Élio, Arnaud, Candice, Paul, Elie, Louis C., Boris, Florian, Luca, Jan-Luka. Attendez vous tous à me revoir à l'occasion d'évènements course-à-pédestres !

Merci de plus à Mitja, Virgile, Simon, Lucas D.L., Mahmoud, Benjamin M., Nico E., Benjamin L., Kim-Han, Thibault, Gauthier, Denis, et tant d'autres, (je m'excuse par avance auprès de ceux que j'aurais oublié), pour tous ces instants de vie passés au laboratoire !

Des remerciements tout particuliers s'adressent à Alexandre, Anthony et Pauline. Vous côtoyer pendant ces années fut un véritable plaisir, et je suis fier de vous compter parmi mes amis proches. Merci de supporter au quotidien le mauvais perdant que je suis, j'espère que vous comptez continuer pendant encore de nombreuses années !

Il serait injuste de ne remercier que les amitiés récentes, quand tant d'autres, plus anciennes, se sont révélées si importantes à mes yeux au cours des années. À ce titre, procédons par ordre

chronologique : merci à Killian, le streamer Mariokart, et à Nicolas G., également, pour toutes ces années sur le mode zombie. Le bon vieux temps.

C'est au lycée que j'ai réellement pris goût aux mathématiques, et pour cela, commençons par mentionner Mme. Draghi, professeure exceptionnelle avec qui tout à commencé. Merci pour tout. Le lycée, c'est aussi des amis, et le crew domontois se devait évidemment d'être mentionné. Merci à Clément, Victor, Axel, Laurie, Inès, Florian. Mention spéciale à Loïc, qui nous a rejoint à Toulouse, mais aussi les champions de la course à pied : Valentin et Nicolas, toujours partants pour parcourir la France et courir 21km de plus avec moi. En route pour les JOs !

Le début de mon aventure mathématique doit beaucoup à la classe préparatoire, et à ce titre je me sens redevable auprès de Mme. Monier. Merci également à Léa, Marie, Pierre, Sophie, Achille, Jean-Camille, Damien, Alba, Mélissa, Charles-Frédérique, Rodolphe, parmi tant d'autres. On se retrouve bientôt, en région parisienne !

Enfin, mon périple m'a mené à Lyon, et c'est tout naturellement qu'il faut saluer Thibault Noëlle, Julia, Léonard, Mathilde, Léa F., Léa C., Clara, Clarisse. Pour tous ces moments et ces moments de gênes passés ensemble au RA, je vous remercie. J'adresse une pensée toute particulière à Julien, désormais prof de prépa, pour m'avoir porté à l'agreg, et pour toutes tes visites à Toulouse. À très vite pour ta soutenance et à Paris ;).

Rien de tout cela ne serait possible sans ma famille géniale pour leur amour inconditionnel et leur affection. Merci à Papapi, Mamichris, qui me sauvent pour la rentrée prochaine ! Merci à Anne, Vincent, Cécile, Cédric, Marc, Estelle, Perrine, Agathe, Fanny, Alix, Guillaume, Romain, Thomas. Hâte de faire du ski à Vars, ou de vous retrouver en Ardèche pour fêter cela. Merci à Papou, Coco, Philippe, Quentin et Célia. Merci enfin à Nanou pour toutes ces galettes et tous ces bons moments que je ne saurais énumérer. Tu nous manques terriblement.

Il est maintenant temps de remercier mes parents extraordinaires. Merci de m'avoir donné le goût du travail et de l'effort, d'avoir cultivé ma curiosité. Entre tant d'autres choses car 200 pages ne suffiraient pas à tout lister : merci maman de m'avoir poussé quand je préférais jouer à la console. Merci papa de m'avoir amené tous ces samedis matin à Paris. C'est sans l'ombre d'un doute grâce à vous que je suis là où j'en suis aujourd'hui.

Enfin, il est temps d'écrire en lettres capitales MERCI à mon soleil du quotidien, sans qui jamais ce manuscrit n'aurait pu être fini à temps. Merci Erwanne de me soutenir dans tout ce que j'entreprends, de ta bonne humeur, de ton humour et de ton amour. Merci Wanou.

TABLE DES MATIÈRES

CHAPITRE 1

INTRODUCTION

Cette thèse de doctorat se concentre sur l'analyse mathématique ainsi que sur la résolution numérique d'équations modélisant les plasmas de fusion nucléaire. Les plasmas dans un tokamak peuvent être décrits à l'échelle microscopique par les équations de Newton couplées aux équations de Maxwell, ce qui serait trop coûteux à simuler numériquement. Une description statistique des particules, permet de réduire en partie ce coût. On appelle alors équations cinétiques les équations décrivant la dynamique de la distribution statistique des particules et on qualifie l'échelle de description de mésoscopique. À l'échelle macroscopique, on retrouve les modèles fluides, moins précis d'un point de vue physique mais permettant des calculs numériques très efficaces. Dans ce manuscrit, différents travaux seront présentés, dérivant rigoureusement ou formellement certains modèles réduits à partir de descriptions cinétiques du plasma. En outre, des méthodes numériques précises et peu coûteuses seront présentées pour simuler l'évolution du plasma.

L'objectif du chapitre 1 est d'introduire le lecteur aux enjeux mathématiques et numériques de la description des plasmas thermonucléaires, afin de mieux contextualiser les trois articles qui constituent la suite de cette thèse. Dans un premier temps, l'introduction présentera la physique des plasmas ainsi que des modèles mathématiques associés à différentes échelles de descriptions : on dérivera formellement des modèles cinétiques classiques de la physique des plasmas, collisionnels ou non, à partir de descriptions microscopiques. Nous présenterons également un panorama de questions centrales concernant ces modèles. Dans la seconde partie de cette introduction, nous nous intéresserons à l'analyse asymptotique permettant de dériver des modèles fluides, simplifiés, qui décrivent à moindre coût numérique le plasma dans des situations physiques spécifiques. Enfin, nous présenterons nos contributions scientifiques à l'étude des plasmas dans la sous-section 1.5, avec quelques perspectives.

La suite du manuscrit regroupe trois articles publiés ou soumis durant cette thèse de doctorat, cités ci-dessous :

- Etienne Lehman, Claudia Negulescu. "Vlasov-Poisson-Fokker-Planck equation in the adiabatic asymptotics", à paraître dans *Communications in Mathematical Sciences* (2024).
- Etienne Lehman, Claudia Negulescu, Stefan Possanner. "Asymptotic study of an anisotropic Fokker-Planck collision operator in a strong magnetic field", publié dans *Kinetic and Related Models* [1] (2024).
- Etienne Lehman, Claudia Negulescu. "Fokker-Planck equation for energetic particles. The κ-distribution function", soumis pour publication.

Un autre travail de synthèse portant sur les modélisations microscopiques, mésoscopiques et macroscopiques de drones et sur les méthodes d'entropie a également été publié au cours de cette thèse de doctorat :

- Claudia Negulescu, Etienne Lehman, Axel Maupoux. "Entropy methods and application in the field of collective behaviour", *Le Matematiche*, Vol. 78, No. 1 (2023).

Dans les sous-sections 1.3.1 à 1.3.4 de l'introduction, on reprend de cet article la dérivation de l'opérateur de collision de Fokker-Planck par souci de complétude.

1. doi : 10.3934/krm.2024004

1.1 Introduction à la physique des plasmas

Le plasma est un état de la matière composé de différentes espèces de particules, telles que les ions, les électrons, et les particules neutres comme les neutrons. Le plasma est l'état le plus courant de la matière. Quoique rare sur Terre en raison des fortes contraintes nécessaires pour le produire à partir d'un gaz neutre, il est présent en abondance dans l'espace. L'étude des plasmas est importante pour la recherche fondamentale, ainsi que pour diverses applications industrielles, dont la fusion nucléaire contrôlée en est l'une des plus importantes.

La fusion est une réaction nucléaire où deux noyaux d'atomes se combinent pour former un noyau plus lourd et lors de laquelle une grande quantité d'énergie est libérée. De ce fait, la fusion est au centre de nombreux travaux de recherche visant à exploiter cette source d'énergie à des fins civiles.

Une telle réaction ne se produit que dans des conditions de pression et de température très précises : deux noyaux d'atomes (chargés positivement) se repoussent *a priori*, à cause de l'interaction coulombienne. Cependant, la fusion nucléaire se produit s'ils sont si proches que l'interaction coulombienne est négligeable par rapport à l'interaction forte, attractive mais de très courte portée. Ainsi, il est nécessaire de maintenir une température et une pression très élevées, pour qu'en moyenne les noyaux d'atomes soient si proches que la réaction de fusion ait lieu.

Des réactions nucléaires ont lieu continûment au cœur du soleil : la gravitation permet en effet de maintenir une pression et une densité élevées, tandis que l'énergie dégagée par la fusion nucléaire permet d'entretenir une haute température. Il est en revanche difficile de maintenir ces conditions artificiellement sur Terre. Il est alors nécessaire de choisir minutieusement les éléments physiques qui contribueront à la réaction. En choisissant la réaction impliquant le deutérium et le tritium :

$$ {}^{2}_{1}D + {}^{3}_{1}T \rightarrow {}^{4}_{2}He + {}^{1}_{0}n + 17,6\text{MeV}\,, $$

les conditions de température et de pression sont réalisables en laboratoire. Ce choix de réaction est également raisonnable car le deuterium est présent en abondance dans l'eau de mer. Le tritium, quant à lui, est présent en quantités relativement abondantes dans la croute terrestre.

La réalisation de fusion nucléaire contrôlée à visée civile présenterait en effet des avantages majeurs : les matériaux nécessaires à sa mise en œuvre sont présents en abondance, et elle ne produit pas de déchets radioactifs, contrairement à la fission nucléaire, tout en produisant de grandes quantités d'énergie. La réalisation d'un tel procédé reste toutefois difficile, pour plusieurs raisons :

- Le plasma doit être confiné dans une région limitée pour permettre la réaction de fusion nucléaire et garantir que l'énergie libérée entretienne la réaction. Pour ce faire, l'approche la plus courante est le confinement magnétique, lors duquel le plasma est enfermé tout en circulant dans une enceinte torique. Un champ magnétique intense, généré par l'enceinte, maintient le plasma éloigné des parois tout en le retenant dans

une zone limitée de l'espace. Différentes conceptions sont possibles : à Cadarache, dans le sud de la France, le projet ITER privilégie l'utilisation d'un tokamak (voir figure 1.1a). À l'Institut Max-Planck de physique de Munich, le choix s'est porté sur le stellarator (voir figure 1.1b).

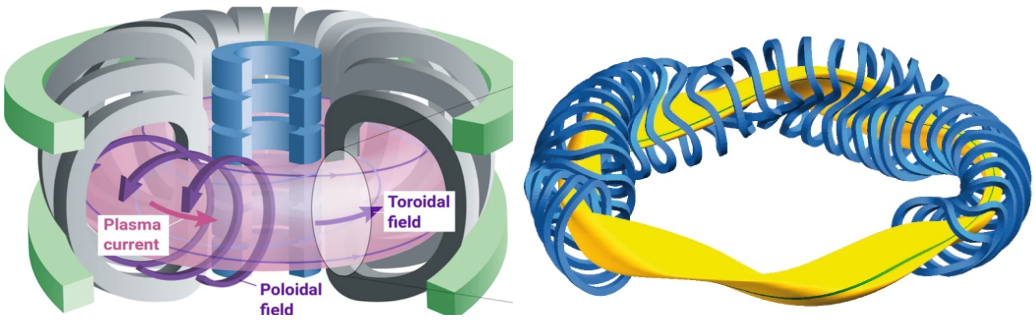

(a) Tokamak [2] (b) Stellarator [3]

FIGURE 1.1 – Deux exemples d'enceintes de confinement du plasma pour la fusion nucleaire.

- Le plasma est sujet à de nombreuses instabilités. La présence de la moindre impureté dans le réacteur peut entrainer la rupture du confinement. Dans le cas où le confinement est perdu, le plasma, à très haute température et électriquement chargé, entre en contact avec les parois du réacteur. Au-delà de l'arrêt de la production d'électricité, l'intégrité des parois du réacteur est mise en péril.
- Lors de la reaction sont produits des neutrons qui, n'étant pas chargés électriquement, échappent au confinement magnétique, et sont envoyés à très haute vitesse contre les parois du tokamak, ce qui a pour effet de rendre les parois radioactives et d'altérer leur intégrité.

La mise en œuvre de la fusion nucléaire représente un enjeu industriel majeur, dont le succès pourrait révolutionner la production de l'électricité. Cependant, cette mise en œuvre présente des difficultés significatives, et le soutien de la recherche fondamentale reste essentiel pour les surmonter. Il est en particulier crucial de développer des modèles mathématiques ainsi que des méthodes numériques précises et peu coûteuses pour décrire les instabilités et le comportement turbulent du plasma, et ainsi surmonter ces difficultés.

1.2 De l'échelle microscopique à l'échelle macroscopique

Dans cette section, nous nous intéressons à certains modèles très étudiés de la littérature. Les équations de Newton constituerons notre point de départ, et nous dériverons l'équation de Vlasov tout en détaillant ses propriétés.

2. Image de EUROfusion
3. https ://www.engineering.com/story/stellarators-back-online-after-decades-in-the-dark

1.2.1 Équations de Newton et de Maxwell

Une approche naturelle dans la modélisation des plasmas consiste à modéliser directement le comportement individuel de chaque particule chargée électriquement par les équations de Newton. Considérons un système de N particules distinctes, indexées par $k \in \{1, \dots, N\}$ et caractérisées par leurs positions et vitesses respectives $(\mathbf{x}_k(t), \mathbf{v}_k(t)) \in \mathbb{R}^3 \times \mathbb{R}^3$. On dénote en outre leurs masses et charges respectives m_k et q_k. Les équations de Newton s'écrivent alors :

$$\left\{ \begin{array}{rcl} \mathbf{x}_k'(t) & = & \mathbf{v}_k(t)\,, \\ m_k\,\mathbf{v}_k'(t) & = & q_k \displaystyle\sum_{\substack{i=1 \\ i\neq k}}^{N} \left(\mathbf{E}_i(t, \mathbf{x}_k(t)) + \mathbf{v}_k(t) \times \mathbf{B}_i(t, \mathbf{x}_k(t))\right)\,, \end{array} \right. \qquad \forall k \in \{1, \dots, N\}, \tag{1.2.1}$$

où $(\mathbf{E}_i(t, \mathbf{x}_k(t)),\ \mathbf{B}_i(t, \mathbf{x}_k(t)))$ est le champ électromagnétique produit par la particule i, mesuré à la position $\mathbf{x}_k(t)$ de la particule k. Le champ électromagnétique $(\mathbf{E}_i(t, \mathbf{x}),\ \mathbf{B}_i(t, \mathbf{x}))$ est calculé à partir des équations de Maxwell :

$$\varepsilon_0\,\mu_0\,\partial_t \mathbf{E}_i(t, \mathbf{x}) = \nabla_{\mathbf{x}} \times \mathbf{B}_i(t, \mathbf{x}) - \mu_0\,\mathbf{J}_i\,, \tag{1.2.2}$$

$$\partial_t \mathbf{B}_i(t, \mathbf{x}) = -\nabla_{\mathbf{x}} \times \mathbf{E}_i(t, \mathbf{x})\,, \tag{1.2.3}$$

$$\nabla_{\mathbf{x}} \cdot \mathbf{B}_i = 0\,, \tag{1.2.4}$$

$$\nabla_{\mathbf{x}} \cdot \mathbf{E}_i = \frac{\rho_i}{\varepsilon_0}\,, \tag{1.2.5}$$

où ε_0 et μ_0 désignent respectivement la permittivité diélectrique et la perméabilité magnétique du vide. La distribution de la charge de la particule i, $\rho_i(t, \mathbf{x})$, est donnée par

$$\rho_i(t, \mathbf{x}) = q_i\,\delta_{\mathbf{x}_i(t)}(\mathbf{x})\,, \tag{1.2.6}$$

et la densité de courant de la particule i est calculée *via*

$$\mathbf{J}_i(t, \mathbf{x}) = q_i\,\mathbf{v}_i(t)\delta_{\mathbf{x}_i(t)}(\mathbf{x})\,.$$

Le champ électromagnétique total $(\mathbf{E}^{\text{tot}}(t, \mathbf{x}), \mathbf{B}^{\text{tot}}(t, \mathbf{x}))$ peut alors se calculer en considérant la somme des champs produits individuellement par les particules :

$$\mathbf{E}^{\text{tot}}(t, \mathbf{x}) = \sum_{i=1}^{N} \mathbf{E}_i(t, \mathbf{x})\,, \qquad \mathbf{B}^{\text{tot}}(t, \mathbf{x}) = \sum_{i=1}^{N} \mathbf{B}_i(t, \mathbf{x})\,. \tag{1.2.7}$$

Ainsi, au regard des équations de Maxwell, soulignons que

- La présence de la particule i, chargée électriquement, donne lieu à un champ électrique $\mathbf{E}_i$ (1.2.5).
- L'évolution temporelle de ce champ électrique $\partial_t \mathbf{E}_i$ ainsi que la densité de courant $\mathbf{J}_i$ (traduisant le déplacement de la particule i) font émerger un champ magnétique $\mathbf{B}_i$ (1.2.2).

- Le champ électromagnetique $(\mathbf{E}_i, \mathbf{B}_i)$ accelère les particules (1.2.1) *via* la force de Lorentz.

Il est aussi possible de considérer le nuage de particules dans un champ électromagnétique imposé, ce qui ajoute des termes dans le système (1.2.1). Cela ne sera pas considéré dans cette section.

Une approximation électrostatique peut être faite si on travaille dans un régime où les variations temporelles du champ magnétique sont négligeables. En effet, dans ce cas, l'équation de Maxwell-Faraday (1.2.3) peut se réécrire :

$$\nabla_{\mathbf{x}} \times \mathbf{E}_i = 0\,. \tag{1.2.8}$$

Cela implique que le champ électrique $\mathbf{E}_i$ dérive d'un potentiel scalaire, c'est-à-dire qu'il existe une quantité scalaire $\Phi_i(t, \mathbf{x})$, telle que :

$$\mathbf{E}_i = -\nabla_{\mathbf{x}} \Phi_i\,. \tag{1.2.9}$$

Insérer cette égalité dans l'équation de Maxwell-Gauss (1.2.5) permet alors de calculer directement le potentiel Φ_i, *via* l'équation de Poisson :

$$\mathbf{E}_i = -\nabla_{\mathbf{x}} \Phi_i\,, \tag{1.2.10}$$

$$-\Delta_{\mathbf{x}} \Phi_i = \frac{\rho_i}{\varepsilon_0}\,. \tag{1.2.11}$$

Au vu de la définition de ρ_i (1.2.6), on peut donner une expression des solutions Φ_i de (1.2.11) qui vérifient

$$\lim_{|\mathbf{x}| \to +\infty} \Phi_i(t, \mathbf{x}) = 0\,.$$

En effet, dans ce cas :

$$\Phi_i(t, \mathbf{x}) = \frac{q_i}{4\,\pi\,\varepsilon_0} \frac{1}{|\mathbf{x} - \mathbf{x}_i(t)|}\,, \qquad \forall \mathbf{x} \neq \mathbf{x}_i(t)\,. \tag{1.2.12}$$

Une quantité ponctuelle de charge donne alors naissance à un potentiel électrique global. Il s'agit d'un potentiel perçu en un point donné $\mathbf{x}$ de l'espace vide de particules. Par linéarité des équations de Maxwell, le champ électrique total $\mathbf{E}^{\text{tot}}$ dérive alors d'un potentiel Φ^{tot}, donné par

$$\Phi^{\text{tot}}(t, \mathbf{x}) = \sum_{i=1}^{N} \frac{q_i}{4\,\pi\,\varepsilon_0} \frac{1}{|\mathbf{x} - \mathbf{x}_i(t)|}\,, \qquad \forall \mathbf{x} \notin \{\mathbf{x}_1(t), \dots, \mathbf{x}_N(t)\}. \tag{1.2.13}$$

Posons maintenant la fonction

$$V(\mathbf{x}) := \frac{1}{4\,\pi\,\varepsilon_0} \frac{1}{|\mathbf{x}|}\,, \qquad \forall \mathbf{x} \neq 0\,,$$

et prolongeons V et ∇V par 0 en $\mathbf{x} = 0$. On a alors le potentiel et le champ électrique total en tout point de l'espace donnés par

$$\Phi^{\rm tot}(t,\mathbf{x}) = V * \rho^{\rm tot}(t,\mathbf{x}), \tag{1.2.14}$$

$$\mathbf{E}^{\rm tot}(t,\mathbf{x}) = -\nabla_{\mathbf{x}}\Phi^{\rm tot}(t,\mathbf{x}) = -\nabla V * \rho^{\rm tot}(t,\mathbf{x}), \qquad \forall \mathbf{x} \notin \{\mathbf{x}_1(t),\dots,\mathbf{x}_N(t)\}, \tag{1.2.15}$$

où $*$ désigne le produit de convolution suivant la variable $\mathbf{x}$, et où la densité totale de charge est donnée par

$$\rho^{\rm tot}(t,\mathbf{x}) := \sum_{i=1}^{N} q_i\, \delta_{\mathbf{x}_i(t)}(\mathbf{x}).$$

Notons qu'au point $\mathbf{x} = \mathbf{x}_k(t)$, la convention $V(0) = 0$ et $\nabla V(0) = 0$ permet d'écrire

$$\Phi^{\rm tot}(t,\mathbf{x}_k(t)) := \sum_{\substack{i=1\\ i\neq k}}^{N} \frac{q_i}{4\,\pi\,\varepsilon_0}\frac{1}{|\mathbf{x}_k(t)-\mathbf{x}_i(t)|}, \qquad \mathbf{E}^{\rm tot}(t,\mathbf{x}_k(t)) := \sum_{\substack{i=1\\ i\neq k}}^{N} \frac{q_i}{4\,\pi\,\varepsilon_0}\frac{\mathbf{x}_k(t)-\mathbf{x}_i(t)}{|\mathbf{x}_k(t)-\mathbf{x}_i(t)|^3}. \tag{1.2.16}$$

Ce champ $\mathbf{E}^{\rm tot}(t,\mathbf{x}_k(t))$ correspond au champ perçu par la particule k qui intervient dans les équations de Newton (1.2.1). Si on suppose de plus le champ magnétique $\mathbf{B}^{\rm tot}$ nul, les équations de Newton (1.2.1) se réécrivent alors :

$$\left\{\begin{array}{rcl} \mathbf{x}_k'(t) &=& \mathbf{v}_k(t), \\ m_k\,\mathbf{v}_k'(t) &=& q_k\,\mathbf{E}^{\rm tot}(t,\mathbf{x}_k(t)), \end{array}\right. \qquad \forall k \in \{1,\dots,N\}. \tag{1.2.17}$$

Les plasmas de fusion sont constitués d'un grand nombre de particules (dans un plasma de fusion contrôlée, il y aurait de l'ordre de 10^{20} particules par mètre cube). Il est alors impossible en pratique de décrire individuellement les particules avec les équations de Newton pour une simulation numérique. Toutefois, une approche statistique peut être mise en œuvre, afin de permettre des descriptions plus économiques.

1.2.2 Échelle mésoscopique, limite des champs moyens et problèmes connexes

Considérons un nuage composé de N électrons de charge $q = -e$, où e est la charge élémentaire. On suppose ces électrons immergés dans un bain d'ions de charge $q = +e$. À partir de maintenant, on distinguera les ions des électrons, et on modélisera leurs dynamiques séparément. Par souci de simplicité, on se place ici dans le cas où $\mathbf{B}^{\rm tot} = 0$, et où le champ électrique $\mathbf{E}^{\rm tot}$ est donné par l'approximation électrostatique. On décrit alors le mouvement des électrons par l'équation de Newton

$$\left\{\begin{array}{rcl} \mathbf{x}_i'(t) &=& \mathbf{v}_i(t), \\ \mathbf{v}_i'(t) &=& -\dfrac{e}{m_e}\,\mathbf{E}^{\rm tot}(t,\mathbf{x}_i(t)), \end{array}\right. \qquad \forall i = 1,\dots,N, \tag{1.2.18}$$

où m_e est la masse d'un électron. On a vu dans (1.2.16) que la contribution des particules chargées au champ électrique total est une somme des contributions individuelles de chacune des particules. Dans l'état actuel des choses, faire tendre le nombre de particules $N \to +\infty$ résulterait en la divergence du champ électrique $\mathbf{E}^{\text{tot}}$. Pour corriger ce problème, la contribution des électrons au champ électrique $\mathbf{E}^{\text{tot}}$ est souvent rééchelonnée de sorte que $\mathbf{E}^{\text{tot}}$ converge formellement dans la limite $N \to +\infty$. On considère alors plutôt dans l'équation de Newton le champ moyenné $\mathbf{E}^N$, donné par :

$$\Phi^N(t,\mathbf{x}) = e\,V * \left(n_i - n_e^N\right)(t,\mathbf{x}), \tag{1.2.19}$$

$$\mathbf{E}^N(t,\mathbf{x}) = -\nabla_{\mathbf{x}}\Phi^N(t,\mathbf{x}) = -e\,\nabla V * \left(n_i - n_e^N\right)(t,\mathbf{x}), \qquad \forall \mathbf{x} \in \mathbb{R}^3, \tag{1.2.20}$$

au lieu de $\mathbf{E}^{\text{tot}}$, où on a dénoté par $n_i(t,\mathbf{x})$ la densité statistique spatiale de particules, et par n_e^N la densité spatiale d'électrons, donnée par

$$n_e^N(t,\mathbf{x}) = \frac{1}{N}\sum_{i=1}^{N} \delta_{\mathbf{x}_i(t)}(\mathbf{x}). \tag{1.2.21}$$

Notons qu'on a incorporé dans la définition de n_e^N un facteur N^{-1}. On considère alors les équations de Newton associées au champ $\mathbf{E}^N$:

$$\begin{cases} \mathbf{x}_i'(t) &= \mathbf{v}_i(t), \\ \mathbf{v}_i'(t) &= -\dfrac{e}{m_e}\,\mathbf{E}^N(t,\mathbf{x}_i(t)), \end{cases} \qquad \forall i = 1,\dots,N. \tag{1.2.22}$$

Ce système est complémenté par l'équation de Poisson (1.2.19)-(1.2.20).

Comme mentionné précédemment, considérer le mouvement individuel de chaque électron serait impossible en pratique, notamment d'un point de vue numérique. Ceux-ci étant présents en très grand nombre, il est pertinent de considérer la distribution empirique des électrons :

$$\mu^N(t,\mathbf{x},\mathbf{v}) = \frac{1}{N}\sum_{i=1}^{N} \delta_{(\mathbf{x}_i(t),\mathbf{v}_i(t))}(\mathbf{x},\mathbf{v}), \qquad \mu_0^N := \mu^N(t=0,\cdot,\cdot).$$

$\mu^N(t,\mathbf{x},\mathbf{v})$ correspond alors à la distribution de la charge au temps t dans un petit voisinage autour du point $(\mathbf{x},\mathbf{v})$ de l'espace des phases.

Il s'agit alors de comprendre le comportement de μ^N quand $N \to +\infty$, et de donner une équation d'évolution associée à sa limite éventuelle $f_e(t,\mathbf{x},\mathbf{v})\,\mathrm{d}\mathbf{x}\,\mathrm{d}\mathbf{v}$. Commençons par remarquer qu'alors, (on rappelle qu'on a fixé $\mathbf{E}^N$ donné par l'approche électrostatique, et $\mathbf{B}^N = 0$, pour simplifier), les équations de Newton (1.2.1) peuvent être réécrites de manière équivalente en termes de μ^N :

$$\partial_t \mu^N + \mathbf{v}\cdot\nabla_{\mathbf{x}}\mu^N - \frac{e}{m_e}\mathbf{E}^N\cdot\nabla_{\mathbf{v}}\mu^N = 0, \tag{1.2.23}$$

au sens des distributions. Cela veut dire, par définition, que

$$\frac{\mathrm{d}}{\mathrm{d}t}\left\langle \mu^N, \varphi \right\rangle_{\mathcal{D}'\times\mathcal{D}} - \left\langle \mu^N, \left(\mathbf{v}\cdot\nabla_{\mathbf{x}} - \frac{e}{m_e}\mathbf{E}^N\cdot\nabla_{\mathbf{v}} \right) \varphi \right\rangle_{\mathcal{D}'\times\mathcal{D}} = 0\,, \qquad \forall \varphi \in \mathcal{D}(\mathbb{R}^3_{\mathbf{x}}\times\mathbb{R}^3_{\mathbf{v}})\,. \tag{1.2.24}$$

Cela se réécrit exactement

$$\begin{aligned}
&\frac{1}{N}\sum_{i=1}^{N}\left(\frac{\mathrm{d}}{\mathrm{d}t}\mathbf{x}_i(t) - \mathbf{v}_i(t) \right)\cdot\nabla_{\mathbf{x}}\,\varphi(\mathbf{x}_i(t),\mathbf{v}_i(t)) \\
&+ \frac{1}{N}\sum_{i=1}^{N}\left(\frac{\mathrm{d}}{\mathrm{d}t}\mathbf{v}_i(t) + \frac{e}{m_e}\,\mathbf{E}^N(t,\mathbf{x}_i(t)) \right)\cdot\nabla_{\mathbf{v}}\,\varphi(\mathbf{x}_i(t),\mathbf{v}_i(t)) = 0\,, \qquad \forall \varphi \in \mathcal{D}(\mathbb{R}^3_{\mathbf{x}}\times\mathbb{R}^3_{\mathbf{v}})\,.
\end{aligned}$$

Supposons que $\mu^N \to f_e\,\mathrm{d}\mathbf{x}\,\mathrm{d}\mathbf{v}$ et $\mathbf{E}^N \to \mathbf{E}$ quand $N \to +\infty$ dans un sens suffisament fort (nous reviendrons sur cette hypothèse dans la sous-section suivante). En passant à la limite dans (1.2.23), on obtient une équation d'évolution pour f_e :

$$\partial_t f_e + \mathbf{v}\cdot\nabla_{\mathbf{x}} f_e - \frac{e}{m_e}\mathbf{E}\cdot\nabla_v f_e = 0\,. \tag{1.2.25}$$

Cette équation est appelée équation de Vlasov. Formellement, le champ électrique limite est donné par

$$\mathbf{E} = -\nabla_{\mathbf{x}}\Phi\,, \tag{1.2.26}$$

$$\Phi(t,\mathbf{x}) = e\,V * (n_i - n_e)\,(\mathbf{x},t)\,, \tag{1.2.27}$$

où n_e est la densité spatiale d'électrons, donnée par

$$n_e(t,\mathbf{x}) = \int_{\mathbb{R}^3_{\mathbf{v}}} f_e(t,\mathbf{x},\mathbf{v})\,\mathrm{d}\mathbf{v}\,. \tag{1.2.28}$$

Notons qu'on peut formellement dériver le système de Vlasov-Poisson pour les ions de manière analogue, en changeant e en $-e$. Le système (1.2.25)-(1.2.27) est appelé système de Vlasov-Poisson ; il s'agit d'une équation d'évolution, hyperbolique. Remarquons que le champ électrique, qui intervient dans le terme de transport de (1.2.25), est calculé à partir de la densité spatiale de particules $n_i - n_e^N$, elle-même calculée à partir de f_e. Cela fait du système de Vlasov-Poisson une équation non-linéaire. Pour cette raison, le comportement qualitatif des solutions f_e de (1.2.25)-(1.2.27) est extrêmement riche, et est au cœur d'une immense littérature, mathématique comme physique.

1.2.2.1 La limite des champs moyens dans la littérature

Le passage à la limite $N \to \infty$ est couramment appelé dans la littérature passage à la limite des champs moyens. Celui-ci peut être justifié rigoureusement dans le cas ou le potentiel V dans

(1.2.15) est régulier. Notons que ce n'est pas le cas du potentiel de l'interaction coulombienne, qui est singulier en $|\mathbf{x}| = 0$. Plus particulièrement on a le résultat suivant (prenons la masse des particules égale à 1, pour simplifier ici).

Théorème 1.2.1. *[Vil10] Soit $W \in C^1(\mathbb{R}^3_{\mathbf{x}})$, tel que ∇W soit uniformément continu. Considérons $(\mathbf{x}_i(t),\, \mathbf{v}_i(t))_{i=1,\dots,N}$ les solutions du système*

$$\begin{cases} \mathbf{x}_i'(t) &= \mathbf{v}_i(t)\,, \\ \mathbf{v}_i'(t) &= \mathbf{F}^N(t, \mathbf{x}_i(t)) := -\dfrac{1}{N} \displaystyle\sum_{\substack{j=1 \\ j\neq i}}^{N} \nabla W(\mathbf{x}_i(t) - \mathbf{x}_j(t))\,, \end{cases} \qquad \forall i = 1, \dots, N\,. \tag{1.2.29}$$

Denotons par μ^N la mesure empirique, définie par

$$\mu^N(t, \mathbf{x}, \mathbf{v}) = \frac{1}{N} \sum_{i=1}^{N} \delta_{(\mathbf{x}_i(t), \mathbf{v}_i(t))}(\mathbf{x}, \mathbf{v})\,, \qquad \mu_0^N := \mu^N(t = 0, \cdot, \cdot)\,.$$

Supposons que $\mu_0^N \to \mu_0$ faiblement quand $N \to +\infty$. Alors, à extraction d'une sous-suite près,

$$\mu^N \underset{N\to+\infty}{\to} \mu, \quad \text{dans } C([0,T]; \mathcal{D}'(\mathbb{R}^3_{\mathbf{x}} \times \mathbb{R}^3_{\mathbf{v}}))\,,$$

où μ est une mesure dépendante du temps, et $\mathbf{F}^N$ converge uniformément vers un champ $\mathbf{F}$ sur $[0,T] \times \mathbb{R}^3_{\mathbf{x}} \times \mathbb{R}^3_{\mathbf{v}}$ quand $N \to +\infty$. De plus, μ est solution au sens des distributions de l'équation

$$\begin{cases} \partial_t \mu + \mathbf{v} \cdot \nabla_{\mathbf{x}} \mu + \mathbf{F} \cdot \nabla_{\mathbf{v}} \mu = 0\,, \\ \mathbf{F}(t, \mathbf{x}) = -\displaystyle\iint_{\mathbb{R}^3_{\mathbf{x}} \times \mathbb{R}^3_{\mathbf{v}}} \nabla_{\mathbf{x}} W(\mathbf{x} - \mathbf{y})\, \mu(t,\, \mathrm{d}\mathbf{y}\, \mathrm{d}\mathbf{v})\,. \end{cases} \tag{1.2.30}$$

En d'autres termes, lorsque le potentiel W est régulier, le passage à la limite des champs moyens est justifié. Ce problème devient en revanche extrêmement difficile si on considère des potentiels singuliers, comme V donné par l'interaction coulombienne. Si μ est une mesure générale, l'une des difficultés est de donner un sens au produit $\mathbf{E}\,\mu$ même pour des distributions. Si on fait tendre μ_0^N vers une distribution continue quand $N \to +\infty$, les particules sont initialement de plus en plus proches. Or rapprocher les particules rend $\mathbf{E}^N$ singulier : il est alors nécessaire de contrôler finement l'espacement des particules au temps $t = 0$, de sorte que $\mathbf{E}\,\mu$ ait un sens pour tout temps t. La question de la limite des champs moyens se pose alors de la manière suivante : "Pour quels choix de limite $\mu_0^N \underset{N\to+\infty}{\to} \mu_0$ le passage à la limite des champs moyens est-il justifié ?" Ce domaine de recherche est particulièrement actif et on pourra orienter le lecteur intéressé vers [Vil10 ; Gol03] pour une introduction à ce sujet ou bien vers [Jab14 ; CC21] pour des revues de la littérature contenant de multiples références. Citons également un résultat récent de Hauray et Jabin [HJ07] qui répond à la question de l'éloignement des particules dans le cadre de potentiels singuliers, mais plus réguliers que V.

Discutons maintenant des propriétés du système de Vlasov-Poisson (1.2.25)-(1.2.27), en commençant par les propriétés d'existence et d'unicité de cette équation.

1.2.2.2 Existence et unicité du système de Vlasov-Poisson

Donnons-nous une fonction de distribution f d'un nuage de particules de charge q et de masse m soumises à un champ électrique $\mathbf{E}$, supposé pour l'instant contraint. On supposera également dans cette partie qu'il n'y a qu'une seule espèce de particules dans le système modélisé. La question du caractère bien posé de l'équation linéaire de Vlasov,

$$\partial_t f + \mathbf{v}\cdot\nabla_{\mathbf{x}} f + \frac{q}{m}\,\mathbf{E}(t,\mathbf{x})\cdot\nabla_{\mathbf{v}} f = 0\,,$$

se résout simplement à l'aide des caractéristiques. Une question plus difficile mais résolue par [Ars75] est celle de l'existence de solutions faibles de l'équation non-linéaire de Vlasov-Poisson. Les hypothèses d'Arsen'ev sont relativement faibles, car elles supposent seulement $f_{in} \in L^1(\mathbb{R}^3_{\mathbf{x}}\times\mathbb{R}^3_{\mathbf{v}}) \cap L^2(\mathbb{R}^3_{\mathbf{x}}\times\mathbb{R}^3_{\mathbf{v}})$, en plus de l'hypothèse physique que la condition initiale soit d'énergie finie :

$$\frac{m}{2}\iint_{\mathbb{R}^3_{\mathbf{x}}\times\mathbb{R}^3_{\mathbf{v}}} |\mathbf{v}|^2\, f_{in}(\mathbf{x},\mathbf{v})\,\mathrm{d}\mathbf{x}\,\mathrm{d}\mathbf{v} + \frac{\varepsilon_0}{2}\int_{\mathbb{R}^3_{\mathbf{x}}} |\mathbf{E}_{in}(\mathbf{x})|^2\,\mathrm{d}\mathbf{x} < +\infty\,. \tag{1.2.31}$$

La seule hypothèse *a priori* non-physique est l'hypothèse $f_{in} \in L^2$. Elle permet cependant de donner sens au produit $\mathbf{E}(t,\mathbf{x})\cdot\nabla_{\mathbf{v}} f$ au sens des distributions. Pour lever cette hypothèse, il arrive d'utiliser ce qui s'appelle des solutions dites renormalisées, mais nous n'en discuterons pas d'avantage ici.

L'idée d'Arsen'ev pour construire des solutions faibles est de considérer le schéma d'approximation suivant. On cherche les solutions f_k du probleme régularisé

$$\partial_t f_k + \mathbf{v}\cdot\nabla_{\mathbf{x}} f_k + \frac{q}{m}\,\mathbf{E}_k(t,\mathbf{x})\cdot\nabla_{\mathbf{v}} f_k = 0\,, \tag{1.2.32}$$

$$\mathbf{E}_k(t,\mathbf{x}) = -\nabla_{\mathbf{x}}\Phi_k\,, \qquad -\varepsilon_0\left(\Delta_{\mathbf{x}} + \frac{1}{n}(\mathbb{I}\mathrm{d} - \Delta_{\mathbf{x}})^s\right)\Phi_k = q\int_{\mathbb{R}^3_{\mathbf{v}}} f_k\,\mathrm{d}\mathbf{v}\,, \tag{1.2.33}$$

avec s suffisamment grand pour que le champ $\mathbf{E}_k$ soit régulier. Comme le problème est régularisé, il est plus simple de produire des solutions à l'aide de la méthode des caractéristiques, puis d'une méthode de point fixe pour gérer le couplage non-linéaire. Un passage à la limite $n \to +\infty$ est alors réalisé. Le champ électrique $\mathbf{E}_k$ converge fortement, grâce à des estimations d'interpolation, tandis que la distribution f_k converge faiblement, menant donc, en passant à la limite dans (1.2.32) grâce à un argument de convergence forte-faible, à l'existence de solutions faibles au probleme de Vlasov-Poisson :

$$\begin{cases} \partial_t f + \mathbf{v}\cdot\nabla_{\mathbf{x}} f + \dfrac{q}{m}\,\mathbf{E}(t,\mathbf{x})\cdot\nabla_{\mathbf{v}} f = 0\,, \\[2ex] \mathbf{E}(t,\mathbf{x}) = -\nabla_{\mathbf{x}}\Phi\,, \qquad -\varepsilon_0\,\Delta_{\mathbf{x}}\Phi = q\displaystyle\int_{\mathbb{R}^3_v} f\,\mathrm{d}\mathbf{v}\,. \end{cases} \tag{1.2.34}$$

La question de l'unicité des solutions est en revanche plus difficile. Un article relativement récent de [Loe06] prouve l'unicité en se servant de techniques venant du transport optimal, en supposant seulement que la densité spatiale $n = \int_{\mathbb{R}^3_v} f \, \mathrm{d}\mathbf{v} \in L^\infty([0,T) \times \mathbb{R}^3_{\mathbf{x}})$.

Finalement, mentionnons [DL89], qui montre l'existence globale de solutions faibles pour l'équation de Vlasov, mais couplé avec un champ électromagnétique donné par les équations de Maxwell, tout en redonnant divers résultats d'existence.

Détaillons maintenant certaines propriétés qualitatives de l'équation de Vlasov-Poisson.

1.2.2.3 Comportement physique et instabilités

Nous avons déjà mentionné que le système de Vlasov-Poisson (1.2.34) était une équation de transport non-linéaire, ce qui est la source d'une riche variété de comportement possible. On se propose ici de recenser quelques comportements typiques de cette équation, d'origine linéaire ou non-linéaire.

- L'un des effets les plus connus associés à cet équation est l'amortissement Landau (*Landau Damping*). Cet effet se caractérise par une convergence exponentielle vers 0 du champ électrique due uniquement aux effets du transport conservatif des particules. Landau découvre en 1946 [Lan65] ce phénomène au niveau de l'équation linéarisée de Vlasov-Poisson autour d'un équilibre. Cet effet est surprenant, dans la mesure où l'équation de Vlasov-Poisson est une équation préservant l'entropie du système, c'est-à-dire qu'aucune information n'est perdue au cours de l'évolution temporelle de la solution. Cet effet est aussi observé physiquement [MW64], mais il faudra attendre les travaux récents de C. Mouhot et C. Villani [MV11] pour démontrer que ce phénomène apparaît également dans l'équation complète non-linéaire (1.2.34), pour des petites perturbations d'un équilibre. Toutefois, s'il est démontré que l'amortissement Landau subsiste au niveau non-linéaire pour des petites perturbations, ce n'est pas forcément le cas si l'équilibre est trop fortement perturbé. Si la perturbation est trop importante, il est possible que le champ électrique décroisse d'abord en amplitude, mais qu'il connaisse ensuite une phase de croissance, d'oscillation, puis de stagnation. Cet effet est purement lié à la non-linéarité, et n'apparaît pas dans la théorie linéarisée de Landau [Lan65]. On se réfère également à [Bed20] qui clarifie les conditions de stabilité de l'amortissement Landau en fonction de la régularité de la perturbation.
- Malgré le caractère homogénéisant de l'amortissement Landau, l'équation de (1.2.34) reste réversible, comme précédemment mentionné, c'est-à-dire qu'aucune information n'est perdue par le plasma. Un phénomène illustrant ce principe est la possibilités d'échos dans le plasma. Les "échos plasma" (*Plasma Echoes*) surviennent dans le cas où deux ondes, de fréquences respectives ω_1 et ω_2, bien qu'entièrement atténuées par l'amortissement Landau se rencontrent dans un plasma. Une nouvelle onde de fréquence $\omega_1 - \omega_2$ peut alors être observée comme résultat de cette interaction. Cet effet est bien documenté, et physiquement observé [Mal+68].
  Mathématiquement, depuis la description mésoscopique (1.2.34), cet effet résulte de

l'interaction entre deux aspects : d'une part, la non-linéarité qui excite en fréquence la solution, renforçant son caractère oscillatoire ; d'autre part, le caractère homogénéisant qui tend à faire décroître le champ électrique vers 0. Une explication purement géométrique de ce phénomène peut être trouvée dans [BAW68].

- On a mentionné l'amortissement Landau, qui est un effet de stabilité linéaire préservé au niveau de l'équation non-linéaire, tant que les perturbations de l'équilibre sont bien choisies. Cependant, même à l'échelle linéaire, l'équation de Vlasov-Poisson présente des instabilités. Mentionnons ici l'instabilité bi-courant, qui émerge quand la densité d'électrons est perturbée par une onde électrique se déplaçant légèrement moins vite que les électrons présents au voisinage de cette onde. Dans ce cas, les électrons vont donner de leur énergie à l'onde, et l'amplifier. Cela génère alors une croissance exponentielle du champ électrique [Che12 ; AFL01].

Finalement, en raison de sa non-linéarité et de ses propriétés de stabilité et d'instabilité linéaires, l'équation de Vlasov-Poisson (1.2.34) présente une grande richesse de comportements mesurés expérimentalement et étudiés analytiquement. Les simulations numériques des équations cinétiques comme (1.2.34) sont nécessaires pour étudier l'ensemble des phénomènes émergeant de ces équations. La grande dimensionnalité de l'espace des phases ($3\,\mathrm{D}_{\mathbf{x}}\,3\,\mathrm{D}_{\mathbf{v}}$) rend toutefois coûteuse les simulations numériques. Nous mentionnons dans la section suivante les équations fluides associées à (1.2.34), qui réduisent cette dimensionnalité.

1.2.3 Équations fluides

L'équation cinétique (1.2.34) détermine la distribution statistique $f(t,\mathbf{x},\mathbf{v})\,\mathrm{d}\mathbf{x}\,\mathrm{d}\mathbf{v}$ des particules au temps t entre des positions $\mathbf{x}$ et $\mathbf{x}+\mathrm{d}\mathbf{x}$, et de vitesse entre $\mathbf{v}$ et $\mathbf{v}+\mathrm{d}\mathbf{v}$. Il peut paraître étonnant de considérer de cette manière la distribution en vitesse des particules, car représenter ainsi l'espace des phases en 6 dimensions ($3\,\mathrm{D}_{\mathbf{x}}\,3\,\mathrm{D}_{\mathbf{v}}$) peut être coûteux d'un point de vue numérique. Par ailleurs, les quantités observables associées à la distribution des particules sont accessibles en calculant les moments de la fonction de distribution par rapport à $\mathbf{v}$. Par exemple, la densité spatiale de particules $n(t,\mathbf{x})$ est donnée par

$$n(t,\mathbf{x}) := \int_{\mathbb{R}^3_{\mathbf{v}}} f(t,\mathbf{x},\mathbf{v})\,\mathrm{d}\mathbf{v}\,.$$

On peut également calculer la quantité de mouvement grâce à ce formalisme :

$$n(t,\mathbf{x})\,\mathbf{u}(t,\mathbf{x}) := \int_{\mathbb{R}^3_{\mathbf{v}}} \mathbf{v}\,f(t,\mathbf{x},\mathbf{v})\,\mathrm{d}\mathbf{v}\,,$$

où $\mathbf{u}$ représente la vitesse moyenne des particules. L'énergie w et la température T associée à la distribution f sont quant à elles accessibles *via* les formules suivantes :

$$w(t,\mathbf{x}) := m\int_{\mathbb{R}^3_{\mathbf{v}}}\frac{1}{2}|\mathbf{v}|^2 f(t,\mathbf{x},\mathbf{v})\,\mathrm{d}\mathbf{v} = \frac{m}{2}n\,|\mathbf{u}(t,\mathbf{x})|^2 + \frac{3\,k_B}{2}n(t,\mathbf{x})\,T(t,\mathbf{x}),$$
$$\frac{3}{2}k_B\,n(t,\mathbf{x})\,T(t,\mathbf{x}) := \frac{m}{2}\int_{\mathbb{R}^3_{\mathbf{v}}}|\mathbf{v}-\mathbf{u}|^2 f(t,\mathbf{x},\mathbf{v})\,\mathrm{d}\mathbf{v}.$$

Dans certaines situations physiques, il est possible de caractériser la fonction de distribution des particules uniquement à partir de quelques moments de f. C'est notamment le cas lorsque les particules sont soumises à un champ magnétique très fort, ou lorsque les particules sont soumises à des collisions fréquentes. On reviendra en détail sur ces questions dans la section 1.4, tandis qu'une introduction aux modèles collisionnels de Fokker-Planck fera l'objet de la section 1.3. En toute généralité, intégrer le système de Vlasov-Poisson (1.2.34) contre 1, $\mathbf{v}$, $\frac{m}{2}|\mathbf{v}|^2$ donne lieu à une hierarchie d'équations dites fluides :

$$\begin{cases}\partial_t n + \nabla_{\mathbf{x}}\cdot(n\,\mathbf{u}) = 0,\\ \partial_t(n\,\mathbf{u}) + \nabla_{\mathbf{x}}\cdot(n\,\mathbf{u}\otimes\mathbf{u}) + \nabla_{\mathbf{x}}\cdot\mathbb{P} - \dfrac{q}{m}n\,\mathbf{E} = 0,\\ \partial_t w + \nabla_{\mathbf{x}}\cdot(w\,\mathbf{u} + \mathbb{P}\cdot\mathbf{u} + \mathbf{q}) - q\,n\,\mathbf{u}\cdot\mathbf{E} = 0,\end{cases} \tag{1.2.35}$$

où $\mathbb{P}$ et $\mathbf{q}$ dénotent respectivement le tenseur de pression et le flux de chaleur, qui sont donnés par

$$\mathbb{P}(t,\mathbf{x}) = m\int_{\mathbb{R}^3_{\mathbf{v}}}(\mathbf{v}-\mathbf{u})\otimes(\mathbf{v}-\mathbf{u})\,f(t,\mathbf{x},\mathbf{v})\,\mathrm{d}\mathbf{v}, \quad \mathbf{q}(t,\mathbf{x}) = \frac{m}{2}\int_{\mathbb{R}^3_{\mathbf{v}}}(\mathbf{v}-\mathbf{u})\,|\mathbf{v}-\mathbf{u}|^2 f(t,\mathbf{x},\mathbf{v})\,\mathrm{d}\mathbf{v}. \tag{1.2.36}$$

Utiliser la description donnée par le système d'équations fluides (1.2.35) est alors attrayant car l'espace des phases associé à ces équations est seulement de dimension 3. La difficulté est que (1.2.35) est un système d'équations non-fermées. En effet, $\mathbb{P}$ et $\mathbf{q}$ ne peuvent *a priori* pas s'exprimer en fonction des moments d'ordre inférieurs $n, \mathbf{u}$ et w. Afin de pouvoir utiliser la description fluide, il est nécessaire de fermer le système (1.2.35). Cela peut se faire *via* des lois empiriques ou bien en étudiant l'équation cinétique (1.2.34) dans un certain régime physique, notamment lorsque les particules sont soumises à de fortes collisions. Nous étudierons en détail la fermeture des équations fluides d'un système dans la sous-section 1.4.2.

Dans cette section, nous avons présenté une hiérarchie de modèles (microscopique, mésoscopique, et macroscopique) décrivant la dynamique des particules chargées. Cependant, notre modélisation ne prend pas en compte la notion de collision, pourtant très importante en physique des plasmas. Les particules subissent en effet des phénomènes de friction, de dérive et de diffusion liés à l'interaction avec leur environnement et entre elles. L'objet de la prochaine section sera de dériver l'opérateur de Fokker-Planck, qui décrit des interactions de longue

portée entre les particules. Cette description est appropriée pour des particules chargées électriquement. De plus, dans les contextes physiques où les collisions sont fréquentes, les équations fluides associées se ferment, contrairement au cas (1.2.35) qu'on a mentionné précédemment.

Les interactions entre les effets non-linéaires du transport et ceux des collisions sont complexes, et les effets mentionnés en sous-section 1.2.2.3 peuvent subsister ou disparaitre selon le contexte physique considéré. Des travaux récents tels que ceux de Bedrossian *et al.* [Bed17 ; BZZ24] précisent les interactions entre effets collisionnels et effets du transport, et posent la question de la persistance des échos du plasma dans la limite de faibles collisions.

Les opérateurs de collisions que nous allons considérer par la suite sont des opérateurs simplifiés de Fokker-Planck, plus faciles à traiter mathématiquement que l'opérateur de Fokker-Planck-Landau, dont nous ne traiterons pas ici. On réfère le lecteur à [Vil96] pour un résultat d'existence de solutions de l'équation de Fokker-Planck-Landau, et à [Des04] pour une revue de la littérature étudiant cette équation. D'autres opérateurs de collisions existent, comme l'opérateur de Boltzmann qui permet de modéliser des collisions élastiques entres particules neutres, ou encore l'opérateur de Bhatnagar-Gross-Krook (souvent dénoté BGK). Nous ne traiterons pas non plus de ces opérateurs dans la suite de cette thèse.

1.3 L'équation de Fokker-Planck

Les sous-sections 1.3.1 à 1.3.4 sont traduites et adaptées de la publication suivante :

- Claudia Negulescu, Etienne Lehman, Axel Maupoux. Entropy methods and application in the field of collective behaviour, *Le Matematiche*, Vol. 78, No. 1 (2023).

Nous allons expliquer la dérivation de l'équation de Fokker-Planck à partir des équations de Newton, comprenant un processus stochastique pour décrire l'interaction d'une particule avec son environnement. Cette dérivation est menée dans un contexte unidimensionnel par simplicité.

1.3.1 L'équation de Langevin

Au XIX$^{\text{ème}}$ siècle, le mouvement imprévisible des particules de pollen en suspension dans l'eau a été étudié une première fois par le botaniste Robert Brown (1773-1858). Influencée par l'aspect déterministe des équations de Newton, la communauté scientifique de l'époque éprouvait toutefois des difficultés à modéliser le mouvement erratique de ces particules.

Par la suite, le physicien Paul Langevin (1872-1946) observa que les équations de Newton de la mécanique classique demeuraient valides en moyenne pour décrire le mouvement erratique des particules, qualifié de Brownien. Ainsi, dans un environnement visqueux de coefficient de frottement $\alpha > 0$, la dynamique moyennée d'une particule est donnée par les équations de Newton suivantes :

$$m \frac{d}{dt}\langle v(t)\rangle = -\alpha \langle v(t)\rangle , \quad \text{où} \quad \langle v(t)\rangle = \frac{d}{dt}\langle x(t)\rangle , \quad \forall t \in \mathbb{R} .$$

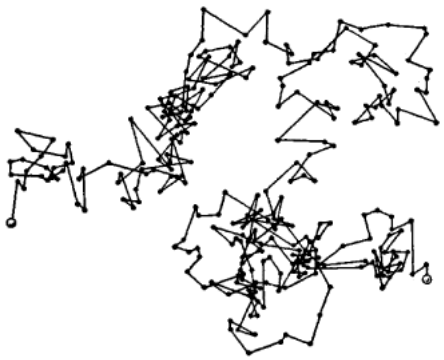

FIGURE 1.2 – Exemple de la dynamique erratique d'une particule.

Dans cette section, la moyenne $\langle\cdot\rangle$ prend en compte toutes les trajectoires possibles des particules soumises à une force aléatoire $\eta(t)$. L'équation qui gouverne en détail la dynamique d'une particule soumise au champ de force aléatoire $\eta(t)$, appelée équation de Langevin, est donnée par :

$$\frac{d}{dt}v(t) = -\gamma\, v(t) + \eta(t)\,, \qquad \text{où } \gamma = \frac{\alpha}{m}\,, \qquad \forall t \in \mathbb{R}\,. \tag{1.3.1}$$

L'équation différentielle stochastique (1.3.1) incorpore deux forces : les frottements visqueux $-\gamma\, v(t)$, et le bruit $\eta(t)$ qui représente les impacts incessants de l'environnement sur la particule brownienne. Le choix du champ de force $\eta(t)$ permet de modéliser de manière réaliste les effets des collisions microscopiques sur la particule. Le champ $\eta(t)$ est inconnu et difficile à décrire, de sorte qu'il est généralement traité de manière stochastique. Supposons en effet que $\eta(t)$ suit une distribution gaussienne (bruit blanc gaussien) de moyenne nulle, et qu'il est totalement décorrélé dans le temps, c'est-à-dire :

$$\langle\eta(t)\rangle = 0\,, \qquad \langle\eta(t)\,\eta(t')\rangle = \Gamma\,\delta_0(t-t')\,, \qquad \Gamma > 0\,, \qquad \forall t,\, t' > 0\,. \tag{1.3.2}$$

La constante $\Gamma > 0$ mesure l'intensité du champ de force fluctuant. Chaque solution de l'équation de Langevin (1.3.1) représente une trajectoire différente de la particule, laquelle dépend à la fois de la condition initiale v_0 et du champ de force aléatoire $\eta(t)$, donnée par la formule de Duhamel :

$$v(t) = v_0\, e^{-\gamma\, t} + \int_0^t e^{-\gamma\,(t-s)}\,\eta(s)\,ds\,, \qquad \forall t > 0\,. \tag{1.3.3}$$

Comme $\eta(t)$ est un processus stochastique gaussien et que l'intégrale de variables gaussiennes est aussi une variable gaussienne, nous pouvons en déduire que $v(t)$ est également un processus stochastique gaussien. Par conséquent, pour le caractériser, il suffit de calculer la moyenne $\mu(t) = \langle v(t)\rangle$ et la variance $\sigma(t)$. On définit alors la fonction de distribution en vitesse corres-

pondante :

$$f(t,v) := \frac{1}{\sqrt{2\pi\sigma^2(t)}}\, e^{-\frac{|v-\mu(t)|^2}{2\,\sigma^2(t)}}\,. \tag{1.3.4}$$

Compte tenu des propriétés (1.3.2), en moyennant (1.3.3), on obtient, d'une part

$$\langle v(t)\rangle = v_0\, e^{-\gamma\, t} \to_{t\to\infty} 0\,,$$

et d'autre part

$$\begin{aligned} v^2(t) &= v_0^2\, e^{-2\,\gamma\, t} + 2v_0\, e^{-\gamma\, t} \int_0^t e^{-\gamma\,(t-s)}\, \eta(s)\, ds \\ &\quad + \int_0^t \int_0^t e^{-\gamma\,(t-s)}\, e^{-\gamma\,(t-s')}\, \eta(s)\, \eta(s')\, ds'\, ds\,, \end{aligned}$$

de sorte que

$$\begin{aligned} \langle v^2(t)\rangle &= v_0^2\, e^{-2\,\gamma\, t} + \int_0^t \int_0^t e^{-\gamma\,(t-s)}\, e^{-\gamma\,(t-s')}\, \Gamma\, \delta_0(s-s')\, ds'\, ds \\ &= v_0^2\, e^{-2\,\gamma\, t} + \frac{\Gamma}{2\,\gamma}\left(1 - e^{-2\,\gamma\, t}\right) \to_{t\to\infty} \frac{\Gamma}{2\,\gamma}\,. \end{aligned}$$

Dans ces deux calculs, on peut observer que les conditions initiales sont perdues après un certain temps. En outre, la vitesse moyenne tend vers zéro dans la limite $t \to +\infty$, et la vitesse quadratique moyenne a une limite finie non-nulle. Dans la limite du temps long $t \to \infty$, la particule brownienne est en équilibre avec le milieu environnant. Si celui-ci est à l'équilibre thermodynamique, caractérisé par une température T (bain thermique), le théorème d'équipartition de la thermodynamique relie la température du milieu à l'énergie cinétique moyenne de la particule *via*

$$\frac{m}{2}\langle v_\infty^2\rangle = \frac{1}{2}\, k_B\, T \qquad \Rightarrow \qquad \Gamma = 2\,\frac{k_B\, T}{m}\,\gamma\,, \tag{1.3.5}$$

où k_B est la constante de Boltzmann. En d'autres termes, dans la limite du temps long, $\langle v^2(t)\rangle$ se rapproche du carré de la vitesse thermique donnée par $v_{th} := \sqrt{\frac{k_B\, T}{m}}$. L'identité (1.3.5) relie une quantité associée aux fluctuations, *i.e.* Γ, au coefficient décrivant la dissipation, *i.e.* γ. La relation fluctuation-dissipation (1.3.5) exprime l'équilibre entre le frottement, qui tend à conduire le système vers un état inactif, et le bruit qui tend à maintenir le système en mouvement.

Nous sommes maintenant en mesure de caractériser la solution de l'équation de Langevin (1.3.1) comme un processus gaussien de moyenne

$$\mu(t) := \langle v(t)\rangle = v_0\, e^{-\gamma\, t}\,, \qquad \forall t > 0\,, \tag{1.3.6}$$

et de variance

$$\sigma^2(t) := \langle [v(t) - \langle v(t)\rangle]^2\rangle = \frac{k_B\, T}{m}\left(1 - e^{-2\,\gamma\, t}\right)\,, \qquad \forall t > 0\,. \tag{1.3.7}$$

Dans la limite $t \to +\infty$, on obtient alors la distribution d'équilibre en vitesse pour la particule brownienne :

$$f_\infty(v) := \frac{1}{\sqrt{2\pi\sigma_\infty^2}}\, e^{-\frac{v^2}{2\,\sigma_\infty^2}} \quad \text{with} \quad \sigma_\infty^2 := \frac{k_B\, T}{m} = v_{th}^2\,, \quad \mu_\infty = 0\,, \tag{1.3.8}$$

qui est appelée la distribution de Maxwell-Boltzmann.

1.3.2 L'équation de Fokker-Planck

La question est maintenant de savoir comment obtenir la distribution des vitesses pour chaque instant t. En d'autres termes, au lieu de nous concentrer, comme dans la sous-section précédente, sur la solution $v(t)$ de l'équation de Langevin (1.3.1), nous nous intéresserons plutôt à trouver une équation régissant la dynamique de la fonction de distribution des vitesses $f(t,v)$, où $f(t,v)\,\mathrm{d}v$ représente la probabilité de trouver, à l'instant t, la particule brownienne ayant une vitesse dans le volume $\mathrm{d}v$ autour de v. Cette équation sera trouvée en faisant le bilan entre les termes de gain et de perte en la variable v. L'évolution temporelle de la quantité $f(t,v)$ est donnée par

$$\partial_t f(t,v) = \int_{-\infty}^{\infty} \left[\tilde{b}(v,v')\, f(t,v') - \tilde{b}(v',v)\, f(t,v)\right]\, dv'\,, \quad \forall (t,v) \in \mathbb{R}^+ \times \mathbb{R}\,, \tag{1.3.9}$$

où $\tilde{b}(v,v')$ est appelée la section transversale (*cross-section*), qui donne la probabilité par unité de temps d'une transition de vitesse de v' vers v. Nous supposons ici que cette section transversale est indépendante du temps, de sorte que les effets de mémoire sont négligés, et que seuls de petits changements de vitesse peuvent se produire.

Introduisons maintenant une nouvelle variable en vitesse $y := v - v'$, ainsi que la nouvelle section transversale

$$b(u-w,w) := \tilde{b}(u,w)\,, \quad \forall u, w \in \mathbb{R}\,.$$

En supposant la régularité nécessaire, on obtient :

$$\begin{aligned}
\partial_t f(t,v) &= \int_{-\infty}^{\infty} \left[b(v-v',v')\, f(t,v') - b(v'-v,v)\, f(t,v)\right]\, dv' \\
&= \int_{-\infty}^{\infty} \left[b(y,v-y)\, f(t,v-y) - b(-y,v)\, f(t,v)\right]\, dy \\
&= \int_{-\infty}^{\infty} \left[b(y,v-y)\, f(t,v-y) - b(y,v)\, f(t,v)\right]\, dy\,,
\end{aligned}$$

où dans le second terme de la dernière ligne, nous avons effectué le changement de variable $y \to -y$. Un développement de Taylor autour de v avec $|y| \ll |v|$ donne

$$b(y,v-y)\, f(t,v-y) = b(y,v)\, f(t,v) - y\, \partial_v \left[b(y,v)\, f(t,v)\right] + \frac{y^2}{2}\, \partial_{vv}^2 \left[b(y,v)\, f(t,v)\right] + \cdots$$

Alors, comme seuls des petits changements de vitesse peuvent se produire, b est concentrée autour de $y \approx 0$, ce qui implique

$$\begin{aligned}\partial_t f(t,v) &\approx \int_{-\infty}^{\infty} \left\{ -y\,\partial_v \left[b(y,v)\, f(t,v) \right] + \frac{y^2}{2}\,\partial_{vv}^2 \left[b(y,v)\, f(t,v) \right] \right\} dy \\ &= -\partial_v \left\{ \left(\int_{-\infty}^{\infty} y b(y,v)\, dy \right) f(t,v) \right\} + \frac{1}{2}\partial_{vv}^2 \left\{ \left(\int_{-\infty}^{\infty} y^2 b(y,v)\, dy \right) f(t,v) \right\} .\end{aligned}$$

Cette équation se réécrit

$$\partial_t f(t,v) = -\partial_v \left[A(v)\, f(t,v) \right] + \frac{1}{2}\partial_{vv}^2 \left[B(v)\, f(t,v) \right] , \tag{1.3.10}$$

où

$$A(v) := \int_{-\infty}^{\infty} y\, b(y,v)\, dy , \qquad B(v) := \int_{-\infty}^{\infty} y^2\, b(y,v)\, dy . \tag{1.3.11}$$

On peut désormais utiliser l'expression de la solution de l'équation de Langevin (1.3.1) pour calculer $A(v)$ et $B(v)$:

$$A(v) = -\gamma v , \qquad B(v) = 2\gamma \frac{k_B\, T}{m} .$$

En effet, en remplaçant d'abord $y = v' - v$ et $dy = dv'$ dans (1.3.11), puis en rappelant que $\tilde{b}(v', v)$ est la probabilité par unité de temps d'une transition de vitesse de v vers v', et enfin en désignant par $v' := v(\Delta t)$ la solution de l'équation de Langevin (1.3.1) munie de la condition initiale v, alors on obtient

$$A(v) = \lim_{\Delta t \to 0} \langle v(\Delta t) - v \rangle \frac{1}{\Delta t} = \lim_{\Delta t \to 0} v \frac{e^{-\gamma\, \Delta t} - 1}{\Delta t} = -\gamma\, v ,$$

où la moyenne $\langle \cdot \rangle$ prend compte toute les réalisations du champ de force aléatoire $\eta(t)$. Des calculs similaires donnent lieu à l'expression de $B(v)$. L'équation (1.3.10) se réécrit alors comme l'équation de Fokker-Planck suivante

$$\partial_t f(t,v) = \gamma \partial_v \left[v\, f(t,v) + \frac{k_B\, T}{m}\, \partial_v f \right] . \tag{1.3.12}$$

Il s'agit d'une équation aux dérivées partielles déterministe sur la fonction de distribution de probabilité f, qui prend la forme d'une équation de dérive-diffusion en la variable v. Soulignons ici l'interprétation de $\frac{k_B\, T}{m}$ comme un coefficient de diffusion en v. Le membre de droite de (1.3.12) peut être réécrit sous la forme $\gamma \partial_v \left[\frac{k_B\, T}{m}\, f_{eq}\, \partial_v \left(\frac{f}{f_{eq}} \right) \right]$, où f_{eq} est défini dans (1.3.13). Cette reformulation de (1.3.12) permet d'obtenir de manière simple les solutions stationnaires de l'équation de Fokker-Planck.

Il peut être intéressant de voir l'équation de Fokker-Planck comme une équation de continuité

$$\partial_t f(t,v) + \partial_v \mathcal{J}(t,v) = 0 ,$$

où le courant de probabilité est donné par

$$\mathcal{J}(t,v) := -\gamma v\, f(t,v) - \gamma \frac{k_B\, T}{m}\, \partial_v f(t,v)\,.$$

L'intégration de l'équation de continuité sur l'intervalle de vitesse $[v_-, v_+]$ donne

$$\partial_t \int_{v_-}^{v_+} f(t,v)\, dv = \mathcal{J}(t,v_-) - \mathcal{J}(t,v_+)\,,$$

ce qui signifie qu'un changement dans la distribution de la densité de probabilité dans l'intervalle $[v_-, v_+]$ provient de changements dans les flux de courant à travers les frontières de l'intervalle.

1.3.3 Propriétés et remarques

L'équation de Fokker-Planck est une équation fondamentale dans de nombreux domaines de la physique et de la biologie. Elle modélise un ensemble de particules soumises à la fois à la diffusion et à la dérive. L'interaction entre ces deux effets est à la source de la plupart de ses propriétés, lesquelles seront brièvement résumées ici dans un cadre multidimensionnel.

Solutions stationnaires

Si l'environnement de notre particule brownienne est à l'équilibre thermique de température T, les solutions stationnaires de (1.3.12) sont alors données par la fonction de distribution de Maxwell-Boltzmann

$$f_{eq}(v) := \left(\frac{m}{2\pi k_B\, T}\right)^{d/2} e^{-\frac{m|v|^2}{2k_B T}}\,, \qquad \forall v \in \mathbb{R}^d\,. \tag{1.3.13}$$

Solutions fondamentales

Il est possible de donner sous forme explicite les solutions fondamentales de (1.3.12), aussi appelées fonctions de Green. En d'autres termes, les solutions de l'équation de Fokker-Planck, munies d'une condition initiale $g(0,v;v_0) := \delta_0(v-v_0)$ pour un $v_0 \in \mathbb{R}^d$ arbitraire, sont données par

$$g(t,v;v_0) := \left(\frac{1}{2\pi\, \sigma^2(t)}\right)^{d/2} e^{-\frac{|v-\mu(t)|^2}{2\,\sigma^2(t)}} \qquad \forall t > 0\,,$$

qui est une distribution gaussienne de vitesse moyenne $\mu(t)$ et d'écart type $\sigma(t)$ donnés dans (1.3.6)-(1.3.7). Les solutions fondamentales permettent maintenant d'obtenir les solutions de l'équation de Fokker-Planck (1.3.12), pour toute condition initiale f_0, *via* :

$$f(t,v) = \int_{\mathbb{R}^d} g(t,v;v_0)\, f(v_0)\, dv_0\,.$$

Propriétés physiques

Considérons maintenant l'équation linéaire de Fokker-Planck suivante

$$\partial_t f(t,v) = \nabla_v \cdot [v\, f(t,v) + \nabla_v f]\,, \qquad \forall (t,v) \in \mathbb{R}^+ \times \mathbb{R}^d\,,$$

et observons qu'elle présente les caractéristiques suivantes :

— Une loi de conservation, donnée par :

$$\partial_t \rho = 0\,, \qquad \rho(t) := \int_{\mathbb{R}^d} f(t,v)\, dv\,.$$

— Une fonction de Lyapunov naturelle, l'énergie libre, composée de la somme de l'entropie et de l'énergie cinétique, c'est-à-dire :

$$\mathcal{E}(f) := \int_{\mathbb{R}^d} f\, \log(f)\, dv + \int_{\mathbb{R}^d} \frac{|v|^2}{2}\, f\, dv\,.$$

— Un terme de dissipation

$$\mathcal{D}(f)(t) := -\frac{d}{dt}\mathcal{E}(f(t)) = \int_{\mathbb{R}^d} \frac{1}{f}\, |\nabla_v f + v\, f|^2\, dv \geq 0\,, \quad \forall t \in \mathbb{R}^+\,,$$

qui peut être réécrit comme l'information de Fisher de f par rapport à la distribution d'équilibre $f_{eq}(v) = \frac{1}{(2\pi)^{d/2}}\, e^{-\frac{|v|^2}{2}}$, c'est-à-dire $\mathcal{D}(f) = \mathcal{I}(f|f_{eq})$, où

$$\mathcal{I}(f|g) := \int_{\mathbb{R}^d} f \left| \nabla_v \log\left(\frac{f}{g}\right)\right|^2 dv\,.$$

Il est maintenant possible d'utiliser les inégalités de Sobolev afin d'obtenir une estimation de la vitesse de retour de la fonction de distribution f vers l'équilibre f_{eq}.

Champ de force dérivant d'un potentiel

Remarquons enfin que, si la particule est immergée dans un potentiel extérieur $\phi(x)$, engendrant une force supplémentaire $F_{ext}(t,x) := -\nabla_x \phi(t,x)$, alors les équations de Fokker-Planck deviennent dépendantes de l'espace et s'écrivent sous la forme

$$\partial_t f(t,x,v) + v \cdot \nabla_x f - \nabla_x \phi(t,x) \cdot \nabla_v f = \gamma \nabla_v \cdot \left[v\, f(t,x,v) + \frac{k_B\, T}{m}\, \nabla_v f \right]\,. \tag{1.3.14}$$

Conditions de bord

Lorsque l'on considère l'équation de Fokker-Planck dans un domaine borné $\Omega \subset \mathbb{R}^d$, avec une frontière $\partial\Omega$ et un vecteur normal unitaire orienté vers l'extérieur $n(x)$, des conditions de bord doivent être spécifiées. Par exemple, on peut implémenter des conditions réflechissantes (mur impénétrable) :

$$f(t,x,R_x\, v) = f(t,x,v)\,, \quad \forall x \in \partial\Omega\,, \qquad R_x v := v - 2(v \cdot n(x))\, n(x)\,,$$

ou des conditions de bord absorbantes (mur absorbant), ce qui signifie que $f(t,x,v) = 0$ pour toutes les vitesses entrantes v au point $x \in \Omega$. En revanche, si $\Omega = \mathbb{R}^d$, des conditions limites naturelles imposent que la fonction de distribution tende vers 0 lorsque $|x| \to \infty$.

1.3.4 Cadre variationnel de l'équation de Fokker-Planck

L'équation linéaire de Fokker-Planck

$$\begin{cases} \partial_t f(t,v) - \nabla_v \cdot [v\, f + \nabla_v f] = 0\,, \qquad \forall (t,v) \in \mathbb{R}^+ \times \mathbb{R}^d\,, \\ f(0,\cdot) = f_{in}\,, \end{cases} \tag{1.3.15}$$

est de type parabolique et possède un cadre variationnel très appréciable. Introduisons les espaces de Hilbert pondérés

$$L^2_\mu := \left\{ f \in L^2(\mathbb{R}^d) \;/\; \int_{\mathbb{R}^d} |f|^2\, d\mu < \infty \right\}, \qquad (f,g)_\mu := \int_{\mathbb{R}^d} f\, g\, d\mu\,, \tag{1.3.16}$$

$$H^1_\mu := \left\{ f \in L^2_\mu \;/\; \nabla_v f \in (L^2_\mu)^d \right\}, \qquad (f,g)_{H^1_\mu} := (f,g)_\mu + (\nabla_v f, \nabla_v g)_\mu\,, \tag{1.3.17}$$

avec les mesures $d\mu := \mathcal{M}^{-1}\, dv$ et $\mathcal{M}(v) := \frac{1}{(2\pi)^{d/2}} e^{-|v|^2/2}$. On peut montrer que $\mathcal{Q}(f) := \nabla_v \cdot [v\, f + \nabla_v f]$, défini par

$$\mathcal{Q} \,:\, H^1_\mu \to H^{-1}_\mu\,, \qquad \langle \mathcal{Q}(f), g \rangle_{H^{-1}_\mu, H^1_\mu} := -(vf + \nabla_v f, vg + \nabla_v g)_\mu\,,$$

est un opérateur linéaire borné, où H^{-1}_μ désigne l'espace dual de H^1_μ. Il est également important de remarquer que pour $f \in H^1_\mu$ on a $vf \in L^2_\mu$. Ceci peut être démontré en $1D$ via une décomposition d'Hermite. En effet, en définissant les fonctions d'Hermite $\{\psi_k\}_{k\mathbb{N}}$ récursivement comme suit

$$\sqrt{k+1}\, \psi_{k+1}(v) = v\, \psi_k(v) - \sqrt{k}\, \psi_{k-1}\,, \qquad \psi_{-1} \equiv 0\,, \;\; \psi_0 \equiv \mathcal{M}\,, \;\; \psi_1 \equiv v\, \mathcal{M}\,, \tag{1.3.18}$$

celles-ci forment une base complète et orthogonale de L^2_μ et satisfont de plus

$$\psi_k'(v) = -\sqrt{k+1}\, \psi_{k+1}(v)\,, \qquad \int_{-\infty}^{\infty} \psi_k(v)\, \psi_l(v)\, \mathcal{M}^{-1}\, dv = \delta_{kl}\,.$$

La solution de (1.3.15) peut alors être décomposée de façon unique, comme suit :

$$f(t,v) := \sum_{k=0}^{\infty} \alpha_k(t)\, \psi_k(v)\,, \tag{1.3.19}$$

ce qui permet de montrer la propriété désirée.

On obtient un cadre mathématique plus courant si l'on rééchelonne la fonction de distribution f avec la distribution d'équilibre $\mathcal{M}(v) := \frac{1}{(2\pi)^{d/2}} e^{-|v|^2/2}$, notamment en introduisant $g := f/\mathcal{M}$, qui résout alors l'équation suivante :

$$\begin{cases} \partial_t g - \Delta_v g + v \cdot \nabla_v g = 0\,, \qquad \forall (t,v) \in \mathbb{R}^+ \times \mathbb{R}^d\,, \\ g(0,\cdot) = g_{in}\,. \end{cases} \tag{1.3.20}$$

En désignant le nouvel opérateur de collision par $\mathcal{L}(g) := \Delta_v g - v \cdot \nabla_v g$, et en introduisant les espaces de Hilbert correspondants associés à la mesure $d\gamma := \mathcal{M}\, dv$:

$$\mathcal{H} := L^2_\gamma\,, \qquad \mathcal{V} := H^1_\gamma\,, \tag{1.3.21}$$

on peut montrer que $\mathcal{L} : \mathcal{V} \to \mathcal{V}^\star$ est un opérateur linéaire borné, défini par la relation

$$\langle \mathcal{L}(f), g\rangle_{H^{-1}_\gamma, H^1_\gamma} := -(\nabla_v f, \nabla_v g)_\gamma$$

pour tout $f, g \in H^1_\gamma$. En introduisant l'opérateur $\nabla_v^\star$ du gradient *via*

$$\nabla_v^\star : L^2_\gamma \to H^{-1}_\gamma\,, \quad \nabla_v^\star\, \xi := v\, \xi - \nabla_v\, \xi\,,$$

on peut réécrire l'opérateur de collision sous la forme simplifiée suivante : $\mathcal{L} = -\nabla_v^\star \cdot \nabla_v$.

Proposition 1.3.1. L'opérateur restreint à L^2_γ, donné par $\mathcal{L} : D(\mathcal{L}) \subset L^2_\gamma \to L^2_\gamma$, vérifie les propriétés suivantes :
(i) L'opérateur $\mathcal{L} : D(\mathcal{L}) \subset \mathcal{H} \to \mathcal{H}$ est symétrique négatif.
(ii) Le noyau de $\mathcal{L}$ est donné par

$$\ker(\mathcal{L}) := \{\rho \in \mathbb{R}\}\,.$$

(iii) L'orthogonal de $\ker(\mathcal{L})$ dans L^2_γ est donné par

$$(\ker(\mathcal{L}))^\perp := \left\{ f \in \mathcal{H} \;/\; \int_{\mathbb{R}^d} f(v)\, \mathcal{M}\, dv = 0 \right\}.$$

En outre, on a $L^2_\gamma = \ker(\mathcal{L}) \oplus (\ker(\mathcal{L}))^\perp$, où $f = \Pi f + (Id - \Pi)\, f$ avec Π la projection orthogonale sur $\ker(\mathcal{L})$, donnée par

$$\Pi : L^2_\gamma \to \ker(\mathcal{L}) \qquad f \mapsto \int_{\mathbb{R}^d} f(v)\, \mathcal{M}\, dv\,.$$

(iv) $-\mathcal{L}$ est coercive sur $D(\mathcal{L}) \cap (\ker(\mathcal{L}))^\perp$, *i.e.*

$$-(\mathcal{L}(f), f)_\gamma = -\langle \mathcal{L}(f), f\rangle_{H^{-1}_\gamma, H^1_\gamma} \geq C\|f\|^2_{\mathcal{H}}\,, \quad \forall f \in D(\mathcal{L}) \cap (\ker(\mathcal{L}))^\perp\,.$$

(v) L'image $\mathrm{Im}(\mathcal{L})$ de $\mathcal{L}$ est fermée dans L^2_γ et coïncide avec $(\ker(\mathcal{L}))^\perp$. On a de plus la correspondance bijective suivante :

$$\mathcal{L} : D(\mathcal{L}) \cap (\ker(\mathcal{L}))^\perp \to (\ker(\mathcal{L}))^\perp\,.$$

Introduire la forme bilinéaire donnée par

$$l : \mathcal{V} \times \mathcal{V} \to \mathbb{R}\,, \qquad l(f, g) := (\nabla_v f, \nabla_v g)_\gamma\,,$$

qui est associée à $\mathcal{L} : \mathcal{V} \to \mathcal{V}^\star$ permet d'entrer dans le cadre mathématique donné par les théorèmes de Lax-Milgram et de Lions. Le caractère bien posé du problème (1.3.20) en est alors une conséquence naturelle. Plus spécifiquement, pour chaque temps $T > 0$, il existe une unique solution faible g de (1.3.20) satisfaisant aux conditions suivantes :

$$g \in W^1_2(0, T; \mathcal{V}, \mathcal{H}) \subset C([0, T]; \mathcal{H})\,.$$

Il s'agit alors de considérer le triplet d'évolution $\mathcal{V} \subset \mathcal{H} = \mathcal{H}^\star \subset \mathcal{V}^\star$.

1.3.5 Quelques variantes de l'équation de Fokker-Planck

Revenons au cadre tridimensionnel. Dans cette thèse, on considèrera essentiellement l'équation de Vlasov-Fokker-Planck ainsi que ses variantes, quelles soient linéaires ou non-linéaires, avec ou sans transport et avec ou sans champ magnétique. Dans le chapitre 1, nous travaillerons sur l'opérateur de Fokker-Planck présent dans (1.3.15), c'est-à-dire l'opérateur de Fokker-Planck linéaire standard :

$$\mathcal{Q}_{\mathrm{FPlin}}(f) = \nabla_{\mathbf{v}} \cdot [\mathbf{v}\, f + \nabla_{\mathbf{v}} f] \,. \tag{1.3.22}$$

Il est à noter que cet opérateur de Fokker-Planck décrit l'interaction de la densité de particules f avec un fond de particules fixées, qui relaxe f vers un équilibre thermodynamique. C'est un opérateur inter-espèce, car il modélise les collisions d'une espèce avec une autre espèce. Signalons toutefois dans cette section que de multiples opérateurs de Fokker-Planck existent pour modéliser toute une variété de situations différentes.

Un exemple particulier est l'opérateur de Fokker-Planck non-linéaire choisi par [Bed17] :

$$\mathcal{Q}_{\mathrm{FPnonlin}}(f) \;:=\; \nu(t,\mathbf{x})\, \nabla_{\mathbf{v}} \cdot \left((\mathbf{v}-\mathbf{u})\, f + \frac{k_B T}{m} \nabla_{\mathbf{v}} f \right) , \tag{1.3.23}$$

où $\nu(t,\mathbf{x})$ est la fréquence de collision pouvant dépendre de f. Dans [Ric19] et [Bed17], $\nu(t,\mathbf{x})$ est en effet proportionnelle à la densité spatiale. L'opérateur $\mathcal{Q}_{\mathrm{FPnonlin}}(f)$ modélise la diffusion des particules en fonction de leur température, mais aussi de leur friction avec l'ensemble (*bulk*) des autres particules modélisées par f. C'est un opérateur de collision intra-espèce, car il modélise les collisions d'une espèce avec elle-même. Les quantités macroscopiques $(n, \mathbf{u}, T)$ sont calculés de la façon suivante :

$$\begin{cases} n(t,x) \;:=\; \displaystyle\int_{\mathbb{R}^3} f(t,x,v)\, \mathrm{d}\mathbf{v}\,, \\ n\,\mathbf{u}(t,x) \;:=\; \displaystyle\int_{\mathbb{R}^3} \mathbf{v}\, f(t,x,v)\, \mathrm{d}\mathbf{v} \\ 3\, k_B\; n\; T(t,\mathbf{x}) \;:=\; m \displaystyle\int_{\mathbb{R}^3} |\mathbf{v}-\mathbf{u}|^2\, f(t,\mathbf{x},\mathbf{v})\; \mathrm{d}\mathbf{v}\,, \end{cases}$$

avec k_B la constante de Boltzmann.

L'opérateur (1.3.23) préserve toutes les propriétés importantes de la distribution des particules. En effet, la masse, la quantité de mouvement et l'énergie sont préservées :

$$\int_{\mathbb{R}^3} \mathcal{Q}_{\mathrm{FPnonlin}}(f) \begin{pmatrix} 1 \\ \mathbf{v} \\ \dfrac{|\mathbf{v}|^2}{2} \end{pmatrix} \mathrm{d}\mathbf{v} \;=\; 0\,.$$

Cet opérateur vérifie également la propriété de décroissance de l'entropie (mathématique)

$$\int_{\mathbb{R}^3} \mathcal{Q}_{\text{FPnonlin}}(f)\,\ln(f)\,\mathrm{d}\mathbf{v} \;\leqslant 0\,,$$

ce qui mène vers un équilibre thermodynamique :

$$\int_{\mathbb{R}^3} \mathcal{Q}_{\text{FPnonlin}}(f)\ln(f)\,\mathrm{d}\mathbf{v} \;=\; 0 \quad\Longleftrightarrow\quad f \;=\; \mathcal{M}_{n,\mathbf{u},T}\,,$$

où $\mathcal{M}_{n,\mathbf{u},T}$ est une distribution Maxwellienne définie par

$$\mathcal{M}_{n,\mathbf{u},T}(\mathbf{v}) \;:=\; n\left(\frac{m}{2\pi\,k_B\,T}\right)^{3/2}\exp\left(-m\frac{|\mathbf{v}-\mathbf{u}|^2}{2k_BT}\right). \tag{1.3.24}$$

Ce sera une variante de cet opérateur non-linéaire et conservatif qui sera choisie dans le Chapitre 3.

Terminons cette section en précisant qu'il est également possible de modéliser deux espèces simultanément à l'aide d'opérateurs de Fokker-Planck. Prenons f_i et f_e des distributions respectives d'ions et d'électrons dans $\mathbb{R}^3$ (ou le domaine périodique $\mathbb{T}^3$), données par les équations couplées de Vlasov-Fokker-Planck suivantes [FN22] (auxquelles on a rajouté les effets du champ magnétique) :

$$\begin{cases} \partial_t f_i \;+\; \mathbf{v}\cdot\nabla_{\mathbf{x}} f_i \;+\; \dfrac{e}{m_i}\,(\mathbf{E}+\mathbf{v}\times\mathbf{B})\cdot\nabla_{\mathbf{v}} f_i \;=\; \mathcal{Q}_{ii}(f_i,f_i) \;+\varepsilon\,\mathcal{Q}_{ie}(f_i,f_e)\,, \\ \varepsilon\partial_t f_e \;+\; \mathbf{v}\cdot\nabla_{\mathbf{x}} f_e \;-\; \dfrac{e}{m_e}\,(\mathbf{E}+\mathbf{v}\times\mathbf{B})\cdot\nabla_{\mathbf{v}} f_e \;=\; \mathcal{Q}_{ee}(f_e,f_e) \;+\; \mathcal{Q}_{ei}(f_e,f_i)\,. \end{cases} \tag{1.3.25}$$

On a dénoté par $-e$, m_e la charge et la masse d'un élection, respectivement e, m_i la charge et la masse d'un ion. Tous les opérateurs de collisions sont de la forme Fokker-Planck, c'est-à-dire si $\alpha,\beta\in\{e,i\}$:

$$\mathcal{Q}_{\alpha\beta}(f_\alpha,f_\beta) \;:=\; \nu_{\alpha\beta}\,\nabla_{\mathbf{v}}\cdot\left((\mathbf{v}-\mathbf{u}_{\alpha\beta})f_\alpha + \frac{k_BT_{\alpha\beta}}{m_\alpha}\nabla_{\mathbf{v}} f_\alpha\right). \tag{1.3.26}$$

où $\nu_{\alpha\beta}>0$ sont les fréquences de collisions correspondant au couple (α,β) de particules. On définit les quantités macroscopiques des ions et des électrons séparément, mais avec les même formules que pour l'opérateur $\mathcal{Q}_{\text{FPnonlin}}$. En d'autres termes, si $\alpha\in\{e,\,i\}$, on définit de la façon suivante :

$$\begin{cases} n_\alpha(t,\mathbf{x}) \;:=\; \displaystyle\int_{\mathbb{R}^3} f_\alpha(t,\mathbf{x},\mathbf{v})\,\mathrm{d}\mathbf{v}\,, \\ n_\alpha\mathbf{u}_\alpha(t,\mathbf{x}) \;:=\; \displaystyle\int_{\mathbb{R}^3} \mathbf{v}\,f_\alpha(t,\mathbf{x},\mathbf{v})\,\mathrm{d}\mathbf{v}\,, \\ 3\,k_B\,n_\alpha\,T_\alpha(t,\mathbf{x}) \;:=\; m_\alpha\displaystyle\int_{\mathbb{R}^3}|\mathbf{v}-\mathbf{u}_\alpha|^2\,f_\alpha(t,\mathbf{x},\mathbf{v})\,\mathrm{d}\mathbf{v}\,. \end{cases} \tag{1.3.27}$$

Avec la convention $X_{\alpha\alpha} := X_\alpha$ pour toute quantité X. Pour les collisions ion-ion et électron-électron (c'est-à-dire Q_{ii} et Q_{ee}), le choix est fait d'un opérateur comme [Bed17], (1.3.23). Le

choix des opérateurs inter-espèces est plus subtil. La forme choisie (1.3.26) demande d'éclaircir le sens de la "vitesse moyenne inter-particules" $\mathbf{u}_{\alpha\beta}$ et de la "température inter-particules" $T_{\alpha\beta}$. Dans [FN22], il est fait le choix de définir ces quantités en mélangeant les expressions des quantités macroscopiques (1.3.27). Ce choix est fait de sorte que le modèle vérifie des propriétés physiques particulières. En effet, les ions et les électrons peuvent échanger de l'énergie et de la quantité de mouvement, de sorte que la conservation de la quantité de mouvement totale du système {ions, électrons} s'écrit

$$m_e \int_{\mathbb{R}^3} \mathcal{Q}_{ei}(f_e, f_i)\, \mathbf{v}\, \mathrm{d}\mathbf{v} + m_i \int_{\mathbb{R}^3} \mathcal{Q}_{ie}(f_i, f_e)\, \mathbf{v}\, \mathrm{d}\mathbf{v} = 0\,, \tag{1.3.28}$$

tandis que la conservation de l'énergie doit s'écrire

$$m_e \int_{\mathbb{R}^3} \mathcal{Q}_{ei}(f_e, f_i)\, \frac{|\mathbf{v}|^2}{2}\, \mathrm{d}\mathbf{v} + m_i \int_{\mathbb{R}^3} \mathcal{Q}_{ie}(f_i, f_e)\, \frac{|\mathbf{v}|^2}{2}\, \mathrm{d}\mathbf{v} = 0\,. \tag{1.3.29}$$

De plus, l'entropie du système complet doit décroître :

$$\int_{\mathbb{R}^3} \mathcal{Q}_{ei}(f_e, f_i)\, \ln(f_e)\, \mathrm{d}\mathbf{v} + \int_{\mathbb{R}^3} \mathcal{Q}_{ie}(f_i, f_e) \ln(f_i)\, \mathrm{d}\mathbf{v} \leqslant 0\,. \tag{1.3.30}$$

Ces propriétés physiques sont satisfaites dans [FN22], le lecteur intéressé peut s'y référer pour plus de détails.

Ces opérateurs sont très riches d'un point de vue physique, mais sont aussi très fortement non-linéaires, ce qui rend leur analyse mathématique difficile. Cependant, le lecteur intéressé peut se référer à [HJZ24], où un résultat d'existence de solutions associées à une large classe d'opérateurs similaires est démontré, dans le cas homogène en espace. Notons que de tels opérateurs pour modéliser les collisions intra et inter-espèces existaient déjà avec d'autres opérateurs, appelés opérateurs de Bhatnagar-Gross-Krook pour des mixtures [Bob+18 ; HHM17 ; Neg18].

Nous avons jusqu'ici discuté en détail d'équations cinétiques donnant la distribution en position et en vitesse des particules considérées. Dans le cadre de simulations numériques réalistes, l'espace des phases est alors de 6 dimensions, 3 d'espace et 3 de vitesse. La simulation de l'évolution temporelle d'une équation cinétique, parfois plusieurs si l'on s'intéresse à la modélisation d'un système multi-espèces comme (1.3.25), reste encore un défi. La situation est encore plus compliquée si, dans ces équations cinétiques, d'autres opérateurs collision plus complexes et plus réalistes que des opérateurs de type Fokker-Planck sont considérés.

Pour répondre à cette difficulté, une approche consiste à simplifier ces modèles cinétiques en tenant compte des conditions physiques spécifiques de la situation étudiée.

1.4 Limites fluides : l'exemple des électrons adiabatiques

Dans certaines situations, la distribution f de particules considérées peut être caractérisée uniquement par certaines des quantités macroscopiques $n, \mathbf{u}, T$ associées à f. Dans ce contexte,

il est souvent possible de dériver des modèles réduits qui répondent à la fois aux exigences de précision physique et d'efficacité numérique. Pour montrer cela, on va prendre en exemple la dérivation complète du modèle étudié au chapitre 2. Une exposition plus complète, partant d'un modèle bi-espèces est donnée dans [Neg18].

1.4.1 Procédure d'adimensionnement

Partons de la description des électrons donnée par l'équation de Vlasov-Poisson-Fokker-Planck avec champ magnétique :

$$\partial_t f_e + \mathbf{v}\cdot\nabla_{\mathbf{x}} f_e - \frac{e}{m_e}\,(\mathbf{E}+\mathbf{v}\times\mathbf{B})\cdot\nabla_{\mathbf{v}} f_e = \nu_e\,\mathcal{Q}_{\mathrm{FPlin}}(f_e)\,. \tag{1.4.1}$$

Exprimons maintenant les variables en termes de leur échelle caractéristique (dénotée avec une barre) et d'une fonction rééchelonnée (dénotée avec une apostrophe), par exemple :

$$f_e = \bar{f}_e\, f_e'\,, \qquad \mathbf{E} = \bar{E}\,\mathbf{E}'\,, \qquad \mathbf{B} = \bar{B}\,\mathbf{B}'\,.$$

On normalise l'équation de Vlasov ci-dessus en posant les échelles d'observations suivantes :

$$t = \bar{t}\,t'\,, \qquad \mathbf{x} = \bar{x}\,\mathbf{x}'\,, \qquad \mathbf{v} = v_{\mathrm{th,e}}\mathbf{v}'\,,$$

où la vitesse thermique des électrons $v_{th,e}$ est définie par

$$v_{th,e} := \sqrt{\frac{k_B\,\bar{T}}{m_e}}\,,$$

et $\bar{T} := \bar{T}_e = \bar{T}_i$ désigne la température caractéristique des électrons, supposée égale à celle des ions. On définit de façon analogue la vitesse thermique des ions :

$$v_{th,i} := \sqrt{\frac{k_B\,\bar{T}}{m_i}}\,. \tag{1.4.2}$$

On suppose également

$$\bar{Q}_{\mathrm{FPlin}}(f) = \bar{f}\,.$$

Nous introduisons la fréquence d'observation et la fréquence cyclotronique des électrons :

$$\bar{\omega} = \frac{1}{\bar{t}}\,, \qquad \Omega_c = \frac{e\,\bar{B}}{m_e}\,.$$

L'équation de Vlasov se renormalise de la façon suivante :

$$\partial_{t'} f' + \frac{\bar{t}\,v_{\mathrm{th,e}}}{\bar{x}}\mathbf{v}'\cdot\nabla_{\mathbf{x}'} f' - \frac{\Omega_{\mathrm{c}}}{\bar{\omega}}\left(\frac{\bar{E}}{v_{\mathrm{th,e}}\bar{B}}\mathbf{E}' + \mathbf{v}'\times\mathbf{B}'\right)\cdot\nabla_{\mathbf{v}'} f' = \frac{\bar{\nu}_{\mathrm{e}}}{\bar{\omega}}\,\nu_{\mathrm{e}}'\,Q_{\mathrm{FPlin}}'(f')\,. \tag{1.4.3}$$

Le régime physique est alors déterminé par quatre quantités :

i) $\frac{\bar{t}\, v_{\mathrm{th,e}}}{\bar{x}}$, le ratio entre le déplacement caractéristique des électrons et l'échelle spatiale d'observation choisie ;

ii) $\Omega_{\mathrm{c}}/\bar{\omega}$, le rapport entre la fréquence cyclotronique et la fréquence d'observation choisie ;

iii) $\bar{E}/(v_{\mathrm{th,e}}\bar{B})$, le rapport entre la vitesse de dérive $\mathbf{E}\times\mathbf{B}/|\mathbf{B}|^2$ et la vitesse thermique ;

iv) $\bar{\nu}_{\mathrm{e}}/\bar{\omega}$, le ratio entre la frequence de collision et la fréquence d'observation choisie.

On fait le choix de se placer à l'échelle d'observation temporelle des ions, ce qui nous conduit à faire le choix suivant :

$$\bar{x} = \bar{t}\, v_{\mathrm{th,i}}\,.$$

Pour cette raison, le paramètre physique i) se réécrit :

$$\frac{\bar{t}\, v_{\mathrm{th,e}}}{\bar{x}} = \frac{v_{\mathrm{th,e}}}{v_{\mathrm{th,i}}} = \sqrt{\frac{m_e}{m_i}}.$$

Dans la situation d'un plasma de fusion thermonucléaire, le rapport de masse est de l'ordre $m_e/m_i \simeq 1/3600 \ll 1$. On choisit alors de définir le petit paramètre

$$\varepsilon \;:=\; \frac{v_{\mathrm{th,e}}}{v_{\mathrm{th,i}}}\,.$$

On suppose que la fréquence cyclotronique est beaucoup plus grande que l'échelle de fréquence choisie, en raison du fort champ magnétique qui est imposé dans un tokamak. Cette hypothèse peut être formulée comme suit :

$$\frac{\Omega_{\mathrm{c}}}{\bar{\omega}} = \frac{1}{\varepsilon^2} \gg 1\,. \tag{1.4.4}$$

Au sujet du paramètre iii), on fait le choix de fixer la vitesse de dérive comme étant de l'ordre de la vitesse macroscopique des particules. On suppose alors la vitesse de dérive négligeable par rapport à la vitesse thermique (limite bas-Mach) :

$$\frac{\bar{E}}{v_{\mathrm{th,e}}\,\bar{B}} = \varepsilon\,. \tag{1.4.5}$$

Finalement, on suppose la fréquence de collisions électroniques grande devant la fréquence d'observation des ions :

$$\frac{\bar{\nu}_{\mathrm{e}}}{\bar{\omega}} = \frac{1}{\varepsilon} \gg 1\,. \tag{1.4.6}$$

Finalement, l'équation renormalisée se réécrit (on omet l'apostrophe par souci de clarté) :

$$\varepsilon\,\partial_t f_e + \mathbf{v}\cdot\nabla_{\mathbf{x}} f_e - \left(\mathbf{E} + \frac{1}{\varepsilon}\mathbf{v}\times\mathbf{B}\right)\cdot\nabla_{\mathbf{v}} f_e = \nu_e\, Q_{\mathrm{FPlin}}(f_e)\,. \tag{1.4.7}$$

On dit que cette équation cinétique décrit les électrons dans le régime adiabatique. Dans le chapitre 2, nous considérerons uniquement le mouvement parallèle au champ magnétique.

Supposons donc f_e homogène dans la direction perpendiculaire à $\mathbf{B}$. Choisissons l'opérateur de Fokker-Planck linéaire pour modéliser les collisions et supposons la dynamique des ions donnée, modélisée par une densité spatiale n_i. L'équation se réécrit finalement :

$$\varepsilon\,\partial_t f_e + v\,\partial_x f_e - E\,\partial_v f_e = \partial_v\left[v\,f + \partial_v f\right]\,. \tag{1.4.8}$$

Le champ électrique, calculé à partir de l'équation de Poisson, est solution de :

$$-\partial_{xx}\phi = n_i - n_e\,, \qquad E = -\partial_x\phi\,, \qquad n_e := \int_{\mathbb{R}} f_e(t,x,v)\,\mathrm{d}v\,. \tag{1.4.9}$$

Notons que les constantes e et ε_0 de l'équation de Poisson sont fixées à 1 dans (1.4.9).

La procédure d'adimensionnement met alors en évidence un petit paramètre ε. On s'attache donc à dériver un modèle limite réduit pour les électrons modélisés par (1.4.8)-(1.4.9), dans la limite $\varepsilon \to 0$. Pour cela, on omettra l'indice e pour parler des électrons, et on dénotera avec l'exposant ε toute quantité dépendant de ε. Par exemple, f_e, dépendant de ε, sera renommée f^ε. Cette notation sera adoptée jusqu'à la fin de cette section, et pour l'ensemble du chapitre 2. Finalement, on s'intéressera au système suivant :

$$(V)_\varepsilon \quad \begin{cases} \partial_t f^\varepsilon + \dfrac{1}{\varepsilon}\,v\,\partial_x f^\varepsilon - \dfrac{1}{\varepsilon}\,E^\varepsilon\,\partial_v f^\varepsilon = \dfrac{1}{\varepsilon}\partial_v\left[v\,f^\varepsilon + \partial_v f^\varepsilon\right]\,, \\ -\partial_{xx}\phi^\varepsilon = n_i - n^\varepsilon, \qquad E^\varepsilon = -\partial_x\phi^\varepsilon\,. \end{cases} \tag{1.4.10}$$

1.4.2 Limite formelle des électrons adiabatiques $\varepsilon \to 0$.

On rappelle que les quantités macroscopiques associées à f^ε telles que la densité spatiale de particules n^ε, la densité de courant locale j^ε ou l'énergie cinétique locale des électrons sont calculées directement comme des moments de la distribution d'électrons f^ε :

$$n^\varepsilon(t,x) := \int_{\mathbb{R}_v} f^\varepsilon(t,x,v)\,\mathrm{d}v\,, \qquad j^\varepsilon(t,x) := (n^\varepsilon u^\varepsilon)(t,x) = \int_{\mathbb{R}_v} v\,f^\varepsilon\,\mathrm{d}v\,,$$

$$w^\varepsilon(t,x) := \frac{1}{2}\int_{\mathbb{R}_v} v^2\,f^\varepsilon\,\mathrm{d}v\,.$$

En calculant les deux premiers moments de (1.4.10), on obtient le système d'équations de conservation macroscopique suivant :

$$\begin{cases} \partial_t n^\varepsilon + \dfrac{1}{\varepsilon}\,\partial_x j^\varepsilon = 0\,, \\ \partial_t j^\varepsilon + \dfrac{2}{\varepsilon}\,\partial_x w^\varepsilon + \dfrac{1}{\varepsilon}\,n^\varepsilon\,E^\varepsilon = -\dfrac{1}{\varepsilon}\,j^\varepsilon\,. \end{cases} \tag{1.4.11}$$

Ce système n'est pas fermé, comme on l'a souligné en sous-section 1.2.3, car w^ε dépend encore de la fonction de distribution f^ε. Cependant, quand $\varepsilon \to 0$, ce système se ferme, de sorte qu'on arrive à exprimer la quantité w^0 en fonction des autres quantités macroscopiques d'ordre inférieur n^0 , j^0. Explorons maintenant formellement la limite $\varepsilon \to 0$ du modèle cinétique (1.4.10).

Théorème 1.4.1. *[LN24b] **(Modèle limite : électrons adiabatiques)** Soit pour tout $\varepsilon > 0$ une solution (f^ϵ, E^ϵ) de (1.4.10) satisfaisant la contrainte de masse*

$$\int_{\mathbb{R}_v}\int_{\mathbb{T}_x} f^\varepsilon(t,x,v)\,\mathrm{d}v\,\mathrm{d}x = \mathfrak{m}\,, \qquad \forall (x,v)\in \mathbb{T}_x\times\mathbb{R}_v\,.$$

Dans la limite $\varepsilon \to 0$, la solution $(f^\varepsilon, E^\varepsilon)$ converge formellement vers (f^0, E^0), donnée par le modèle macroscopique, elliptique, non-linéaire suivant :

$$(L)\quad \begin{cases} f^0(t,x,v) = c(t)\; e^{\phi^0(t,x)}\,\mathcal{M}(v)\,, & c(t) = \mathfrak{m}/\displaystyle\int_{\mathbb{T}_x} e^{\phi^0(t,x)}\,\mathrm{d}x\,, \\ -\partial_{xx}\phi^0 + c(t)\,e^{\phi^0(t,x)} = n_i(t,x)\,, & E^0 = -\partial_x\phi^0\,, \end{cases} \tag{1.4.12}$$

où $\mathcal{M}(v)$ est une distribution maxwellienne en une dimension de vitesse :

$$\mathcal{M}(v) = \frac{1}{\sqrt{2\,\pi}} e^{-v^2/2}\,. \tag{1.4.13}$$

On dit que les électrons suivent la relation de Maxwell-Boltzmann.

Preuve du Théoreme 1.4.1. Une preuve de ce Théorème est donnée dans le chapitre 2. On présente toutefois ici une preuve différente qui illustre la fermeture du système des moments (1.4.11) dans le cas de la limite adiabatique. La preuve de la convergence formelle de la solution f^ε repose sur plusieurs étapes :

(a) Théorème-H : remarquons que le membre de droite de (1.4.10), c'est-à-dire le terme de collision, se réécrit

$$\partial_v\left(v\,f^\varepsilon + \partial_v f^\varepsilon\right) = \partial_v\left(\mathcal{M}\,\partial_v\left(\frac{f^\varepsilon}{\mathcal{M}}\right)\right)\,. \tag{1.4.14}$$

Alors, multiplier l'équation cinétique (1.4.10) par $\ln(\frac{f^\varepsilon}{e^{\phi^\varepsilon}\mathcal{M}})$ et faire tendre formellement $\varepsilon \to 0$ permet de montrer que

$$0 = \int_{\mathbb{T}_x}\int_{\mathbb{R}_v} \partial_v\left(\mathcal{M}\,\partial_v\left(\frac{f^0}{\mathcal{M}}\right)\right)\ln\left(\frac{f^0}{e^{\phi^0}\,\mathcal{M}}\right)\,\mathrm{d}v\,\mathrm{d}x \tag{1.4.15}$$

$$= \int_{\mathbb{T}_x}\int_{\mathbb{R}_v} \partial_v\left(\mathcal{M}\,\partial_v\left(\frac{f^0}{\mathcal{M}}\right)\right)\ln(f^0/\mathcal{M})\,\mathrm{d}v\,\mathrm{d}x \tag{1.4.16}$$

$$= -\int_{\mathbb{T}_x}\int_{\mathbb{R}_v} \frac{\mathcal{M}^2}{f^0}\left|\partial_v\frac{f^0}{\mathcal{M}}\right|^2\,\mathrm{d}v\,\mathrm{d}x\,. \tag{1.4.17}$$

On en déduit donc

$$f^0(t,x,v) = n^0(t,x)\,\mathcal{M}(v)\,, \qquad \forall (t,x,v) \in \mathbb{R}^+ \times \mathbb{T}_x \times \mathbb{R}_v\,,$$

où $n^0(t,x)$ reste à calculer dans les étapes (b) et (c).

(b) Convergence des moments : en utilisant la forme trouvée en (*a*), *i.e.* $f^0(t,x,v) = n^0(t,x)\,\mathcal{M}(v)$, on trouve les convergences formelles

$$j^\varepsilon \underset{\varepsilon\to 0}{\to} j^0 = \int_{\mathbb{R}_v} v\, f^0\, \mathrm{d}v = 0$$

et

$$w^\varepsilon \underset{\varepsilon\to 0}{\to} w^0 = \frac{1}{2}\int_{\mathbb{R}_v} v^2\, f^0\, \mathrm{d}v = n^0\,.$$

(c) Passage à la limite formel : Dans la limite où $\varepsilon \to 0$, la deuxième équation de (1.4.11) conduit alors formellement à

$$\partial_x n^0 + n^0\, E^0 = \partial_x n^0 - n^0\, \partial_x \phi^0 = 0\,.$$

On en conclut que

$$n^0(t,x) = c(t)\, e^{\phi^0(t,x)}\,.$$

Intégrer cette égalité par rapport à $x \in \mathbb{T}_x$ permet de conclure, *via* la conservation de la masse quant à la forme de $c(t)$.

□

Remarquons que dans l'étape (c), on a passé à la limite $\varepsilon \to 0$ dans le produit $n^\varepsilon\, E^\varepsilon$. Pour cette raison, le Théorème 1.4.1 donné ici est seulement formel. Dans [BD95], pour l'étude de l'asymptotique $t \to +\infty$, les auteurs concluent par un argument de compacité forte pour passer à la limite dans le produit. Dans le chapitre 2, on donnera une preuve rigoureuse de la convergence en utilisant une autre approche.

Cette preuve formelle a illustré que dans le régime $\varepsilon \to 0$, les électrons sont caractérisés exclusivement par quelques quantités macroscopiques, c'est-à-dire les moments de f^0. De manière générale, les modèles limites issus d'une procédure d'adimensionnement et d'analyse asymptotique présentent une dimensionnalité réduite, permettant alors des simulations numériques bien plus efficaces.

On trouve dans la littérature une grande variété de régimes physiques étudiés à l'aide de l'analyse asymptotique. Mentionnons que beaucoup d'hypothèses différentes peuvent être faites lors de l'adimensionnement de l'équation de Vlasov pour les électrons [NP16]. Parmi d'autres régimes possibles en théorie cinétique, citons [GS99 ; Sai02] pour l'étude du système de Vlasov-Poisson modélisant des ions dans un champ électrique fort :

$$\partial_t f^\varepsilon + \mathbf{v}\cdot\nabla_{\mathbf{x}} f^\varepsilon + \mathbf{E}^\varepsilon \cdot \nabla_{\mathbf{v}} + \frac{1}{\varepsilon}(\mathbf{v}\times\mathbf{B})\cdot\nabla_{\mathbf{v}} f^\varepsilon = 0\,,$$

le régime hydrodynamique [BGL91 ; Deg04 ; Gol05 ; Nis78 ; Bob18], basé sur l'équation

$$\partial_t f^\varepsilon + v\,\partial_x f^\varepsilon = \frac{1}{\varepsilon} C(f^\varepsilon)\,, \tag{1.4.18}$$

le régime de dérive-diffusion [PS00 ; EM00 ; Add+21 ; AT04 ; Bar+13 ; Bob95], basé sur l'équation

$$\partial_t f^\varepsilon + \frac{1}{\varepsilon} v\,\partial_x f^\varepsilon - \frac{1}{\varepsilon} E^\varepsilon\,\partial_v f^\varepsilon = \frac{1}{\varepsilon^2} C(f^\varepsilon)\,,$$

ou encore la limite d'un champ électrique dominant [Arn+01 ; BS01 ; NPS01] :

$$\partial_t f^\varepsilon + v\,\partial_x f^\varepsilon - \frac{1}{\varepsilon} E^\varepsilon\,\partial_v f^\varepsilon = \frac{1}{\varepsilon} C(f^\varepsilon)\,.$$

La dérivation de modèles réduits grâce à l'analyse asymptotique constitue une grande partie de ce travail de thèse.

Avant de détailler le contenu de nos contributions, discutons de la simulation numérique des modèles que nous avons présentés.

1.4.3 Schémas préservant une limite asymptotique.

Les modèles présentés dans la sous-section 1.4.2 sont des modèles singuliers, raides et caractérisés par un petit paramètre $\varepsilon \ll 1$. La simulation numérique de tels modèles peut être coûteuse en temps de calcul. En effet, certains phénomènes peuvent se produire à une échelle de temps $\mathcal{O}(\varepsilon) \ll 1$, ce qui nécessite de discrétiser la variable de temps finement. En l'absence de telle précaution, la solution approchée par le schéma peut diverger significativement de la solution réelle et le schéma numérique peut même être instable. Par exemple, une discrétisation explicite en temps du problème (1.4.10) présenterait une condition de stabilité contraignant le pas de temps Δt à dépendre de $\varepsilon \ll 1$. Même en choisissant un autre type de discrétisation en temps, il est possible que le schéma numérique ne soit pas uniformément consistant et stable par rapport à ε (voir Figure 2.10).

Dans le chapitre 2, on présentera un schéma numérique qui permet de calculer la solution de (1.4.10) sans contrainte sur le maillage en temps. Ainsi, il est possible de fixer Δt et de faire tendre ε vers 0, tout en maintenant une erreur numérique uniforme. Dans la littérature, un tel schéma est qualifié de "schéma préservant l'asymptotique" (*Asymptotic-Preserving*, ci-après dénoté AP). Pour une introduction complète aux "schémas préservant l'asymptotique", le lecteur intéressé pourra consulter [Jin22 ; Neg13].

Notre travail de doctorat a porté sur l'analyse mathématique et numérique de différents modèles liés à la physique des plasmas. Dans le chapitre 1, nous avons introduit les enjeux numériques et analytiques qui seront développés tout au long de ce manuscrit. On expose dans la prochaine section les contributions scientifiques réalisées au cours de cette thèse.

1.5 Résumé de chaque contribution de cette thèse

Le but de cette dernière section de l'introduction est de synthétiser les contributions apportées tout le long de cette thèse dans le domaine des plasmas de fusion thermonucléaire. On apporte également des perspectives de recherches, à la suite de chaque sous-section.

Le chapitre 2 porte sur l'analyse de la distribution d'électrons au cœur du tokamak, dans le régime adiabatique. Le chapitre 3 s'intéresse à la dérivation d'un modèle hybride cinétique-fluide pour les ions évoluant dans la couche extérieure d'un tokamak (*Scrape-off layer*, ci-après dénoté SOL). Nous faisons l'hypothèse de différents régimes de collisions dans les directions parallèles et perpendiculaires au champ magnétique. Enfin, le chapitre 4 s'intéresse à la modélisation des particules rapides dans un tokamak et en astrophysique. On étudie mathématiquement et numériquement des opérateurs de Fokker-Planck sans trou spectral.

1.5.1 Chapitre 2 : Électrons Boltzmanniens

Le contenu de ce chapitre est en anglais, et est tiré de la publication scientifique suivante :

- Etienne Lehman, Claudia Negulescu. "Vlasov-Poisson-Fokker-Planck equation in the adiabatic asymptotics", à paraître dans *Communications in Mathematical Sciences* (2024).

On s'intéresse dans ce chapitre à la modélisation d'électrons dans le cœur du plasma. Le point de départ de l'analyse de ce chapitre est l'équation de Vlasov-Poisson-Fokker-Planck dans le régime adiabatique :

$$(V)_\varepsilon \quad \begin{cases} \partial_t f^\varepsilon + \dfrac{1}{\varepsilon} v\, \partial_x f^\varepsilon - \dfrac{1}{\varepsilon} E^\varepsilon\, \partial_v f^\varepsilon = \dfrac{1}{\varepsilon} \partial_v \left[v\, f^\varepsilon + \partial_v f^\varepsilon \right], \\ -\partial_{xx} \phi^\varepsilon = n_i - n^\varepsilon, \qquad E^\varepsilon = -\partial_x \phi^\varepsilon, \end{cases} \tag{1.5.1}$$

où $\varepsilon > 0$ représente le petit rapport de masse électrons-ions : on renvoie à la section 1.4.1, dans laquelle on a adimensionné l'équation de Vlasov-Poisson-Fokker-Planck. Dans notre étude, les particules sont confinées dans un domaine periodique $\mathbb{T}_x$ à une dimension, correspondant à la direction parallèle au champ magnétique d'un tokamak. La variable de vitesse v appartient quant à elle à $\mathbb{R}_v$.

Jusqu'à présent, la communauté mathématique s'était surtout intéressée au cas où la densité ionique n_i ne dépend pas du temps. Le régime adiabatique correspond dans ce cas à l'étude en temps long de l'équation, par un simple changement de variable en temps. Cette limite en temps long fut étudiée par [BD95] qui montre la convergence de $f^\varepsilon(t,x,v)$ vers une distribution de Maxwell-Boltzmann (1.4.12) quand $t \to +\infty$. L'originalité théorique de notre travail vient de notre hypothèse : la densité d'ions $n_i(t,x)$ est imposée et dépendante du temps. Ici, la limite $\varepsilon \to 0$ ne correspond plus à la limite $t \to +\infty$. Il est alors intéressant de comprendre le comportement de la distribution d'électrons f^ε dans le régime $\varepsilon \ll 1$.

Contribution analytique : preuve rigoureuse de la convergence vers la limite adiabatique $\varepsilon \to 0$, avec exhibition de deux régimes temporels.

La première partie de notre étude est purement analytique. Pour introduire notre théorème principal, donnons quelques notations. Soit $\mathcal{M}(v) := \frac{1}{\sqrt{2\pi}} e^{-v^2/2}$ une distribution maxwellienne centrée normalisée, et définissons les mesures pondérées $\mathrm{d}\gamma(v) := \mathcal{M}^{-1}(v)\,\mathrm{d}v$ sur $\mathbb{R}_v$ ainsi que $\mathrm{d}\sigma(x,v) := \mathrm{d}x\,\mathrm{d}\gamma(v)$ sur $\mathbb{T}_x \times \mathbb{R}_v$. Nous dénoterons dans ce chapitre $L^2_\sigma(\mathbb{T}_x \times \mathbb{R}_v)$ l'espace L^2 associé à cette mesure $\mathrm{d}\sigma$. On a alors le théorème suivant.

Théorème 1.5.1. *[LN24b] **(Comportement asymptotique)** Soit $(f^\varepsilon, E^\varepsilon)$ une solution au sens des distributions de (1.5.1), avec la densité ionique imposée $n_i \in W^{1,\infty}((0,T); L^1(\mathbb{T}_x))$, vérifiant $\int_{\mathbb{T}_x} n_i(t,x)\,\mathrm{d}x \equiv \mathfrak{m}$. Notons $(f^\varepsilon_{in}, E^\varepsilon_{in})$ sa condition initiale. On dénote par (f^0, E^0) la solution du problème limite (1.4.12), et (f^0_{in}, E^0_{in}) la solution de ce problème pour $t = 0$. On suppose de plus que $f^\varepsilon \in C^0([0,T], L^2_\sigma(\mathbb{T}_x \times \mathbb{R}_v))$ et $E^\varepsilon = -\partial_x \phi^\varepsilon \in L^\infty((0,T)\times\mathbb{T}_x)$. Il existe alors une constante $\eta_0 > 0$ telle que, si f^ε_{in} est assez proche de f^0_{in}, au sens où*

$$\|f^\varepsilon_{in} - f^0_{in}\|^2_{L^2_\sigma(\mathbb{T}_x\times\mathbb{R}_v)} \leqslant \eta_0, \qquad \forall \varepsilon > 0, \tag{1.5.2}$$

il existe des constantes $C_0, C_1, C_2, \varepsilon_0 > 0$ telles que

$$\|f^\varepsilon(t) - f^0(t)\|^2_{L^2_\sigma(\mathbb{T}_x\times\mathbb{R}_v)} \leqslant C_0 \|f^\varepsilon_{in} - f^0_{in}\|^2_{L^2_\sigma(\mathbb{T}_x\times\mathbb{R}_v)} e^{-\frac{C_1 t}{\varepsilon}} + C_2 \varepsilon^2, \qquad \forall \varepsilon \leqslant \varepsilon_0, \forall t \in [0,T]. \tag{1.5.3}$$

La preuve de ce résultat s'appuie sur des méthodes d'hypocoercivité, directement adaptées de [Add+21] à notre cadre dépendant du temps. L'estimation (1.5.3) permet d'identifier deux régimes temporels : une couche limite de taille ε en temps et un régime permanent.

- Pour comprendre l'apparition de la couche limite initiale, remarquons que le problème limite (1.4.12) n'est pas un problème d'évolution temporelle. Pour cette raison, la solution du problème (1.4.12) dépend de t *via* $n_i(t,\cdot)$, et le temps est alors un paramètre. Ainsi, la solution f^0 de (1.4.12) a une condition initiale imposée qui dépend de $n_i(t=0,\cdot)$. La condition initiale f^ε_{in} ne doit pas nécessairement être bien préparée. On observe donc un phénomène de couche limite où l'écart entre les deux conditions initiales disparaît. Cela correspond au premier terme exponentiellement décroissant dans (1.5.3).
- Une fois cette couche initiale dépassée, une situation de régime permanent se produit. Dans ce régime, la solution de (1.5.1) reste à distance d'ordre ε de la solution du problème limite (1.4.12). Dans la preuve du théorème 1.5.1, donnée au chapitre 2, il est démontré que la constante C_2 dans (1.5.3) ne dépend que de la dérivée en temps de f^0 et disparaît donc si on prend n_i indépendant du temps.

Contributions numériques : calcul du problème limite (1.4.12) et schéma AP discrétisant le problème cinétique (1.5.1) avec un maillage indépendant de ε.

La deuxième partie du chapitre 2 est consacrée à une étude numérique du problème *via* une méthode spectrale de Hermite-Fourier. Les fonctions de Hermite en vitesse sont

introduites en (1.3.18) et diagonalisent l'opérateur linéaire de Fokker-Planck. Il s'agit donc d'un choix particulièrement adapté à notre problème. Nos contributions numériques peuvent être synthétisées en plusieurs points :

- On analyse numériquement dans un premier temps les taux de convergences donnés par le théorème 1.5.1 et vérifions nos résultats théoriques. En particulier, on vérifie la taille de la couche limite en temps.
- On présente une méthode simple et efficace permettant une simulation numérique de la solution du problème limite (1.4.12), c'est à dire de l'équation elliptique et non-linéaire

$$-\partial_{xx}\phi^* + \mathfrak{m}\frac{e^{\phi^*(t,x)}}{\displaystyle\int_{\mathbb{T}_x} e^{\phi^*(t,y)}\,\mathrm{d}y} = n_i(t,x), \qquad \forall x \in \mathbb{T}_x\,.$$

  La méthode itérative naïve de point fixe

$$-\partial_{xx}\phi^{j+1}(t,x) + \mathfrak{m}\,\frac{e^{\phi^j}(t,x)}{\displaystyle\int_{\mathbb{T}_x} e^{\phi^j}(t,y)\,\mathrm{d}y} = n_i(t,x), \qquad \forall j \geqslant 0,$$

  ne converge pas, et on propose alors le schéma semi-implicite suivant :

$$-\partial_{xx}\phi^{j+1} + n^j\phi^{j+1} = n_i - n^j(1-\phi^j), \qquad \text{avec} \quad n^j = \mathfrak{m}\,\frac{e^{\phi^j}}{\int_{\mathbb{T}_x} e^{\phi^j(t,y)}\,\mathrm{d}y}. \tag{1.5.4}$$

  Notre méthode émerge de la procédure semi-implicite et non-linéaire suivante :

$$-\partial_{xx}\phi^{j+1}(t,x) + \mathfrak{m}\,\frac{e^{\phi^{j+1}}(t,x)}{\int_{\mathbb{T}_x} e^{\phi^j}(t,y)\,\mathrm{d}y} = n_i(t,x), \quad \forall j \geqslant 0,$$

  pour laquelle on a linéarisé le terme exponentiel implicite. En effet, quand $\phi^{j+1} - \phi^j \ll 1$, on a

$$e^{\phi^{j+1}} = e^{\phi^j}\, e^{\phi^{j+1}-\phi^j} \simeq e^{\phi^j}\left(1 + \phi^{j+1} - \phi^j\right).$$

  On trouve numériquement que cette méthode est d'ordre 2 (voir Figure 2.1).
- On introduit enfin en détail un schéma numérique préservant l'asymptotique $\varepsilon \to 0$. Ce schéma AP décompose la solution de (1.5.1) en la somme du problème limite f^0, solution de (1.4.12), avec la fluctuation $f^\varepsilon - f^0$. La distribution f^0 est calculée à l'aide de la procédure de point fixe (1.5.4), tandis que la fluctuation $f^\varepsilon - f^0$ est calculée à partir d'une méthode de Hermite-Fourier discrétisée en temps à l'aide d'un schéma de Newton implicite. Ce schéma AP permet de calculer la solution de (1.5.1) dans la limite $\varepsilon \ll 1$ à un coût numérique très réduit. Dans la section 2.6, on montre numériquement que notre schéma est AP. On analyse de plus l'erreur et le temps de calcul associé à cette méthode en la comparant à une méthode naïve.

Perspectives de ce travail. Ce travail peut être poursuivi dans plusieurs directions. Tout d'abord, il peut être intéressant d'étudier une nouvelle fois rigoureusement la limite adiabatique $\varepsilon \to 0$, mais cette fois en considérant l'équation complète sur les électrons

$$\varepsilon\, \partial_t f_e + \mathbf{v} \cdot \nabla_{\mathbf{x}} f_e - \left(\mathbf{E} + \frac{1}{\varepsilon} \mathbf{v} \times \mathbf{B} \right) \cdot \nabla_{\mathbf{v}} f_e = \nu_e\, \mathcal{Q}_{\mathrm{FPlin}}(f_e)\,, \tag{1.5.5}$$

de dimensionnalité $3D_{\mathbf{x}}3D_{\mathbf{v}}$, ainsi qu'un champ magnétique fort. On pourrait pour cela adapter les méthodes développées dans le chapitre 2, en conjonction avec celles de [HM19], qui applique des méthodes d'hypocoercivité au cadre du transport de particules dans un champ magnétique. La difficulté serait alors d'adapter [HM19] tout en gardant le champ électrique non-linéaire, calculé par l'équation de Poisson. Il serait également intéressant de montrer le résultat pour le modèle bi-espèces de [FN22], qui présente de nombreuses lois de conservations.

On a également proposé dans ce travail une méthode numérique AP pour la résolution de l'équation de Vlasov-Poisson-Fokker-Planck, tout en préservant l'asymptotique des électrons adiabatiques $\varepsilon \to 0$. Il serait intéressant de faire de même pour le modèle bi-espèce de [FN22]. Une discrétisation minutieuse de ce modèle doit être menée au niveau numérique, afin de préserver les propriétés de conservations physiques de ce modèle, même dans l'asymptotique $\varepsilon \to 0$.

1.5.2 Chapitre 3 : Modèle hybride cinétique-fluide pour les ions dans la couche extérieure d'un tokamak

Le contenu de ce chapitre est en anglais, et est tiré de la publication scientifique suivante :

- Etienne Lehman, Claudia Negulescu, Stefan Possanner. "Asymptotic study of an anisotropic Fokker-Planck collision operator in a strong magnetic field", publié dans *Kinetic and Related Models* [4] (2024).

Dans cette partie, nous nous intéressons aux ions se déplaçant dans la couche extérieure d'un tokamak (*Scrape-off layer* ou SOL).

Au sein de la SOL d'un tokamak, les ions se déplacent très rapidement dans la direction parallèle au champ magnétique, de sorte que leur dynamique est souvent modélisée par une équation cinétique. Dans la littérature [CHM16 ; Mou+13 ; MHD10], la distribution d'espèces est parfois donnée par la forme suivante :

$$f_{\mathrm{s}}(t, x, v_{\parallel}, \mathbf{v}_{\perp}) = g_{\mathrm{s}}(t, x, v_{\parallel}) \frac{m_{\mathrm{s}}}{2\pi k_{\mathrm{B}} T_{\mathrm{s},\perp}(t, x)} \exp\left(-\frac{m_{\mathrm{s}} |\mathbf{v}_{\perp}|^2}{2 k_{\mathrm{B}} T_{\mathrm{s},\perp}(t, x)} \right), \tag{1.5.6}$$

où les indices $\perp$ et $\parallel$ indiquent respectivement les vitesses dans les directions perpendiculaires et parallèles au champ magnétique, supposé ici droit et pointant dans une direction fixe $\mathbf{e}_z$. La

4. doi : 10.3934/krm.2024004

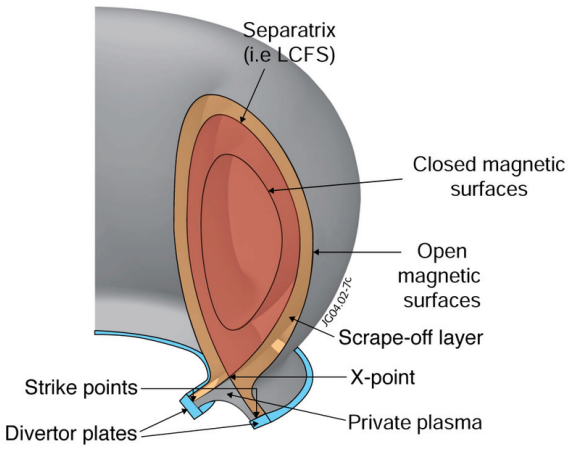

FIGURE 1.3 – Différentes zones dans un tokamak.

constante de Boltzmann est dénotée k_B, tandis que m_s est la masse de l'espèce s. Dans [CHM16], les auteurs proposent un système couplé d'équations aux dérivées partielles pour l'évolution de g_s et de la température perpendiculaire $T_{s,\perp}$.

Le premier objectif de notre travail était d'obtenir la forme (1.5.6) depuis une description complètement cinétique des ions par le biais d'une limite asymptotique.

Contribution mathématique et physique : dérivation du modèle (1.5.6) depuis l'échelle cinétique.

Dans [CHM16 ; Mou+13 ; MHD10], la dynamique est lente dans le plan perpendiculaire au champ magnétique, et la fonction de distribution est donc supposée thermalisée dans cette direction. En revanche, dans la direction parallèle au champ magnétique, la fonction de distribution n'a pas nécessairement atteint un équilibre thermodynamique car elle est soumise à beaucoup moins de collisions. En effet, le libre parcours moyen des particules dépasse la longueur totale de la SOL d'un tokamak. Dans notre modélisation, nous postulerons donc une anisotropie dans les processus de collisions : un opérateur de collision sera supposé dominant dans la dimension perpendiculaire au champ magnétique. Notre point de départ est donné par l'équation suivante :

$$\partial_t f + \mathbf{v} \cdot \nabla_{\mathbf{v}} f + \frac{q}{m}(\mathbf{E} + \mathbf{v} \times \mathbf{B}) \cdot \nabla_{\mathbf{v}} f = \nu_\perp Q_\perp(f) + \nu_r Q_r \,, \tag{1.5.7}$$

où on postule l'existence de deux processus collisionnels différents, modélisés par des opérateurs de type Fokker-Planck. Le premier opérateur, donné par $Q_\perp$, n'agit que dans la direction perpendiculaire au champ magnétique. Le second opérateur, modélisé par Q_r, est un processus thermalisant les ions de manière isotrope en temps très long. L'expression exacte des opérateurs Q_r, $Q_\perp$ est donnée dans (3.1.14). Les opérateurs ont été choisis afin de préserver des propriétés de conservation et de dissipation réalistes, telles que :

— La préservation de la masse, de la quantité de mouvement, et de l'énergie :

$$\int_{\mathbb{R}^3_v} \begin{pmatrix} 1 \\ \mathbf{v} \\ \frac{|\mathbf{v}|^2}{2} \end{pmatrix} Q_{\mathrm{r}}(f)\,\mathrm{d}\mathbf{v} = 0\,; \tag{1.5.8}$$

— La thermalisation entre les directions parallèles et perpendiculaires :

$$m \int_{\mathbb{R}^3_v} \frac{|\mathbf{v}_\perp|^2}{2} Q_{\mathrm{r}}(f)\,\mathrm{d}\mathbf{v} = \eta\, n\, k_B\,(T - T_\perp) = \frac{\eta}{3}\, n\, k_B\,(T_\parallel - T_\perp)\,, \tag{1.5.9}$$

où $T = (2\,T_\perp + T_\parallel)/3$, $\eta > 0$ est un coefficient donné, et

$$n\,u_\parallel(t,\mathbf{x}) := \int_{\mathbb{R}^3_v} v_\parallel\, f\ \mathrm{d}\mathbf{v}\,, \qquad \frac{1}{2}\, n\, k_{\mathrm{B}}\, T_\parallel(t,\mathbf{x}) := \frac{m}{2} \int_{\mathbb{R}^3_v} |v_\parallel - u_\parallel|^2\, f\,\mathrm{d}\mathbf{v}\,. \tag{1.5.10}$$

— La conservation de l'énergie perpendiculaire sur des échelles de temps très courts, de l'ordre de $\mathcal{O}(\nu_\perp^{-1})$:

$$\int_{\mathbb{R}^3_v} \frac{|\mathbf{v}_\perp|^2}{2}\, Q_\perp(f)\,\mathrm{d}\mathbf{v} = 0\,, \tag{1.5.11}$$

qui est une propriété naturelle dans le cadre d'un champ magnétique très fort [ONe83].

On procède alors à un adimensionnement de l'équation (1.5.7) en supposant $\nu_{\mathrm{r}} \ll \nu_\perp$ ainsi qu'un champ magnétique très fort. Une telle procédure (conduite intégralement dans l'annexe 3.A) donne lieu à l'équation adimensionnée suivante :

$$\partial_t f^\varepsilon + \mathbf{v}\cdot\nabla_{\mathbf{x}} f^\varepsilon + \mathbf{E}\cdot\nabla_{\mathbf{v}} f^\varepsilon + \frac{1}{\varepsilon}\,\mathbf{v}\times\mathbf{B}\cdot\nabla_{\mathbf{v}} f^\varepsilon = \frac{\nu_\perp}{\varepsilon}\, Q_\perp(f^\varepsilon) + \nu_{\mathrm{r}}\, Q_{\mathrm{r}}(f^\varepsilon)\,. \tag{1.5.12}$$

Dans la limite $\varepsilon \to 0$, on retrouve le modèle postulé par [CHM16]. Dénotons

$$\langle\theta\rangle_\parallel(t,\mathbf{x},\mathbf{v}_\perp) := \int_{\mathbb{R}_v} \theta(t,\mathbf{x},\mathbf{v}_\perp,v_\parallel)\,\mathrm{d}v_\parallel\,.$$

On montre alors le théorème suivant :

Théorème 1.5.2. *[LNP24] (**Modèle limite : ions dans le régime de collisions anisotropes.**) Dans la limite où $\varepsilon \to 0$, la solution f^ε de (1.5.12) converge (formellement) vers une fonction f^0 de la forme factorisée suivante :*

$$f^0(t,\,\mathbf{x},\,\mathbf{v}) = g^0(t,\mathbf{x},v_\parallel)\,\mathcal{M}_\perp^{T_\perp^0(t,\mathbf{x})}(\mathbf{v}_\perp)\,, \tag{1.5.13a}$$

où la distribution maxwellienne perpendiculaire $\mathcal{M}_\perp^{T_\perp^0(t,\mathbf{x})}$ *est donnée par*

$$\mathcal{M}_\perp^{T_\perp^0(t,\mathbf{x})}(\mathbf{v}_\perp) := \frac{1}{2\,\pi\,T_\perp^0(t,\mathbf{x})}\, e^{-\frac{|\mathbf{v}_\perp|^2}{2\,T_\perp^0(t,\mathbf{x})}}. \tag{1.5.13b}$$

La "distribution cinétique réduite g^0*" et la température perpendiculaire* $T_\perp^0$ *satisfont le système couplé d'équations suivant :*

$$\begin{cases} \partial_t g^0 + v_\parallel\,\partial_z g^0 + E_\parallel\,\partial_{v_\parallel} g^0 = \nu_{\mathrm{r}}\,\partial_{v_\parallel}\left[(v_\parallel - u_\parallel^0)\,g^0 + T^0\,\partial_{v_\parallel} g^0\right], \\ \partial_t(n^0\,T_\perp^0) + \partial_z(n^0\,T_\perp^0\,u_\parallel^0) = \dfrac{2}{3}\,\nu_{\mathrm{r}}\,n^0\,\left(T_\parallel^0 - T_\perp^0\right), \end{cases} \tag{1.5.13c}$$

avec $T^0 = (T_\parallel^0 + 2\,T_\perp^0)/3$ *et*

$$n^0 = \langle g^0\rangle_\parallel, \qquad n^0\,u_\parallel^0 = \left\langle v_\parallel\,g^0\right\rangle_\parallel, \qquad \frac{1}{2}n^0\,T_\parallel^0 = \frac{1}{2}\left\langle (v_\parallel - u_\parallel^0)^2\,g^0\right\rangle_\parallel. \tag{1.5.14}$$

Ce système (1.5.13) *est complété par une condition initiale bien préparée*

$$f_{\mathrm{in}}^0(\mathbf{x},\,\mathbf{v}) = g_{\mathrm{in}}^0(\mathbf{x},v_\parallel)\,\mathcal{M}_\perp^{T_{\perp,\mathrm{in}}^0(\mathbf{x})}(\mathbf{v}_\perp), \tag{1.5.15}$$

où $f_{\mathrm{in}}^0 := \lim_{\varepsilon\to 0} f_{\mathrm{in}}^\varepsilon$.

Dans la seconde partie de notre analyse, on dérive des termes correcteurs au problème limite.

Contribution physique et mathématique : Calcul de la correction à l'ordre 1 du modèle (1.5.12).

La seconde partie de cette étude s'intéresse à la dérivation d'un modèle plus précis que le modèle limite (1.5.13), tout en étant plus simple à simuler numériquement que le modèle cinétique (1.5.12). Ce modèle plus précis est caractérisé par une fonction $\widehat{f^\varepsilon}$ proche de la fonction de distribution des ions f^ε, solution de (1.5.12), dans le sens où, quand $\varepsilon \to 0$:

$$f^\varepsilon = \widehat{f^\varepsilon} + \mathcal{O}(\varepsilon^2). \tag{1.5.16}$$

Afin de dériver le système d'équations associé à $\widehat{f^\varepsilon}$, on développe

$$f^\varepsilon = f^0 + \varepsilon\,f^1 + \mathcal{O}(\varepsilon^2), \tag{1.5.17}$$

où f^0 est donné par le modèle limite. Un tel développement est appelé "développement de Hilbert." Cet *Ansatz* engendre une hiérarchie d'équations sur les coefficients f^0, f^1, ... :

$$\mathcal{O}(\varepsilon^{-1}) : \ \mathbb{A}(f^0) = 0, \tag{1.5.18a}$$

$$\mathcal{O}(1) : \ \partial_t f^0 + \mathbf{v}\cdot\nabla_{\mathbf{x}} f^0 + \mathbf{E}\cdot\nabla_{\mathbf{v}} f^0 + \mathbb{A}_{f^0}^{\mathrm{lin}}(f^1) = \nu_{\mathrm{r}}\,Q_{\mathrm{r}}(f^0), \tag{1.5.18b}$$

$$\mathcal{O}(\varepsilon) : \ \partial_t f^1 + \mathbf{v}\cdot\nabla_{\mathbf{x}} f^1 + \mathbf{E}\cdot\nabla_{\mathbf{v}} f^1 + \mathbb{A}_{f^0}^{\mathrm{lin}}(f^2) - \nu_\perp\,\delta^2 Q_\perp(f^1) = \nu_{\mathrm{r}}\,\delta Q_{\mathrm{r}}[f^0](f^1). \tag{1.5.18c}$$

Cette hiérarchie implique l'opérateur dominant $\mathbb{A}$ dans (1.5.12) ainsi que sa linéarisation $\mathbb{A}^{\mathrm{lin}}_{f^0}$ autour de f^0. Une étude rigoureuse de $\mathbb{A}^{\mathrm{lin}}_{f^0}$ nous permet de caractériser f^1 par l'examen des équations (1.5.18b) et (1.5.18c). La connaissance de f^0 et de f^1 permet de calculer une distribution $\widehat{f}^\varepsilon$ qui approxime f^ε avec une précision de l'ordre de $\mathcal{O}(\varepsilon^2)$. Le théorème 1.5.3 donne le système d'équations qui permet de calculer $\widehat{f}^\varepsilon$:

Théorème 1.5.3. *[LNP24] (**Correction à l'ordre 1 : ions dans le régime de collisions anisotropes.**) Soit f^ε la solution de l'équation (1.5.12). On peut alors approximer la fonction de distribution f^ε par $\widehat{f}^\varepsilon$ vérifiant*

$$f^\varepsilon = \widehat{f}^\varepsilon + \mathcal{O}(\varepsilon^2)\,,$$

quand $\varepsilon \to 0$. La distribution approchée $\widehat{f}^\varepsilon$ a la forme suivante (pour des raisons de visibilité, l'exposant ε a été omis de la factorisation) :

$$\widehat{f}^\varepsilon(t,\mathbf{x},\mathbf{v}) = \widehat{g}(t,\,\mathbf{x},\,v_\parallel)\,\mathcal{M}_\perp^{\widehat{T}_\perp(t,\mathbf{x})}(\mathbf{v}_\perp)\left(1+\,\varepsilon\,\Lambda_{\widehat{g},\widehat{T}_\perp}\right). \tag{1.5.19a}$$

La "distribution cinétique réduite" $\widehat{g}$ et la température perpendiculaire $\widehat{T}_\perp$ satisfont le système couplé suivant :

$$\begin{cases} \partial_t \widehat{g} + v_\parallel\,\partial_z \widehat{g} + E_\parallel\,\partial_{v_\parallel}\widehat{g} + \varepsilon\,\nabla_{\mathbf{x}_\perp}\cdot(\widehat{\mathbf{u}}^{\mathrm{K}}_{\mathrm{drift}}\,\widehat{g}) = \nu_{\mathrm{r}}\,\partial_{v_\parallel}\left[(v_\parallel-\widehat{u}_\parallel)\,\widehat{g} + \widehat{T}\,\partial_{v_\parallel}\widehat{g}\right] \\ \qquad\qquad + \varepsilon\,\nabla_{\mathbf{x}_\perp}\cdot\left(\widehat{n}\,\widehat{T}_\perp\,\mathbb{D}_2\nabla_{\mathbf{x}_\perp}\dfrac{\widehat{g}}{\widehat{n}}\right), \\ \partial_t(\widehat{n}\,\widehat{T}_\perp) + \partial_z(\widehat{n}\,\widehat{T}_\perp\,\widehat{u}_\parallel) + \varepsilon\,\nabla_{\mathbf{x}_\perp}\cdot(2\,\widehat{n}\,\widehat{T}_\perp\,\widehat{\mathbf{u}}_{\mathrm{drift}}) + \varepsilon\,\nabla_{\mathbf{x}}\cdot\mathbf{q} = \varepsilon\,\widehat{n}\,\widehat{\mathbf{u}}_{\mathrm{drift}}\cdot\mathbf{E}_\perp \\ \qquad\qquad + \dfrac{2}{3}\,\nu_{\mathrm{r}}\,\widehat{n}\,(\widehat{T}_\parallel - \widehat{T}_\perp). \end{cases} \tag{1.5.19b}$$

Ici, les vitesses de dérive sont données par :

$$\widehat{\mathbf{u}}^{\mathrm{K}}_{\mathrm{drift}} = \frac{\mathbf{E}_\perp\times\mathbf{B}}{|B|^2} - \frac{\nabla_{\mathbf{x}_\perp}(\widehat{g}\,\widehat{T}_\perp)\times\mathbf{B}}{\widehat{g}\,|B|^2}, \qquad \widehat{\mathbf{u}}_{\mathrm{drift}} = \frac{\mathbf{E}_\perp\times\mathbf{B}}{|B|^2} - \frac{\nabla_{\mathbf{x}_\perp}(\widehat{n}\,\widehat{T}_\perp)\times\mathbf{B}}{\widehat{n}\,|B|^2}. \tag{1.5.19c}$$

La température $\widehat{T}$ est calculée via *$\widehat{T} = (\widehat{T}_\parallel + 2\,\widehat{T}_\perp)/3$, les quantités macroscopiques $(\widehat{n},\,\widehat{u}_\parallel,\,\widehat{T}_\parallel)$ sont définies par*

$$\widehat{n} = \langle\widehat{g}\rangle_\parallel, \qquad \widehat{n}\,\widehat{u}_\parallel = \langle v_\parallel\widehat{g}\rangle_\parallel, \qquad \frac{1}{2}\widehat{n}\,\widehat{T}_\parallel = \frac{1}{2}\left\langle (v_\parallel-\widehat{u}_\parallel)^2\,\widehat{g}\right\rangle_\parallel, \tag{1.5.19d}$$

et le flux de chaleur est donné comme suit :

$$\mathbf{q} = \begin{pmatrix}\mathbf{q}_\perp\\ q_\times\end{pmatrix}, \qquad \mathbf{q}_\perp = -2\,\widehat{n}\,\widehat{T}_\perp\,\mathbb{D}_1\,\nabla_{\mathbf{x}_\perp}\widehat{T}_\perp, \qquad q_\times = -\frac{1}{2\,\nu_\perp}\,\widehat{n}\,\widehat{T}_\parallel\,\partial_z\widehat{T}_\perp. \tag{1.5.19e}$$

La quantité $\Lambda_{\widehat{g},\widehat{T}_\perp}$, entièrement définie en termes de $\widehat{g}$, $\widehat{T}_\perp$, est donnée par la formule

$$\Lambda_{\widehat{g},\widehat{T}_\perp}(\mathbf{v}) := \frac{\widehat{\mathbf{u}}^{\mathrm{K}}_{\mathrm{drift}} \cdot \mathbf{v}_\perp}{\widehat{T}_\perp} - \left(\mathbb{D}_1 \frac{\nabla_{\mathbf{x}_\perp} \widehat{T}_\perp}{\widehat{T}_\perp} \right) \cdot \mathbf{v}_\perp \left[\frac{|\mathbf{v}_\perp|^2}{2\,\widehat{T}_\perp} - 2 \right] + \frac{\partial_z \widehat{T}_\perp}{\widehat{T}_\perp} \frac{\widehat{u}_\parallel - v_\parallel}{2} \left[\frac{|\mathbf{v}_\perp|^2}{2\,\widehat{T}_\perp} - 1 \right] - \left(\mathbb{D}_2 \frac{\nabla_{\mathbf{x}_\perp} (\widehat{g}/\widehat{n})}{(\widehat{g}/\widehat{n})} \right) \cdot \mathbf{v}_\perp, \tag{1.5.19f}$$

où les matrices de diffusion, positives, sont données par

$$\mathbb{D}_1 = \frac{1}{B^2 + 9\,\nu_\perp^2} \begin{bmatrix} 3\,\nu_\perp & B \\ -B & 3\,\nu_\perp \end{bmatrix}, \qquad \mathbb{D}_2 = \frac{\nu_\perp}{B} \frac{1}{B^2 + \nu_\perp^2} \begin{bmatrix} B & -\nu_\perp \\ \nu_\perp & B \end{bmatrix}. \tag{1.5.19g}$$

Ce système (1.5.19b) *est complété par la condition initiale bien préparée de la forme*

$$f^\varepsilon_{\mathrm{in}}(\mathbf{x},\mathbf{v}) = g^\varepsilon_{\mathrm{in}}(\mathbf{x}, v_\parallel)\, \mathcal{M}_\perp^{T^\varepsilon_{\perp,\mathrm{in}}}(\mathbf{v}_\perp) \left(1 + \varepsilon\, \Lambda_{g^\varepsilon_{\mathrm{in}},\, T^\varepsilon_{\perp,\mathrm{in}}}\right). \tag{1.5.19h}$$

On revient en détail sur ce résultat et ses propriétés dans le chapitre 3. Soulignons que ce modèle est cinétique dans la direction parallèle au champ magnétique et fluide dans la direction perpendiculaire. L'espace des phases est de trois dimensions spatiales pour une dimension en vitesse. La dimensionnalité ($3\mathrm{D}_\mathbf{x}1\mathrm{D}_\mathbf{v}$) est alors réduite par rapport à d'autres modèles utilisés dans la littérature. Par exemple, les modèles gyrocinétiques ont un espace des phases de cinq dimensions.

Le lecteur intéressé pourra consulter [Deg04 ; MRS12] pour une introduction complète sur ces méthodes ainsi que sur les développements de Hilbert. Ajoutons qu'une version de ce modèle, réécrit en unités physiques est donnée en annexe 3.A du chapitre 3.

Perspectives de ce travail. Ce travail possède quelques limitations théoriques, qu'il pourrait être intéressant de dépasser. Par exemple, une perspective possible serait l'étude de l'équation de Vlasov-Fokker-Planck (1.5.12) dans le même régime, mais avec des géométries de champ magnétique différentes. On conjecture dans ce cas l'apparition de termes de dérives associés au gradient de $\mathbf{B}$ et à sa courbure.

En outre, ce travail a consisté en une étude formelle, de sorte qu'une démonstration rigoureuse du passage à la limite $\varepsilon \to 0$ reste à mener. Une étude analytique ou physique complète du modèle corrigé à l'ordre 1 (1.5.19) doit également être menée. La démonstration du caractère bien posé des systèmes (1.5.13) et (1.5.19) pourrait par exemple faire l'objet d'une direction de recherche future.

Une discrétisation de ce problème et son implémentation dans la bibliothèque Python STRUPHY sont en cours, afin de continuer les recherches sur ce modèle d'un point de vue numérique. Par exemple, la dimensionnalité (4D) de (1.5.19) est plus faible que dans les descriptions gyrocinétiques (5D), de sorte qu'on peut s'attendre à un gain de performance significatif.

1.5.3 Chapitre 4 : Modélisation des particules rapides : électrons en fuite et κ-distributions

Le contenu de ce chapitre est en anglais, et est tiré de la publication scientifique suivante :

- Etienne Lehman, Claudia Negulescu. "Fokker-Planck equation for energetic particles. The κ-distribution function", soumis pour publication.

Certains contextes physiques ne sont pas adaptés à la modélisation donnée par l'opérateur de Fokker-Planck (1.3.22). Dans la littérature physique, l'opérateur est souvent considéré avec un coefficient de diffusion $D(v)$ qui dépend de la variable de vitesse v. En d'autres termes, un opérateur plus général permettant de modéliser la distributions d'électrons s'écrit sous la forme

$$v\,\partial_v\left[\frac{2\,D(v)}{v_{th}^2}\left(v\,f_e+\frac{v_{th}^2}{2}\partial_v f_e\right)\right],\qquad v\in\mathbb{R}\,, \tag{1.5.20}$$

où v_{th} est la vitesse thermique des électrons, supposée donnée et constante. Cet opérateur modélise les collisions des électrons avec un plasma à l'équilibre thermodynamique. Dans la littérature mathématique, le coefficient de diffusion $D(v)$ est souvent supposé constant, ce qui correspond, à un changement de variable près, à l'opérateur de Fokker-Planck linéaire (1.3.22), et dont la dérivation est présentée en section 1.3. Dans la littérature [Bia+14; CN; WC15; HM03], il est parfois supposé $D(v)=\frac{G(v/v_{th}))}{v/v_{th}}$, où la fonction G est la fonction de Chandrasekar, donnée par :

$$G(x)=\frac{\phi(x)-x\phi'(x)}{2x^2}\,,\qquad \phi(x)=\frac{2}{\sqrt{\pi}}\int_0^x e^{-y^2}\,\mathrm{d}y\,. \tag{1.5.21}$$

Dans ce cas, la fonction $D(v)$ décroit comme une fonction de l'ordre de v^{-3} quand $v\to+\infty$ et l'opérateur de Fokker-Planck (1.5.20) relaxe tout de même la fonction de distribution vers un équilibre maxwellien.

Au sein d'un tokamak comme en astrophysique, il arrive que des électrons approchent des vitesses relativistes. Ces électrons doivent être modélisés à part pour plusieurs raisons.

- D'une part, ces électrons de très haute énergie sont source d'instabilité et peuvent perturber le confinement magnétique ou mettre en danger les structures présentes dans l'espace.
- D'autre part, ces particules rapides sont moins sujettes à des collisions avec l'ensemble des autres particules. On les appelle pour cela "électrons en fuite" (*runaway electrons*).

Pour modéliser les collisions des "électrons en fuite" avec le plasma, la littérature physique considère parfois l'opérateur

$$v\,\partial_v\left[\gamma(v)\left(v\,f_e+\left(\frac{v_{th}^2}{2}+D_{turb}(v)\right)\partial_v f_e\right)\right], \tag{1.5.22}$$

où γ est une fonction de l'ordre de v^{-3} quand $v \to +\infty$. Le coefficient $D_{turb}(v) := \frac{D_0}{v^2}$ avec $D_0 > 0$ est un terme ajouté empiriquement et modélise l'accélération turbulente du flux d'électrons. Dans ce contexte, la distribution d'équilibre de cet opérateur n'est plus une distribution maxwellienne mais une κ-distribution, donnée par

$$h_\kappa(v) = \frac{C_\kappa}{\left(1 + \frac{v^2}{\kappa\, v_{th}^2}\right)^\kappa}, \qquad \kappa = \frac{1}{2\, D_0}, \tag{1.5.23}$$

où C_κ est une constante de normalisation, et D_0 est donné par le choix de fonction $D_{turb}(v) = \frac{D_0}{v^2}$. Toutes ces classes d'opérateurs de Fokker-Planck linéaires peuvent être rassemblées sous la forme générale

$$\mathcal{Q}_{D,eq}(f) = \partial_v \left[D(v)\, f_{eq} \partial_v \left(\frac{f}{f_{eq}} \right) \right], \tag{1.5.24}$$

où $D(v)$ et f_{eq} sont respectivement le coefficient de diffusion et la distribution d'équilibre, qui doivent être choisis en fonction du modèle. On considère alors l'équation parabolique générale suivante

$$\begin{cases} \partial_t f = \mathcal{Q}_{D,eq}(f), \\ f(t=0) = f_{\text{in}}. \end{cases} \tag{1.5.25}$$

Dans le chapitre 4, on étudie quatre cas :

(I) Le cas $D(v) = 1$ et $f_{eq} = \mathcal{M}(v)$, où $\mathcal{M}(v) := \frac{1}{\sqrt{2\,\pi}} e^{-v^2/2}$ est une distribution maxwellienne. Ce cas correspond à l'opérateur de Fokker-Planck linéaire standard ;

(II) Le cas $D(v) = 1$ et $f_{eq} = f_\kappa$, où $f_\kappa := \alpha_\kappa \left(1 + \frac{v^2}{\kappa}\right)^{-\kappa}$ est une κ-distribution et α_κ est une constante de normalisation ;

(III) Le cas $D(v) = G(v)/v$ et $f_{eq} = \mathcal{M}$;

(IV) Le cas $D(v) = G(v)/v$ et $f_{eq} = f_\kappa$.

Contribution analytique : Taux de convergence algébrique vers l'équilibre dans les cas (III) et (IV).

Dans la première partie du chapitre 4, on rappelle les propriétés classiques de l'opérateur de Fokker-Planck linéaire (1.3.22) relaxant vers une distribution maxwellienne. Dans le cas (I), la distribution f, solution de (1.5.25), est relaxée vers son équilibre $f_\infty = \alpha\, \mathcal{M}(v)$, où $\alpha = \int_{\mathbb{R}_v} f_{\text{in}}\, \mathrm{d}v$, à une vitesse exponentielle :

$$\int_{\mathbb{R}_v} |f(t) - f_\infty|^2 \frac{1}{f_{eq}}\, \mathrm{d}v \leqslant e^{-2t} \int_{\mathbb{R}_v} |f_{\text{in}} - f_\infty|^2 \frac{1}{f_{eq}}\, \mathrm{d}v, \qquad \forall t \geqslant 0. \tag{1.5.26}$$

La preuve de cette estimation se fait à l'aide d'une inégalité de Poincaré-Wirtinger. De plus, l'opérateur de Fokker-Planck est diagonalisable dans l'espace $L^2(\mathrm{d}v\, f_{eq}^{-1}(v))$ par les fonctions

de Hermite, introduites en (1.3.18).

La situation dans les cas (II) à (IV) est profondément différente. On montre que la distribution f, solution de (1.5.25), est relaxée vers l'équilibre $f_\infty = \alpha\, f_\kappa(v)$, où $\alpha = \int_{\mathbb{R}_v} f_{\text{in}}\, \mathrm{d}v$, à une vitesse polynomiale. Ce fait était déjà connu dans le cas (II) [BDZ23]. On adapte dans le chapitre 4 leur méthode aux cas (III) et (IV), ce qui donne lieu au théorème suivant :

Théorème 1.5.4. *[LN24a] **(Cas (III) et (IV) : convergence vers l'équilibre.)** Soit f la solution du problème d'évolution (1.5.25), avec une condition initiale vérifiant $f_{in}/f_{eq} \in L^\infty(\mathbb{R}_v)$. Alors, si on note $f_\infty = \bar{f}\, f_{eq} := \int_{\mathbb{R}} f(v)\, \mathrm{d}v\, f_{eq} = \bar{f}_{\text{in}}\, f_{eq}$, on a :*

- *Dans le cas (III), pour tout $p > 0$:*

$$\int_{\mathbb{R}_v} |f(t) - f_\infty|^2 \leqslant \left[\left(\int_{\mathbb{R}_v} |f_{\text{in}} - f_\infty|^2 \frac{1}{f_{eq}}\, \mathrm{d}v \right)^{-3/p} + K_p^{III}\, \frac{6\, t}{p} \right]^{-p/3}, \quad \forall t \geqslant 0\,, \tag{1.5.27}$$

  où K_p^{III} est une constante explicite donnée dans (4.3.17).

- *Dans le cas (IV), si $\kappa > 1/2$, pour tout $0 < p < 2\,\kappa - 1$, on a l'estimation suivante :*

$$\int_{\mathbb{R}_v} |f(t) - f_\infty|^2 \frac{1}{f_{eq}}\, \mathrm{d}v \leqslant \left[\left(\int_{\mathbb{R}_v} |f_{\text{in}} - f_\infty|^2 \frac{1}{f_{eq}}\, \mathrm{d}v \right)^{-5/p} + K_{p,\kappa}^{IV} \frac{10\, t}{p} \right]^{-p/5}, \quad \forall t \geqslant 0\,, \tag{1.5.28}$$

  où $K_{p,\kappa}^{IV} > 0$ est une constante explicite donnée dans (4.3.21).

Remarquons que dans le cas (III), on peut choisir n'importe quel p dans (1.5.27), tandis que dans le cas (IV), p doit être majoré par $2\,\kappa - 1$ dans (1.5.28), où le paramètre κ intervient dans la distribution d'équilibre $f_{eq} = f_\kappa$.

La méthode utilisée pour trouver ce résultat s'appuie sur des inégalités de Hardy-Poincaré, qui sont des formes plus faibles des inégalités de Poincaré standard. Une inégalité de Poincaré dérive d'un trou spectral et permet de démontrer la convergence de la distribution vers son équilibre en un temps exponentiel. Dans la proposition 4.4.1, on montre qu'au contraire, dans les cas (II) à (IV), l'opérateur de Fokker-Planck $Q_{D,eq}$ a un spectre continu et ne présente pas de trou spectral. Pour le démontrer, on exploite des résultats connus de l'équation de Schrödinger.

Contribution numérique : Présentation d'un schéma préservant les basses énergies.

L'absence de trou spectral a une importance d'un point de vue numérique. Dans la seconde partie du chapitre 4, on discute l'absence de méthodes numériques permettant de rendre compte des taux de convergences algébriques donnés dans le théorème 1.5.4. Le début de cette réflexion est le théorème spectral pour des opérateurs différentiels auto-adjoints d'ordre 2, qui permet de représenter la solution f de (1.5.25) à l'aide de fonctions propres généralisées.

Pour l'écrire, posons

$$h(t,v) := f(t,v)/\, f_{eq}(v)\,,$$

et définissons

$$\Phi(v,\lambda) = \begin{pmatrix} \varphi_0(v,\lambda) \\ \varphi_1(v,\lambda) \end{pmatrix},$$

où les fonctions $\varphi_0,\ \varphi_1$ forment une base de solutions fondamentales du problème aux valeurs propres généralisé

$$-\frac{1}{f_{eq}}\mathcal{Q}_{D,eq}\,(f_{eq}\,\varphi) = \lambda\,\varphi\,, \qquad \forall\lambda\in\mathbb{R}\,. \tag{1.5.29}$$

On impose à $\varphi_0,\ \varphi_1$ des conditions appropriées en $v=0$. On définit également les coefficients spectraux suivants :

$$\mathfrak{A}(t,\lambda) := \begin{pmatrix} \mathfrak{A}_0(t,\lambda) \\ \mathfrak{A}_1(t,\lambda) \end{pmatrix}, \qquad \mathfrak{A}_l(t,\lambda) = e^{-\lambda\, t}\,\mathfrak{A}_{in,l}(\lambda)\,, \qquad \mathfrak{A}_{in,l}(\lambda) = \int_{\mathbb{R}} f_{in}(v)\,\varphi_l(v,\lambda)\,\mathrm{d}v\,. \tag{1.5.30}$$

La solution $f = f_{eq}\,h$ de (1.5.25) se décompose alors spectralement de la façon suivante [CL55] :

$$h(t,v) = \mathfrak{A}_0(t,0) + \int_0^{+\infty} \mathfrak{A}(t,\lambda)^T\,P(\lambda)\,\Phi(v,\lambda)\,\mathrm{d}\lambda\,, \tag{1.5.31}$$

où la matrice spectrale $P(\lambda)$ ne dépend que du paramètre λ. On introduit $P(\lambda)$ en détail dans la sous-sous-section 4.4.2.1, et l'omettons ici pour des raisons de clarté. Soulignons ici la ressemblance entre l'expansion (1.5.31) et une transformation de Fourier.

Discutons maintenant des méthodes numériques permettant de résoudre le problème d'évolution (1.5.25). De nombreux schémas numériques s'appuient sur la troncature du domaine en vitesse à partir de $v=\pm L$. Cela est notamment le cas des discrétisations s'appuyant sur des différences, des éléments ou des volumes finis. Dans chacun de ces cas, on introduit numériquement un trou spectral artificiel dont la taille dépend du paramètre de discrétisation. En d'autres termes, ces méthodes numériques n'approchent que

$$h^{\varepsilon}_{st}(t,v) = \mathfrak{A}_0(t,0) + \int_{\varepsilon}^{+\infty} \mathfrak{A}(t,\lambda)^T\,P(\lambda)\,\Phi(v,\lambda)\,\mathrm{d}\lambda\,, \tag{1.5.32}$$

où ε est un petit paramètre. La partie

$$\mathcal{C}_{\varepsilon}(t,v) := \int_0^{\varepsilon} \mathfrak{A}(t,\lambda)^T\,P(\lambda)\,\Phi(v,\lambda)\,\mathrm{d}\lambda\,, \qquad \forall(t,v)\in\mathbb{R}^+\times\mathbb{R} \tag{1.5.33}$$

est alors omise. Cette partie de l'intégrale est pourtant dominante dans la limite $t\to+\infty$. En particulier, elle est la raison du taux de convergence algébrique dans le théorème 1.5.4. On propose alors d'approximer finement l'intégrale $\mathcal{C}_{\varepsilon}$, qui est associé aux basses énergies. On utilise pour cela des techniques de perturbation. En effet, on écrit

$$\mathfrak{A}_{in}(\lambda) = \mathfrak{A}^0_{in} + \lambda\,\tilde{\mathfrak{A}}_{in,\lambda}\,, \qquad P(\lambda) = \lambda^{\alpha}P_0 + \lambda^{\alpha+\beta}\,\tilde{P}_{\lambda}\,, \tag{1.5.34}$$

et on suppose $\tilde{\mathfrak{A}}_{in,\lambda}$ et $\tilde{P}_\lambda$ bornées, $\alpha > -1$ et $\beta > 0$. Cela permet de faire l'approximation

$$C_\varepsilon(t,v) = \int_0^\varepsilon e^{-\lambda t}\, \mathfrak{A}_{in}^T(\lambda)\, P(\lambda)\, \Phi(v,\lambda)\, \mathrm{d}\lambda \simeq \tilde{C}_{\varepsilon,\alpha}(t,v) := \left(\int_0^\varepsilon e^{-\lambda t}\, \lambda^\alpha \ \mathrm{d}\lambda \right) (\mathfrak{A}_{in}^0)^T\, P_0\, \Phi(v,0)\,. \tag{1.5.35}$$

On revient sur les hypothèses (1.5.34) dans la section 4.5.2. On décrit notre méthode comme "préservant les basses énergies" (*Low-Energy Accurate Scheme*, ci-après dénoté LEAS). Il est possible d'introduire le correcteur $\tilde{C}_{\varepsilon,\alpha}$ dans toutes les méthodes de discrétisation standard. L'ajout de $\tilde{C}_{\varepsilon,\alpha}$ permet une approximation numérique précise de l'équation (1.5.25) dans le cas où l'opérateur $Q_{D,eq}$ ne présente pas de trou spectral, même dans des temps très longs. En particulier, introduire le correcteur $\tilde{C}_{\varepsilon,\alpha}$ permet de retrouver au niveau numérique le taux de convergence algébrique vers l'équilibre. Notre théorème 9 précise l'erreur commise dans l'approximation de C_ε (1.5.35).

Perspectives de ce travail. Ce travail peut naturellement être poursuivi dans plusieurs directions de recherche. Tout d'abord, il reste à mettre en œuvre le correcteur $\tilde{C}_{\varepsilon,\alpha}$ dans des contextes appliqués de la physique des plasmas. Pour cela, le point clé est de déterminer, numériquement ou mathématiquement, la forme asymptotique de la matrice spectrale $P(\lambda)$. Cette matrice dépend de l'opérateur de Fokker-Planck considéré, et on conjecture que la forme asymptotique (1.5.34) est adaptée aux cas (II) et (IV). La forme (1.5.34) correspond également à beaucoup d'équations de Fokker-Planck et de Schrödinger intervenant dans des domaines variés [Miy08]. Toutefois, dans le cas (III), la littérature [Yaf82 ; WC15] nous fait conjecturer que la matrice $P(\lambda)$ a une autre forme que (1.5.34) quand $\lambda \to 0+$. Connaître l'asymptotique exacte de $P(\lambda)$ permettrait de dériver un correcteur adapté au cas (III). En raison de la convergence vers 0 très rapide de $P(\lambda)$, quand $\lambda \to 0+$ [WC15], il est cependant attendu que l'implémentation du correcteur $\tilde{C}_{\varepsilon,\alpha}$ donne lieu à des bénéfices moins importants.

Il reste de plus à évaluer les effets concrets de ce correcteur dans des simulations appliquées de la physique des plasmas. On pourra implémenter le schéma LEAS dans le cadre homogène en espace du chapitre 4, ou encore dans le cadre d'une simulation inhomogène en espace. Pour cela, une méthode de *splitting* entre le transport et les collisions semble appropriée.

CHAPTER 2

VLASOV-POISSON-FOKKER-PLANCK EQUATION IN THE ADIABATIC ASYMPTOTICS

Le contenu de ce chapitre est en anglais, et est tiré de la publication scientifique suivante :

- Etienne Lehman, Claudia Negulescu. "Vlasov-Poisson-Fokker-Planck equation in the adiabatic asymptotics", à paraître dans *Communications in Mathematical Sciences* (2024).

Abstract: The main concern of this article is the study of a nonlinear Vlasov-Poisson-Fokker-Planck equation describing the electron dynamics in a thermonuclear fusion plasma, in the regime of a small electron-to-ion mass ratio ($\varepsilon \ll 1$). The first part of this work focuses on the rigorous $\varepsilon \to 0$ asymptotic study, based on hypocoercive techniques, permitting to understand the electron transition from the kinetic level to the macroscopic, adiabatic level. The second part introduces a Hermite-Fourier spectral method enabling to treat without too much numerical effort the above mentioned electron transition. This scheme has in particular the nice property of being *Asymptotic Preserving* in the sense that ε-independent meshes can be chosen, permitting a considerable gain in simulation time without degrading the accuracy. Some numerical tests are finally performed validating on one hand the scheme and underscoring on the other hand the mathematical results.

Contents

2.1 Introduction/Motivation

The concern of the present work is the theoretical as well as numerical study of the $\varepsilon \to 0$ asymptotic limit of the following coupled, nonlinear $1D_x\,1D_v$ Vlasov-Poisson-Fokker-Planck model

$$(V)_\varepsilon \quad \begin{cases} \partial_t f^\varepsilon + \dfrac{1}{\varepsilon}\, v\, \partial_x f^\varepsilon - \dfrac{1}{\varepsilon}\, E^\varepsilon\, \partial_v f^\varepsilon = \dfrac{1}{\varepsilon}\partial_v \left[v\, f^\varepsilon + \partial_v f^\varepsilon \right] , \\ -\partial_{xx}\phi^\varepsilon = n_i - n^\varepsilon, \qquad E^\varepsilon = -\partial_x \phi^\varepsilon , \end{cases} \tag{2.1.1}$$

associated with an initial condition $f^\varepsilon(t = 0, \cdot, \cdot) = f^\varepsilon_{in}$ and evolving on the phase-space $(x, v) \in \mathbb{T}_x \times \mathbb{R}_v$ with $\mathbb{T}_x$ a periodic domain. System (2.1.1) describes the time evolution of the electron distribution function $f^\varepsilon(t, x, v)$ in a thermonuclear fusion plasma. The electron density n^ε is defined as $n^\varepsilon(t, x) := \int_{\mathbb{R}_v} f^\varepsilon\, dv$ and the ions are assumed to form a given background interacting with the electrons only via the self-consistent electric field E^ε. We shall also assume the conservation of the particle number or the so-called mass constraint $\int_{\mathbb{T}_x} n^\varepsilon(t, x)\, \mathrm{d}x = \int_{\mathbb{T}_x} n_i(t, x)\, \mathrm{d}x = \mathfrak{m}$. The given ion density $n_i(t, x)$ is considered time-dependent and sufficiently smooth, *typically* $n_i \in W^{1,\infty}((0, T); L^1(\mathbb{T}_x))$. The small parameter $\varepsilon \in (0, 1)$ is related to the small electron-to-ion mass ratio and the asymptotic regime $\varepsilon \ll 1$ corresponds to a situation where the electron dynamics is very fast as compared to the ion motion, which fixes the reference time-scale in current simulations [CVB00; CP01; Gar+01; Kwo08]. In particular, to avoid the cumbersome resolution of an electron kinetic equation, present codes describe the electron dynamics through the so-called *electron Boltzmann relation*

$$n(t, x) = c(t)\, e^{\phi(t,x)}, \qquad \forall (t, x) \in \mathbb{R}_+ \times \mathbb{T}_x , \tag{2.1.2}$$

with $c(t)$ defined by the mass constraint. This relation (2.1.2) says that in the regime of a small mass ratio $\varepsilon \ll 1$, the electrons tend towards a thermodynamic equilibrium relating directly the electron equilibrium density to the electric potential. The validity of this adiabatic electron model is however rather controversial. Indeed, this model seems to break down in some situations, as for example near the edge of the tokamak [Dom+12]. Unusual electron temperature enhancement are observed when using this relation to describe the electron dynamics rather than a fully kinetic model. It is hence of first importance to understand the asymptotic passage from the kinetic (mesoscopic) model (2.1.1) towards the adiabatic (macroscopic) one (2.1.2) and to propose some corrections. For more details about the scaling of the electron kinetic model (2.1.1) we refer the interested reader to the previous papers [FN22; Neg18], where the physical context is explained in a more exhaustive way.

The asymptotic limit $\varepsilon \to 0$ of (2.1.1) is a singular limit, thus the theoretical as well as numerical investigations are rather complex. Different scalings are usually studied in literature, for example the hydrodynamic scaling, studied for instance in [BGL91; Deg04; Gol05; Nis78], which is based on the equation

$$\partial_t f^\varepsilon + v\, \partial_x f^\varepsilon = \frac{1}{\varepsilon} \mathcal{C}(f^\varepsilon),$$

where C is some collision operator. One encounters often also the drift-diffusive regime [PS00; EM00; Add+21; AT04], based on the following scaling

$$\partial_t f^\varepsilon + \frac{1}{\varepsilon} v\, \partial_x f^\varepsilon - \frac{1}{\varepsilon} E^\varepsilon\, \partial_v f^\varepsilon = \frac{1}{\varepsilon^2} C(f^\varepsilon)\,.$$

Our present scaling (2.1.1) is a different one, the main particularity coming from the fact that the collision (diffusive) operator acts at the same order as the transport (mixing) operator, leading to a more delicate struggle between these two very different operators.

In this paper, we shall firstly focus on a rigorous obtention of the electron Boltzmann relation (2.1.2) starting from the fully kinetic model (2.1.1) and performing the adiabatic asymptotic limit $\varepsilon \to 0$. Our rigorous treatment uses the tools of *hypocoercivity theory*. More precisely, we decide to follow the so-called *"Auxiliary operator method"* [DMS15; Add+21; Hér17; Hér07] build upon a weighted L^2-setting. Usually, hypocoercivity is a tool useful in the study of the long time asymptotics $t \to \infty$, but we adapt it to our needs, especially for time-dependent ion-densities n_i, in which case the limit $\varepsilon \to 0$ of (2.1.1) is not equivalent to the long time asymptotics. We underline that other approaches also exist, set down for instance in a H^1-framework [Vil09], in a H^{-1}-setting [Bri23; Alb+19] or in a general H^s-setting [HJ12]. For some introductory material on hypocoercivity theory, one may read [Vil09; Hér07].

The second aim of our paper is the design of an efficient, in particular so-called *Asymptotic-Preserving* numerical method, able to cope with the above mentioned electron adiabatic asymptotic without too much numerical effort (low memory and time requirements). This scheme shall be based on a Hermite spectral approach, such that, for consistency reasons, we shall carry out even the theoretical analysis in a Hermite spectral formalism. Specifically, let us denote by $\mathcal{M}(v) := \frac{1}{\sqrt{2\pi}} e^{-v^2/2}$ a Gaussian velocity distribution function and introduce the following weighted measures $\mathrm{d}\gamma(v) := \mathcal{M}^{-1}(v)\,\mathrm{d}v$ on $\mathbb{R}_v$ as well as $\mathrm{d}\sigma(x,v) := \mathrm{d}x\,\mathrm{d}\gamma(v)$ on $\mathbb{T}_x \times \mathbb{R}_v$. Furthermore we shall denote for a measured space $(\Omega, \mathrm{d}\mu)$, by $L^2_\mu(\Omega)$ and $H^s_\mu(\Omega)$ respectively the L^2- and H^s-spaces associated with the measure $\mathrm{d}\mu$. With this, we expand our particle distribution function f^ε, solution of (2.1.1), in a Hermite basis corresponding to the velocity variable v

$$f^\varepsilon(t,x,v) = \sum_{k\geqslant 0} \alpha_k^\varepsilon(t,x)\psi_k(v), \tag{2.1.3}$$

where $\{\psi_k\}_{k\in\mathbb{N}}$ are well-chosen Hermite functions, forming a complete, orthonormal basis of $L^2_\gamma(\mathbb{R}_v)$ and defined in Section 2.3.1. There are several advantages, when using a Hermite spectral method for the discretization of the velocity variable. Firstly the functions $\{\psi_k\}_{k\in\mathbb{N}}$ form a complete, orthonormal basis of $L^2_\gamma(\mathbb{R}_v)$ with respect to the Gaussian weights, such that these basis functions seem to be optimal to approach Maxwellian-like distribution functions in v, such as our limit distribution function f^0. Secondly, the lower-order terms in the expansion (2.1.3) are related to the low-order moments of the distribution function f^ε, namely to the macroscopic quantites like density, momentum and energy, quantities which are usually

of interest. Thus, such a Hermite spectral method will permit somehow to make the link between the kinetic and the fluid descriptions, and is particularly well suited for our numerical asymptotic study $\varepsilon \to 0$.

The idea to describe the particle density function as an (infinite) sum of orthogonal polynomials related to the Maxwellian form of the equilibrium is not new. In [Bur35], the author used Sonine's polynomials, in order to simplify the integral forms of collision operators, and in [Gra49], the author used N-dimensional Hermite polynomials to approximate the particle density function, solution of the Boltzmann equation. The use of such type of Hermite expansions for the numerical resolution of $1D_x\,1D_v$ Vlasov-Poisson equations goes back as soon as the end of the 60's [Arm67; GF67]. The community then lost interest in these methods, as the computational capacities of that time were not enough to compute - with a high resolution - systems like Vlasov-Poisson. However, in the last decades, these techniques regained interest, and were widely studied and used in the design of numerical schemes [FX20; BF22; SH98; Tan93; PD15; LRW21; KY21].

To summarize, in the first part of this paper we performed a mathematical analysis of the asymptotic behaviour of f^ε, solution of the kinetic model (2.1.1), analysis based on a Hermite-decomposition. We deduced in particular some rates of convergence (with respect to ε) of the Hermite coefficients : the higher the coefficient in the Hermite hierarchy, the faster the convergence, *i.e.* we shall show that $\alpha_k^\varepsilon = \mathcal{O}(\sqrt{\frac{\varepsilon}{k}})$ in some specific norm. This idea is also illustrated in [FN22] and justifies that the Hermite spectral method is particularly well adapted for this kinetic-to-adiabatic transition, as one may neglect for small ε the high order coefficients in the hierarchy, fact which will lead to large computational savings.

In the second part we designed a Hermite-Fourier-Implicit-Euler numerical scheme for (2.1.1) and investigate its main features in the regime of a reasonably small $\varepsilon \ll 1$. In particular, we measure accurately the decay rate of several Hermite coefficients with respect to ε as well as to their height in the hierarchy. This numerical scheme will however, at first, not be designed to efficiently handle the singular limit $\varepsilon \to 0$, due to the still present time-stiffness.

As a consequence, we dedicate the last part of this article to the modification of the above-mentioned scheme, to construct an efficient *Asymptotic Preserving* (AP) method to manage this asymptotic $\varepsilon \to 0$ passage on the discrete level, and this without extensive numerical efforts. An AP scheme has the essential property of being uniformly stable and accurate with respect to a small parameter -in our case ε- and this for a fixed grid. For a complete introduction to the subject, the interested reader may read [Jin22; Neg13].

2.1.1 Main results

Let us summarize here the main results of the theoretical analysis of this paper, the second numerical part of this work shall underscore or reinforce this first analytical part. Firstly a formal asymptotic analysis is carried out to identify the $\varepsilon \to 0$ adiabatic regime of (2.1.1). In

this limit $\varepsilon \to 0$, the electron particle distribution function converges towards a Maxwellian distribution of the form $n^0(t,x)\mathcal{M}(v)$.

Theorem 1. **(Limit model)** Let $(f^\varepsilon, E^\varepsilon)$ be a solution to (2.1.1), for each fixed $\varepsilon > 0$, satisfying the mass constraint

$$\int_{\mathbb{R}_v}\int_{\mathbb{T}_x} f^\varepsilon(t,x,v)\ \mathrm{d}v\,\mathrm{d}x = \mathfrak{m}\,, \qquad \forall (x,v) \in \mathbb{T}_x \times \mathbb{R}_v\,.$$

Then, in the limit $\varepsilon \to 0$ this solution converges towards (f^0, E^0), given by the following nonlinear, elliptic **Limit-model**

$$(L)\quad \begin{cases} f^0(t,x,v) = c(t)\ e^{\phi^0(t,x)}\,\mathcal{M}(v)\,, & c(t) = \mathfrak{m}/\displaystyle\int_{\mathbb{T}_x} e^{\phi^0(t,x)}\ \mathrm{d}x\,, \\ -\partial_{xx}\phi^0 + c(t)\,e^{\phi^0(t,x)} = n_i(t,x)\,, & E^0 = -\partial_x\phi^0\,. \end{cases} \tag{2.1.4}$$

Remark 1. Notice that t is only a parameter in this Limit-model, coming from the time-dependency of the ion density. Therefore, the value of f^0 at $t = 0$ could be *a priori* incompatible with the initial condition of the electron distribution function f^ε solution of the kinetic equation (2.1.1). We need thus to address subtly the question of the transition between the kinetic regime (2.1.1) and the macroscopic description (2.1.4) for an ill-prepared initial datum. This specific point of an initial layer is also addressed in Theorem 2.

The identification and well-posedness of the non-linear elliptic L-model will be investigated in Section 2.2.2. In Section 2.3, the rigorous convergence of $(f^\varepsilon, E^\varepsilon)$, solution to (2.1.1), towards the solution (f^0, E^0) of the limit model (2.1.4), is done via hypocoercivity arguments, the latter being directly inspired by [Add+21]. It is an analysis conducted in a perturbative context, and based on the linearization of the transport operator $v\,\partial_x - E^\varepsilon\,\partial_v$.

Theorem 2. **(Asymptotic behaviour)** Let $(f^\varepsilon, E^\varepsilon)$ be a distributional solution of the nonlinear system (2.1.1), with a given ion density $n_i \in W^{1,\infty}((0,T); L^1(\mathbb{T}_x))$, such that $\int_{\mathbb{T}_x} n_i(t,x)\,\mathrm{d}x \equiv \mathfrak{m}$. We denote by $(f^\varepsilon_{in}, E^\varepsilon_{in})$ its initial data. Denote as well by (f^0, E^0) the solution of the limit problem (2.1.4), and by (f^0_{in}, E^0_{in}) its solution at $t = 0$. Assume furthermore that $f^\varepsilon \in \mathcal{C}^0([0,T], L^2_\sigma(\mathbb{T}_x \times \mathbb{R}_v))$ and $E^\varepsilon = -\partial_x\phi^\varepsilon \in L^\infty((0,T)\times\mathbb{T}_x)$. There exists then a constant $\eta_0 > 0$ such that, if the initial condition of the perturbation is small enough, in the sense

$$\|f^\varepsilon_{in} - f^0_{in}\|^2_{L^2_\sigma(\mathbb{T}_x\times\mathbb{R}_v)} \leqslant \eta_0, \qquad \forall \varepsilon > 0, \tag{2.1.5}$$

one finds constants $C_0, C_1, C_2, \varepsilon_0 > 0$ such that

$$\|f^\varepsilon(t) - f^0(t)\|^2_{L^2_\sigma(\mathbb{T}_x\times\mathbb{R}_v)} \leqslant C_0\|f^\varepsilon_{in} - f^0_{in}\|^2_{L^2_\sigma(\mathbb{T}_x\times\mathbb{R}_v)} e^{-\frac{C_1 t}{\varepsilon}} + C_2\varepsilon^2, \qquad \forall \varepsilon \leqslant \varepsilon_0, \forall t \in [0,T]. \tag{2.1.6}$$

This theorem permits to highlight the presence of an initial layer of size ε in time. Furthermore, as we shall see in the proof (see Remark 6), the constant C_2 in this Theorem depends solely on the time derivative of the limit density $n^0(t,x) = c(t)e^{\phi^0}$ defined by (2.1.4). Therefore, C_2 is zero when n_i does not depend on time.

Estimate (2.1.6) allows also to find an explicit convergence rate towards the adiabatic regime, after integrating in time, namely

$$\|f^\varepsilon - n^0\mathcal{M}\|_{L^p((0,T);L^2_\sigma(\mathbb{T}_x\times\mathbb{R}_v))} \underset{\varepsilon\to 0}{=} \mathcal{O}(\varepsilon^{1/p}), \qquad \text{for all } p\in[1,+\infty[. \tag{2.1.7}$$

Notice that the term related to the dissipation of the initial layer $C_0\|f^\varepsilon_{in} - n^0_{in}\mathcal{M}\|^2_{L^2_\sigma(\mathbb{T}_x\times\mathbb{R}_v)}e^{-\frac{C_1 t}{\varepsilon}}$, is the dominant term. If we assume that the initial condition is well prepared in the sense

$$\|f^\varepsilon_{in} - n^0_{in}\mathcal{M}\|_{L^2_\sigma(\mathbb{T}_x\times\mathbb{R}_v)} = \mathcal{O}(\varepsilon^{1-\frac{1}{p}}),$$

we will get an improved behaviour

$$\|f^\varepsilon - n^0\mathcal{M}\|_{L^p((0,T);L^2_\sigma(\mathbb{T}_x\times\mathbb{R}_v))} \underset{\varepsilon\to 0}{=} \mathcal{O}(\varepsilon), \qquad \text{for all } p\in[1,+\infty[. \tag{2.1.8}$$

This result will be proven in this paper in a Hermite spectral setting. One may wonder about the optimality of assumption (2.1.5). The reason for this assumption is the perturbative nature of our approach. In [Add+21], the authors manage to avoid this assumption thanks to a convergence argument based on the $H-$theorem. In a context of a time-dependent ion density n_i, this latter approach however fails, and getting rid of assumption (2.1.5) remains an open question.

Estimate (2.1.6) of Theorem 2 permits also to evaluate the convergence rates of the Hermite modes, as summarized in the following Corollary.

Corollary 1. **(Hermite coefficient behaviour)** Assume that the conditions of Theorem 2 are met. Then decomposing the particle distribution density f^ε in the Hermite basis via (2.1.3) yields

$$\|\alpha^\varepsilon_k\|_{L^2((0,T)\times\mathbb{T}_x)} = \mathcal{O}\left(\sqrt{\frac{\varepsilon}{k}}\right), \qquad \forall k\geqslant 1 \quad \text{and} \quad \varepsilon\ll 1. \tag{2.1.9}$$

This corollary is a first step towards an efficient numerical treatment of the adiabatic $\varepsilon\to 0$ regime of (2.1.1). The higher the index in the infinite hierarchy of Hermite coefficients, the smaller the importance of the coefficient. This estimate is not a pointwise-in-time estimate, but rather an L^2-result. Furthermore, the estimate in k is not sharp, as our analysis is conducted in a $L^2_\sigma(\mathbb{T}_x\times\mathbb{R}_v)$ setting . A way to get sharper results would be to carry out an analysis in a $H^s_\sigma(\mathbb{T}_x\times\mathbb{R}_v)$ setting, with a general $s\in\mathbb{R}$, as in [HJ12]. This may be the object of future works.

2.1.2 Outline of the paper

The paper is organised as follows : in Section 2.2, we quickly state a result on the well-posedness of system (2.1.1) for fixed ε, and give some physical properties of (2.1.1). In Section 2.2.2 we identify formally the limit problem when $\varepsilon\to 0$ and prove some related existence,

uniqueness and regularity results that will be useful in the rigorous treatment. Section 2.3 introduces the Hermite formalism we will work with, along with the functional spaces and operators and their respective properties. In subsection 2.3.3.1, in particular, we adapt the formalism of [Add+21] to our time-dependent setting, and state the hypocoercivity properties that will lead to our Theorem 2. Theorem 2 is proven in Section 2.4, along with Corollary 1. Finally, in Section 2.5, numerical schemes are presented both for the computation of the kinetic problem (2.1.1), and of the limit problem (2.1.4). We validate the kinetic scheme thanks to the features of our Theorem 2. Numerical investigations aimed to highlight Corollary 1 are performed. Finally, in Section 2.6, we investigate the properties of this numerical scheme in the singular limit $\varepsilon \to 0$, considering a fixed mesh. Then we adjust it in such a way that the scheme becomes *Asymptotic-Preserving* and demonstrate numerically this last essential property. The paper finishes with some conclusions and open problems for future works.

2.2 The Kinetic Vlasov-Poisson-Fokker-Planck equation and its Limit model

Before starting with the asymptotic study, we shall firstly recall some existence and uniqueness results about the Vlasov-Poisson-Fokker-Planck model (2.1.1), and state some properties of this equation as well of its solution.

2.2.1 The kinetic model for fixed $\varepsilon > 0$

Many authors have worked on the mathematical study of this type of Fokker-Planck equation for given electric force fields, showing the existence/uniqueness of strong/weak solutions, local/global in time. For the coupled, nonlinear Vlasov-Poisson-Fokker-Planck problem (2.1.1), see for ex. [Deg86] for a global strong existence result in $2D_x2D_v$, or [Bou93] where an existence result in the $3D_x3D_v$ setting is proven, assuming only the initial condition to be in $L^1 \cap L^\infty$, with finite moments of order 6.

The long-time behaviour of the solutions, in the case of a time-independent ion density is also well documented : see [BD95] for instance, for a method based on compactness techniques. More recently, [Add+21] extends those results by giving an explicit convergence rate towards the long-time equilibrium, in a $L^2_\sigma(\mathbb{T}_x \times \mathbb{R}_v)$ setting and using hypocoercivity techniques. The long-time asymptotics in a $H^s_\sigma(\mathbb{T}_x \times \mathbb{R}_v)$ framework is studied in [HJ12].

Our problem (2.1.1) is slightly different due to the presence of a time-dependent ion density and we state the following existence and uniqueness result based on bootstrap arguments, fixed point techniques, Duhamel formulations and short time regularizations (see [NH05; Vil09; Hér07; Hér17] for this last point) of the operator $P : \mathcal{D}(P) \subset L^2_\sigma(\mathbb{T}_x \times \mathbb{R}_v) \to L^2_\sigma(\mathbb{T}_x \times \mathbb{R}_v)$,

$P := v\partial_x - \partial_v\,[v + \partial_v]$. One can check [Hér07] for a proof of the following theorem, proof that adapts without any difficulty to our setting.

Theorem 3. **(Existence and Uniqueness)** Let $\varepsilon > 0$ fixed, $n_i \in L^\infty((0,T);L^1(\mathbb{T}_x))$ and an initial condition $f^\varepsilon_{in} \in L^2_\sigma(\mathbb{T}_x \times \mathbb{R}_v)$. Then there exists a unique couple $(f^\varepsilon, E^\varepsilon)$ of mild solutions of (2.1.1), satisfying $f^\varepsilon \geqslant 0$ and

— $f^\varepsilon \in C^0([0,T], L^2_\sigma(\mathbb{T}_x \times \mathbb{R}_v))$,

— $E^\varepsilon \in L^\infty((0,T)\times\mathbb{T}_x)$.

A mild solution of (2.1.1) is a couple of functions $(f^\varepsilon, E^\varepsilon)$ satisfying

$$\begin{cases} f^\varepsilon(t) = f^\varepsilon_{in} + \dfrac{1}{\varepsilon}\displaystyle\int_0^t e^{-(t-s)P/\varepsilon}(\partial_v(E^\varepsilon f^\varepsilon)(s))\,\mathrm{d}s, \\ E^\varepsilon = -\partial_x\phi^\varepsilon, \qquad -\partial_{xx}\phi^\varepsilon = n_i - n^\varepsilon_e = n_i - \displaystyle\int_{\mathbb{R}_v} f^\varepsilon\,\mathrm{d}v, \end{cases}$$

where $e^{-tP/\varepsilon}$ is the semigroup generated by the operator P/ε.

Remark 2. Notice that with this definition of a mild solution, f^ε is also a solution in the distributional sense, and one can show furthermore that $f^\varepsilon \in L^2((0,T)\times\mathbb{T}_x; H^1_\gamma(\mathbb{R}_v))$.

Remark 3. Let us remark also that ϕ^ε is unique up to an additive constant. How this constant shall be fixed is of no importance for the computation of the distribution function f^ε, however it has to be specified if one is interested in the computation of the potential.

For the study of the asymptotics of f^ε towards f^0 it is important to know more about the linear Fokker-Planck collision operator, given by

$$C \,:\, D(C) \subset L^2_\gamma(\mathbb{R}_v) \to L^2_\gamma(\mathbb{R}_v), \qquad C(f) := \partial_v\,[v\,f + \partial_v f] = \partial_v\left[\mathcal{M}\,\partial_v\left(\frac{f}{\mathcal{M}}\right)\right], \qquad (2.2.1)$$

with definition domain

$$D(C) := \{f \in L^2_\gamma(\mathbb{R}_v) \;/\; C(f) \in L^2_\gamma(\mathbb{R}_v)\}.$$

Remark that C acts only on the velocity variable, the time and space variables are considered as parameters. The following proposition summarizes now the properties of conservation and entropy decay, which are very easily proven using (2.2.1).

Proposition 2.2.1. **(The Fokker-Planck Operator)** The Fokker-Planck collision operator C defined in (2.2.1) satisfies the following properties:

— Mass conservation:

$$\int_{\mathbb{R}_v} C(f)\,\mathrm{d}v = 0, \qquad \forall f \in D(C);$$

— Entropy Decay:

$$\int_{\mathbb{R}_v} C(f)\ln(f/\mathcal{M})\,\mathrm{d}v \leq 0, \qquad \forall f \in D(C), \quad C(f)\ln(f/\mathcal{M}) \in L^1(\mathbb{R}_v);$$

— Thermal equilibrium:

$$\int_{\mathbb{R}_v} C(f)\ln(f/\mathcal{M})\,\mathrm{d}v = 0 \quad \Leftrightarrow \quad f(v) = n\,\mathcal{M}(v), \quad n \in \mathbb{R}\,,$$
$$\forall f \in D(C), \quad C(f)\ln(f/\mathcal{M}) \in L^1(\mathbb{R}_v).$$

Let us observe furthermore that this collision operator does not preserve momentum and energy.

2.2.2 Formal Identification and Well-Posedness of the limit model

Let us investigate now formally the $\varepsilon \to 0$ limit of the kinetic model (2.1.1) in the aim to identify the asymptotic limit model. We shall prove Theorem 1, saying that if f^ε is a strong solution of (2.1.1), of mass $\mathfrak{m}$, then formally $f^\varepsilon \to f^0$, where f^0 is given by the limit model (2.1.4), which we remind here

$$(L)\quad \begin{cases} f^0(t,x,v) = c(t)\ e^{\phi^0(t,x)}\,\mathcal{M}(v)\,, \quad c(t) = \dfrac{\mathfrak{m}}{\int_{\mathbb{T}_x} e^{\phi^0(t,x)}\,\mathrm{d}x}\,, \quad \mathfrak{m} := \displaystyle\int_{\mathbb{T}_x}\int_{\mathbb{R}_v} f^0_{in}(x,v)\ \mathrm{d}v\,\mathrm{d}x\,, \\ -\partial_{xx}\phi^0 + c(t)\,e^{\phi^0(t,x)} = n_i\,. \end{cases}$$

Proof of Theorem 1. To obtain the Limit-model, several steps are performed:

(a) H-theorem: Multiplying the kinetic equation (2.1.1) by $\ln(\frac{f^\varepsilon}{e^{\phi^\varepsilon}\mathcal{M}})$ and letting formally $\varepsilon \to 0$ permits to show that

$$\int_{\mathbb{T}_x}\int_{\mathbb{R}_v} C(f^0)\ln\left(\frac{f^0}{e^{\phi^0}\,\mathcal{M}}\right)\mathrm{d}v\,\mathrm{d}x = \int_{\mathbb{T}_x}\int_{\mathbb{R}_v} C(f^0)\ln(f^0/\mathcal{M})\,\mathrm{d}v\,\mathrm{d}x = 0\,,$$

yielding (see Proposition 2.2.1)

$$f^0(t,x,v) = n^0(t,x)\,\mathcal{M}\,, \qquad \forall (t,x) \in \mathbb{R}^+ \times \mathbb{T}_x\,,$$

with $n^0(t,x)$ still to be determined.

(b) Struggle between transport and collision operator: If we make now use of the kinetic equation (2.1.1), we get at highest order in ε the equation

$$v\,\partial_x f^0 - E^0\,\partial_v f^0 = C(f^0)\,.$$

Inserting the Maxwellian $f^0 = n^0(t,x)\,\mathcal{M}$ obtained in the first step into this last equation, yields

$$v\,\partial_x n^0\,\mathcal{M} - E^0\,n^0\,\partial_v\mathcal{M} = 0 \quad \Rightarrow \quad \partial_x n^0 - n^0\,\partial_x\phi^0 = 0\,,$$

permitting to get finally the Limit-model (2.1.4).

□

Thus it is the combination between the dissipative operator (H-theorem, step (a)) and the transport operator (step (b)) which permits to converge towards the Boltzmann equilibrium. The existence and uniqueness of a solution of the obtained limit-model (2.1.4) for a fixed ion density n_i is given in the following proposition.

Proposition 2.2.2. **(Existence, uniqueness and regularity)** Let us fix the total electron mass $\mathfrak{m} > 0$ and furthermore assume that the ion density is known, satisfying $n_i \in L^\infty(\mathbb{R}_+; L^1(\mathbb{T}_x))$ as well as the constraint $\int_{\mathbb{T}_x} n_i \, \mathrm{d}x = \mathfrak{m}$.
(i) Then the non-linear elliptic problem

$$-\partial_{xx}\phi^0 + c(t)\, e^{\phi^0(t,x)} = n_i \,, \tag{2.2.2}$$

associated with the intrinsic solvability condition

$$c(t) \int_{\mathbb{T}_x} e^{\phi^0(t,x)} \, \mathrm{d}x = \mathfrak{m} \,, \tag{2.2.3}$$

periodic boundary conditions in $x \in \mathbb{T}_x$ and the additional constraint

$$\int_{\mathbb{T}_x} \phi^0(t,x) \, \mathrm{d}x = 0 \,, \tag{2.2.4}$$

admits a unique solution $\phi^0 \in L^\infty(\mathbb{R}_+; H^1(\mathbb{T}_x))$. Furthermore, thanks to (2.2.2) one has even

$$\partial_x \phi^0 \in L^\infty(\mathbb{R}_+, W^{1,1}(\mathbb{T}_x)) \subset L^\infty(\mathbb{R}_+ \times \mathbb{T}_x).$$

(ii) If $n_i \in L^\infty(\mathbb{R}_+; L^2(\mathbb{T}_x))$ one gets more regular solutions, namely $\phi^0 \in L^\infty(\mathbb{R}_+; H^2(\mathbb{T}_x))$.
(iii) Let now $n_i \in W^{1,\infty}((0,T); L^1(\mathbb{T}_x))$ and denote by ϕ^0 the solution of (2.2.2)-(2.2.3) associated with the different constraint

$$\int_{\mathbb{T}_x} e^{\phi^0(t,y)} \, \mathrm{d}y \equiv 1 \,. \tag{2.2.5}$$

Then the solution actually has the regularity $\phi^0 \in W^{1,\infty}((0,T); H^1(\mathbb{T}_x))$. One can further show that

$$\partial_t \phi^0 \in L^\infty((0,T); W^{1,\infty}(\mathbb{T}_x)).$$

Proof. The proof of this theorem is rather standard, based essentially on the minimization of the strictly convexe, Gateaux differentiable functional

$$\mathcal{L}(\phi) := \frac{1}{2} \int_{\mathbb{T}_x} |\partial_x \phi|^2 \, \mathrm{d}x + \mathfrak{m} \, \ln\left(\int_{\mathbb{T}_x} e^{\phi} \, \mathrm{d}x \right) - \int_{\mathbb{T}_x} n_i \, \phi \, \mathrm{d}x \,.$$

A more general proof can be found in the previous paper [FN22]. □

2.3 Rigorous asymptotic via hypocoercivity arguments

In this section we shall treat rigorously the $\varepsilon \to 0$ asymptotic limit of the Vlasov-Poisson-Fokker-Planck system (2.1.1) with initial condition $f_{in}^{\varepsilon} \in L^2_\sigma(\mathbb{T}_x \times \mathbb{R}_v)$ and a given time-dependent ion density $n_i \in W^{1,\infty}((0,T); L^1(\mathbb{T}_x))$. This shall be done using hypocoercivity arguments. Let us begin by recalling our starting kinetic problem

$$(V)_\varepsilon \quad \begin{cases} \partial_t f^\varepsilon + \dfrac{1}{\varepsilon} v\, \partial_x f^\varepsilon - \dfrac{1}{\varepsilon} E^\varepsilon\, \partial_v f^\varepsilon = \dfrac{1}{\varepsilon} \partial_v \left[v\, f^\varepsilon + \partial_v f^\varepsilon \right], \\ -\partial_{xx}\phi^\varepsilon = n_i - n^\varepsilon, \qquad E^\varepsilon = -\partial_x \phi^\varepsilon, \qquad n^\varepsilon = \displaystyle\int_{\mathbb{R}_v} f^\varepsilon(t,x,v)\, \mathrm{d}v, \\ f^\varepsilon(t=0,x,v) = f_{in}^\varepsilon(x,v), \end{cases}$$

which admits (Theorem 3) for each $\varepsilon > 0$ a unique mild solution $(f^\varepsilon, E^\varepsilon)$ verifying

- $f^\varepsilon \in C^0([0,T], L^2_\sigma(\mathbb{T}_x \times \mathbb{R}_v)) \cap L^2((0,T) \times \mathbb{T}_x, H^1_\gamma(\mathbb{R}_v))$,
- $E^\varepsilon = -\partial_x \phi^\varepsilon \in L^\infty((0,T) \times \mathbb{T}_x)$.

The corresponding nonlinear elliptic limit problem (2.2.2)-(2.2.3), with the additional constraint (2.2.5) to fix ϕ^0

$$(L) \quad \begin{cases} n^0(t,x) = \mathfrak{m}\, e^{\phi^0(t,x)}, \\ -\partial_{xx}\phi^0 = n_i - n^0, \\ \displaystyle\int_{\mathbb{T}_x} e^{\phi^0(t,x)}\, \mathrm{d}x \equiv 1, \end{cases} \tag{2.3.1}$$

has (Proposition 2.2.2) a unique solution $\phi^0 \in W^{1,\infty}((0,T); H^1(\mathbb{T}_x))$, such that $\partial_t \phi^0 \in L^\infty((0,T); W^{1,\infty}(\mathbb{T}_x))$. The $\varepsilon \to 0$ asymptotic study will be performed in a Hermite spectral formalism we shall define now.

2.3.1 The Hermite spectral formalism

Let us start by expanding the electron distribution function $f^\varepsilon(t,x,v)$ as follows

$$f^\varepsilon(t,x,v) = \sum_{k=0}^{\infty} \alpha_k^\varepsilon(t,x)\, \psi_k(v), \qquad f_{in}(x,v) = \sum_{k=0}^{\infty} \alpha_{k,in}(x) \psi_k(v), \tag{2.3.2}$$

where $\{\psi_k\}_{k\in\mathbb{N}}$ are Hermite functions defined recursively as

$$\sqrt{k+1}\, \psi_{k+1}(v) = v\, \psi_k(v) - \sqrt{k}\, \psi_{k-1}, \qquad \psi_{-1} \equiv 0, \quad \psi_0 \equiv \mathcal{M}, \quad \psi_1 \equiv v\, \mathcal{M}, \tag{2.3.3}$$

and which satisfy

$$\psi_k'(v) = -\sqrt{k+1}\, \psi_{k+1}(v), \qquad \int_{-\infty}^{\infty} \psi_k(v)\, \psi_l(v)\, \mathrm{d}\gamma(v) = \delta_{kl}, \quad \forall k,l \in \mathbb{N}.$$

These Hermite functions form a complete, orthonormal basis of $L^2_\gamma(\mathbb{R}_v)$. System (2.1.1) therefore rewrites as an infinite hierarchy of nonlinear, coupled PDEs

$$\begin{cases} \varepsilon\,\partial_t \alpha_k^\varepsilon(t,x) + \sqrt{k}\,\partial_x \alpha_{k-1}^\varepsilon - \sqrt{k}\,\partial_x\phi^\varepsilon(t,x)\,\alpha_{k-1}^\varepsilon + \sqrt{k+1}\,\partial_x\,\alpha_{k+1}^\varepsilon + k\,\alpha_k^\varepsilon = 0\,, \quad \forall k \in \mathbb{N}, \\ -\partial_{xx}\phi^\varepsilon = n_i - \alpha_0^\varepsilon, \\ \alpha_k^\varepsilon(t=0,\cdot) = \alpha_{k,in}, \end{cases} \tag{2.3.4}$$

where we set $\alpha_{-1}^\varepsilon := 0$. Remark that the Fokker-Planck collision operator becomes now in the Hermite-framework a simple multiplication operator.

We shall prove in the next sections the $\varepsilon \to 0$ convergence of the distribution function f^ε towards the limit problem (2.3.1) by using this Hermite-approach and showing that in some sense

$$\begin{cases} \alpha_0^\varepsilon & \to_{\varepsilon\to 0} & n^0, \\ \alpha_k^\varepsilon & \to_{\varepsilon\to 0} & 0, \qquad \forall k \in \mathbb{N}^*, \\ \partial_x\phi^\varepsilon & \to_{\varepsilon\to 0} & \partial_x\phi^0, \end{cases}$$

where the quantities (n^0, ϕ^0) are solutions of (2.3.1).

2.3.2 Filtering of the equilibrium

Our strategy is to use a perturbative approach, based on the decomposition

$$f^\varepsilon = \underbrace{n^0(t,x)\mathcal{M}(v)}_{\text{asymptotic regime}} + \underbrace{g^\varepsilon}_{\text{fluctuation}}\,,$$

which reformulates, in Hermite variables, as

$$f^\varepsilon(t,x,v) = \sum_{k=0}^{\infty} \alpha_k^\varepsilon(t,x)\psi_k(v), \qquad g^\varepsilon(t,x,v) = \sum_{k=0}^{\infty} \gamma_k^\varepsilon(t,x)\psi_k(v),$$

with

$$\begin{cases} \alpha_0^\varepsilon &=& n^0 + \gamma_0^\varepsilon, \\ \alpha_k^\varepsilon &=& 0 + \gamma_k^\varepsilon, \qquad \forall k \in \mathbb{N}^*, \\ \phi^\varepsilon &=& \phi^0 + \varphi^\varepsilon, \end{cases}$$

and we want to show that these new variables $(\{\gamma_k^\varepsilon\}_{k\in\mathbb{N}}, \varphi^\varepsilon)$ converge to zero in a way that we shall specify later. The decomposition in asymptotic and fluctuating part leads to the following set of equations for the fluctuating Hermite variables $(\{\gamma_k^\varepsilon\}_{k\in\mathbb{N}}, \varphi^\varepsilon)$

$$\begin{cases} \varepsilon\,\partial_t \gamma_0^\varepsilon + \partial_x \gamma_1^\varepsilon = -\varepsilon \partial_t n^0, \\ \varepsilon\,\partial_t \gamma_1^\varepsilon + \partial_x \gamma_0^\varepsilon - \partial_x \phi^0 \gamma_0^\varepsilon + \sqrt{2}\partial_x \gamma_2^\varepsilon - \partial_x \varphi^\varepsilon n^0 + \gamma_1^\varepsilon = \partial_x \varphi^\varepsilon \gamma_0^\varepsilon, \\ \varepsilon\,\partial_t \gamma_k^\varepsilon + \sqrt{k}\,\partial_x \gamma_{k-1}^\varepsilon - \sqrt{k}\,\partial_x \phi^0 \gamma_{k-1}^\varepsilon + \sqrt{k+1}\,\partial_x \gamma_{k+1}^\varepsilon + k\gamma_k^\varepsilon = \sqrt{k}\partial_x \varphi^\varepsilon \gamma_{k-1}^\varepsilon, \quad \forall k \geqslant 2 \\ -\partial_{xx}\varphi^\varepsilon = -\gamma_0^\varepsilon, \end{cases} \tag{2.3.5}$$

where we used that the limiting density verifies $\partial_x n^0 = \partial_x \phi^0 n^0$. In the following, the fluctuation variable vector $\{\gamma_k^\varepsilon\}_{k\in\mathbb{N}}$ will be simply denoted by γ^ε and we shall fix the fluctuating potential by imposing $\int_{\mathbb{T}_x} \varphi^\varepsilon \,\mathrm{d}x = 0$.

Remark 4. Notice that integrating with respect to $x \in \mathbb{T}_x$ the relation $\alpha_0^\varepsilon = n^0 + \gamma_0^\varepsilon$ yields the constraint

$$\int_{\mathbb{T}_x} \gamma_0^\varepsilon(t,x)\,\mathrm{d}x = 0, \quad \forall t \in [0,T].$$

This remark, along with the functional space to which f^ε belongs, invites to define the following Hilbert spaces for the fluctuating Hermite-coefficient vector γ^ε

$$l_0^2(\mathbb{N}, L^2(\mathbb{T}_x)) := \left\{ \gamma \in l^2(\mathbb{N}, L^2(\mathbb{T}_x)) \;\Big/\; \int_{\mathbb{T}_x} \gamma_0(x)\,\mathrm{d}x = 0 \right\},$$

$$h_0^1(\mathbb{N}, L^2(\mathbb{T}_x)) := \left\{ \gamma \in l_0^2(\mathbb{N}, L^2(\mathbb{T}_x)) \;\Big/\; \sum_k k \|\gamma_k\|^2_{L^2(\mathbb{T}_x)} < \infty \right\}.$$

Therefore for

$$f^\varepsilon \in C^0([0,T], L^2_\sigma(\mathbb{T}_x \times \mathbb{R}_v)) \cap L^2((0,T)\times \mathbb{T}_x; H^1_\gamma(\mathbb{R}_v)),$$

and $\phi^0 \in W^{1,\infty}((0,T); H^1(\mathbb{T}_x))$, we have the following regularity of the fluctuation variable

$$\gamma^\varepsilon \in C^0([0,T], l_0^2(\mathbb{N}, L^2(\mathbb{T}_x))) \cap L^2((0,T), h_0^1(\mathbb{N}, L^2(\mathbb{T}_x))).$$

Let us introduce now some notation enabling to write system (2.3.5) in a more concise way, namely

$$\varepsilon\,\partial_t \gamma^\varepsilon + \mathcal{T}_t \gamma^\varepsilon - \mathcal{L}\gamma^\varepsilon = \varepsilon\,\mathcal{S} + \mathcal{Q}[\gamma^\varepsilon], \tag{2.3.6}$$

where for smooth $\xi = \{\xi_k\}_{k\in\mathbb{N}} \in l_0^2(\mathbb{N}, L^2(\mathbb{T}_x))$ the time-dependent *linearized* transport operator is defined (for given (n^0, ϕ^0)) as

$$\mathcal{T}_t \xi := \begin{bmatrix} \partial_x \xi_1 & & & & \\ \partial_x \xi_0 & - & \partial_x \phi^0(t,\cdot)\xi_0 & + & \sqrt{2}\,\partial_x \xi_2 & - & \partial_x \varphi_\xi n^0(t,\cdot) \\ \sqrt{2}\,\partial_x \xi_1 & - & \sqrt{2}\,\partial_x \phi^0(t,\cdot)\xi_1 & + & \sqrt{3}\,\partial_x \xi_3 & & \\ & & & \vdots & & & \\ \sqrt{k}\,\partial_x \xi_{k-1} & - & \sqrt{k}\,\partial_x \phi^0(t,\cdot)\xi_{k-1} & + & \sqrt{k+1}\,\partial_x \xi_{k+1} & & \\ & & & \vdots & & & \end{bmatrix}, \tag{2.3.7}$$

with domain $\mathcal{D}(\mathcal{T}_t) := \{\xi \in l^2_0(\mathbb{N}, L^2(\mathbb{T}_x)),\ \mathcal{T}_t\xi \in l^2_0(\mathbb{N}, L^2(\mathbb{T}_x))\}$ and φ_ξ computed via

$$-\partial_{xx}\varphi_\xi = -\xi_0\,, \qquad \int_{\mathbb{T}_x} \varphi_\xi \,\mathrm{d}x = 0\,.$$

The linear Fokker-Planck collision operator $\mathcal{L}$ has the simple form

$$\mathcal{L}\xi := [0, -\xi_1, \cdots, -k\xi_k, \cdots]^t, \tag{2.3.8}$$

with domain $\mathcal{D}(\mathcal{L}) = h^2(\mathbb{N}, L^2(\mathbb{T}_x)) := \{\xi \in l^2(\mathbb{N}, L^2(\mathbb{T}_x)),\ \sum_k k^2 \|\xi_k\|^2_{L^2(\mathbb{T}_x)} < \infty\}$.

The source term $\mathcal{S}$ contains terms coming from the time-dependence of the density

$$\mathcal{S}(t,x) := [-\partial_t n^0(t,x), 0, \cdots]^t\,,$$

and $\mathcal{Q}$ is the term regrouping all the "small" quadratic fluctuation terms

$$\mathcal{Q}[\xi] := \left[0,\ \partial_x\varphi_\xi\xi_0,\ \ldots,\ \sqrt{k}\,\partial_x\varphi_\xi\xi_{k-1}\ \ldots\right]^t.$$

Finally, in order to distinguish between the macroscopic part and the mesoscopic part of the distribution function, we define the following projection operator

$$\Pi\xi := [\xi_0, 0, \cdots]^t, \quad \text{and} \quad (\mathbb{I}\mathrm{d} - \Pi)\xi := [0, \xi_1, \cdots, \xi_k, \cdots]^t, \tag{2.3.9}$$

where $\Pi : l^2(\mathbb{N}, L^2(\mathbb{T}_x)) \to \ker \mathcal{L}$ is the orthogonal projection on the set of local equilibria of the Fokker-Planck operator.

2.3.3 The functional space and its properties

The aim of this subsection is to introduce all the necessary ingredients required to prove our main theorem, in particular the functional spaces, functional inequalities *etc.* Let us consider the time-dependent measure defined on $\mathbb{T}_x$ by $\mathrm{d}\eta_t(x) = (n^0(t,x))^{-1}\mathrm{d}x$ and the space $L^2_{\eta_t}(\mathbb{T}_x)$, which is nothing but the $L^2(\mathbb{T}_x)$-space endowed with the slightly different Hilbert scalar-product, given for fixed $t \in [0,T]$ and $a, b \in L^2(\mathbb{T}_x)$ by

$$\langle a, b\rangle_{L^2_{\eta_t}(\mathbb{T}_x)} := \int_{\mathbb{T}_x} a(x)b(x)\,\mathrm{d}\eta_t(x).$$

We will work in this paper with the space $l^2(\mathbb{N}, L^2_{\eta_t}(\mathbb{T}_x))$. This last choice of space is actually the same as in [Add+21], however with the difference that we are using the Hermite spectral formalism for the velocity variable, and a time-dependent setting. Adapting their work, let us use the following time-dependent norm on the closed subspace $l^2_0(\mathbb{N}, L^2_{\eta_t}(\mathbb{T}_x)) := \{\xi \in l^2(\mathbb{N}, L^2_{\eta_t}(\mathbb{T}_x)), \int_{\mathbb{T}_x} \xi_0\,\mathrm{d}x \equiv 0\}$

$$\|\xi\|^2_t := \sum_{k=0}^{\infty} \|\xi_k\|^2_{L^2_{\eta_t}(\mathbb{T}_x)} + \int_{\mathbb{T}_x} (\partial_x\varphi_\xi)^2\,\mathrm{d}x, \tag{2.3.10}$$

where $-\partial_{xx}\varphi_\xi = -\xi_0$ defines φ_ξ through the constraint $\int_{\mathbb{T}_x} \varphi_\xi \,\mathrm{d}x = 0$. We are thus incorporating a nonlocal term in our norm. We denote by $\langle\cdot,\cdot\rangle_t$ the associated time-dependent scalar product.

We will furthermore make use of the adjoint operator and the orthogonal to a functional space X. These notions depend on t, but since we will never consider simultaneously two times, we just denote them as usual by $*$ and $X^\perp$ and without ambiguity.

In the following proposition, we shall regroup the properties of $l^2_0(\mathbb{N}, L^2_{\eta_t}(\mathbb{T}_x))$ endowed with the $\|\cdot\|_t$ norm.

Proposition 2.3.1. **($\|\cdot\|_t$ norm)**

1. The space $L^2_{\eta_t}(\mathbb{T}_x)$ is uniformly in t equivalent to $L^2(\mathbb{T}_x)$, more specifically, there exist time-independent constants $c, C > 0$ such that
$$c\|h\|^2_{L^2(\mathbb{T}_x)} \leqslant \|h\|^2_{L^2_{\eta_t}(\mathbb{T}_x)} \leqslant C\|h\|^2_{L^2(\mathbb{T}_x)}, \qquad \forall h \in L^2(\mathbb{T}_x), \quad \forall t \in [0,T].$$
2. There exist furthermore time-independent constants $c, C > 0$ such that we have the norm equivalence
$$c\|\xi\|^2_{l^2(\mathbb{N},L^2(\mathbb{T}_x))} \leqslant \|\xi\|^2_t \leqslant C\|\xi\|^2_{l^2(\mathbb{N},L^2(\mathbb{T}_x))}, \qquad \forall \xi \in l^2_0(\mathbb{N}, L^2(\mathbb{T}_x)), \quad \forall t \in [0,T].$$
3. $\mathcal{T}_t$ is skew-symmetric, namely
$$\langle \mathcal{T}_t\xi, \xi\rangle_t = 0, \qquad \forall \xi \in \mathcal{D}(\mathcal{T}_t), \quad \forall t \in [0,T].$$
4. Π is symmetric, i.e.
$$\langle \Pi\xi, \chi\rangle_t = \langle \xi, \Pi\chi\rangle_t, \qquad \forall \xi, \chi \in l^2(\mathbb{N}, L^2(\mathbb{T}_x)), \quad \forall t \in [0,T].$$

Proof. The first point is a result of the fact that $\phi^0 \in L^\infty((0,T)\times\mathbb{T}_x)$. The second point is due to the the first point, and the following sequence of inequalities, obtained from the classical Poincaré-Wirtinger inequality
$$0 \leqslant \int_{\mathbb{T}_x} (\partial_x\varphi_\xi)^2 \,\mathrm{d}x \leqslant \kappa \int_{\mathbb{T}_x} (\xi_0)^2 \,\mathrm{d}x \leqslant \kappa\, \|n^0\|_\infty \|\xi_0\|^2_{L^2_{\eta_t}(\mathbb{T}_x)}.$$
For the third point, we compute
$$\begin{aligned}
\langle \mathcal{T}_t\xi, \xi\rangle_t &= \sum_{k=0}^{\infty} \langle \sqrt{k+1}\,\partial_x\xi_{k+1} + \sqrt{k}\,\partial_x\xi_{k-1} - \sqrt{k}\,\partial_x\phi^0(t,\cdot)\xi_{k-1}, \xi_k\rangle_{L^2_{\eta_t}(\mathbb{T}_x)} \\
&\quad + \underbrace{\int_{\mathbb{T}_x} \partial_x\varphi_{\mathcal{T}_t\xi}\partial_x\varphi_\xi \,\mathrm{d}x}_{\text{non-local part of the scalar product}} \quad \underbrace{- \langle \partial_x\varphi_\xi n^0, \xi_1\rangle_{L^2_{\eta_t}(\mathbb{T}_x)}}_{\text{additional term of k=1}} \\
&= \sum_{k=0}^{\infty} \langle \sqrt{k+1}\,\partial_x\xi_{k+1} + \sqrt{k}\,\partial_x\xi_{k-1} - \sqrt{k}\,\partial_x\phi^0(t,\cdot)\xi_{k-1}, \xi_k\rangle_{L^2_{\eta_t}(\mathbb{T}_x)} \\
&\quad + \int_{\mathbb{T}_x} \partial_x\varphi_{\mathcal{T}_t\xi}\partial_x\varphi_\xi \,\mathrm{d}x - \int_{\mathbb{T}_x} \partial_x\varphi_\xi\xi_1 \,\mathrm{d}x.
\end{aligned}$$

The first term in this equality sums to zero, because of an integration by parts and a telescopic sum, and the two other terms cancel out, because of an integration by parts and the fact that $\partial_{xx}\varphi_{\mathcal{T}_t\xi} = (\mathcal{T}_t\xi)_0 = \partial_x\xi_1$. The fourth point is straightforward. □

Remark 5. To simplify the notation and due to the equivalence property of Proposition 2.3.1 (1) and (2), we shall denote in the following simply by $L^2(\mathbb{T}_x)$ the space $L^2_{\eta_t}(\mathbb{T}_x)$ endowed with the norm (2.3.10).

Proposition 2.3.2. **(The linear Fokker-Planck operator)** The linear Fokker-Planck operator $\mathcal{L} : \mathcal{D}(\mathcal{L}) = h^2(\mathbb{N}, L^2(\mathbb{T}_x)) \to l^2(\mathbb{N}, L^2(\mathbb{T}_x))$ satisfies the following properties

1. $\mathcal{L}$ can be extended to an operator

$$\tilde{\mathcal{L}} : h^1(\mathbb{N}, L^2(\mathbb{T}_x)) \to h^{-1}(\mathbb{N}, L^2(\mathbb{T}_x)) := \left\{ \{\xi_k\}_{k\in\mathbb{N}} \in L^2(\mathbb{T}_x)^{\mathbb{N}} \Big/ \sum_{k>1} \frac{1}{k}\|\xi_k\|^2_{L^2(\mathbb{T}_x)} < \infty \right\}.$$

2. $\mathcal{L}$ is self-adjoint, namely, $\mathcal{D}(\mathcal{L}) = \mathcal{D}(\mathcal{L}^*)$, and

$$\langle \mathcal{L}\xi, \chi\rangle_t = \langle \xi, \mathcal{L}\chi\rangle_t, \qquad \forall \xi, \chi \in \mathcal{D}(\mathcal{L}), \quad \forall t \in [0, T].$$

3. $\mathcal{L}$ is a closed operator, and we have that

$$\operatorname{Im}\mathcal{L} = (\ker \mathcal{L})^\perp = (\ker \tilde{\mathcal{L}})^\perp = \{\xi \in l^2(\mathbb{N}, L^2(\mathbb{T}_x)) \ / \ \xi_0 = 0\}.$$

4. **Microscopic coercivity :** The operator $-\mathcal{L}$ is coercive on $(\ker \mathcal{L})^\perp \cap \mathcal{D}(\mathcal{L})$, namely

$$-\langle \mathcal{L}\xi, \xi\rangle_t \geqslant \|(\mathrm{Id} - \Pi)\xi\|^2_t, \qquad \forall t \in [0, T], \quad \forall \xi \in h^2(\mathbb{N}, L^2(\mathbb{T}_x)). \tag{2.3.11}$$

The Microscopic coercivity property (2.3.11) expresses the fact that the collision operator relaxes the electron density towards a local Maxwellian distribution function belonging to the kernel of $\mathcal{L}$. We only prove the fourth point, as the first three ones are immediate from the definition of $\mathcal{L}$ and its expression in terms of the Hermite coefficients (2.3.8).

Proof of (4). The micro-coercivity property is the reformulation of the following inequality

$$\sum_{k=1}^{\infty} k\|\xi_k\|^2_{L^2_{\eta_t}(\mathbb{T}_x)} \geqslant \sum_{k=1}^{\infty} \|\xi_k\|^2_{L^2_{\eta_t}(\mathbb{T}_x)},$$

where we keep in mind that $\varphi_{\mathcal{L}\xi} = 0$. The conclusion follows from Pareseval's theorem. □

Now that we have introduced the notations and explicited some properties of the functional space, we are ready to move to the next subsection, dealing with hypocoercivity and aimed to be a toolbox that we will use in Section 2.5.

2.3.3.1 Hypocoercivity toolbox.

Entropy methods are strategies for proving the exponential decay of solutions of evolution equations of the type

$$\begin{cases} \partial_t u + \mathcal{B} u = 0\,, \\ u(t=0,\cdot) = u_0\,, \end{cases} \tag{2.3.12}$$

towards the equilibrium solution u_{eq} satisfying $\mathcal{B} u_{eq} = 0$. The main idea is to find a suitable entropy functional (Lyapunov functional) in terms of the considered operator $\mathcal{B}$ and equivalent to the underlying Hilbert-norm, permitting to measure the decay towards the equilibrium. For ex. to find a scalar-product $\langle\cdot,\cdot\rangle_{\mathcal{B}}$, equivalent to the underlying scalar-product, however for which $\mathcal{B}$ is coercive, meaning

$$\langle \mathcal{B}\, u, u\rangle_{\mathcal{B}} \geqslant \lambda \|u\|^2_{\mathcal{B}}\,, \quad \forall u \in D(\mathcal{B}) \cap (\ker \mathcal{B})^{\perp}\,,$$

such that one obtains from (2.3.12)

$$\frac{1}{2}\frac{\mathrm{d}}{\mathrm{d}t}\|u\|^2_{\mathcal{B}} = \langle \partial_t u, u\rangle_{\mathcal{B}} \leqslant -\lambda \|u\|^2_{\mathcal{B}}\,,$$

leading with Gronwall's lemma to the desired exponential decay

$$\|u(t)\|^2_{\mathcal{B}} \leqslant e^{-2\,\lambda\, t}\, \|u_0\|^2_{\mathcal{B}}\,, \qquad \forall t \geqslant 0\,.$$

In order to prove Theorem 2, namely the exponential decay of f^ε in the t/ε variable, towards the asymptotic regime $n^0\mathcal{M}$, we shall investigate the convergence towards zero of the fluctuations, solutions of the Hermite system

$$\varepsilon\, \partial_t \gamma^\varepsilon + \mathcal{T}_t \gamma^\varepsilon - \mathcal{L}\gamma^\varepsilon = \varepsilon\, \mathcal{S} + \mathcal{Q}[\gamma^\varepsilon], \tag{2.3.13}$$

trying to find a suitable functional $\mathcal{F}_t$, which is equivalent to the norm $\|\cdot\|_t$ (uniformly in time) and which satisfies moreover an inequality of the form

$$\frac{\mathrm{d}}{\mathrm{d}t}\mathcal{F}_t(\gamma^\varepsilon) \leqslant \mathcal{G}_\varepsilon\left(\mathcal{F}_t(\gamma^\varepsilon)\right), \tag{2.3.14}$$

with $\mathcal{G}_\varepsilon$ a certain non-linear function.

Unfortunately the operator $\mathcal{T}_t - \mathcal{L}$ is not coercive for the $\|\cdot\|_t$ norm, we rather have for ξ smooth enough

$$\langle (\mathcal{T}_t - \mathcal{L})\xi, \xi\rangle_t \geqslant \|(\mathbb{I}\mathrm{d} - \Pi)\xi\|^2_t. \tag{2.3.15}$$

This fact is due to both, the skew-symmetry of the transport operator and the microscopic coercivity of $\mathcal{L}$, which is coercive only on $(\ker \mathcal{L}_{|l^2_0(\mathbb{N},L^2(\mathbb{T}_x))})^{\perp}$, and not on the whole space. However, from the formal analysis performed in Section 2.2.2, we observed that the operator

$\mathcal{T}_t - \mathcal{L}$ relaxes nevertheless the macroscopic part $\Pi\xi$ towards zero, so that we can still expect an inequality of the form (2.3.14).

The problem is that the transport operator, skew-symmetric, is absent from the computations, while its mixing properties are essential to get an exponential decay in this $\|\cdot\|_t$ norm. This problematic has been widely called *hypocoercivity*.

There are several ways to introduce the effect of $\mathcal{T}_t$ to get the desired exponential decay for the hypocoercive operator $\mathcal{T}_t - \mathcal{L}$. Inspired by [Add+21], we choose the so-called *auxiliary operator method*. The idea of this method is to add a well-chosen correction operator A_t to the standard entropy functional, and hence instead of working with the usual $\|\cdot\|_t$ norm, to work with the modified functional

$$\mathcal{F}_t(\gamma^\varepsilon(t)) := \frac{1}{2}\|\gamma^\varepsilon\|_t^2 + \delta\,\langle A_t\gamma^\varepsilon, \gamma^\varepsilon\rangle_t, \tag{2.3.16}$$

with $\delta > 0$ to be tuned later on. This functional will be designed in such a manner to be a Lyapunov functional for (2.3.13), and furthermore equivalent to the $\|\cdot\|_t$ norm. The operator A_t shall incorporate somehow the role of the transport operator $\mathcal{T}_t$.

The choice of the operator A_t is inspired by the Drift-Diffusion limit [Add+21] and is defined by

$$A_t := (\mathbb{I}\mathrm{d} + (\mathcal{T}_t\Pi)^*(\mathcal{T}_t\Pi))^{-1}(\mathcal{T}_t\Pi)^*,$$

where the adjoint operator $*$ is, for fixed t, the adjoint operator corresponding to the Hilbertian scalar-product $\langle\cdot,\cdot\rangle_t$. The role of the operator A_t in the modified entropy (2.3.16) is similar to the mixing term $\langle\nabla_x\xi, \nabla_v\xi\rangle$ (see [Hér17]), which, as the name suggests, permits to mix the two space and velocity variables in order to recover the missing space derivatives in the coercivity inequality (2.3.15).

The well-posedness of this operator

$$A_t \,:\, l_0^2(\mathbb{N}, L^2(\mathbb{T}_x)) \to l_0^2(\mathbb{N}, L^2(\mathbb{T}_x))$$

is a consequence of Lax-Milgram theorem, as stated in the next Proposition. In the next subsections some essential properties of this operator A_t will be summarized, being the basis for showing an estimate of the type (2.3.14).

2.3.3.2 Properties of the mixing operator A_t

The first inequality we shall introduce can be seen as the coercivity of the operator $(\mathcal{T}_t)^*\mathcal{T}_t$ on the space $\ker\mathcal{L} \cap \mathcal{D}((\mathcal{T}_t)^*\mathcal{T}_t)$.

Proposition 2.3.3. **(Macroscopic coercivity)** Let $\mathcal{T}_t$ be the transport operator defined in (2.3.7). There exists a constant $\lambda_M > 0$ such that

$$\|\mathcal{T}_t\Pi\xi\|_t^2 \geqslant \lambda_M\|\Pi\xi\|_t^2, \qquad \forall t\in[0,T], \quad \forall\xi\in l_0^2(\mathbb{N}, H^1(\mathbb{T}_x)). \tag{2.3.17}$$

This uniform in time spectral gap inequality leads to the well-definitness of the operator A_t, and furthermore, to the coercivity of $A_t\mathcal{T}_t\Pi$ on $l^2_0(\mathbb{N}, L^2(\mathbb{T}_x))$, namely

$$\langle A_t\mathcal{T}_t\Pi\xi, \xi\rangle_t \geqslant \frac{\lambda_M}{1+\lambda_M}\|\Pi\xi\|_t^2, \qquad \forall t \in [0,T], \quad \forall \xi \in l^2_0(\mathbb{N}, L^2(\mathbb{T}_x)). \tag{2.3.18}$$

Proof. This property is based exclusively on the ideas of [Add+21], with the specificity of the uniform-in-time Poincaré inequality given in Lemma 5, and also on Lax-Milgram theorem. Let us make here some further comments. The first inequality is a spectral gap inequality, indicating a uniform in time lower bound on the first eigenvalue of the positive operator $(\mathcal{T}_t\Pi)^*\mathcal{T}_t\Pi$. The second inequality is a consequence of the first one: since $A_t\mathcal{T}_t\Pi$ is just the composition of $z \mapsto z(1+z)^{-1}$ with the operator $(\mathcal{T}_t\Pi)^*(\mathcal{T}_t\Pi)$, diagonalizing this operator $(\mathcal{T}_t\Pi)^*(\mathcal{T}_t\Pi)$ leads to the second point. □

Decomposing now the space $l^2_0(\mathbb{N}, L^2(\mathbb{T}_x))$ as

$$l^2_0(\mathbb{N}, L^2(\mathbb{T}_x)) = \ker \mathcal{L}_{|l^2_0(\mathbb{N},L^2(\mathbb{T}_x))} \oplus (\ker \mathcal{L}_{|l^2_0(\mathbb{N},L^2(\mathbb{T}_x))})^\perp,$$

we see that the microscopic coercivity (2.3.11) guarantees a coercivity of the operator $\mathcal{T}_t - \mathcal{L}$ on $(\ker \mathcal{L}_{|l^2_0(\mathbb{N},L^2(\mathbb{T}_x))})^\perp$, which is the reason of the relaxation towards zero on this space, whereas on the subspace $\ker \mathcal{L}$, the reason of relaxation towards zero will be the transport operator, and more explicitly, the macroscopic coercivity property (2.3.18) of the operator $\mathcal{T}_t^*\mathcal{T}_t$.

Now, the computation of $\varepsilon \frac{\mathrm{d}}{\mathrm{d}t}\mathcal{F}_t(\gamma^\varepsilon)$ will lead on one hand to the appearance of the microscopic and macroscopic coercivities, but on the other hand also to many other terms, that need to be controlled. We will detail the properties used to bound all these terms in the rest of this subsection. Some of these properties are identical to those introduced in [Add+21] and will hence not be proven here.

Observing that we have

$$\mathcal{T}_t\Pi\xi = \begin{bmatrix} 0 \\ \partial_x\xi_0 - \partial_x\phi^0(t,\cdot)\xi_0 - \partial_x\varphi_\xi n^0(t,\cdot) \\ 0 \\ \vdots \end{bmatrix},$$

yields immediately the so-called *parabolic dynamics property* $\Pi\mathcal{T}_t\Pi = 0$, which implies, as in [DMS15], the following Lemma.

Lemma 1. [DMS15] **(Parabolic macroscopic dynamics)** Let $\xi \in l^2_0(\mathbb{N}, L^2(\mathbb{T}_x))$. First we observe that $\Pi A_t = A_t$, which leads to

$$\|A_t\xi\|_t^2 + \|T_tA_t\xi\|_t^2 = \langle \xi, \mathcal{T}_tA_t\xi\rangle_t\,, \tag{2.3.19}$$

and then to

$$\|A_t\xi\|_t \leqslant \frac{1}{2}\|(\mathbb{Id}-\Pi)\xi\|_t, \quad \forall t \in [0,T]. \tag{2.3.20}$$

We deduce that $A_t = A_t(\mathbb{Id}-\Pi)$ and

$$\|T_tA_t\xi\|_t \leqslant \|(\mathbb{Id}-\Pi)\xi\|_t, \quad \forall t \in [0,T]. \tag{2.3.21}$$

For the remaining terms we have the following Lemma.

Lemma 2. **(Bounded auxiliary operators)** Set $\xi \in l^2_0(\mathbb{N}, L^2(\mathbb{T}_x))$. The auxiliary operator A_t has a regularising effect, namely we have

$$\|A_t\mathcal{L}\xi\|_t \leqslant \frac{1}{2}\|(\mathbb{Id}-\Pi)\xi\|_t, \quad \forall t \in [0,T], \tag{2.3.22}$$

and $\exists \Lambda > 0$ independent on time, such that

$$\|A_t\mathcal{T}_t(\mathbb{Id}-\Pi)\xi\|_t \leqslant \Lambda\|(\mathbb{Id}-\Pi)\xi\|_t, \quad \forall t \in [0,T]. \tag{2.3.23}$$

Proof. The proof of inequality (2.3.22) is exactly as in [Add+21]. The proof of (2.3.23) is quite technical, but follows the lines of [Add+21], Lemma 20, and is mainly based on integration by parts and the use of Poincaré type inequalities. A difference between [Add+21] and our result is the time-independence of the constant Λ that needs to be addressed. This is assured because of our uniform in time Poincaré inequalities (see Lemma 5). The beginning of the proof follows exactly step 1 and 2 of [Add+21]. However, keeping in mind that in our case $n^0,\ \partial_x\phi^0 \in L^\infty((0,T)\times\mathbb{T}_x)$ permits to greatly simplify the proof, as we do not need the estimates of their step 3. Their inequalities (32)-(33) of step 4 are a direct consequence of their inequalities (27)-(28). □

Now, because of the time dependency of the weight, as opposed to [Add+21], there are some additional terms appearing in our computations. We show in the following Lemma that these additional terms can be properly handled.

Lemma 3. **(Specificities due to the time-dependency of n_i)** The commutator $[\partial_t, A_t] := \partial_tA_t - A_t\partial_t$ is uniformly bounded, namely

$$\|[\partial_t, A_t]\xi\|_t \leqslant C_*\|(\mathbb{Id}-\Pi)\xi\|_t, \quad \forall t \in [0,T], \quad \forall \xi \in L^\infty((0,T), l^2_0(\mathbb{N}, L^2(\mathbb{T}_x))), \tag{2.3.24}$$

with $C_* > 0$ a time-independent constant, depending only on the L^∞-norm of $\partial_t\partial_x\phi^0$, $\partial_t\phi^0$, and ϕ^0.

Proof. We prove this lemma in the Appendix. □

With these properties in mind, we are ready to deal with the proof of Theorem 2.

2.4 Proofs of Theorem 2 and Corollary 1

Let us come now to the rigorous asymptotic study of our nonlinear Vlasov-Poisson-Fokker-Planck system (2.1.1). Recalling that we decomposed f^ε in a macroscopic asymptotic part, and a fluctuation part $f^\varepsilon = n^0(t,x)\mathcal{M}(v) + g^\varepsilon$, with $g^\varepsilon = \sum_{k=0}^{\infty} \gamma_k^\varepsilon(t,x)\psi_k(v)$, we shall focus on the fluctuation problem

$$\varepsilon\, \partial_t \gamma^\varepsilon + \mathcal{T}_t \gamma^\varepsilon = \mathcal{L}\gamma^\varepsilon + \varepsilon\, \mathcal{S} + \mathcal{Q}[\gamma^\varepsilon].$$

Reformulating Theorem 2 with our new notation, we need to show that there exists $\eta_0 > 0$ such that, if the initial condition for the perturbation γ_{in}^ε is small enough, namely if

$$\|\gamma_{in}^\varepsilon\|^2_{l^2(\mathbb{N},L^2(\mathbb{T}_x))} = \|f_{in}^\varepsilon - n_{in}^0\mathcal{M}\|^2_{L^2_\sigma(\mathbb{T}_x\times\mathbb{R}_v)} \leqslant \eta_0, \qquad \forall \varepsilon > 0\,,$$

we have the existence of constants $C_0, C_1, C_2, \varepsilon_0 > 0$ such that

$$\|f^\varepsilon(t) - n_0(t)\mathcal{M}\|^2_{L^2_\sigma(\mathbb{T}_x\times\mathbb{R}_v)} = \|\gamma^\varepsilon(t)\|^2_{l^2(\mathbb{N},L^2(\mathbb{T}_x))} \leqslant C_0\|\gamma_{in}^\varepsilon\|^2_{l^2(\mathbb{N},L^2(\mathbb{T}_x))} e^{-\frac{C_1 t}{\varepsilon}} + C_2\varepsilon^2,$$
$$\forall \varepsilon \leqslant \varepsilon_0,\ \forall t \in [0,T].$$

Proof of Theorem 2 : The proof is based on the study of the following entropy functional

$$\mathcal{F}_t(\gamma^\varepsilon(t)) := \frac{1}{2}\|\gamma^\varepsilon\|_t^2 + \delta\,\langle A_t\gamma^\varepsilon, \gamma^\varepsilon\rangle_t\,, \tag{2.4.1}$$

introduced in Section 2.3.3.1. Notice that this functional $\mathcal{F}_t$ is equivalent to $\|\cdot\|_t^2$, uniformly in t, provided that $\delta > 0$ is small enough, i.e. one has, thanks to (2.3.20) and to the definition (2.3.9)

$$\frac{1}{2}(1-\delta)\|\cdot\|_t^2 \leqslant \mathcal{F}_t \leqslant \frac{1}{2}(1+\delta)\|\cdot\|_t^2, \quad \forall t \in [0,T].$$

In the first part of the proof, using the tools of Section 2.3.3.1, we shall show the estimate

$$\varepsilon\frac{\mathrm{d}}{\mathrm{d}t}\mathcal{F}_t(\gamma^\varepsilon) \leqslant -\eta\mathcal{F}_t(\gamma^\varepsilon) + \varepsilon^2\, C_1 + C_2\mathcal{F}_t(\gamma^\varepsilon)^2, \tag{2.4.2}$$

which will lead, in a second time, to the convergence result, thanks to the smallness of the initial condition (2.1.5), Gronwall's Lemma and the equivalence with the $\|\cdot\|_t^2$ norm.

2.4.1 Part 1 : Estimate obtention

Derivating in time the entropy functional $\mathcal{F}_t$ (2.4.1), yields

$$\begin{aligned}
\varepsilon \frac{\mathrm{d}}{\mathrm{d}t}\mathcal{F}_t(\gamma^\varepsilon) =& \langle \mathcal{L}\gamma^\varepsilon, \gamma^\varepsilon\rangle_t - \delta\langle A_t\mathcal{T}_t\Pi\gamma^\varepsilon, \gamma^\varepsilon\rangle_t && \text{('Good dissipative terms')}\\
&- \delta\langle A_t\mathcal{T}_t(\mathbb{I}\mathrm{d}-\Pi)\gamma^\varepsilon, \gamma^\varepsilon\rangle_t + \delta\langle \mathcal{T}_t A_t\gamma^\varepsilon, \gamma^\varepsilon\rangle_t + \delta\langle A_t\mathcal{L}\gamma^\varepsilon, \gamma^\varepsilon\rangle_t + \delta\underbrace{\langle \mathcal{L}A_t\gamma^\varepsilon, \gamma^\varepsilon\rangle_t}_{=0}\\
& && \text{(Signless terms arising in the classical computation)}\\
&+ \varepsilon\langle \mathcal{S}, \gamma^\varepsilon\rangle_t + \varepsilon\delta\underbrace{\langle A_t\mathcal{S}, \gamma^\varepsilon\rangle_t}_{=0} + \varepsilon\delta\langle A_t\gamma^\varepsilon, \mathcal{S}\rangle_t\\
& && \text{(Terms associated with the source term)}\\
&- \frac{\varepsilon}{2}\sum_{k=0}^{\infty}\langle \partial_t\phi^0\gamma_k^\varepsilon, \gamma_k^\varepsilon\rangle_{L^2_{\eta_t}(\mathbb{T}_x)} - \varepsilon\delta\sum_{k=0}^{\infty}\langle \partial_t\phi^0(A_t\gamma^\varepsilon)_k, \gamma_k^\varepsilon\rangle_{L^2_{\eta_t}(\mathbb{T}_x)} + \varepsilon\delta\langle[\partial_t, A_t]\gamma^\varepsilon, \gamma^\varepsilon\rangle_t\\
& && \text{(Terms related to the time dependency of the norms and operators)}\\
&+ \langle \mathcal{Q}[\gamma^\varepsilon], \gamma^\varepsilon\rangle_t + \delta\langle A_t\mathcal{Q}[\gamma^\varepsilon], \gamma^\varepsilon\rangle_t + \delta\underbrace{\langle A_t\gamma^\varepsilon, \mathcal{Q}[\gamma^\varepsilon]\rangle_t}_{=0}.\\
& && \text{(Terms arising due to the nonlinearity } \mathcal{Q})
\end{aligned} \tag{2.4.3}$$

Some terms vanish to zero due to $\mathcal{L}(A_t) = \mathcal{L}(\Pi A_t) = 0$, $A_t\mathcal{S} = A_t(\mathbb{I}\mathrm{d}-\Pi)\mathcal{S} = 0$ and $A_t = \Pi A_t$, which gives $\langle A_t\gamma^\varepsilon, \mathcal{Q}[\gamma^\varepsilon]\rangle_t = 0$.

The first line regroups the dissipation terms, which behave nicely because of the microscopic and macroscopic coercivities. We use estimates identical to the ones occuring in [Add+21; DMS15], to control the terms of the second line by the microscopic and macroscopic coercivity. We compiled them in the Appendix, for the sake of completeness, inequalities (2.8.4) to (2.8.9). We also need to deal with the terms related to the source term and to the time dependency of the norms, gathered in the Appendix (inequality (2.8.10) to (2.8.15)) as they are essentially based on Young's inequality and Lemma 3.

There only remains to control the terms in the last line of (2.4.3), appearing because of the nonlinear coupling, and this will be detailed now.

2.4.1.1 Control of the terms arising because of the nonlinearity

We deal with the quadratic term $\mathcal{Q}[\gamma^\varepsilon]$ in the following way: the first term of the last line of (2.4.3) is controlled by the following sequence of inequalities

$$\begin{aligned}\langle \mathcal{Q}[\gamma^\varepsilon], \gamma^\varepsilon\rangle_t &= \sum_{k=1}^{\infty} \sqrt{k}\,\langle \partial_x \varphi^\varepsilon_\gamma . \gamma^\varepsilon_{k-1}, \gamma^\varepsilon_k\rangle_{L^2_{\eta_t}(\mathbb{T}_x)} \\ &\leqslant \frac{1}{2}\sum_{k=1}^{\infty} k\|\gamma^\varepsilon_k\|^2_{L^2_{\eta_t}(\mathbb{T}_x)} + \frac{1}{2}\sum_{k=0}^{\infty}\|\partial_x\varphi^\varepsilon_\gamma \gamma^\varepsilon_k\|^2_{L^2_{\eta_t}(\mathbb{T}_x)} \\ &\leqslant -\frac{1}{2}\langle \mathcal{L}\gamma^\varepsilon, \gamma^\varepsilon\rangle_t + \frac{\kappa}{2}\|\gamma^\varepsilon\|^4_t. \end{aligned} \tag{2.4.4}$$

The passage from the second line to the third one uses the following sequence of inequalities, coming from the continuous Sobolev injection $H^1(\mathbb{T}_x) \hookrightarrow L^\infty(\mathbb{T}_x)$ and from the definition of the $\|\cdot\|_t$

$$\frac{1}{2}\sum_{k=0}^{\infty}\|\partial_x\varphi^\varepsilon_\gamma \gamma^\varepsilon_k\|^2_{L^2_{\eta_t}(\mathbb{T}_x)} \leqslant \frac{1}{2}\|\partial_x\varphi^\varepsilon_\gamma(t)\|^2_{L^\infty(\mathbb{T}_x)}\sum_{k=0}^{\infty}\|\gamma^\varepsilon_k\|^2_{L^2_{\eta_t}(\mathbb{T}_x)} \leqslant \frac{\kappa}{2}\|\gamma^\varepsilon\|^4_t.$$

The second term of the last line of (2.4.3) is controlled as follows, using (2.3.22)

$$\begin{aligned}\delta\langle A_t\mathcal{Q}[\gamma^\varepsilon], \gamma^\varepsilon\rangle_t &= \delta\langle A_t\mathcal{L}\mathcal{L}^{-1}\mathcal{Q}[\gamma^\varepsilon], \gamma^\varepsilon\rangle_t \\ &\leqslant \delta\|A_t\mathcal{L}\mathcal{L}^{-1}\mathcal{Q}[\gamma^\varepsilon]\|_t\|\gamma^\varepsilon\|_t \\ &\leqslant \frac{\delta}{2}\|\mathcal{L}^{-1}\mathcal{Q}[\gamma^\varepsilon]\|_t\|\gamma^\varepsilon\|_t \\ &\leqslant \frac{\delta}{2}\sqrt{\sum_{k=1}^{\infty}\left\|\frac{\sqrt{k}}{k}\partial_x\varphi^\varepsilon_\gamma . \gamma^\varepsilon_{k-1}\right\|^2_{L^2_{\eta_t}(\mathbb{T}_x)}}\,\|\gamma^\varepsilon\|_t \leqslant \frac{\delta\,\nu_5\,\kappa}{4}\|\gamma^\varepsilon\|^4_t + \frac{\delta}{4\nu_5}\|\gamma^\varepsilon\|^2_t, \end{aligned} \tag{2.4.5}$$

where $\nu_5 > 0$ will be adequately fixed later on. Notice that $\mathcal{L}^{-1}\mathcal{Q}$ is well defined, since $\Pi\mathcal{Q} = 0$.

2.4.1.2 Summarizing the previous estimates

Assembling and reorganizing the terms of (2.4.3) and using all the estimates obtained so far, leads to

$$\begin{aligned}\varepsilon\frac{\mathrm{d}}{\mathrm{d}t}\mathcal{F}_t(\gamma^\varepsilon) \leqslant\ & \delta\left(\frac{1}{2\nu_1}+\frac{1}{2\nu_2}+\frac{1}{2\nu_3}-\frac{\lambda_M}{1+\lambda_M}\right)\|\Pi\gamma^\varepsilon\|^2_t && \text{(Dissipation of } \Pi\gamma\text{)} \\ &+\left(\delta\Lambda^2\frac{\nu_1}{2}+\delta\frac{5}{4}+\delta\frac{\nu_2}{8}+\delta\frac{1}{8\nu_4}-\frac{1}{2}\right)\|(1-\Pi)\gamma^\varepsilon\|^2_t && \text{(Dissipation of } (\mathbb{I}\mathrm{d}-\Pi)\gamma\text{)} \\ &+\frac{\varepsilon^2}{2}\left(\frac{\nu_3}{\delta}+\delta\nu_4\right)\|S\|^2_t && \text{(Source term)} \\ &+\varepsilon\,C_{\delta,\phi}\|\gamma^\varepsilon\|^2_t && \text{(Time dependency)} \\ &+\kappa\left(\frac{1}{2}+\frac{\delta\nu_5}{4}\right)\|\gamma^\varepsilon\|^4_t+\frac{\delta}{4\nu_5}\|\gamma^\varepsilon\|^2_t, && \text{(Nonlinearity } \mathcal{Q}\text{)} \end{aligned}$$

where $C_{\delta,\phi} := \left(\frac{\|\partial_t \phi^0\|_\infty}{2} + \frac{\delta}{2}\|\partial_t \phi^0\|_\infty + \delta C_* \right)$ and $\nu_1, \nu_2, \nu_3, \nu_4, \nu_5 > 0$ are some constants to be tuned later on.

Choosing firstly $\nu_1, \nu_2, \nu_3 > 0$ such that the first line becomes strictly negative, tuning then $\delta > 0$ and $\nu_4 > 0$ in order to get a strictly negative second line, permits to obtain the existence of an $\eta > 0$ such that

$$\varepsilon \frac{\mathrm{d}}{\mathrm{d}t}\mathcal{F}_t(\gamma^\varepsilon) \leqslant -(\eta - \frac{\delta}{4\nu_5} - \varepsilon\, C_{\delta,\phi})\,\|\gamma^\varepsilon\|_t^2 + \frac{\varepsilon^2}{2}\left(\frac{\nu_3}{\delta} + \delta\nu_4\right)\|S\|_t^2 + \kappa\left(\frac{1}{2} + \frac{\delta\nu_5}{4}\right)\|\gamma^\varepsilon\|_t^4.$$

Taking now $0 < \eta_1 < \eta$ and a small $\varepsilon_0 > 0$, and choosing furthermore $\nu_5 > 0$ big enough, depending on η, yields the existence of constants C', $C'' > 0$ such that

$$\varepsilon \frac{\mathrm{d}}{\mathrm{d}t}\mathcal{F}_t(\gamma^\varepsilon) \leqslant -\eta_1\,\|\gamma^\varepsilon\|_t^2 + \varepsilon^2 C' + C''\,\|\gamma^\varepsilon\|_t^4, \quad \forall t \in [0,T], \quad \forall \varepsilon < \varepsilon_0. \tag{2.4.6}$$

Remark 6. Notice that the constant C' depends solely on the source term S, which is zero when the density n_i is time-independent.

Using the equivalence between $\mathcal{F}_t$ and $\|\cdot\|_t^2$, estimate (2.4.6) rewrites, up to changing the names of the constants, as

$$\frac{\mathrm{d}}{\mathrm{d}t}\mathcal{F}_t(\gamma^\varepsilon) \leqslant -\frac{\eta}{\varepsilon}\mathcal{F}_t(\gamma^\varepsilon) + \varepsilon\, C_1 + \frac{C_2}{\varepsilon}\mathcal{F}_t(\gamma^\varepsilon)^2 = \frac{\mathcal{F}_t(\gamma^\varepsilon)}{\varepsilon}(C_2\mathcal{F}_t(\gamma^\varepsilon) - \eta) + \varepsilon\, C_1. \tag{2.4.7}$$

We now want to conclude by Gronwall's lemma, but we need to be cautious, because of the quadratic term, and this is precisely where we will use the assumption on the smallness of the initial condition.

2.4.2 Part 2 : Gronwall's Lemma with smallness of the initial condition

If the initial condition is too big, the quadratic term in (2.4.7) is bigger than the linear term, and $\mathcal{F}_t$ can explode in finite time. If, however the initial condition is very small, the first term on the right-hand side of (2.4.7) is negative, and the functional remains controlled. We write this rigorously in the following Lemma.

Lemma 4. Assume that there exists constants $\eta,\ C_1,\ C_2 > 0$ such that the function $t \in [0,T] \to \mathcal{F}_t(\gamma^\varepsilon)$ verifies inequality (2.4.7). Assume now that $\mathcal{F}_0(\gamma_{in}^\varepsilon) \leqslant \frac{\eta}{2C_2}$. Then if $\varepsilon_1 > 0$ is such that $\varepsilon_1 C_1 \leqslant \frac{\eta}{8C_2 T}$, we have

$$\mathcal{F}_t(\gamma^\varepsilon) \leqslant \frac{3}{4}\frac{\eta}{C_2}, \qquad \forall \varepsilon < \varepsilon_1,\ \ \forall t \in [0,T].$$

Proof. We are going to prove the following intermediate result

$$\mathcal{F}_t(\gamma^\varepsilon) \leqslant \frac{\eta}{2C_2} + \frac{t\eta}{4TC_2}, \qquad \forall \varepsilon < \varepsilon_1,\ \ \forall t \in [0,T],$$

which implies immediately the Lemma. To do this, we fix $\varepsilon < \varepsilon_1$, and define

$$E := \left\{ t \in [0,T] \ / \ \mathcal{F}_s(\gamma^\varepsilon(s)) \leqslant \frac{\eta}{2C_2} + \frac{s\eta}{4TC_2} \quad \forall s \in [0,t] \right\}.$$

Let us prove that $\sup E = T$. Firstly, this set is nonempty, because of the smallness of the initial condition, which imposes $0 \in E$. Furthermore, because of Gronwall's Lemma applied to inequality (2.4.7), we will prove *by contradiction* that $\sup E = T$.

Assume indeed that $\sup E = t^* < T$. Then, using (2.4.7) for $t = t^*$, and the following inequality

$$\mathcal{F}_{t^*}(\gamma^\varepsilon) \leqslant \frac{\eta}{2C_2} + \frac{t^*\eta}{4TC_2} \leqslant \frac{3}{4}\frac{\eta}{C_2},$$

gives

$$\frac{\mathrm{d}}{\mathrm{d}t}\mathcal{F}_t(\gamma^\varepsilon)_{|t=t^*} \leqslant \frac{\mathcal{F}_{t^*}(\gamma^\varepsilon)}{\varepsilon}(C_2\mathcal{F}_{t^*}(\gamma^\varepsilon) - \eta) + \varepsilon\, C_1 \leqslant -\frac{\eta\,\mathcal{F}_{t^*}(\gamma^\varepsilon)}{4\varepsilon} + \varepsilon\, C_1.$$

We then use the assumption $\varepsilon_1 C_1 \leqslant \frac{\eta}{8C_2T}$, to get that

$$\frac{\mathrm{d}}{\mathrm{d}t}\mathcal{F}_t(\gamma^\varepsilon)_{|t=t^*} \leqslant \frac{\eta}{8C_2T}.$$

Using the definition of the derivative at time t^* gives that $\sup E > t^*$, which is a contradiction. □

Now let us assume that we have the smallness condition (2.1.5) on the initial condition, with η_0 so small that $\mathcal{F}_0(\gamma^\varepsilon_{in}) \leqslant \frac{\eta}{2C_2}$ holds. The conditions of the previous lemma are thus satisfied and the estimate (2.4.7) rewrites now

$$\frac{\mathrm{d}}{\mathrm{d}t}\mathcal{F}_t(\gamma^\varepsilon) \leqslant \frac{\mathcal{F}_t(\gamma^\varepsilon)}{\varepsilon}(C_2\mathcal{F}_t(\gamma^\varepsilon) - \eta) + \varepsilon\, C_1 \leqslant -\frac{\eta}{4}\frac{\mathcal{F}_t(\gamma^\varepsilon)}{\varepsilon} + \varepsilon\, C_1.$$

The result follows, using Gronwall's Lemma and the equivalence between $\|\cdot\|_{l^2(\mathbb{N},L^2(\mathbb{T}_x))}$ and $\sqrt{\mathcal{F}_t}$, along with Parseval's theorem. □

We conclude this section with the proof of Corollary 1.

Proof of Corollary 1. Taking the scalar-product of (2.3.13) with γ^ε yields

$$\begin{aligned}\varepsilon\,\frac{\mathrm{d}}{\mathrm{d}t}\|\gamma^\varepsilon\|_t^2 - \langle \mathcal{L}\gamma^\varepsilon, \gamma^\varepsilon\rangle_t &= \varepsilon\,\langle \mathcal{S}, \gamma^\varepsilon\rangle_t - \frac{\varepsilon}{2}\sum_{k=0}^{\infty}\langle \partial_t\phi^0\gamma_k^\varepsilon, \gamma_k^\varepsilon\rangle_{L^2_{\eta_t}(\mathbb{T}_x)} + \langle \mathcal{Q}[\gamma^\varepsilon], \gamma^\varepsilon\rangle_t \\ &\leqslant \frac{\varepsilon^2}{2}\|\mathcal{S}\|_t^2 + \left(\frac{1}{2} + \frac{\varepsilon}{2}\|\partial_t\phi^0\|_\infty\right)\|\gamma^\varepsilon\|_t^2 + \langle \mathcal{Q}[\gamma^\varepsilon], \gamma^\varepsilon\rangle_t.\end{aligned}$$

Using the bound (2.4.4) for the quadratic term and integrating in time over $[0, T]$, implies

$$\varepsilon \|\gamma^\varepsilon\|_T^2 + \frac{1}{2}\int_0^T \langle -\mathcal{L}\gamma^\varepsilon(s),\, \gamma^\varepsilon(s)\rangle_s \,\mathrm{d}s \leqslant \varepsilon^2 \sup_{s\in[0,T]} \|S\|_s^2 + \int_0^T C(\|\gamma^\varepsilon(s)\|_s^2 + \|\gamma^\varepsilon(s)\|_s^4)\,\mathrm{d}s$$
$$\leqslant c_1\,\varepsilon^2 + c_2\,\varepsilon,$$

where we injected the result of Theorem 2 to pass from the first line to the second one. The control of the second term of the left-hand side gives the desired result, thanks to Parseval's equality. □

2.5 Numerical investigations

In the rest of this paper we shall be concerned with the introduction of a performant numerical scheme for the resolution of the kinetic problem (2.1.1). In this aim, we firstly present a Newton strategy to compute the solution of the limit problem (2.1.4). Then a Hermite-Fourier spectral approach is proposed for the resolution of the kinetic equation (2.1.1). And finally, we use these schemes to investigate further the mathematical results obtained in the previous parts.

2.5.1 Numerical Scheme for the Limit problem

In this subsection we present the methodology chosen to discretize the limit problem (2.1.4), called Poisson-Boltzmann model, task which is not so trivial due to the occurrence of the exponential term. Our numerical scheme is an iterative method based on Newton's procedure.

In more details, the nonlinear elliptic limit problem (2.1.4) for the electric potential ϕ^* reads

$$-\partial_{xx}\phi^* + \mathfrak{m}\frac{e^{\phi^*(t,x)}}{\displaystyle\int_{\mathbb{T}_x} e^{\phi^*(t,y)}\,\mathrm{d}y} = n_i(t,x), \qquad \forall x \in \mathbb{T}_x\,, \tag{2.5.1}$$

associated with periodic boundary conditions in x and where $t \in [0, T]$ is a fixed parameter. Given ϕ^*, the corresponding limiting electron density is given by Boltzmann's relation $n^*(t,x) = \mathfrak{m}\frac{e^{\phi^*(t,x)}}{\int_{\mathbb{T}_x} e^{\phi^*(t,y)}\,\mathrm{d}y}$. Notice that the solution ϕ^* of (2.5.1) is uniquely defined up to an additive constant, we shall fix it by imposing $\int_{\mathbb{T}_x} \phi^*(t,x)\,\mathrm{d}x \equiv 0$. In the aim to solve (2.5.1), the first idea could be a naive fixed point strategy of the following form : given ϕ^j, compute the next iteration ϕ^{j+1} via

$$-\partial_{xx}\phi^{j+1}(t,x) + \mathfrak{m}\,\frac{e^{\phi^j}(t,x)}{\int_{\mathbb{T}_x} e^{\phi^j}(t,y)\,\mathrm{d}y} = n_i(t,x), \qquad \forall j \geqslant 0.$$

This strategy does however not converge, neither with a Fourier nor with a finite difference discretization, and this due to stability reasons brought in by the exponential term.

Instead, our numerical scheme is based on the following semi-implicit procedure

$$-\partial_{xx}\phi^{j+1}(t,x) + \mathfrak{m}\,\frac{e^{\phi^{j+1}}(t,x)}{\int_{\mathbb{T}_x} e^{\phi^j}(t,y)\,\mathrm{d}y} = n_i(t,x), \quad \forall j \geqslant 0, \tag{2.5.2}$$

with a further manipulation to linearize the implicit exponential term. Supposing ϕ^j known, one can write $e^{\phi^{j+1}} = e^{\phi^j}\, e^{\phi^{j+1}-\phi^j}$. Assuming furthermore that two subsequent iterations are sufficiently close, namely assuming that $\|\phi^{j+1} - \phi^j\|_{L^2(\mathbb{T}_x)} \ll 1$, one can approximate

$$e^{\phi^{j+1}-\phi^j} \simeq 1 + \phi^{j+1} - \phi^j,$$

thus leading to the numerical scheme

$$-\partial_{xx}\phi^{j+1} + n^j\phi^{j+1} = n_i - n^j(1-\phi^j), \qquad \text{where} \quad n^j = \mathfrak{m}\,\frac{e^{\phi^j}}{\int_{\mathbb{T}_x} e^{\phi^j(t,y)}\,\mathrm{d}y}. \tag{2.5.3}$$

This last equation can now be solved with either a finite difference scheme or a Fourier spectral method and gives good results as shown in the following.

To illustrate the convergence of our method (2.5.3), let us take the following test case : on a periodic domain $[0, L]$ of length $L = 12$, choose the ion density

$$n_i(x) = k^2\sin(kx) + \frac{e^{\sin(kx)}}{\int_{\mathbb{T}_x} e^{\sin(ky)}\,\mathrm{d}y}, \qquad k = 2\pi/L, \quad \forall x \in [0,L].$$

In this case, the exact solution to the associated nonlinear elliptic problem (2.1.4) is $\phi^*(x) := \sin(kx)$, and hence $n^*(x) = \frac{e^{\sin(kx)}}{\int_{\mathbb{T}_x} e^{\sin(ky)}\,\mathrm{d}y}$.

We choose for this test case a standard second order finite difference discretization of (2.5.3) with several grids Δx, and an initial guess $\phi^{j=0} = 0$. In Figure 2.1, the error on the spatial densities $\|n^j - n^*\|_{L^2(\mathbb{T}_x)}$ (left) and the error on the electric potential (right) are both plotted with respect to the iteration number j. Since the constraint on the asymptotic electric potential $\int_{\mathbb{T}_x}\phi^*\,\mathrm{d}x = 0$ is not necessarily compatible with the various iterations ϕ^j, we plot the L^2-error between the iterated electric potential with rescaled average $\phi^j - \frac{1}{|\mathbb{T}_x|}\int_{\mathbb{T}_x}\phi^j\,\mathrm{d}x$ and the asymptotic electric potential ϕ^*. What can be remarked is that after very few iterations ($j = 3$), the iterative procedure gives an acceptable result, the order of magnitude being negligible when compared to the amplitude of the limit problem solution. Numerically the convergence rate is of order 2 in Δx.

2.5.2 Numerical Scheme for the Kinetic problem with not too small $\varepsilon > 0$

We shall now present a numerical scheme for the resolution of the Vlasov-Poisson-Fokker-Planck system

$$\begin{cases} \partial_t f^\varepsilon + \dfrac{1}{\varepsilon}\,v\,\partial_x f^\varepsilon - \dfrac{1}{\varepsilon}\,E^\varepsilon\,\partial_v f^\varepsilon = \dfrac{1}{\varepsilon}\,\partial_v\left[v\,f^\varepsilon + \partial_v f^\varepsilon\right], \\ -\partial_{xx}\phi^\varepsilon = n_i - n^\varepsilon, \qquad E^\varepsilon = -\partial_x\phi^\varepsilon\,. \end{cases}$$

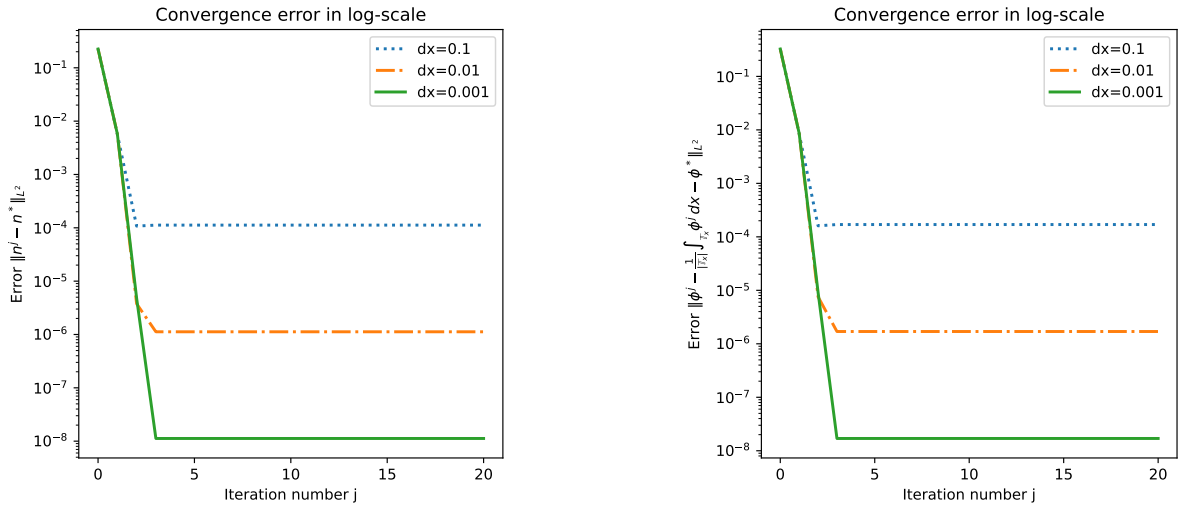

Figure 2.1 – Left: Convergence of the density $n^j = \mathfrak{m}\,\frac{e^{\phi^j}}{\int_{\mathbb{T}_x} e^{\phi^j(y)}\,\mathrm{d}y}$ computed via (2.5.3) towards the exact density n^* of the limit problem (2.1.4). Right: Convergence of ϕ^j - after rescaling its average to 0 - towards the exact electric potential ϕ^*

In the velocity space, we shall make use of a complete, orthogonal Hermite basis to approach the distribution functions (Hermite spectral method). For the space discretization, due to the periodicity, a standard Fourier spectral method is used. In the present section, $\varepsilon \in (0,1]$ is chosen not too small, the numerical procedure requiring a time-step Δt of order ε. In the next section, however, we will adapt this method in such a manner to recover automatically for $\varepsilon \to 0$ the limit problem, and this with an ε-independent mesh (*Asymptotic-Preserving* procedure).

2.5.2.1 Discretization in the velocity variable

Let us start with expanding the electron distribution function $f^\varepsilon(t,x,v)$ as in (2.3.2), and truncate it at $k = N_v - 1$, where N_v is the number of considered Hermite modes. Thus the exact solution $(f^\varepsilon, E^\varepsilon)$ of (2.1.1) is approximated by the couple $(f^\varepsilon_{N_v}, E^\varepsilon_{N_v})$ defined through

$$f^\varepsilon_{N_v}(t,x,v) := \sum_{k=0}^{N_v-1} \alpha^\varepsilon_k(t,x)\,\psi_k(v)\,, \quad E^\varepsilon_{N_v} = -\partial_x \phi^\varepsilon_{N_v}, \quad -\partial_{xx}\phi^\varepsilon_{N_v} = n_i - \alpha^\varepsilon_0, \tag{2.5.4}$$

where $\{\psi_k\}_{k\in\mathbb{N}}$ are the Hermite basis-functions defined in (2.3.3). In this section the constraint $\int_{\mathbb{T}_x} \phi^\varepsilon_{N_v}\,\mathrm{d}x \equiv 0$ determines uniquely $\phi^\varepsilon_{N_v}$, for all $\varepsilon \geqslant 0$. The coefficients $\alpha^\varepsilon_k(t,x)$ are still to be determined by solving the coupled PDE-system

$$\varepsilon\,\partial_t \alpha^\varepsilon_k(t,x) + \sqrt{k}\,\partial_x \alpha^\varepsilon_{k-1} + \sqrt{k+1}\,\partial_x\,\alpha^\varepsilon_{k+1} + E^\varepsilon(t,x)\,\sqrt{k}\,\alpha^\varepsilon_{k-1} + k\alpha^\varepsilon_k = 0\,, \quad \forall k \in \{0,\dots,N_v-1\}, \tag{2.5.5}$$

where we set $\alpha^{\varepsilon}_{-1} = \alpha^{\varepsilon}_{N_v} = 0$. For the sake of notational simplicity, we denote from now on again $(f^{\varepsilon}, E^{\varepsilon})$, instead of $(f^{\varepsilon}_{N_v}, E^{\varepsilon}_{N_v})$ for the truncated solution. This system is a closed system, coupled with Poisson's equation, and is well posed in $(L^2([0,T]\times\mathbb{T}_x))^{N_v}\times L^{\infty}([0,T]\times\mathbb{T}_x)$. Letting formally ε tend towards zero in (2.5.5) yields the PDE-hierarchy

$$\begin{cases} \sqrt{k}\,\partial_x\alpha^0_{k-1} + \sqrt{k+1}\,\partial_x\,\alpha^0_{k+1} + E^0(t,x)\,\sqrt{k}\,\alpha^0_{k-1} + k\alpha^0_k = 0 \\ -\partial_{xx}\phi^0 = n_i - \alpha^0_0, \qquad E^0 = -\partial_x\phi^0\,. \end{cases} \tag{2.5.6}$$

By equivalence with the Limit-model (2.1.4), one proves the well-posedness of this PDE-system, with a solution satisfying $\alpha^0_k \equiv 0$ for $k \neq 0$ and α^0_0 solution of the limit-problem

$$\begin{cases} \partial_x\alpha^0_0 - \partial_x\phi^0\,\alpha^0_0 = 0\,, \\ -\partial_{xx}\phi^0 = n_i - \alpha^0_0, \qquad E^0 = -\partial_x\phi^0\,, \end{cases} \tag{2.5.7}$$

associated with the constraint of zero average.

2.5.2.2 Discretization in the space variable

Dealing with a periodic framework in $x \in \mathbb{T}_x$, one can treat the discretization in the space variable via a Fourier spectral method. One approximates thus the Hermite coefficients $\alpha^{\varepsilon}_k(t,x)$ and the potential function $\phi^{\varepsilon}(t,x)$ as follows

$$\alpha^{\varepsilon}_k(t,x) \simeq \alpha^{\varepsilon,N_x}_k(t,x) := \sum_{l=-N_x}^{N_x} \alpha^{\varepsilon}_{k,l}(t)\,e^{\frac{2\pi\mathbf{i}\,lx}{L}}\,, \qquad \phi^{\varepsilon}(t,x) \simeq \phi^{\varepsilon}_{N_x}(t,x) := \sum_{l=-N_x}^{N_x} \beta^{\varepsilon}_l(t)\,e^{\frac{2\pi\mathbf{i}\,lx}{L}}\,, \tag{2.5.8}$$

with $L := |\mathbb{T}_x|$ and $2N_x+1$ considered Fourier modes. Again, for notational simplicity, we drop the N_x exponent, keeping in mind that all of the considered numerical quantities have their Fourier decomposition truncated at order N_x.

We decompose the ion and electron density as

$$n_i(x) := \sum_{l=-N_x}^{N_x} \widehat{n_{i,l}}\,e^{\frac{2\pi\mathbf{i}\,lx}{L}}\,, \qquad n^{\varepsilon}(t,x) = \alpha^{\varepsilon}_0(t,x) := \sum_{l=-N_x}^{N_x} \alpha^{\varepsilon}_{0,l}(t)\,e^{\frac{2\pi\mathbf{i}\,lx}{L}}\,,$$

and plug this decomposition into (2.5.5), yielding the following coupled ODE system

$$\begin{aligned} \varepsilon\,{\alpha^{\varepsilon}_{k,l}}'(t) + \left(\frac{2\pi\mathbf{i}\,l}{L}\right)\,\sqrt{k}\,\alpha^{\varepsilon}_{k-1,l}(t) + \left(\frac{2\pi\mathbf{i}\,l}{L}\right)\,\sqrt{k+1}\,\alpha^{\varepsilon}_{k+1,l}(t) + k\,\alpha^{\varepsilon}_{k,l}(t) \\ -\sqrt{k}\sum_{\substack{m=-N_x \\ l-m\in\{-N_x,\dots,N_x\}}}^{N_x} \left(\frac{2\pi\mathbf{i}\,(l-m)}{L}\right)\,\beta^{\varepsilon}_{l-m}(t)\,\alpha^{\varepsilon}_{k-1,m}(t) = 0\,, \end{aligned} \tag{2.5.9}$$

for $k \in \{0, \cdots, N_v - 1\}$ and $l \in \{-N_x, \cdots, N_x\}$. The nonlinear coupling is due to Poisson's equation

$$\left(\frac{2\pi l}{L}\right)^2 \beta_l^\varepsilon(t) = \widehat{n_{i,l}} - \alpha_{0,l}^\varepsilon(t)\,, \quad \forall l \in \{-N_x, \cdots, N_x\}\,,$$

and we impose $\beta_l^\varepsilon = 0$ if $l \notin \{-N_x, \cdots, N_x\}$, and also for $l = 0$ due to the potential constraint of zero mean. .

Thus, using a Hermite method in the variable v and a Fourier method in the variable x leads to a system of ODE equations for the computation of the Hermite-Fourier coefficients $\alpha_{k,l}^\varepsilon(t)$. Coupling between the different modes arises from particle streaming as well as from the non-linear term involving the electric potential. To simplify the notation, let us introduce the vector $W^\varepsilon(t) := \{\alpha_{k,l}^\varepsilon(t)\}_{k,l}$ and rewrite this ODE system (2.5.9) simply as

$$\varepsilon \frac{\mathrm{d}}{\mathrm{d}t} W^\varepsilon(t) + B(t)\, W^\varepsilon(t) = 0\,, \quad \forall t \in [0, T]\,, \tag{2.5.10}$$

where we underline that the matrix $B(t)$ depends on W.

Remark 7. Usually, when dealing with spectral methods, and notably for the Vlasov-Poisson equation, Gibbs effects appear due to filamentation. Due to particle streaming, there is a coupling between various Hermite modes, propagating perturbations towards low order modes. This effect is called recurrence. To solve these problems, a filter is usually applied on high-order modes. Thankfully, as opposed to Vlasov-Poisson system, in the Vlasov-Poisson-Fokker-Planck case the collision operator has a strong smoothing effect, and strongly dissipates high order modes. The mixing properties of the transport operator permits to propagate this gain of regularity in the space variable, and therefore filamentation does not occur. Because of these facts, it is not necessary to apply a filter in order to damp artificially high-order Hermite-Fourier coefficients.

2.5.2.3 Discretization in time

The last step concerns the time-discretization of the ODE system (2.5.10). In the following, we will omit the exponent ε, and we dedicate the exponent index to the iteration in time.

Let us discretize homogeneously the time interval $[0, T]$ into N_t sub-intervals via $t^j := j\,\Delta t$ where $j = 0, \ldots, N_t$, and $\Delta t := T/N_t$, and approximate (2.5.10) via the Euler implicit scheme

$$\varepsilon \frac{W^{j+1} - W^j}{\Delta t} + B^{j+1} W^{j+1} = 0\,, \tag{2.5.11}$$

where B^j is given through $\beta_l^j \simeq \beta_l(t^j)$, computed with the help of Poisson's equation, in other words

$$\left(\frac{2\pi l}{L}\right)^2 \beta_l^j = \widehat{n_{i,l}(t_j)} - \alpha_{0,l}^j\,, \quad \forall l \in \{-N_x, \cdots, N_x\}\backslash\{0\}\,, \quad \beta_0^j := 0. \tag{2.5.12}$$

Thus we observe that for every time iteration of (2.5.11) we have to solve a nonlinear equation and for its resolution we use a fixed point technique. Fix $j \in \{0, \dots, N_t\}$ and start the fixed point procedure by setting $W^{j,0} := W^j$. Then we construct an iterative sequence $\{W^{j,m}\}_{m\in\mathbb{N}}$ via

$$\varepsilon \frac{W^{j,m+1} - W^j}{\Delta t} + B^{j,m} W^{j,m+1} = 0\,, \quad \forall m \in \mathbb{N}.$$

We observe numerically that the sequences $\{W^{j,m}\}_{m\in\mathbb{N}}, \{B^{j,m}\}_{m\in\mathbb{N}}$ converge, as $m \to \infty$, towards the unique fixed point (W^{j+1}, B^{j+1}) solution of (2.5.11). In practice only a few $k^* = 3$ iterations are necessary to reach a close enough approximation of the requested fixed point, and we therefore set $B^{j+1} := B^{j,k^*}$ as well as $W^{j+1} := W^{j,k^*}$. The fully discretized system (2.5.11) ensures the conservation of mass, like its continuous counterpart (2.1.1), as shown in the next Proposition.

Proposition 2.5.1 (**Mass conservation**). For any $N_x, N_v, N_t > 1$, $\varepsilon > 0$, consider the solution $\{(W^j, \beta^j)\}\}_{0\leqslant j\leqslant N_t}$ of the approximate system (2.5.11). Then the mass is preserved, namely, if we denote as before $W^j = \{\alpha^j_{k,l}\}_{\substack{0\leqslant k\leqslant N_v,\\ -N_x\leqslant l\leqslant N_x}}$, we have the following **conservation of mass** property

$$\alpha^j_{0,0} = \alpha^{in}_{0,0}, \quad \forall j \in \{0, \dots, N_t\}.$$

Proof. Denote the vector $e_{0,0} := {}^t[e_0, 0_{2N_x+1}, \cdots 0_{2N_x+1}]$, where $e_0 := {}^t[0, \cdots, 0, 1, 0, \cdots, 0]$ is a vector whose $(N_x + 1)^{th}$ coordinate is 1. In other terms, the vector $e_{0,0}$ is the vector of the canonical basis associated to the average in space and velocity in our Hermite-Fourier framework.

The property is then a simple consequence of the fact that $e_{0,0}$ is in the kernel of B^j, for all $j \in \mathbb{N}$ by construction : the $(N_x + 1)^{th}$ column of B^j is zero. □

2.5.3 Numerical investigation and validation of the numerical scheme

We shall now perform some numerical simulations based on the scheme (2.5.11)-(2.5.12) detailed above, in order to approximate the particle distribution function of (2.1.1). In the first test case, we will study the case of a time independent ion density, and the second test case will focus on the specificities due to a time-dependent ion density. The numerical procedure (2.5.11)-(2.5.12) will be validated thanks to the mathematical analysis performed in the first part of this paper, and more specifically thanks to the convergence results of Theorem 2.

2.5.3.1 Test case 1 : time-independent ion density

In this subsection, we choose to take the following space homogeneous two-stream initial condition for the electron distribution function

$$f_0(x, v) := \frac{1}{7\sqrt{2\pi}} \left(2 + 5v^2\right) e^{-v^2/2} = \psi_0(v) + \frac{5\sqrt{2}}{7}\psi_2(v), \quad \forall (x, v) \in [0, L] \times \mathbb{R}_v\,, \tag{2.5.13}$$

and fix the following background ion density

$$n_i(x) = 1 + \kappa \left[\frac{\cos(2kx) + \cos(3kx)}{1.2} + \cos(kx) \right], \quad \forall x \in [0, L], \tag{2.5.14}$$

where $k = 2\pi/L$, $L = 12$, and $\kappa = 0,4$. Recall that in this context, the limit $\varepsilon \to 0$ is equivalent to the long-time asymptotics $t \to \infty$.

We plot in Figure 2.2 some snapshots in the (x, v) phase-space of the particle density function f^ε at several instants and for a fixed $\varepsilon = 0.01$. As one can see, the particle density function approaches very rapidly a distribution close to a Maxwellian ($t = 0.005$) in the velocity space. It is only afterwards that the mass starts to be distributed by the transport operator also in the x direction. In the long-time limit, the distribution function approaches finally the Maxwell-Boltzmann equilibrium, as will be also shown in the following plots. Remark here that due to the collision term, the plots in Figure 2.2 are smoothed out and the filamentation usually observed in such kind of simulations is here not observable.

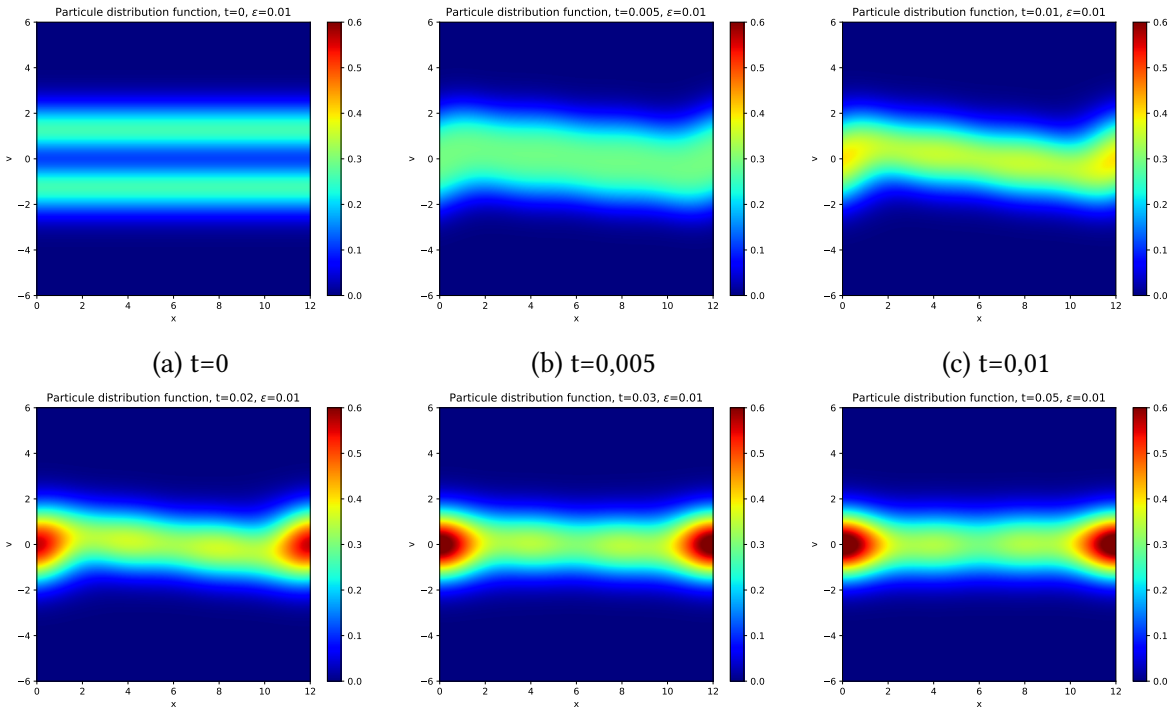

(a) t=0 (b) t=0,005 (c) t=0,01

(d) t=0,02 (e) t=0,03 (f) t=0,05

Figure 2.2 – Time-evolution of the particle distribution function f^ε solution of (2.1.1), for $\varepsilon = 0.01$, $N_v = 60$, $N_x = 40$, $\Delta t = \varepsilon/40$.

In Figure 2.3 we displayed the time evolution of the spatial density n^ε and of the electric potential ϕ^ε. Observe that these quantities converge, as $t \to \infty$, towards the solution of the limit problem (2.1.4) computed thanks to Newton's procedure (2.5.3) and plotted also on the Figure.

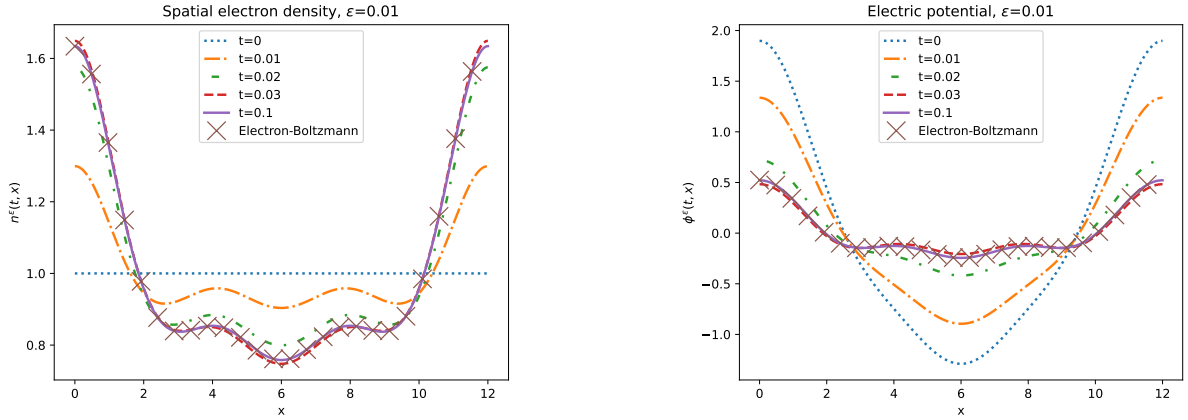

(a) n^ε (b) ϕ^ε

Figure 2.3 – Snapshots at various instants of the spatial density n^ε and the electric potential ϕ^ε corresp. to the solution of (2.1.1), for $\varepsilon = 0.01$, $N_v = 60$, $N_x = 40$. The X markers correspond to the Electron-Boltzmann relation computed thanks to (2.5.3).

Next we performed several simulations for different values of $\varepsilon \in \{0.1, 0.005\}$, and plotted in Figure 2.4 the evolution over time of the macroscopic error $\|n^\varepsilon \mathcal{M} - n^0 \mathcal{M}\|^2_{L^2_\sigma}$, the microscopic error $\|f^\varepsilon - n^\varepsilon \mathcal{M}\|^2_{L^2_\sigma}$ and the total error $\|f^\varepsilon - n^0 \mathcal{M}\|^2_{L^2_\sigma}$. The asymptotic density n^0 is computed thanks to our Newton procedure (2.5.3) discretized with a finite difference method. Notice that in Figure 2.4b the macroscopic error decreases quickly before saturating at a value of approximately 10^{-10}. The saturation occurs at the order of magnitude of the error obtained by the limit problem procedure (2.5.3) (see Figure 2.1 for this saturation). This numerical convergence matches that of Theorem 2 and therefore supports the validity of our numerical scheme (2.5.11)-(2.5.12). Notice also that letting ε become smaller is, in this situation, nothing else than accelerating the time, such that Figure 2.4a is a zoom of Figure 2.4b, showing more details in the initial layer. This Figure 2.4a permits to illustrate the effects of the struggle between the transport operator and the collision operator during the transient regime. The convergence towards the equilibrium arises iteratively, the collision operator reduces firstly the microscopic error at the price of a small increase of the macroscopic error, and then the transport operator becomes predominant, decreasing the macroscopic error at the price of an increased microscopic error. This is related to what is called (for instance in [Vil09]) the interplay between the dissipation introduced by the collision operator, and the conservative, mixing role played by the nonlinear, kinetic transport.

In Figure 2.5 we plotted the norms of several Hermite modes, thus investigating further the behaviour of the microscopic error of Figure 2.4 by decomposing it in several modes.

One can see, as expected from Theorem 2, that the norm of the first coefficient α_0 does not vanish in time. Indeed, we have seen in Figure 2.4 that it converges towards the solution of the

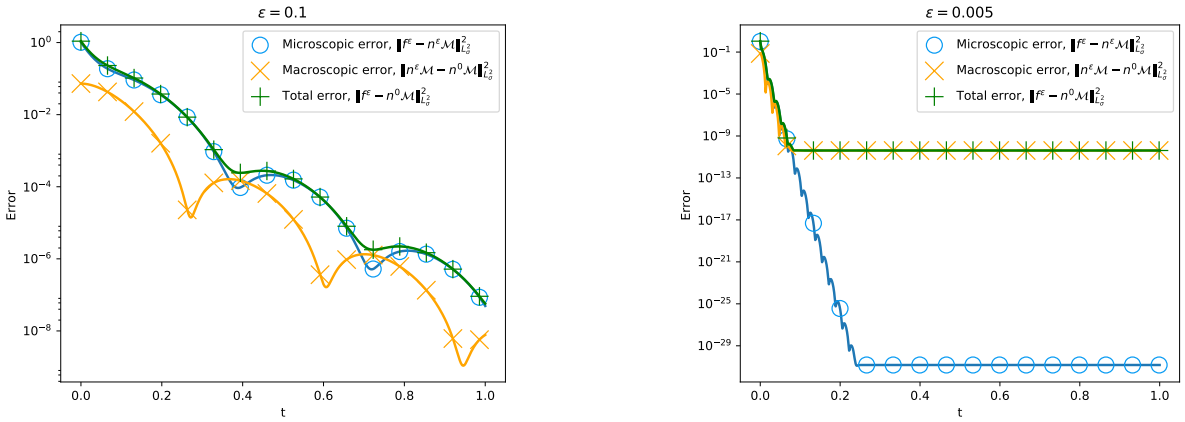

(a) ε=0.1 (b) ε=0.005

Figure 2.4 – Convergence of the particle distribution function solution of (2.1.1) over time, for two different ε-values and $N_v = 20$, $N_x = 28$, $\Delta t = \varepsilon/35$.

limit problem. We can also notice that although the Hermite mode α_2 has a greater importance than the others at the initial time, it is quickly damped and becomes then smaller in L^2_x-norm than the coefficient α_1. Finally, due to the particle streaming induced by the transport operator, even the modes that were initially zero (namely, all of them, except α_0 and α_2), increase slightly during an initial layer before converging again towards zero.

One may wonder if this initial layer is actually of size ε in time. To investigate this, we underline that this initial layer is exactly the reason of a convergence of order $\mathcal{O}(\sqrt{\varepsilon})$ for all of the Hermite modes in (2.1.7), when considering the $L^2_{dt}L^2_\sigma-$norm. To see this, one can integrate in time the result of Theorem 2, yielding, after applying the square root

$$\|f^\varepsilon - n^0\mathcal{M}\|_{L^2((0,T);L^2_\sigma(\mathbb{T}_x\times\mathbb{R}_v))} \leqslant \sqrt{\varepsilon}\,\|f^\varepsilon_{in} - n^0_{in}\mathcal{M}\|_{L^2_\sigma(\mathbb{T}_x\times\mathbb{R}_v)}\sqrt{C_0\left[1-e^{-\frac{C_1 T}{\varepsilon}}\right]} + \varepsilon\sqrt{C_2\,T},$$
$$\forall \varepsilon \leqslant \varepsilon_0, \forall t \in [0,T].$$

As one can see, the dominant term is the first one, namely, the term associated with the initial layer, and is of order $\mathcal{O}(\sqrt{\varepsilon})$ as $\varepsilon \to 0$. In this specific case of a time-independent ion density function n_i, the constant C_2 is even zero, such that we remain only with the initial layer term. The object of Figure 2.6, is therefore to confirm the theoretical expected rate of convergence of $\mathcal{O}(\sqrt{\varepsilon})$, which in turn confirms the size of the initial layer of our numerical scheme (2.5.11).

Corollary 1 addresses the behaviour of the Hermite coefficients with respect to their index k in the Hermite hierarchy. The object of Figure 2.7 is to investigate this rate of $\mathcal{O}(\sqrt{k^{-1}})$. As one can see, for small $\varepsilon \ll 1$, the convergence with respect to k is rather of order $\mathcal{O}(e^{-rk})$, with $r \simeq 0.627$. The hypocoercive study performed in this paper was in a general L^2_σ setting. Following the approach of [HJ12] would yield a more accurate rate of convergence of order

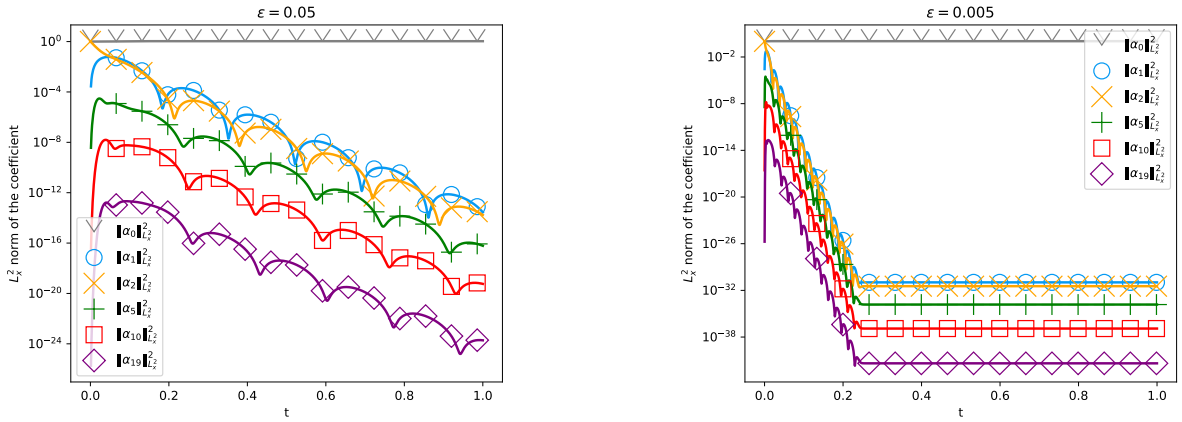

(a) ε=0.05 (b) ε=0.005

Figure 2.5 – Convergence of various Hermite modes of the solution of (2.1.1) over time, $N_v = 20$, $N_x = 28$, $\Delta t = \varepsilon/35$, for various ε.

$\mathcal{O}(k^{-s/2})$, for H^s_σ initial data. Finding rigorous evidence of an exponential rate is however an open question. Finally, one can notice that the very last computed Hermite coefficient seems not to follow this exponential trend. This is a numerical artefact due to the brutal truncation of the Hermite hierarchy in (2.5.5).

2.5.3.2 Test case 2 : time-dependent ion density

In this test case, we choose the following space inhomogeneous two-stream initial condition

$$f_{in}(x,v) := \left(\frac{4}{7} + 0.4\cos(2kx) + \frac{3}{7}v^2\right)\frac{e^{-v^2/2}}{\sqrt{2\pi}} = [1 + 0.4\cos(2kx)]\psi_0(v) + \frac{3\sqrt{2}}{7}\psi_2(v), \quad (2.5.15)$$

and a time-dependent ion density n_i, defined as follows

$$n_i(t,x) := 1 + \kappa\sin(4\pi t)\left[\frac{\cos(2kx) + \cos(3kx)}{1.2} + \cos(kx)\right], \quad \forall x \in [0,L], \quad (2.5.16)$$

with $k = 2\pi/L$, $L = 12$, and $\kappa = 0,3$.

This time, the result of Theorem 2 still predicts an initial layer of size ε in time, but also an error of size ε^2 during the permanent regime. This is closely related to the fact that, as underlined in Remark 6, if n_i depends on time, the constant C_2 in Theorem 2 is non-zero and depends only on $\partial_t n^0$. This effect is illustrated in Figure 2.8. Notice also that the error schrinks dramatically at the times at which $\partial_t n_i$ becomes zero (namely at times $t = 1/8, 3/8, 5/8, 7/8$).

We also plotted in Figure 2.9a the rate of convergence of various Hermite coefficients with respect to ε, and confirm again the rate of convergence $\mathcal{O}(\sqrt{\varepsilon})$ of (2.1.7). We see that our scheme renders accurately the order of magnitude of the initial layer even when the permanent regime is nontrivial.

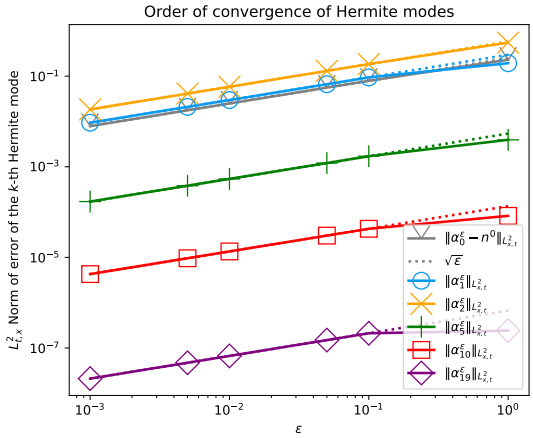

Figure 2.6 – Convergence in ε of the $L^2_{t,x}$-norm of the Hermite modes of the solution of (2.1.1), for $N_v = 20$, $N_x = 28$, $\Delta t = \varepsilon/35$. The dotted lines represent a behaviour of the order of $\mathcal{O}(\sqrt{\varepsilon})$.

One can then wonder if the size of the permanent regime is accurately computed. For this, note that our Theorem 2 predicts that

$$\sup_{t\in[s,T]} \|f^\varepsilon(t) - f^0(t)\|^2_{L^2_\sigma} = \mathcal{O}(\varepsilon^2), \qquad \text{as } \varepsilon \to 0, \quad \forall\, 0 < s < T.$$

We plotted in Figure 2.9b the macroscopic error $\sup_{t\in[T/2,T]} \|n^\varepsilon(t)\mathcal{M} - n^0(t)\mathcal{M}\|^2_{L^2_\sigma}$ and the microscopic one $\sup_{t\in[T/2,T]} \|n^\varepsilon(t)\mathcal{M} - n^0(t)\mathcal{M}\|^2_{L^2_\sigma}$ in the permanent regime. As one can see, they are both numerically of order $\mathcal{O}(\varepsilon^2)$, and we conclude that indeed the scheme renders accurately the permanent regime.

Finally we mention that the numerical conservation of mass is guaranteed up to machine precision for reasonably small $\varepsilon > 0$ (up to about $\varepsilon \simeq 10^{-3}$).

2.6 Asymptotic preserving approach

The focus of this section is the investigation of the asymptotic properties of our numerical scheme (2.5.11)-(2.5.12) when ε becomes smaller and smaller. In order to get an *Asymptotic-preserving* (AP) scheme which shall permit the choice of an ε-independent time step Δt, we shall slightly reformulate the previous scheme.

2.6.1 Enforcing the numerical mass conservation

Our first problem in the $\varepsilon \to 0$ limit concerns the numerical mass conservation. The constraint $\int_{\mathbb{T}_x} n^\varepsilon(t,x)\,\mathrm{d}x \equiv \mathfrak{m}$ shall be valid for all $\varepsilon \geqslant 0$, in particular also in the limit. However one remarks that solving (2.5.11) for $\varepsilon = 0$ loses this mass conservation. Reformulated in other words, the condition number of the matrix $(\varepsilon I_{N_v(2N_x+1)} + \Delta t\, B^{j+1})$ is of order ε^{-1}.

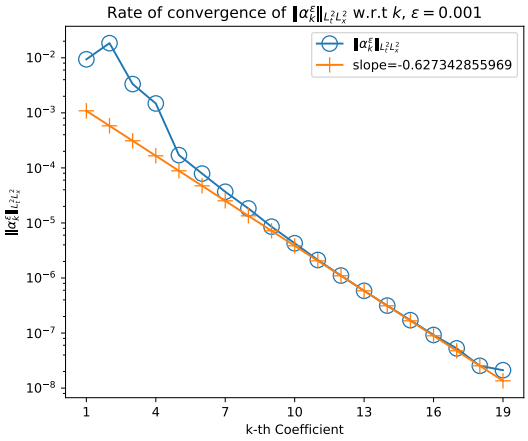

Figure 2.7 – $L^2_{t,x}$-norm of the Hermite coefficients of the solution of (2.1.1), as a function of k (log-scale) and for $N_v = 20$, $N_x = 28$, $\Delta t = \varepsilon/35$, $\varepsilon = 0.001$.

To cope with this problem, we can multiply the $(N_x + 1)^{th}$ - line of the system

$$(\varepsilon I_{N_v(2N_x+1)} + \Delta t\, B^{j+1})\, W^{j+1} = \varepsilon\, W^j\,,$$

by ε^{-1}, line which corresponds to the mass conservation. This leads to an equivalent mathematical problem for $\varepsilon > 0$, all the while numerically guaranteeing a non singular condition number of the matrix, and being compatible with the limit $\varepsilon \to 0$. Heuristically, we enforced the numerical conservation of mass, for all $\varepsilon \geqslant 0$.

2.6.2 Difficulties related to the computation of the limit problem

Now that we reformulated our problem so that the limit $\varepsilon \to 0$ is regular, we focus on the accuracy of our scheme when ε becomes zero. For the sake of the exposition, we shall omit here to underline again the multiplication by ε^{-1} of the $(N_x + 1)^{th}$ line of system (2.5.11), but we shall keep in mind that the conservation of the mass must be ensured for the matrices to be invertible in the limit $\varepsilon \to 0$.

We plotted in Figure 2.10 the evolution over time of the microscopic and macroscopic errors for the solution of (2.1.1) thanks to procedure (2.5.11)-(2.5.12), with the additional enforcing of the mass conservation, but this time, we took $\Delta t > \varepsilon$. Compare now both Figures 2.10 and 2.8d, the only different parameter being the time-step. As one can see, in Figure 2.10, the microscopic part of the particle distribution function gets immediately damped, as expected, but the macroscopic part fails to converge towards the desired limit problem. The convergence problem therefore lies at the macroscopic level. To investigate this problem, we examine our numerical procedure when ε becomes smaller.

The procedure obtained when taking $\varepsilon = 0$ in (2.5.11)-(2.5.12) is a naive fixed point technique

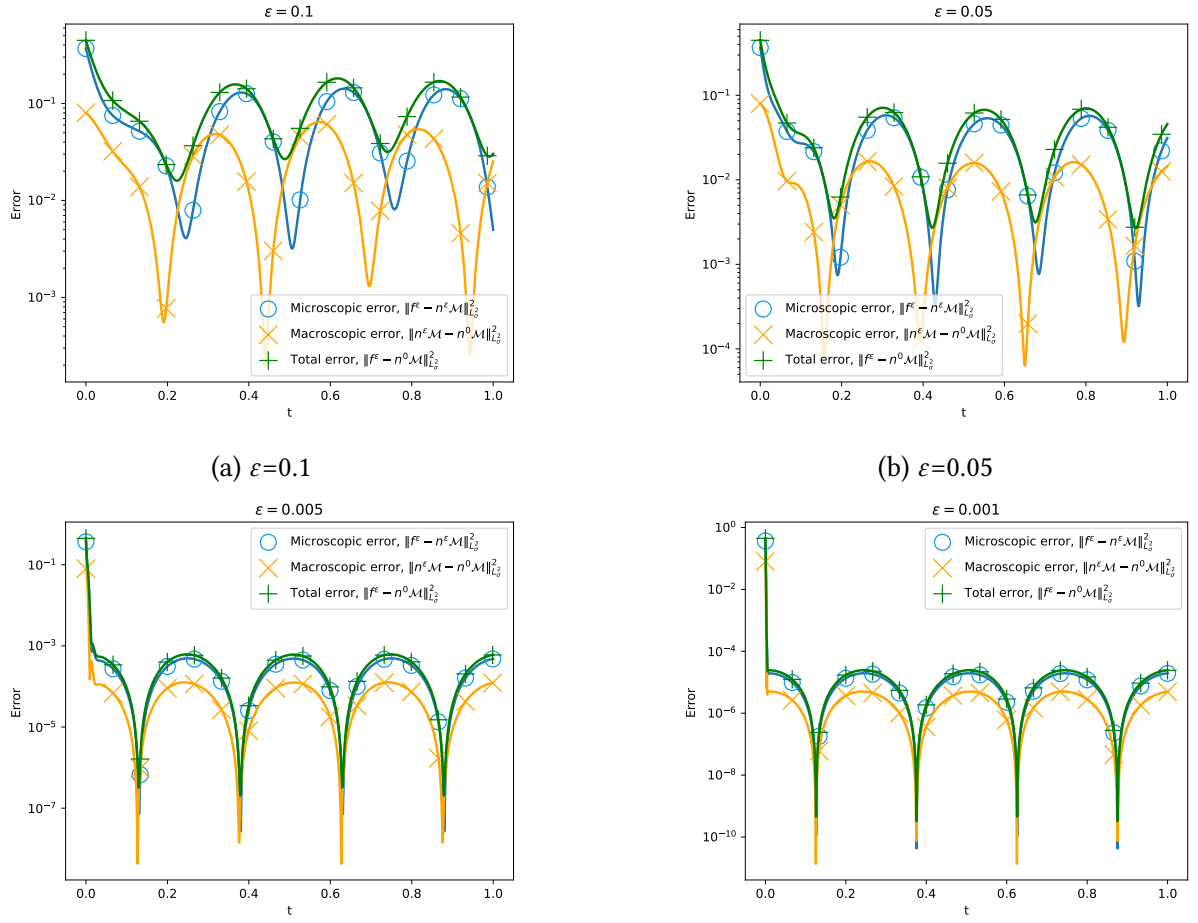

(a) ε=0.1

(b) ε=0.05

(c) ε=0.005

(d) ε=0.001

Figure 2.8 – Convergence of the particle distribution function solution of (2.1.1) over time, $N_v = 20$, $N_x = 28$, $\Delta t = \varepsilon/35$, for various ε.

for the resolution of

$$B^{j+1} W^{j+1} = 0. \tag{2.6.1}$$

Sadly, this procedure does not converge, and for this reason, neither does our numerical scheme (2.5.11)-(2.5.12) when $\varepsilon < \Delta t$. Actually, the same difficulty arises when trying to solve the limit problem (which is macroscopic) not by a Newton procedure, as we did in (2.5.3), but with a naive fixed point of the form

$$\begin{cases} \partial_x n^j - \partial_x \phi^j n^j = 0, \\ -\partial_{xx} \phi^{j+1} = n_i - n^j, \end{cases}$$

with either a Fourier or a finite difference discretization (see Section 2.5.1).

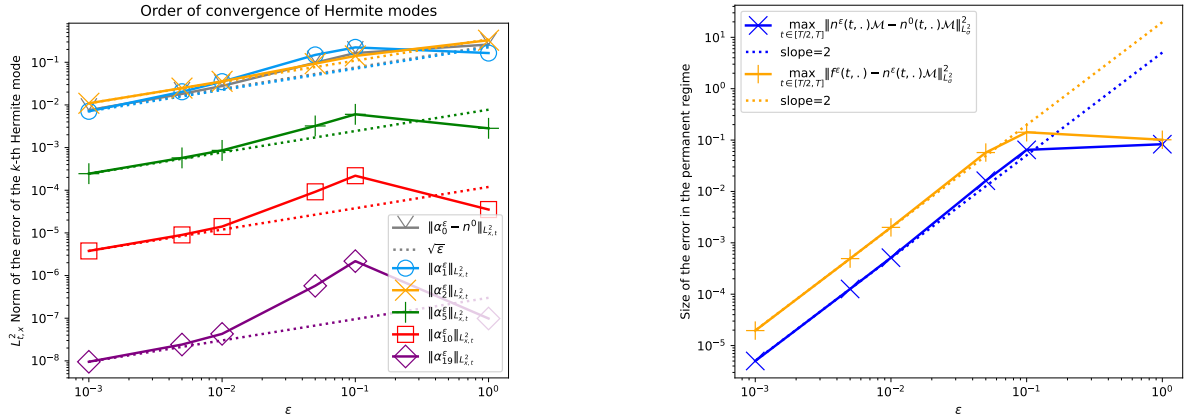

(a) (b)

Figure 2.9 – $N_v = 20$, $N_x = 28$, $\Delta t = \varepsilon/35$ (A) $L^2_{t,x}-$convergence of various Hermite modes, the dotted lines represent a behaviour of $\mathcal{O}(\sqrt{\varepsilon})$. (B) Size of the (squared) error in the permanent regime, the dotted lines represent a behaviour of $\mathcal{O}(\varepsilon^2)$.

In order to cope with this difficulty, rather than computing directly a numerical approximation of the full distribution function f^ε, we are going to use the decomposition introduced in the proof of Theorem 2, namely in the asymptotic and the fluctuation part.

2.6.3 Separate computation of the fluctuation and the limit part

Thanks to the procedure (2.5.3), we have access to the limit particle density function f^0 given by the resolution of the limit problem (2.1.4). Now, rather than directly computing the particle distribution function f^ε, we decide to decompose $f^\varepsilon = f^0 + g^\varepsilon$ and to expand the fluctuating part in the Hermite basis as

$$g^\varepsilon(t,x,v) = \sum_{k=0}^{N_v-1} \gamma_k^\varepsilon(t,x)\,\psi_k(v),$$

with the coefficients $\{\gamma_k\}_k$ satisfying the following truncated PDE-system

$$\begin{cases} \varepsilon\,\partial_t\gamma_0^\varepsilon + \partial_x\gamma_1^\varepsilon = -\varepsilon\partial_t n^0, \\ \varepsilon\,\partial_t\gamma_1^\varepsilon + \partial_x\gamma_0^\varepsilon - \partial_x\phi^\varepsilon\gamma_0^\varepsilon + \sqrt{2}\partial_x\gamma_2^\varepsilon - \partial_x\varphi^\varepsilon n^0 + \gamma_1^\varepsilon = 0, \\ \varepsilon\,\partial_t\gamma_k^\varepsilon + \sqrt{k}\,\partial_x\gamma_{k-1}^\varepsilon - \sqrt{k}\,\partial_x\phi^\varepsilon\gamma_{k-1}^\varepsilon + \sqrt{k+1}\,\partial_x\gamma_{k+1}^\varepsilon + k\gamma_k^\varepsilon = 0\,, \quad \forall k\in\{2,\dots,N_v-1\} \\ -\partial_{xx}\varphi^\varepsilon = -\gamma_0^\varepsilon, \qquad \phi^\varepsilon = \phi^0 + \varphi^\varepsilon, \end{cases} \tag{2.6.2}$$

with $\gamma_{-1} = \gamma_{N_v} \equiv 0$. As we did before, we discretize this equation (2.6.2) with an implicit Euler-Fourier spectral approach. Thus our AP-strategy is based on the resolution of (2.5.3) for

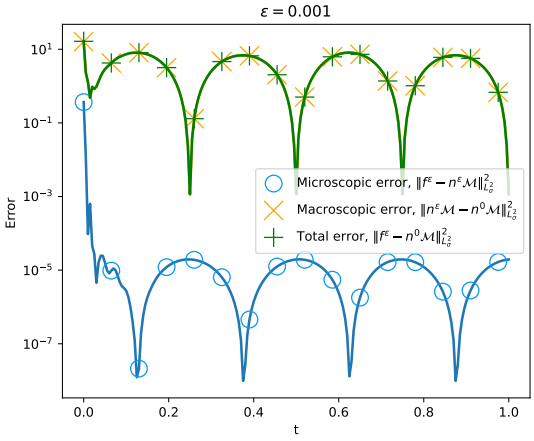

Figure 2.10 – Default of convergence of the particle distribution function solution of (2.1.1) (method (2.5.11)) for $\Delta t = 0.005 > \varepsilon = 0.001$ and $N_v = 20$, $N_x = 28$, $\Delta t = 0.005$

the macroscopic part and (2.6.2) for the microscopic part.

2.6.4 Analysis of the AP-Scheme

Let us now study the AP properties of the scheme based on the fluctuation computation. An AP-scheme should be stable and uniformly accurate with respect to the small parameter ε, for a fixed mesh.

To illustrate that this is the case, we first start by fixing a time step $\Delta t = 0.005$. In Figure 2.11, we computed the spatial density of electrons n^ε and the electric potential ϕ^ε for various values of ε. We chose in this case to take the time-independent ion spatial density n_i as in (2.5.14), and the associated initial condition (2.5.13). In this case the $\varepsilon \to 0$ limit is equivalent to the $t \to \infty$ limit, which explains the resemblance between Figures 2.11 and 2.3. In Figure 2.11, the scheme has the correct behaviour even when $\varepsilon \ll \Delta t$.

Let us now investigate the accuracy of our numerical scheme. For this, we take the spatial ion density n_i to be time-dependent, as given by (2.5.16), and the associated initial condition (2.5.15). Firstly, we test our numerical scheme on its ability to successfully pass the initial layer. As we reminded before, the solution f^ε of (2.1.1) should verify the following uniform estimate in the permanent regime

$$\sup_{t\in[\Delta t,T]} \|f^\varepsilon(t) - f^0(t)\|^2_{L^2_\sigma} = \mathcal{O}(\varepsilon^2), \quad \text{as } \varepsilon \to 0, \quad \forall \Delta t > 0.$$

Our Figure 2.12 validates this rate of uniform in time convergence. This shows that our numerical scheme successfully passes the initial layer after a single iteration Δt, even for very small $\varepsilon \ll \Delta t$.

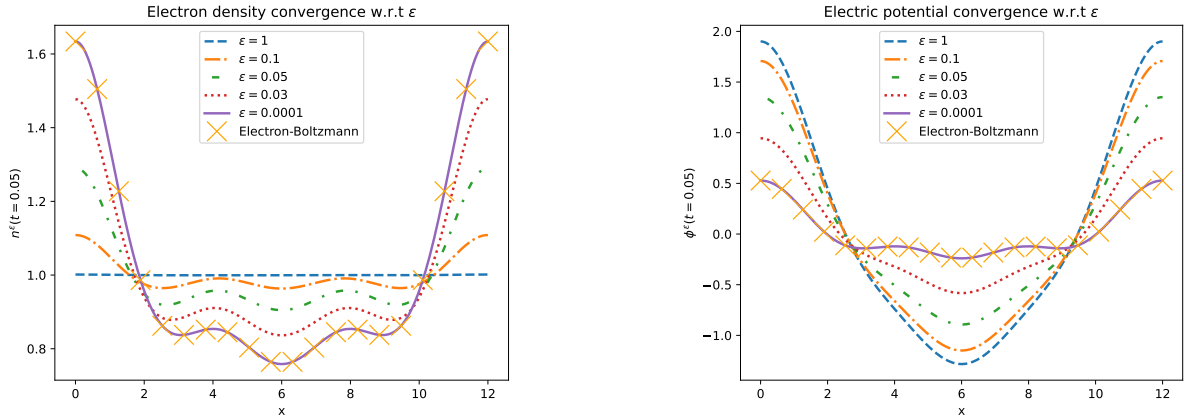

(a) $n^\varepsilon(t = 0.05)$ (b) $\phi^\varepsilon(t = 0.05)$

Figure 2.11 – Spatial density n^ε and electric potential ϕ^ε computed with our AP-method for various ε and fixed $t = 0.05$, with $N_v = 20$, $N_x = 20$, $\Delta t = 0.005$. The ion density n_i is chosen as in (2.5.14).

We then examine how the accuracy of our AP procedure is affected by the time-step, both during the initial layer, and during the permanent regime. In Figure 2.13, we plotted the macroscopic error over time, with various time-steps Δt and fixed $\varepsilon = 0.003$. First, let us compare the case of $\Delta t = 0.01$ and $\Delta t = 0.001$. As one can see, in both cases, the permanent regime is accurately represented. The only difference lies in the treatment of the initial layer : for the case of $\Delta t = 0.001$, since the time step is small when compared to ε, the initial layer is represented with precision. When $\Delta t = 0.01$, the time step is of the same order of magnitude as ε, and thus the details of the initial layer are not rendered accurately, but without impairing the precision of the permanent regime, and with a lower computational cost. When taking an even bigger time step $\Delta t = 0.05$, the details of the initial layer are completely forgotten, but the macroscopic error is still correctly computed.

At this point, we want to emphasize that the computational benefits of our AP-procedure are important for small values of ε, because of the ε-independence of the time-step. In order to measure quantitatively this fact, we computed, for several values of ε, a reference distribution function f^ε_{ref}, with a very refined time-step $\Delta t = 5 \times 10^{-5}$, using the classical method (that is, the numerical scheme presented in (2.5.11)), with enforced mass conservation, as explained in subsection 2.6.1. This solution will serve as reference in order to compare the numerical errors of two numerical solutions computed by two distinct methods. The first numerical solution, denoted by f^ε_C, the subscript 'C' standing for 'Classical method', will be computed with the same numerical scheme, but using a coarser time step. The second one, denoted by f^ε_{AP}, shall be also computed with a coarse time step, but using this time the AP approach, separating the computation of the fluctuation and the limit part. In order to compare the efficiency of the classical scheme with the AP-scheme, we shall compute the following quantities, referred to

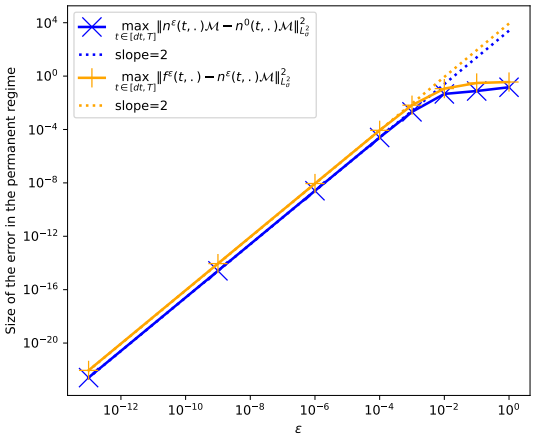

Figure 2.12 – ε-Behaviour of the microscopic/macroscopic errors of the AP-method right after the first time step, with $\Delta t = 0.005$, $N_v = 20$, $N_x = 20$. The ion density n_i is chosen as in (2.5.16), $\kappa = 0.3$. The dotted lines represent a behaviour of $\mathcal{O}(\varepsilon^2)$.

Experiment	ε	Δt_{AP}	Δt_C	Computational time AP	Computational time C	Relative error f^ε_{AP}	Relative error f^ε_C
1	10^{-3}	0.05	0.005	$7.2\ s + 10.57\ s$	$74.0\ s$	7.6×10^{-8}	9.4×10^{-6}
2	10^{-4}	0.05	0.001	$6.8\ s + 10.57\ s$	$360.1\ s$	1.9×10^{-8}	1.1×10^{-6}
3	0.1	0.005	0.005	$66.4\ s + 63.4\ s$	$68.9\ s$	3.8×10^{-8}	1.0×10^{-8}

Table 2.1 – Computational time of the different methods, and relative errors computed as in (2.6.3), for various time steps and values of ε. The computational times associated with the AP method are the sums of the times necessary for the computation of the fluctuation+the limit problem.

as *relative errors between* f^ε_{ref} *and* f^ε_C (respectively f^ε_{AP})

$$\left\| \frac{\|f^\varepsilon_{ref} - f^\varepsilon_{num}\|_{L^2_\sigma}}{\|f^\varepsilon_{ref}\|_{L^2_\sigma}} \right\|_{L^2_t}, \qquad num \in \{C, AP\}. \tag{2.6.3}$$

We shall thus consider these errors and put them in perspective with the simulation time for f^ε_C and f^ε_{AP}. We sum up the details of three experiments that we conducted in Table 2.1 and make some comments. All computations are realised with $N_x = N_v = 20$ and the ion spatial density n_i was chosen as in (2.5.16), $\kappa = 0.3$.

- Experiment 1 highlights the benefits of our method for small ε. The computational time for the AP method was much lower than that of the classical one, and furthermore this lower computational time was also met with a much better accuracy with an improvement factor of about 100 for the relative error.
- Experiment 2 shows that the computational benefit is even bigger when taking smaller values of ε. There is the same factor of about 100 in terms of the accuracy, but the

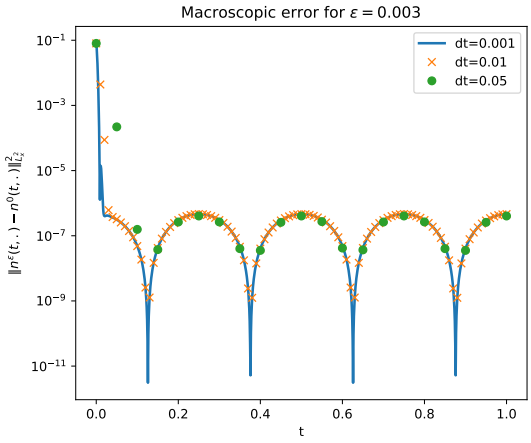

Figure 2.13 – Behaviour of the macroscopic error of (2.1.1) (AP-method) during the initial layer and in the permanent regime for various time-steps Δt. $N_v = 20$, $N_x = 20$, $\varepsilon = 0.003$. The ion density n_i is chosen as in (2.5.16), $\kappa = 0.03$.

difference in computational time is even greater.

— Experiment 3 is here to precise the conditions under which our AP-method should be used. When taking $\varepsilon \gg \Delta t$, the numerical errors of the two methods are equivalent. Remark however that our AP-method requires firstly the computation of the limit model. For accuracy reasons, this limit-model computation can be prohibitive for small time-steps. The relative errors of both methods are of the same order of magnitude, but the total computational time for the AP-method is much longer.

Concluding, the AP-scheme is very useful if one wants to solve the singular kinetic problem in the small $\varepsilon \ll 1$ regime, but without being interested in all details, meaning when one wants to choose a large time-step $\Delta t \gg \varepsilon$. However, when one needs a very refined computation of the initial layer of the system, which requires to take a very small time-step $\Delta t \ll \varepsilon$, it is better to use a more classical method.

2.7 Concluding remarks and perspectives

We shall now summarize what has been achieved in this paper, and state some of the open problems one can investigate in future works.

The aim of this article was to investigate, both from a mathematical and from a numerical point of view, the small electron-to-ion mass ratio limit $\varepsilon \to 0$ of the Vlasov-Poisson-Fokker-Planck system (2.1.1), in a setting of a given, time-dependent ion density, limit which does not correspond to the long-time asymptotics $t \to \infty$.

After a short introduction of the properties of the model (2.1.1) and a formal study of the limit $\varepsilon \to 0$, the rigorous asymptotic analysis was performed thanks to a study of the regularity

of the limit problem and an adaptation of existing hypocoercivity methods to the setting of time-dependent coefficients. This analysis was performed under a condition of smallness of the initial fluctuations (assumption (2.1.5)). This is due to our approach, which was perturbative in nature, and one may try, in future works, to lift this assumption.

Furthermore, all these studies were performed in a simplified, non-physical, one species model. In future works, one may consider similar questions regarding more physical kinetic, multispecies models with several conservation laws, such as the one developed in [FN22].

The numerical part of this paper was concerned with the development of a performant numerical scheme for the resolution of (2.1.1), with particular focus on the adiabatic regime $\varepsilon \to 0$. For this, a Hermite spectral approach was chosen for the discretization in the velocity variable. This choice is relevant for this asymptotic regime, as the Hermite coefficients vanish in the limit $\varepsilon \to 0$ (except the principal mode), the rate of convergence being dependent on their position in the hierarchy (see Corollary 1). This permits in practice to consider only few Hermite modes for $\varepsilon \ll 1$, and reduces thus dramatically the computational costs.

The numerical computations have however to be treated with care, especially for the time-discretization of this problem, due to the fact that the problem is stiff in time. Thanks to a reformulation and an implicit time-discretization, we were able to treat this problem as a regular limit, which led to the obtention of an *Asymptotic-Preserving* (AP) reformulation. The latter permits to choose an ε-independent time step, saving furthermore computational time.

The numerical analysis of the here presented AP-scheme as well as the construction of an AP-scheme for the more physical two-species model developed in [FN22] will be the object of future works.

2.8 Appendix

This Appendix regroups some lemmata and proofs useful for the paper, regrouped here to render the reading of the paper simpler.

2.8.1 Uniform in time Poincaré inequality

In this subsection, we mention the following elementary uniform in time Poincaré inequality, in the setting of a time-dependent weight. This inequality is essential for estimates such as the macroscopic coercivity (2.3.17) or inequality (2.3.23).

Lemma 5 (Uniform in time Weighted Poincaré Inequality). Let $\phi^0 \in L^\infty((0,T)\times\mathbb{T}_x)$ such that $\int_{\mathbb{T}_x} e^{\phi^0(t,x)}\,\mathrm{d}x \equiv 1$. Then, denoting the weighted average by $\langle u\rangle_t := \int_{\mathbb{T}_x} u(x) e^{\phi^0(t,x)}\,\mathrm{d}x$, we state the following uniform in time Poincaré inequality : there exists a time-independent constant $C_P > 0$ such that

$$C_P \int_{\mathbb{T}_x} |u(x) - \langle u\rangle_t|^2 e^{\phi^0(t,x)}\,\mathrm{d}x \leqslant \int_{\mathbb{T}_x} |\partial_x u(x)|^2 e^{\phi^0(t,x)}\,\mathrm{d}x, \qquad \forall t \in [0,T], \forall u \in H^1(\mathbb{T}_x).$$

Proof. Since the weights are very well controlled, because of the L^∞ bound of ϕ^0, we essentially present here a rough proof in one dimension of the Euclidian Poincaré-Wirtinger inequality.

Set $u \in C^1(\mathbb{T}_x)$ and $y \in \mathbb{T}_x$. We compute, using Taylor's expansion

$$\begin{aligned}|u(y) - \langle u\rangle_t| &= \left|\int_{\mathbb{T}_x} (u(y) - u(z))e^{\phi^0(t,z)}\,\mathrm{d}z\right| \\ &\leqslant \left|\int_{\mathbb{T}_x}\int_0^1 (y-z)\partial_x u(y + s(z-y))e^{\phi^0(t,z)}\,\mathrm{d}s\,\mathrm{d}z\right| \\ &\leqslant |\mathbb{T}_x| e^{\|\phi^0\|_\infty}\int_{\mathbb{T}_x}\int_0^1 |\partial_x u(y + s(z-y))|\,\mathrm{d}s\,\mathrm{d}z.\end{aligned}$$

The result follows from rough estimates of the right-hand side, after squaring and integrating in $\mathrm{d}y$ against $e^{\phi^0(t,y)}$. □

2.8.2 Specificities of the time-dependent case $n_i(t,x)$

Because of the time dependency of the asymptotic electric field ϕ^0, there are some additional terms appearing in the computations, as opposed to [Add+21]. In this subsection, we assume that ξ is time-dependent, and prove each point of the following lemma. This Lemma is a more detailed version of Lemma 3, giving thus the steps of the proof.

Lemma 6. Let $\xi \in C^\infty([0,T]\times\mathbb{T}_x\times\mathbb{R}_v)$, and denote by $[A,B] := AB - BA$ the commutator. Assume that n_i satisfies the assumptions of Proposition 2.2.2, and that ϕ^0, n^0 are the electric potential and density satisfying (2.1.4), with the constraint (2.2.5). Then, if $\mathcal{T}_t$ is defined as in (2.3.7), we have the following properties:

1. We have the commutation relations

$$[\partial_t, (\mathcal{T}_t\Pi)^*] = 0,$$

$$\mathrm{Aux}_t\xi := [\partial_t, (\mathcal{T}_t\Pi)]\xi = \begin{bmatrix} 0 \\ -\partial_t\partial_x\phi^0(t,.)\cdot\xi_0 - \partial_x\varphi_\xi\partial_t\phi^0(t,\cdot)\cdot n^0 \\ 0 \\ \vdots \end{bmatrix}.$$

2. One has that Aux_t is bounded uniformly with respect to time, namely

$$\|\mathrm{Aux}_t\xi\|_t \leqslant c_*\|\xi\|_t, \quad \forall t\in[0,T],$$

with $c_* > 0$ a time independent constant which depends on the L^∞-norm of $\partial_t\partial_x\phi^0$, $\partial_t\phi^0$ and n^0.

3. Because of the commutation $[\partial_t, (\mathcal{T}_t\Pi)^*] = 0$, we get

$$[\partial_t, (\mathbb{I}\mathrm{d} + (\mathcal{T}_t\Pi)^*(\mathcal{T}_t\Pi))] = (\mathcal{T}_t\Pi)^*\mathrm{Aux}_t. \tag{2.8.1}$$

4. As a consequence we obtain

$$[\partial_t, A_t] = -A_t \mathrm{Aux}_t A_t. \tag{2.8.2}$$

This last equality (2.8.2) gives rise to the following sequence of inequalities

$$\|[\partial_t, A_t]\xi\|_t = \|A_t \mathrm{Aux}_t A_t \xi\|_t \leqslant \frac{1}{2}\|\mathrm{Aux}_t A_t \xi\|_t \leqslant \frac{c_*}{2}\|A_t\xi\|_t \leqslant \frac{c_*}{4}\|(\mathbb{Id} - \Pi)\xi\|_t, \tag{2.8.3}$$

which is valid by density for all $\xi \in L^\infty((0,T); l^2_0(\mathbb{N}, L^2(\mathbb{T}_x)))$. We denote $C_* := c_*/4$.

Proof. 1. First of all one notices that $(\mathcal{T}_t\Pi)^*\xi = -\Pi\mathcal{T}_t\xi = \begin{bmatrix} -\partial_x\xi_1 \\ 0 \\ \vdots \end{bmatrix}$. This yields $[\partial_t, (\mathcal{T}_t\Pi)^*] = \partial_t(\mathcal{T}_t\Pi)^* - (\mathcal{T}_t\Pi)^*\partial_t = 0$. The second equality is a consequence of a direct computation on the definition of $\mathcal{T}_t$ in (2.3.7).

2. This point is a direct consequence of the triangle inequality.

3. We compute directly,

$$\begin{aligned}
[\partial_t, (\mathbb{Id} + (\mathcal{T}_t\Pi)^*(\mathcal{T}_t\Pi))] &= \{\partial_t(\mathbb{Id} + (\mathcal{T}_t\Pi)^*(\mathcal{T}_t\Pi)) - (\mathbb{Id} + (\mathcal{T}_t\Pi)^*(\mathcal{T}_t\Pi))\partial_t\} \\
&= \{(\mathcal{T}_t\Pi)^*\partial_t(\mathcal{T}_t\Pi) - (\mathcal{T}_t\Pi)^*(\mathcal{T}_t\Pi)\partial_t\} \\
&= (\mathcal{T}_t\Pi)^*[\partial_t, (\mathcal{T}_t\Pi)] \\
&= (\mathcal{T}_t\Pi)^*\mathrm{Aux}_t,
\end{aligned}$$

where we used, for the second equality, the commutation $[\partial_t,\ (\mathcal{T}_t\Pi)^*] = 0$.

4. The last point is a consequence of the multiplication of (2.8.1) on the left by the operator $(\mathbb{Id} + (\mathcal{T}_t\Pi)^*(\mathcal{T}_t\Pi))^{-1}$, and on the right by A_t. On one hand, the left-hand side is computed as follows

$$\begin{aligned}
&(\mathbb{Id} + (\mathcal{T}_t\Pi)^*(\mathcal{T}_t\Pi))^{-1}[\partial_t, (\mathbb{Id} + (\mathcal{T}_t\Pi)^*(\mathcal{T}_t\Pi))]A_t \\
&\quad = (\mathbb{Id} + (\mathcal{T}_t\Pi)^*(\mathcal{T}_t\Pi))^{-1}[\partial_t, (\mathbb{Id} + (\mathcal{T}_t\Pi)^*(\mathcal{T}_t\Pi))](\mathbb{Id} + (\mathcal{T}_t\Pi)^*(\mathcal{T}_t\Pi))^{-1}(\mathcal{T}\Pi_t)^* \\
&\quad = -[\partial_t, (\mathbb{Id} + (\mathcal{T}_t\Pi)^*(\mathcal{T}_t\Pi))^{-1}](\mathcal{T}\Pi_t)^*,
\end{aligned}$$

using the general computation $B^{-1}[A,B]B^{-1} = -[A, B^{-1}]$ with the operators $A = \partial_t$ and $B = (\mathbb{Id} + (\mathcal{T}_t\Pi)^*(\mathcal{T}_t\Pi))$. Then, because of the commutation $[\partial_t, (\mathcal{T}_t\Pi)^*] = 0$, we deduce

$$\begin{aligned}
(\mathbb{Id} + (\mathcal{T}_t\Pi)^*(\mathcal{T}_t\Pi))^{-1}[\partial_t, (\mathbb{Id} + (\mathcal{T}_t\Pi)^*(\mathcal{T}_t\Pi))]A_t &= -[\partial_t, (\mathbb{Id} + (\mathcal{T}_t\Pi)^*(\mathcal{T}_t\Pi))^{-1}](\mathcal{T}\Pi_t)^* \\
&= -[\partial_t, A_t].
\end{aligned}$$

On the other hand, the right-hand side rewrites

$$(\mathbb{Id} + (\mathcal{T}_t\Pi)^*(\mathcal{T}_t\Pi))^{-1}(\mathcal{T}_t\Pi)^*\mathrm{Aux}_t A_t = A_t\mathrm{Aux}_t A_t,$$

yielding the equality. The last chain of inequalities (2.8.3) follows then immediately from (2.3.20).

□

2.8.3 Handling the different terms in the hypocoercivity estimate (2.4.3)

For the sake of completeness, we will mention in this subsection how we deal with each of the nonlinear terms in (2.4.3).

2.8.3.1 Good dissipative terms

The microscopic and macroscopic coercivity give the dissipation of the two first terms, namely

$$\langle \mathcal{L}\gamma^\varepsilon, \gamma^\varepsilon\rangle_t \leqslant \frac{1}{2}\langle \mathcal{L}\gamma^\varepsilon, \gamma^\varepsilon\rangle_t - \frac{1}{2}\|(\mathbb{I}\mathrm{d}-\Pi)\gamma^\varepsilon\|_t^2, \tag{2.8.4}$$

and

$$-\delta\langle A_t\mathcal{T}_t\Pi\gamma^\varepsilon, \gamma^\varepsilon\rangle_t \leqslant -\delta\frac{\lambda_M}{1+\lambda_M}\|\Pi\gamma^\varepsilon\|_t^2, \quad \text{using} \int_{\mathbb{T}_x}\gamma_0^\varepsilon(t,x)\,\mathrm{d}x = 0. \tag{2.8.5}$$

2.8.3.2 Signless terms arising in the classical computation

We have using (2.3.23) along with $\Pi A_t = A_t$

$$\begin{aligned}-\delta\langle A_t\mathcal{T}_t(\mathbb{I}\mathrm{d}-\Pi)\gamma^\varepsilon, \gamma^\varepsilon\rangle_t &\leqslant \delta\frac{\nu_1}{2}\|A_t\mathcal{T}_t(\mathbb{I}\mathrm{d}-\Pi)\gamma^\varepsilon\|_t^2 + \delta\frac{1}{2\nu_1}\|\Pi\gamma^\varepsilon\|_t^2\\ &\leqslant \delta\Lambda^2\frac{\nu_1}{2}\|(\mathbb{I}\mathrm{d}-\Pi)\gamma^\varepsilon\|_t^2 + \delta\frac{1}{2\nu_1}\|\Pi\gamma^\varepsilon\|_t^2,\end{aligned} \tag{2.8.6}$$

with an $\nu_1 > 0$ to be tuned later. Moreover we also have, using (2.3.19) and then (2.3.20) and (2.3.21)

$$\begin{aligned}\delta\,\langle \mathcal{T}_tA_t\gamma^\varepsilon, \gamma^\varepsilon\rangle_t &= \delta\,\left[\|A_t\gamma^\varepsilon\|_t^2 + \|\mathcal{T}_tA_t\gamma^\varepsilon\|_t^2\right]\\ &\leqslant \frac{\delta}{4}\|(\mathbb{I}\mathrm{d}-\Pi)\gamma^\varepsilon\|_t^2 + \delta\,\|(\mathbb{I}\mathrm{d}-\Pi)\gamma^\varepsilon\|_t^2\\ &= \frac{5\delta}{4}\|(\mathbb{I}\mathrm{d}-\Pi)\gamma^\varepsilon\|_t^2\,.\end{aligned} \tag{2.8.7}$$

Furthermore, using (2.3.22) and for $\nu_2 > 0$ to be tuned later

$$\begin{aligned}\delta\,\langle A_t\mathcal{L}\gamma^\varepsilon, \gamma^\varepsilon\rangle_t = \delta\,\langle A_t\mathcal{L}\gamma^\varepsilon, \Pi\gamma^\varepsilon\rangle_t &\leqslant \delta\frac{\nu_2}{2}\|A_t\mathcal{L}\gamma^\varepsilon\|_t^2 + \frac{\delta}{2\nu_2}\|\Pi\gamma^\varepsilon\|_t^2\\ &\leqslant \delta\frac{\nu_2}{8}\|(\mathbb{I}\mathrm{d}-\Pi)\gamma^\varepsilon\|_t^2 + \frac{\delta}{2\nu_2}\|\Pi\gamma^\varepsilon\|_t^2.\end{aligned} \tag{2.8.8}$$

Finally,

$$\delta\,\langle \mathcal{L}A_t\gamma^\varepsilon, \gamma^\varepsilon\rangle_t = 0, \tag{2.8.9}$$

because of $\mathcal{L}(A_t) = \mathcal{L}(\Pi A_t) = (\mathcal{L}\Pi)A_t = 0.A_t = 0$.

2.8.3.3 Terms associated with the source term

For some $\nu_3 > 0$ to be fixed later, Young's inequality permits to estimate

$$\varepsilon \langle \mathcal{S}, \gamma^\varepsilon \rangle_t = \varepsilon \langle \mathcal{S}, \Pi\gamma^\varepsilon \rangle_t \leqslant \frac{\nu_3 \varepsilon^2}{2\delta} \|\mathcal{S}\|_t^2 + \frac{\delta}{2\nu_3} \|\Pi\gamma^\varepsilon\|_t^2. \tag{2.8.10}$$

Since $\mathcal{S} = \Pi\mathcal{S}$, and $A\Pi = 0$, we have

$$\varepsilon\delta \langle A_t \mathcal{S}, \gamma^\varepsilon \rangle_t = 0. \tag{2.8.11}$$

Finally, using (2.3.20), Young's inequality leads to

$$\varepsilon\delta \langle A_t \gamma^\varepsilon, \mathcal{S} \rangle_t \leqslant \frac{\nu_4 \varepsilon^2 \delta}{2} \|\mathcal{S}\|_t^2 + \frac{\delta}{8\nu_4} \|(1-\Pi)\gamma^\varepsilon\|_t^2. \tag{2.8.12}$$

2.8.3.4 Terms associated with the time dependency of norms and operator

Because of the time dependency of the norms and of the A_t operator, some small ε-order terms appear in our computations. We show how we control them. Cauchy-Schwarz' inequality immediately gives

$$-\frac{\varepsilon}{2} \sum_{k=0}^{\infty} \langle \partial_t \phi^0 \gamma_k^\varepsilon, \gamma_k^\varepsilon \rangle_{L^2_{\eta_t}(\mathbb{T}_x)} \leqslant \frac{\varepsilon}{2} \|\partial_t \phi^0\|_\infty \|\gamma^\varepsilon\|_t^2. \tag{2.8.13}$$

Thanks to (2.3.20), we have

$$-\varepsilon\delta \sum_{k=0}^{\infty} \langle \partial_t \phi^0 (A_t \gamma^\varepsilon)_k, \gamma_k^\varepsilon \rangle_{L^2_{\eta_t}(\mathbb{T}_x)} \leqslant \varepsilon\delta \|\partial_t \phi^0\|_\infty \|A_t \gamma^\varepsilon\|_t \|\gamma^\varepsilon\|_t \leqslant \frac{\varepsilon\delta}{2} \|\partial_t \phi^0\|_\infty \|\gamma^\varepsilon\|_t^2. \tag{2.8.14}$$

Finally, using (2.3.24) yields

$$-\varepsilon\delta \langle [\partial_t, A_t]\gamma^\varepsilon, \gamma^\varepsilon \rangle_t \leqslant \varepsilon\delta\, C_* \|\gamma^\varepsilon\|_t^2. \tag{2.8.15}$$

Acknowledgments. This work has been carried out within the framework of the EUROfusion Consortium, funded by the European Union via the Euratom Research and Training Programme (Grant Agreement No 101052200 — EUROfusion). Views and opinions expressed are however those of the author(s) only and do not necessarily reflect those of the European Union or the European Commission. Neither the European Union nor the European Commission can be held responsible for them. E. Lehman would like to acknowledge the financial support of the Ecole Normale Supérieure de Lyon. The authors would also like to thank Yanick Sarazin and Guilhem Dif-Pradalier for the numerous fruitful discussions.

CHAPTER 3

ASYMPTOTIC STUDY OF AN ANISOTROPIC FOKKER-PLANCK COLLISION OPERATOR IN A STRONG MAGNETIC FIELD

Le contenu de ce chapitre est en anglais, et est tiré de la publication scientifique suivante :

- Etienne Lehman, Claudia Negulescu, Stefan Possanner. "Asymptotic study of an anisotropic Fokker-Planck collision operator in a strong magnetic field", publié dans *Kinetic and Related Models* [1] (2024).

Abstract: The present paper is concerned with the derivation, via asymptotic studies, of a reduced hybrid model describing the anisotropic fusion plasma dynamics. The parallel dynamics is governed by a kinetic equation, whereas the perpendicular dynamics is described by a Maxwellian distribution function, whose temperature $T_\perp$ satisfies an evolution equation, exchanging information with the parallel direction via some coupling terms. The reduced model is obtained from the underlying fully kinetic model, under the assumption of a strong magnetic field and strong collisionality in the perpendicular direction. From a numerical point of view, reduced models are very advantageous, permitting significant savings in computational times and memory. To improve the precision of the reduced description, we propose in this paper also first order correction terms with respect to the parameter describing the anisotropy, and discuss these terms from a physical point of view. This first order truncated model is new to our knowledge, meets the desired requirements of precision and efficiency, and its derivation is clearly exposed in this work, based on formal asymptotic studies.

Contents

1. doi: 10.3934/krm.2024004

3.1 Introduction

Strong anisotropy is naturally present in a broad variety of plasma phenomena. For example, space and laboratory plasma in strong magnetic fields exhibit different properties parallel and perpendicular to the magnetic field lines. To accurately describe such situations, quantities are usually decomposed into distinct parallel and perpendicular components, such as $T_\parallel$ and $T_\perp$ for the temperature. These quantities can evolve according to rather different evolution equations, which are coupled in order to permit exchanges (of energy, momentum, *etc.*) between the parallel and perpendicular directions. For instance, in strongly-magnetized plasma, the diffusion of thermal energy along magnetic field lines can be orders of magnitude faster than across field lines [HM03], and it seems questionable to describe then such anisotropic dynamics with a set of equations based on isotropic assumptions. One of the first studies about the (anisotropic) form of the plasma distribution function in strong magnetic fields has been given in [CGL56], leading to the famous Chew-Goldberger-Low (CGL) expression of the pressure tensor. Since then, many studies followed making use of specific anisotropic plasma distribution functions, of which we can mention here only a small sample: non-linear development of electromagnetic instabilities [Dav+72], Whistler instabilities [OHO72], mirror and ion cyclotron instabilities [Gar92], and transport equations for multi-component space plasmas [BS82], among many others. In many of these models, the anisotropy is manifest in the different temperatures of the velocity distribution function along and perpendicular to the magnetic field. Describing these anisotropic phenomena is crucial for the design of plasma fusion devices, as anisotropy strongly impacts heat diffusion and hence the heat deposition on the device wall [Sta00]. Anisotropy also affects turbulence [Sco21], instabilities, the propagation of energetic particles, *etc.* Briefly, anisotropy is one of the key aspects to be taken into account in electromagnetic plasma simulations.

A precise study of such anisotropic plasma dynamics starts with the fully kinetic description, in which each plasma species of charge q_s and mass m_s is described by the Boltzmann-type equation,

$$\partial_t f_\mathrm{s} + \mathbf{v}\cdot\nabla_\mathbf{x} f_\mathrm{s} + \frac{q_\mathrm{s}}{m_\mathrm{s}}\left(\mathbf{E}+\mathbf{v}\times\mathbf{B}\right)\cdot\nabla_\mathbf{v} f_\mathrm{s} = \sum_\mathrm{r} Q_\mathrm{sr}(f_\mathrm{s}, f_\mathrm{r})\,, \tag{3.1.1}$$

for the particle distribution function $f_\mathrm{s}(t,\mathbf{x},\mathbf{v})$ defined on position-velocity phase-space. The long-range interactions between the species are mediated by the electromagnetic fields $\mathbf{E}$ and $\mathbf{B}$, satisfying Maxwell's equations. The short-range interactions are modeled via collision operators Q_sr, accounting for the thermodynamic processes such as entropy decay and thermal equilibration. In the presence of a strong magnetic field $\mathbf{B}$, charged particles will execute helical movements around the field lines, their dynamics being thus constrained in the perpendicular direction with respect to the magnetic field, whereas in the parallel direction particles move freely. This is the simplest explanation of the creation of anisotropy.

The distribution functions f_s contain all the information about the plasma dynamics. However, solving numerically the whole kinetic system (3.1.1) coupled with Maxwell's equation is out of reach for today's computers. The multiscale nature of the problem requires indeed

prohibitively high spatial and velocity resolutions when standard schemes are used. However, taking advantage of the high anisotropy of the problem could help to design multiscale schemes or to derive reduced models, yielding computational savings. One scenario where reduced models have been fruitfully employed is the study of the propagation of edge-localized modes (ELMs) in the scrape-off layer (SOL) of Tokamak fusion devices [MHD10; Mou+13]. In the latest version of these works [CHM16], the distribution functions of electrons and ions describing the ELMs were assumed of the following form:

$$f_s(t,x,v_\parallel,\mathbf{v}_\perp) = g_s(t,x,v_\parallel)\frac{m_s}{2\pi k_B T_{s,\perp}(t,x)}\exp\left(-\frac{m_s|\mathbf{v}_\perp|^2}{2k_B T_{s,\perp}(t,x)}\right). \tag{3.1.2}$$

Here, f_s is the product of a reduced $1D_x1D_v$ kinetic distribution function g_s in the parallel velocity direction and a $1D_x2D_v$ Maxwellian distribution function in the perpendicular velocity direction. The constant $k_B > 0$ denotes the Boltzmann constant, and $m_s > 0$ denotes the mass of one element of the species s. In [CHM16] the authors propose a coupled system of PDEs for the evolution of g_s and $T_{s,\perp}$, permitting the exchange of thermal energy via a simplified (BGK) collision operator. The above mentioned models were often introduced without a clear mathematical derivation. In this paper, we aim to derive the form of the distribution function f_s given in (3.1.2) as an asymptotic limit solution of equation (3.1.1) in a suitable scaling reflecting the strong anisotropy. Moreover, in this process we shall also derive first order corrections to the limit solution; these will include the well-known plasma drifts across the magnetic field, and thus enhance the physics content of the reduced model. The exact interplay between parallel kinetic and perpendicular fluid aspects of the model shall furthermore be underlined in this work.

What are the physical processes that could lead to a distribution function of the form (3.1.2)? First of all, Maxwellian velocity distributions arise from collisions. In [MHD10; Mou+13; CHM16] it is stated that the dynamics is slow in the perpendicular plane, the distribution function is thus assumed to be thermalized in this perpendicular direction. By contrast, in the parallel velocity direction, the distribution function $g_s(v_\parallel)$ is not necessarily in thermal equilibrium and is subject to far fewer collisions. Indeed, the mean free path of the particles exceeds the total length of the spatial parallel direction in the Scrape-Off Layer of a tokamak. In our modelling, we shall thus postulate an anisotropy in the collisional processes: a perpendicular collisional process shall be assumed dominant. Moreover, we will investigate strongly magnetized plasma, where the Lorentz force is dominated by the magnetic field term.

A more precise description than (3.1.2) of a magnetized plasma is provided by gyrokinetic theory [BH07; Kro12; GHN09]. There the distribution function is assumed to be of the form $f(t,\mathbf{x},v_\parallel,\mu)$, with $\mu := |\mathbf{v}_\perp|^2/(2|\mathbf{B}|)$ the magnetic moment. However in gyrokinetic theory it is not assumed that one has strong collisions in the perpendicular direction such that the whole distribution function remains kinetic. The effect of the strong magnetic field is merely the reduction to a $3D_x\,2D_v$ kinetic distribution function, where μ is however an adiabatic invariant. In situation (3.1.2) which is studied here, the distribution function in the direction perpendicular

to **B** has a Maxwellian form, reducing thus further the complexity of the problem. Indeed, solving the gyrokinetic equation is more demanding (but also more precise) than solving the truncated hybrid kinetic/fluid model we shall present in this paper. Thus, the aim of our paper is to obtain via asymptotic arguments such a reduced hybrid model, which is often encountered in literature to further reduce the numerical complexity of the resolution of a full kinetic or gyrokinetic equation.

This is thus the physical context we are interested in. From now on, we shall consider only a single plasma species in a given electromagnetic field $\mathbf{E}$, $\mathbf{B} : \mathbb{R}_+ \times \mathbb{T}^3_x \to \mathbb{R}^3$ with $\mathbf{B} = B(t,\mathbf{x})\mathbf{e}_z$ pointing along the z-direction (periodic in $\mathbf{x}$). We shall assume that this magnetic field is non-vanishing, namely

$$B(t,\mathbf{x}) > 0 \qquad (t,\ \mathbf{x}) \in \mathbb{R}_+ \times \mathbb{T}^3_x\,. \tag{3.1.3}$$

The starting point of the present work is hence the following *Vlasov-Fokker-Planck equation* (VFP),

$$\partial_t f + \mathbf{v}\cdot\nabla_{\mathbf{x}} f + \frac{q}{m}\,(\mathbf{E} + \mathbf{v}\times B\mathbf{e}_z)\cdot\nabla_{\mathbf{v}} f = \nu_\perp\, Q_\perp(f) + \nu_{\mathrm{r}}\, Q_{\mathrm{r}}(f)\,, \tag{3.1.4}$$

for the particle distribution function $f : \mathbb{R}_+ \times \mathbb{T}^3_x \times \mathbb{R}^3_v \to \mathbb{R}_+$, with the collision frequencies $\nu_{\perp,\mathrm{r}} > 0$. As mentioned above, one key idea of this work is to single out the specific collisions in the plane perpendicular to the magnetic field lines, modelled here by a nonlinear *Fokker-Planck operator*,

$$Q_\perp(f) := \nabla_{\mathbf{v}_\perp}\cdot\left[(\mathbf{v}_\perp - \mathbf{u}_\perp)\,f + \frac{k_{\mathrm{B}}T_\perp}{m}\,\nabla_{\mathbf{v}_\perp} f\right], \tag{3.1.5}$$

where $\mathbf{v}_\perp := (v_x,\, v_y)^t \in \mathbb{R}^2_v$, while the mean perpendicular velocity $\mathbf{u}_\perp$ and the perpendicular temperature $T_\perp$ depend on f in the following way:

$$\begin{aligned} n(t,x) &:= \int_{\mathbb{R}^3_v} f\ \mathrm{d}\mathbf{v}\,,\\ n\,\mathbf{u}_\perp(t,\mathbf{x}) &:= \int_{\mathbb{R}^3_v} \mathbf{v}_\perp\, f\ \mathrm{d}\mathbf{v}\,,\\ n\,k_{\mathrm{B}}\,T_\perp(t,\mathbf{x}) &:= \frac{m}{2}\int_{\mathbb{R}^3_v} |\mathbf{v}_\perp - \mathbf{u}_\perp|^2\, f\,\mathrm{d}\mathbf{v}\,. \end{aligned} \tag{3.1.6}$$

The remaining collision operator Q_{r} will be chosen of the form

$$Q_{\mathrm{r}}(f) := \nabla_{\mathbf{v}}\cdot\left[(\mathbf{v}-\mathbf{u})\,f + \frac{k_{\mathrm{B}}T}{m}\,\nabla_{\mathbf{v}} f\right] - Q_\perp(f)\,, \tag{3.1.7}$$

where

$$\begin{aligned} n\,\mathbf{u}(t,\mathbf{x}) &:= \int_{\mathbb{R}^3_v} \mathbf{v}\, f\ \mathrm{d}\mathbf{v}\,,\\ \frac{3}{2}n\,k_{\mathrm{B}}\,T(t,\mathbf{x}) &:= \frac{m}{2}\int_{\mathbb{R}^3_v} |\mathbf{v}-\mathbf{u}|^2\, f\,\mathrm{d}\mathbf{v}\,. \end{aligned} \tag{3.1.8}$$

This operator is nothing else than a standard isotropic Fokker-Planck operator (leading in the long time limit to a full isotropisation) minus the just introduced perpendicular collision operator, such that if both $Q_\perp(f)$ and $Q_{\mathrm{r}}(f)$ scale equally, the right-hand side of (3.1.4) is a standard isotropic collision operator; however we shall focus in this work on an anisotropic regime, as mentioned above. One can choose for $Q_{\mathrm{r}}(f)$ more general collision operators than (3.1.7), which should however satisfy the following properties:

— Preservation of mass, momentum and energy:

$$\int_{\mathbb{R}^3_v} \begin{pmatrix} 1 \\ \mathbf{v} \\ \frac{|\mathbf{v}|^2}{2} \end{pmatrix} Q_{\mathrm{r}}(f)\,\mathrm{d}\mathbf{v} = 0\,; \tag{3.1.9}$$

— Thermalisation between parallel and perpendicular directions:

$$m \int_{\mathbb{R}^3_v} \frac{|\mathbf{v}_\perp|^2}{2} Q_{\mathrm{r}}(f)\,\mathrm{d}\mathbf{v} = \eta\, n\, k_B\,(T - T_\perp) = \frac{\eta}{3}\, n\, k_B\,(T_\parallel - T_\perp)\,, \tag{3.1.10}$$

where $T = (2\,T_\perp + T_\parallel)/3$, $\eta > 0$ is some given coefficient (equal to $\eta = 2$ for Q_{r} defined in (3.1.7)) and

$$n\,u_\parallel(t,\mathbf{x}) := \int_{\mathbb{R}^3_v} v_\parallel\, f\ \mathrm{d}\mathbf{v}\,, \qquad \frac{1}{2}\, n\, k_{\mathrm{B}}\, T_\parallel(t,\mathbf{x}) := \frac{m}{2} \int_{\mathbb{R}^3_v} |v_\parallel - u_\parallel|^2\, f\,\mathrm{d}\mathbf{v}\,. \tag{3.1.11}$$

Altogether, equation (3.1.4) models a magnetized plasma in a given electromagnetic field, undergoing anisotropic collisions, which lead on long time scales to complete thermalisation. However, on a short time scale the two parallel and perpendicular temperatures need not necessarily be equal, and this is reflected by the choice of our collision operator. On short times of order $\mathcal{O}(\nu_\perp^{-1})$, the perpendicular energy is conserved thanks to

$$\int_{\mathbb{R}^3_v} \frac{|\mathbf{v}_\perp|^2}{2}\, Q_\perp(f)\,\mathrm{d}\mathbf{v} = 0\,, \tag{3.1.12}$$

which is a natural property in a high magnetic field setting [ONe83]. On long time scales, the perpendicular energy is however not anymore conserved because of the operator Q_{r}, which thermalizes and ensures isotropisation of the temperatures as $t \to \infty$, c.f.(3.1.10). However, we recognize that our modeling is limited in the following ways:

— The electromagnetic fields are prescribed and not solved in a self-consistent manner;
— The magnetic field is pointing in a fixed direction and has no curvature;
— The effects of multiple species are excluded;
— The space domain is periodic;
— $Q_\perp$ and Q_{r} are modeled by differential type Fokker-Planck operators (3.1.5)-(3.1.7).

The first four simplifications are not so dramatic and can be easily removed. Additionally, the method given in the present manuscript is general and one can replicate the analysis with different choices of operators $Q_\perp$ and Q_{r}. These assumptions have been made to simplify the analysis in order to focus on the main point, namely the effects of anisotropic collisions.

In this work, we set a physical scaling (given in Appendix A) reflecting the strongly magnetized nature of the plasma and the dominance of collisions perpendicular to $\mathbf{B}$. This scaling makes apparent a small parameter $\varepsilon \ll 1$, and the obtained adimensional model reads

$$\partial_t f^\varepsilon + \mathbf{v}\cdot\nabla_{\mathbf{x}} f^\varepsilon + \mathbf{E}\cdot\nabla_{\mathbf{v}} f^\varepsilon + \frac{1}{\varepsilon}(\mathbf{v}\times B\mathbf{e}_z)\cdot\nabla_{\mathbf{v}} f^\varepsilon = \frac{\nu_\perp}{\varepsilon} Q_\perp(f^\varepsilon) + \nu_{\mathrm{r}}\, Q_{\mathrm{r}}(f^\varepsilon)\,. \tag{3.1.13}$$

Here, the rescaled operators $Q_\perp$, Q_{r} are of the following form

$$\begin{aligned} Q_\perp(f^\varepsilon) =& \nabla_{\mathbf{v}_\perp}\cdot\left[(\mathbf{v}_\perp - \mathbf{u}^\varepsilon_\perp) f^\varepsilon + T^\varepsilon_\perp \nabla_{\mathbf{v}_\perp} f^\varepsilon\right]\,, \\ Q_{\mathrm{r}}(f^\varepsilon) :=& \nabla_{\mathbf{v}}\cdot\left[(\mathbf{v}-\mathbf{u}^\varepsilon) f^\varepsilon + T^\varepsilon \nabla_{\mathbf{v}} f^\varepsilon\right] - Q_\perp(f^\varepsilon)\,, \end{aligned} \tag{3.1.14}$$

where $\mathbf{u}^\varepsilon_\perp$, $\mathbf{u}^\varepsilon$, $T^\varepsilon_\perp$ and $T^\varepsilon := (2T^\varepsilon_\perp + T^\varepsilon_\parallel)/3$ depend on f^ε in the following way:

$$\begin{aligned} n^\varepsilon(t,x) &:= \int_{\mathbb{R}^3_v} f^\varepsilon \,\mathrm{d}\mathbf{v}\,, \\ n^\varepsilon\,\mathbf{u}^\varepsilon_\perp(t,\mathbf{x}) &:= \int_{\mathbb{R}^3_v} \mathbf{v}_\perp\, f^\varepsilon \,\mathrm{d}\mathbf{v}\,, & n^\varepsilon\,\mathbf{u}^\varepsilon(t,\mathbf{x}) &:= \int_{\mathbb{R}^3_v} \mathbf{v}\, f^\varepsilon \,\mathrm{d}\mathbf{v}\,, \\ n^\varepsilon\, T^\varepsilon_\perp(t,\mathbf{x}) &:= \frac{1}{2}\int_{\mathbb{R}^3_v} |\mathbf{v}_\perp - \mathbf{u}^\varepsilon_\perp|^2 f^\varepsilon \,\mathrm{d}\mathbf{v}\,, & \frac{1}{2} n^\varepsilon\, T^\varepsilon_\parallel(t,\mathbf{x}) &:= \frac{1}{2}\int_{\mathbb{R}^3_v} |v_\parallel - u^\varepsilon_\parallel|^2 f^\varepsilon \,\mathrm{d}\mathbf{v}\,. \end{aligned} \tag{3.1.15}$$

This equation is supplemented with a suitable, well-prepared initial condition $f^\varepsilon(t=0) = f^\varepsilon_{\mathrm{in}}$. We do not treat in this work with the possible occurrence of initial layers.

Our goal is to find approximate solutions to equation (3.1.13) in the regime $\varepsilon \ll 1$. The analysis performed in this work is mostly formal and based on a Hilbert expansion:

$$f^\varepsilon = f^0 + \varepsilon\, f^1 + \varepsilon^2 f^2 + \dots$$

This ansatz leads to a hierarchy of coupled equations for the coefficients f^0, f^1, ... The analysis of this hierarchy requires a careful study of the dominant operator in equation (3.1.13), and its linearized version. The study of the latter is performed in a rigorous manner, using well known techniques coming from the isotropic functional analysis framework. A careful truncation permits to get a reduced model corresponding to (3.1.13) in the $\varepsilon \ll 1$ regime. The interested reader is referred to [Deg04; MRS12] for a comprehensive introduction on those methods and on Hilbert expansions.

The field of asymptotic analysis in strongly magnetized plasma is very active. One can for instance cite [GS99; Sai02] for the study of the Vlasov-Poisson system in the case of strong magnetic field, [BG12; AH08] for Vlasov-Poisson-Boltzmann, or even [Bos07] for the coupling

with Maxwell equations. Multi-species plasma also feature a small electron-ion mass ratio and small Debye length; these singular parameters also can be taken into account in scaling assumptions. See [LN24b; NP16; Neg18; FN22] for the former, and [HH15; Gre96; CG00] for instance for the latter. Various assumptions can be made about these parameters, leading to various types of scaling. Some of them are very well studied, such as the hydrodynamic scaling [BGL91; Deg04; Gol05; Nis78; Bob18], the drift-diffusion scaling [PS00; EM00; Add+21; AT04; Bar+13; Bob95], or the high-field scaling [Arn+01; BS01; NPS01].

The document is organized as follows: in Section 3.2 we state the main results, discuss them and give some notation. We then write in subsection 3.2.2 the Hilbert hierarchy. We give in Section 3.3 the proof of Theorem 4, which concerns the limit model. Section 3.4 deals with the proof of Theorem 5, concerning the first order correction. Finally in Section 3.5, we summarize and give an outlook on future applications and improvements of the current work. To simplify the presentation, the Appendix regroups the scaling procedure along with cumbersome proofs and computations.

3.2 Main results

This section contains the two main results of the present work:

1. The first result concerns the derivation of the limit model which approximates the kinetic equation (3.1.13) in the asymptotics $\varepsilon \to 0$. The limit model is stated in Theorem 4, followed by a discussion of its key aspects.
2. The second result addresses the derivation of first order correction terms to the limit model. The corresponding truncated system is stated in Theorem 5, followed by a discussion of its key aspects and novelties.

In all of the following, we will denote by

$$\langle \theta \rangle_\perp := \int_{\mathbb{R}^2_v} \theta \, \mathrm{d}\mathbf{v}_\perp , \qquad \langle \theta \rangle_\parallel := \int_{\mathbb{R}_v} \theta \, \mathrm{d}v_\parallel , \qquad \langle \theta \rangle := \int_{\mathbb{R}^3_v} \theta \, \mathrm{d}\mathbf{v} ,$$

the integration against the orthogonal, parallel and total velocity variable, respectively. One also introduces the following notation for any vector field X taking values in $\mathbb{R}^2$:

$$X^\top := X \times \mathbf{e}_z := \begin{pmatrix} v_y \\ -v_x \end{pmatrix} . \tag{3.2.1}$$

3.2.1 Main results

Theorem 4 (**Limit model**). In the limit $\varepsilon \to 0$, the solution f^ε of (3.1.13) converges (formally) to a function f^0 of the following factorized form

$$f^0(t, \mathbf{x}, \mathbf{v}) = g^0(t, \mathbf{x}, v_\parallel) \, \mathcal{M}_\perp^{T^0_\perp(t,\mathbf{x})}(\mathbf{v}_\perp) , \tag{3.2.2a}$$

where the perpendicular Maxwellian $\mathcal{M}_\perp^{T_\perp^0(t,\mathbf{x})}$ is given by

$$\mathcal{M}_\perp^{T_\perp^0(t,\mathbf{x})}(\mathbf{v}_\perp) := \frac{1}{2\,\pi\,T_\perp^0(t,\mathbf{x})}\, e^{-\frac{|\mathbf{v}_\perp|^2}{2\,T_\perp^0(t,\mathbf{x})}}. \tag{3.2.2b}$$

The "reduced kinetic distribution g^0" and the perpendicular temperature $T_\perp^0$ satisfy the system

$$\begin{cases} \partial_t g^0 + v_\parallel\,\partial_z g^0 + E_\parallel\,\partial_{v_\parallel} g^0 = \nu_{\mathrm{r}}\,\partial_{v_\parallel}\left[(v_\parallel - u_\parallel^0)\,g^0 + T^0\,\partial_{v_\parallel} g^0\right], \\ \partial_t(n^0\,T_\perp^0) + \partial_z(n^0\,T_\perp^0\,u_\parallel^0) = \dfrac{2}{3}\,\nu_{\mathrm{r}}\,n^0\,\left(T_\parallel^0 - T_\perp^0\right), \end{cases} \tag{3.2.2c}$$

where $T^0 = (T_\parallel^0 + 2\,T_\perp^0)/3$ and

$$n^0 = \langle g^0\rangle_\parallel, \qquad n^0\,u_\parallel^0 = \left\langle v_\parallel\,g^0\right\rangle_\parallel, \qquad \frac{1}{2}n^0\,T_\parallel^0 = \frac{1}{2}\left\langle (v_\parallel - u_\parallel^0)^2\,g^0\right\rangle_\parallel. \tag{3.2.3}$$

This system (3.2.2) is supplemented with the following well-prepared initial condition

$$f_{\mathrm{in}}^0(\mathbf{x},\,\mathbf{v}) = g_{\mathrm{in}}^0(\mathbf{x},v_\parallel)\,\mathcal{M}_\perp^{T_{\perp,\mathrm{in}}^0(\mathbf{x})}(\mathbf{v}_\perp), \tag{3.2.4}$$

where $f_{\mathrm{in}}^0 := \lim_{\varepsilon\to 0} f_{\mathrm{in}}^\varepsilon$.

Let us now discuss some key aspects of Theorem 4:

- In the $\varepsilon \to 0$ limit, the particle distribution function f^ε decomposes exactly as a product of a reduced kinetic distribution function g^0 modelling the parallel transport, and a Maxwellian distribution in the perpendicular variable, depending only on the perpendicular temperature $T_\perp^0$ (3.2.2a).
- The two quantities g^0 and $T_\perp^0$ satisfy the coupled system of PDEs (3.2.2c). The reduced distribution function g^0 satisfies a $1\mathrm{D}_x1\mathrm{D}_v$ kinetic equation along the magnetic field lines. The perpendicular temperature is advected along the field lines by the bulk velocity $u_\parallel^0$ associated with g^0.
- Moreover, there is a coupling responsible for the energy exchanges between the parallel and perpendicular directions, represented by the Fokker-Planck term and the relaxation term $n^0(T_\parallel^0 - T_\perp^0)$. On long time scales, these terms lead to isotropisation between $T_\parallel^0$ and $T_\perp^0$.
- Setting $E_\parallel \equiv 0$ in order to not inject energy into the system, the system (3.2.2c) exactly conserves the energy:

$$\frac{\mathrm{d}}{\mathrm{d}t}\int_{\mathbb{T}_x^3}\left[\frac{3}{2}\,n^0\,T^0 + \frac{1}{2}\,n^0\,(u_\parallel^0)^2\right]\mathrm{d}\mathbf{x} = 0\,.$$

- The limit model (3.2.2c) is exactly the one described in [CHM16], without source terms. The temperature equation can be rewritten in non-conservative form

$$\partial_t T_\perp^0 + u_\parallel^0\,\partial_z T_\perp^0 = \frac{2}{3}\,\nu_{\mathrm{r}}\,(T_\parallel^0 - T_\perp^0), \tag{3.2.5}$$

which is obtained from the kinetic equation in (3.2.2c) by using the conservation law

$$\partial_t n^0 + \partial_z (n^0\, u_\parallel^0) = 0\,. \tag{3.2.6}$$

This formulation corresponds to the one given in [CHM16].

Theorem 5 (**First order corrections**). Let f^ε be the solution of equation (3.1.13). Then, one can approximate the distribution function f^ε by $\widehat{f}^\varepsilon$, such that

$$f^\varepsilon = \widehat{f}^\varepsilon + \mathcal{O}(\varepsilon^2)\,, \qquad \text{as} \qquad \varepsilon \to 0\,,$$

and $\widehat{f}^\varepsilon$ has the following form (for notational reasons we kept the index ε in the factorisation)

$$\widehat{f}^\varepsilon(t,\mathbf{x},\mathbf{v}) = \widehat{g}(t,\,\mathbf{x},\,v_\parallel)\,\mathcal{M}_\perp^{\widehat{T}_\perp(t,\mathbf{x})}(\mathbf{v}_\perp)\left(1 + \,\varepsilon\,\Lambda_{\widehat{g},\widehat{T}_\perp}\right). \tag{3.2.7a}$$

The "reduced kinetic distribution" $\widehat{g}$ and the perpendicular temperature $\widehat{T}_\perp$ satisfy the coupled system

$$\begin{cases} \partial_t \widehat{g} + v_\parallel\,\partial_z \widehat{g} + E_\parallel\,\partial_{v_\parallel}\widehat{g} + \varepsilon\,\nabla_{\mathbf{x}_\perp}\cdot(\widehat{\mathbf{u}}^{\mathrm{K}}_{\mathrm{drift}}\,\widehat{g}) = \nu_{\mathrm{r}}\,\partial_{v_\parallel}\left[(v_\parallel - \widehat{u}_\parallel)\,\widehat{g} + \widehat{T}\,\partial_{v_\parallel}\widehat{g}\right] \\ \qquad\qquad + \varepsilon\,\nabla_{\mathbf{x}_\perp}\cdot\left(\widehat{n}\,\widehat{T}_\perp\,\mathbb{D}_2\nabla_{\mathbf{x}_\perp}\frac{\widehat{g}}{\widehat{n}}\right), \\ \partial_t(\widehat{n}\,\widehat{T}_\perp) + \partial_z(\widehat{n}\,\widehat{T}_\perp\,\widehat{u}_\parallel) + \varepsilon\,\nabla_{\mathbf{x}_\perp}\cdot(2\,\widehat{n}\,\widehat{T}_\perp\,\widehat{\mathbf{u}}_{\mathrm{drift}}) + \varepsilon\,\nabla_{\mathbf{x}}\cdot\mathbf{q} = \varepsilon\,\widehat{n}\,\widehat{\mathbf{u}}_{\mathrm{drift}}\cdot\mathbf{E}_\perp \\ \qquad\qquad + \frac{2}{3}\,\nu_{\mathrm{r}}\,\widehat{n}\,(\widehat{T}_\parallel - \widehat{T}_\perp)\,. \end{cases} \tag{3.2.7b}$$

Here, the drift velocities are given by

$$\widehat{\mathbf{u}}^{\mathrm{K}}_{\mathrm{drift}} = \frac{\mathbf{E}_\perp\times\mathbf{B}}{|B|^2} - \frac{\nabla_{\mathbf{x}_\perp}(\widehat{g}\,\widehat{T}_\perp)\times\mathbf{B}}{\widehat{g}\,|B|^2}, \qquad \widehat{\mathbf{u}}_{\mathrm{drift}} = \frac{\mathbf{E}_\perp\times\mathbf{B}}{|B|^2} - \frac{\nabla_{\mathbf{x}_\perp}(\widehat{n}\,\widehat{T}_\perp)\times\mathbf{B}}{\widehat{n}\,|B|^2}, \tag{3.2.7c}$$

the temperature $\widehat{T}$ is computed via $\widehat{T} = (\widehat{T}_\parallel + 2\,\widehat{T}_\perp)/3$, the macroscopic quantities $(\widehat{n},\,\widehat{u}_\parallel,\,\widehat{T}_\parallel)$ are defined through

$$\widehat{n} = \langle\widehat{g}\rangle_\parallel, \qquad \widehat{n}\,\widehat{u}_\parallel = \langle v_\parallel\widehat{g}\rangle_\parallel, \qquad \frac{1}{2}\widehat{n}\,\widehat{T}_\parallel = \frac{1}{2}\left\langle (v_\parallel - \widehat{u}_\parallel)^2\,\widehat{g}\right\rangle_\parallel, \tag{3.2.7d}$$

and the heat flux is given by

$$\mathbf{q} = \begin{pmatrix}\mathbf{q}_\perp \\ q_\times\end{pmatrix}, \qquad \mathbf{q}_\perp = -2\,\widehat{n}\,\widehat{T}_\perp\,\mathbb{D}_1\,\nabla_{\mathbf{x}_\perp}\widehat{T}_\perp, \qquad q_\times = -\frac{1}{2\,\nu_\perp}\,\widehat{n}\,\widehat{T}_\parallel\,\partial_z\widehat{T}_\perp. \tag{3.2.7e}$$

The quantity $\Lambda_{\hat{g},\hat{T}_\perp}$ is a polynomial quantity in $\mathbf{v}_\perp$ entirely defined in terms of the quantities $\hat{g}$, $\hat{T}_\perp$ through

$$\Lambda_{\hat{g},\hat{T}_\perp}(\mathbf{v}) := \frac{\hat{\mathbf{u}}^{\mathrm{K}}_{\mathrm{drift}} \cdot \mathbf{v}_\perp}{\hat{T}_\perp} - \left(\mathbb{D}_1 \frac{\nabla_{\mathbf{x}_\perp} \hat{T}_\perp}{\hat{T}_\perp} \right) \cdot \mathbf{v}_\perp \left[\frac{|\mathbf{v}_\perp|^2}{2\,\hat{T}_\perp} - 2 \right] + \frac{\partial_z \hat{T}_\perp}{\hat{T}_\perp} \frac{\hat{u}_\parallel - v_\parallel}{2} \left[\frac{|\mathbf{v}_\perp|^2}{2\,\hat{T}_\perp} - 1 \right] - \left(\mathbb{D}_2 \frac{\nabla_{\mathbf{x}_\perp} (\hat{g}/\hat{n})}{(\hat{g}/\hat{n})} \right) \cdot \mathbf{v}_\perp, \tag{3.2.7f}$$

where the positive diffusion matrices are given by

$$\mathbb{D}_1 = \frac{1}{B^2 + 9\,\nu_\perp^2} \begin{bmatrix} 3\,\nu_\perp & B \\ -B & 3\,\nu_\perp \end{bmatrix}, \qquad \mathbb{D}_2 = \frac{\nu_\perp}{B} \frac{1}{B^2 + \nu_\perp^2} \begin{bmatrix} B & -\nu_\perp \\ \nu_\perp & B \end{bmatrix}. \tag{3.2.7g}$$

This system (3.2.7b) is supplemented with the following well-prepared initial condition

$$f^\varepsilon_{\mathrm{in}}(\mathbf{x},\mathbf{v}) = g^\varepsilon_{\mathrm{in}}(\mathbf{x}, v_\parallel)\, \mathcal{M}_\perp^{T^\varepsilon_{\perp,\mathrm{in}}}(\mathbf{v}_\perp) \left(1 + \varepsilon\, \Lambda_{g^\varepsilon_{\mathrm{in}},\, T^\varepsilon_{\perp,\mathrm{in}}}\right). \tag{3.2.7h}$$

Let us comment on the key aspects of Theorem 5:

- Setting $\varepsilon = 0$ in (3.2.7b) gives back the limit model from Theorem 4.
- The asymptotic form of $\hat{f}^\varepsilon$ (3.2.7a) resembles (3.1.2) (which was given in [CHM16]). In our case, however, there is the additional correction term $\Lambda_{\hat{g},\hat{T}}$, given in (3.2.7f), which destroys the product structure with respect to $(v_\parallel, \mathbf{v}_\perp)$ in the distribution function.
- The system of PDEs (3.2.7b) satisfied by $(\hat{g},\ \hat{T}_\perp)$ has a higher dimensionality $3\mathrm{D}_x1\mathrm{D}_v$ than the limit model ($1\mathrm{D}_x1\mathrm{D}_v$). This is a) due to the perpendicular plasma drifts that occur at first order in ε in the present scaling, and b) due to perpendicular diffusion arising from collisions $Q_\perp$ at first order. Such diffusion terms are typical first-order corrections in fluid models - the Navier-Stokes equations being the prime example for first-order corrections to Euler equations.
- In the fluid equation for $\hat{T}_\perp$, one observes the classical plasma drift $\hat{\mathbf{u}}_{\mathrm{drift}}$, which is the sum of the $\mathbf{E}\times\mathbf{B}$ drift and the diamagnetic drift. Moreover, in the kinetic equation for $\hat{g}$ appears the new "kinetic diamagnetic drift" term $\hat{\mathbf{u}}^K_{\mathrm{drift}}$ which depends on $v_\parallel$ through $\hat{g}$. The latter seems to be a quite unusual term when comparing for instance to standard guiding-center models for magnetized plasma. There, the diamagnetic drift appears only on the level of the moment equations, and not already on the kinetic level. In the model presented here, the fact that the diamagnetic drift is present in the kinetic equation suggest a sort of "hybrid character" of the model, due to the assumption of high collisionality in the perpendicular direction only.
- The temperature equation features a heat flux $\mathbf{q}$, given in (3.2.7e), of Braginskii type [NP16; Bra65], composed of gyroviscous (antidiagonal) and viscous (diagonal) terms.

— One observes that there is, in the kinetic equation on $\widehat{g}$, a diffusion-type term in the $\mathbf{x}_\perp$ variable, coming from the combined effects of the magnetic field with the collision term. The diffusion frequency associated with this term scales as the matrix $\mathbb{D}_2$, which involves the two frequencies $\nu_\perp$ and qB/m. This term acts on a long time-scale, and is responsible for the homogenisation in the perpendicular plane of the macroscopic quantities. This can be immediately seen by taking the moments of the kinetic equation:

$$\begin{cases} \partial_t \widehat{n} + \partial_z(\widehat{n}\,\widehat{u}_\parallel) + \varepsilon\,\nabla_{\mathbf{x}_\perp}\cdot(\widehat{n}\,\widehat{\mathbf{u}}_{\mathrm{drift}}) = 0\,, \\ \partial_t(\widehat{n}\,\widehat{u}_\parallel) + \partial_z(2\,\widehat{w}_\parallel) + \varepsilon\,\nabla_{\mathbf{x}_\perp}\cdot\left(\dfrac{\mathbf{E}_\perp\times\mathbf{B}}{|B|^2}\,\widehat{n}\,\widehat{u}_\parallel - \dfrac{\nabla_{\mathbf{x}_\perp}(\widehat{n}\,\widehat{u}_\parallel\,T_\perp)\times\mathbf{B}}{|B|^2}\right) - \widehat{n}\,E_\parallel \\ \qquad = \varepsilon\,\nabla_{\mathbf{x}_\perp}\cdot\left(\widehat{n}\,\widehat{T}_\perp\,\mathbb{D}_2\,\nabla_{\mathbf{x}_\perp}\,\widehat{u}_\parallel\right)\,, \\ \partial_t\widehat{w}_\parallel + \partial_z\left\langle\dfrac{v_\parallel^3}{2}\,\widehat{g}\right\rangle_\parallel + \varepsilon\,\nabla_{\mathbf{x}_\perp}\cdot\left(\dfrac{\mathbf{E}_\perp\times\mathbf{B}}{|B|^2}\,\widehat{w}_\parallel - \dfrac{\nabla_{\mathbf{x}_\perp}(\widehat{w}_\parallel\,T_\perp)\times\mathbf{B}}{|B|^2}\right) - \widehat{n}\,\widehat{u}_\parallel\,E_\parallel \\ \qquad = \dfrac{2}{3}\,\nu_{\mathrm{r}}\,\widehat{n}\,(\widehat{T}_\perp - \widehat{T}_\parallel) + \varepsilon\,\nabla_{\mathbf{x}_\perp}\cdot\left(\widehat{n}\,\widehat{T}_\perp\,\mathbb{D}_2\,\nabla_{\mathbf{x}_\perp}\,\dfrac{\widehat{w}_\parallel}{\widehat{n}}\right)\,, \end{cases} \tag{3.2.8a}$$

where we used the following notation for the second moment of $\widehat{g}$:

$$\widehat{w}_\parallel := \left\langle\frac{v_\parallel^2}{2}\,\widehat{g}\right\rangle_\parallel\,. \tag{3.2.9}$$

One notices that the diffusion term does not operate on n, but diffuses higher order moments in the perpendicular plane.

— Setting $\mathbf{E} = 0$ to not inject energy into the system, this first order correction model satisfies the following energy conservation:

$$\frac{\mathrm{d}}{\mathrm{d}t}\int_{\mathbb{T}^3_x}\left[\frac{3}{2}\,\widehat{n}\,\widehat{T} + \frac{1}{2}\,\widehat{n}\,\widehat{u}_\parallel^2\right]\mathrm{d}\mathbf{x} = 0\,.$$

One could be surprised by the fact that only the parallel kinetic energy $\frac{1}{2}\,\widehat{n}\,\widehat{u}_\parallel^2$ appears in this energy conservation. The reason why the perpendicular kinetic energy $\frac{1}{2}\,\widehat{n}\,|\varepsilon\,\widehat{\mathbf{u}}_{\mathrm{drift}}|^2$ does not appear is because it is of order $\mathcal{O}(\varepsilon^2)$. It is therefore within the range of error of the first order correction of the model.

Let us now turn to the strategy followed in this article to derive Theorems 4 and 5.

3.2.2 Strategy: Hilbert hierarchy

The proofs of Theorem 4 and 5 are based on a Hilbert expansion, which we shall present in this subsection. Let us denote by $\mathbb{A}$ the dominant operator in the full Vlasov equation (3.1.13), namely

$$\mathbb{A}(f) := (\mathbf{v}\times B\mathbf{e}_z)\cdot\nabla_{\mathbf{v}} f - \nu_\perp\,Q_\perp(f)\,, \tag{3.2.10}$$

where $Q_\perp$ is defined in (3.1.14). With this notation, equation (3.1.13) rewrites

$$\partial_t f^\varepsilon + \mathbf{v}\cdot\nabla_{\mathbf{x}} f^\varepsilon + \mathbf{E}\cdot\nabla_{\mathbf{v}} f^\varepsilon + \frac{1}{\varepsilon}\mathbb{A}(f^\varepsilon) = \nu_{\mathrm{r}}\, Q_{\mathrm{r}}(f^\varepsilon)\,. \tag{3.2.11}$$

Let us assume that the solution f^ε can be expanded in the following formal power series in ε:

$$f^\varepsilon = f^0 + \varepsilon\, f^1 + \varepsilon^2\, f^2 + \mathcal{O}(\varepsilon^3)\,.$$

Plugging this ansatz into (3.2.11) and comparing terms of the same order in ε leads to the following Hilbert hierarchy:

$$\mathbb{A}(f^0) = 0\,, \qquad : \mathcal{O}(\varepsilon^{-1}) \tag{3.2.12a}$$

$$\partial_t f^0 + \mathbf{v}\cdot\nabla_{\mathbf{x}} f^0 + \mathbf{E}\cdot\nabla_{\mathbf{v}} f^0 + \mathbb{A}^{\mathrm{lin}}_{f^0}(f^1) = \nu_{\mathrm{r}}\, Q_{\mathrm{r}}(f^0)\,, \qquad : \mathcal{O}(1) \tag{3.2.12b}$$

$$\partial_t f^1 + \mathbf{v}\cdot\nabla_{\mathbf{x}} f^1 + \mathbf{E}\cdot\nabla_{\mathbf{v}} f^1 + \mathbb{A}^{\mathrm{lin}}_{f^0}(f^2) - \nu_\perp\,\delta^2 Q_\perp(f^1) = \nu_{\mathrm{r}}\,\delta Q_{\mathrm{r}}[f^0](f^1)\,, \qquad : \mathcal{O}(\varepsilon) \tag{3.2.12c}$$

where we denoted by $\delta^2 Q_\perp(f^1)$ a remainder term, quadratic in the order one quantities (its expression is given later in (3.4.5) for the sake of shortness of the presentation), and by $\delta\mathbb{O}[f^0]$ the linearization of any nonlinear operator $\mathbb{O}$ around a function f^0, namely

$$\delta\mathbb{O}[f^0](\delta f) = \lim_{\|\delta f\|\to 0} \frac{\mathbb{O}(f^0+\delta f) - \mathbb{O}(f^0)}{\|\delta f\|}\,. \tag{3.2.13}$$

The linear part of the dominant operator (3.2.10) is hence

$$\mathbb{A}^{\mathrm{lin}}_{f^0}(\delta f) := \delta\mathbb{A}[f^0](\delta f) = (\mathbf{v}\times B\mathbf{e}_z)\cdot\nabla_{\mathbf{v}}\delta f - \nu_\perp\,\delta Q_\perp[f^0](\delta f)\,. \tag{3.2.14}$$

The investigation of each one of the equation occurring in this hierarchy permits to get step by step information about the coefficients f^0, f^1. Section 3.3 deals thus with the detailed study of equations (3.2.12a)-(3.2.12b), yielding the limit model for f^0 and leading to the proof of Theorem 4. Section 3.4 focuses on equations (3.2.12b)-(3.2.12c), permitting to obtain f^1 and to conclude the proof of Theorem 5.

3.3 Limit model

As expected from (3.2.12a), in order to fully characterize the limit distribution f^0, it is necessary to study in detail the kernel of $\mathbb{A}$. Using then the two equations (3.2.12a)-(3.2.12b) permits to get the limit model and prove Theorem 4. Let us underline that operators $Q_\perp$ and $\mathbb{A}$ act only on the velocity variable $\mathbf{v}$. Therefore in subsections 3.3.1 and 3.3.2, we shall deal with functions of $\mathbf{v}$ only. In subsection 3.3.3 however we shall consider the whole phase-space.

3.3.1 Properties of the collision operator $Q_\perp$

The perpendicular Fokker-Planck collision operator $Q_\perp$ defined in (3.1.14) satisfies the following properties, which are easily checked:

— $Q_\perp$ can be expressed with the following alternative form

$$Q_\perp(f) = \nabla_{\mathbf{v}_\perp} \cdot \left[T_\perp \, \mathcal{M}_\perp^{\mathbf{u}_\perp, T_\perp} \nabla_{\mathbf{v}_\perp} \left(\frac{f}{\mathcal{M}_\perp^{\mathbf{u}_\perp, T_\perp}} \right) \right], \tag{3.3.1}$$

where we denoted

$$\mathcal{M}_\perp^{\mathbf{u}_\perp, T_\perp}(\mathbf{v}_\perp) := \frac{1}{2\pi \, T_\perp} e^{-\frac{|\mathbf{v}_\perp - \mathbf{u}_\perp|^2}{2T_\perp}},$$

and the macroscopic quantities $\mathbf{u}_\perp$, $T_\perp$, associated with f, are defined thanks to (3.1.6).

— Mass, momentum and energy conservation:

$$\int_{\mathbb{R}^3_v} \begin{pmatrix} 1 \\ \mathbf{v}_\perp \\ \frac{|\mathbf{v}_\perp|^2}{2} \end{pmatrix} Q_\perp(f) \, \mathrm{d}\mathbf{v} = 0\,, \qquad \text{and even} \qquad \int_{\mathbb{R}^2_v} Q_\perp(f) \, \mathrm{d}\mathbf{v}_\perp = 0\,. \tag{3.3.2}$$

— Entropy Decay *(H-Theorem)*:

$$\begin{aligned} \int_{\mathbb{R}^3_v} Q_\perp(f) \ln(f) \, \mathrm{d}\mathbf{v} &= \int_{\mathbb{R}^3_v} Q_\perp(f) \ln \left(\frac{f}{\mathcal{M}_\perp^{\mathbf{u}_\perp, T_\perp}} \right) \mathrm{d}\mathbf{v} \\ &= - \int_{\mathbb{R}^3_v} T_\perp \, \frac{(\mathcal{M}_\perp^{\mathbf{u}_\perp, T_\perp})^2}{f} \left| \nabla_{\mathbf{v}_\perp} \frac{f}{\mathcal{M}_\perp^{\mathbf{u}_\perp, T_\perp}} \right|^2 \mathrm{d}\mathbf{v} \leqslant 0, \qquad \forall f > 0\,; \end{aligned} \tag{3.3.3}$$

— Thermal equilibrium:

$$\int_{\mathbb{R}^3_v} Q_\perp(f) \ln(f) \, \mathrm{d}\mathbf{v} = 0 \quad \Leftrightarrow \quad f(\mathbf{v}) = g(v_\parallel) \, \mathcal{M}_\perp^{\mathbf{u}_\perp, T_\perp}(\mathbf{v}_\perp), \qquad \forall f > 0\,. \tag{3.3.4}$$

3.3.2 Study of the dominant operator $\mathbb{A}$

The main properties of $\mathbb{A}$ defined in (3.2.10) are regrouped in the following Proposition 3.3.1.

Proposition 3.3.1 (**Kernel of $\mathbb{A}$.**). The kernel of the operator $\mathbb{A}$, defined in (3.2.10), namely, the set of positive functions such that $\mathbb{A}(f) = 0$, is given by

$$\operatorname{Ker} \mathbb{A} = \{ f = g(v_\parallel) \mathcal{M}_\perp^{T_\perp}(\mathbf{v}_\perp)\,,\ g > 0 \}\,, \tag{3.3.5}$$

where $T_\perp > 0$, and $\mathcal{M}_\perp^{T_\perp}$ is defined in (3.2.2b).

Proof. First, let us notice that if f is a function of the form

$$f(\mathbf{v}) = g(v_\parallel) \mathcal{M}_\perp^{T_\perp}(\mathbf{v}_\perp)\,,$$

then f is both

1. radial in $\mathbf{v}_\perp$, cancelling the rotation term $(\mathbf{v}\times\mathbf{B})\cdot\nabla_{\mathbf{v}} f$,
2. and Maxwellian in $\mathbf{v}_\perp$, leading to $Q_\perp(f) = 0$,

thus leading to $\mathbb{A}(f) = 0$.

Conversely, let us assume that $f \in \ker \mathbb{A}$, namely, assume that

$$(\mathbf{v}\times\mathbf{B})\cdot\nabla_{\mathbf{v}} f - \nu_\perp\, Q_\perp(f) \;= 0\,. \tag{3.3.6}$$

Testing (3.3.6) against $\ln(f)$ and integrating against $\mathrm{d}\mathbf{v}$ yields :

$$\nu_\perp \int_{\mathbb{R}^3_v} Q_\perp(f)\ln(f)\,\mathrm{d}\mathbf{v} = 0\,,$$

noticing that the term involving the magnetic field becomes zero. This implies that f is of the form

$$f(\mathbf{v}) = g(v_\parallel)\,\mathcal{M}_\perp^{\mathbf{u}_\perp,T_\perp}(\mathbf{v}_\perp)\,,$$

using (3.3.4). Plugging this expression of f in equality (3.3.6) cancels the collision term, and we are left with

$$B\,g\,\mathcal{M}_\perp^{\mathbf{u}_\perp,T_\perp}\left\{\frac{v_y\,u_x}{T_\perp} - \frac{v_x\,u_y}{T_\perp}\right\} = 0\,, \qquad \forall v_x, v_y \in \mathbb{R}_v\,,$$

where $u_x,\ u_y$ are the components of $\mathbf{u}_\perp$. The identification of the coefficients of this polynomial expression in v_x, v_y gives $u_x = u_y = 0,$ leading to the required form of f.

□

Now that we characterized the kernel of $\mathbb{A}$, we are in capacity to deal with (3.2.12a). We still however need to study some properties of the linearized operator $\mathbb{A}^{\mathrm{lin}}_{f^0}$ defined in (3.2.14), for the analysis of (3.2.12b). Let us state the following Lemma, which sums up the conservation properties of $\mathbb{A}^{\mathrm{lin}}_{f^0}$:

Lemma 7. The linearized version $\mathbb{A}^{\mathrm{lin}}_{f^0}$ of the dominant operator satisfy the following conservation properties:

$$\left\langle \mathbb{A}^{\mathrm{lin}}_{f^0}(\xi)\right\rangle_\perp = 0\,, \qquad \left\langle |\mathbf{v}_\perp|^2 \mathbb{A}^{\mathrm{lin}}_{f^0}(\xi)\right\rangle = 0\,, \tag{3.3.7}$$

for any arbitrary function ξ.

Proof of Lemma 7. The first step is to notice that these properties hold for the total operator $\mathbb{A}$ as a direct consequence of the conservations of $Q_\perp$ (3.3.2). But then $\mathbb{A}^{\mathrm{lin}}_{f^0}$ also satisfies these conservation properties by linearity, integrating the definition (3.2.13) for $\mathbb{O} = \mathbb{A}$. □

3.3.3 Proof of Theorem 4 (Limit model)

It this section, we shall keep in mind that the previous analysis was carried out for functions of the $\mathbf{v}$ variable only, while the solution f^ε of (3.2.11) depends on the parameters $(t, \mathbf{x})$. The proof is divided into several steps, based on the two first equations of the Hilbert hierarchy (3.2.12):

$$\mathbb{A}(f^0) = 0\,, \qquad : \mathcal{O}(\varepsilon^{-1}) \tag{3.3.8a}$$

$$\partial_t f^0 + \mathbf{v}\cdot\nabla_{\mathbf{x}} f^0 + \mathbf{E}\cdot\nabla_{\mathbf{v}} f^0 + \mathbb{A}^{\mathrm{lin}}_{f^0}(f^1) = \nu_{\mathrm{r}}\, Q_{\mathrm{r}}(f^0)\,. \qquad : \mathcal{O}(1) \tag{3.3.8b}$$

Step 1: the limit distribution f^0. The first equation in the Hilbert hierarchy is

$$\mathbb{A}(f^0) = 0\,.$$

As a consequence, Proposition 3.3.1 yields the existence of two functions $g^0(t,\mathbf{x},v_\parallel)$, $T^0_\perp(t,\mathbf{x})$ such that

$$f^0(t,\mathbf{x},\mathbf{v}) = g^0(t,\mathbf{x},v_\parallel)\,\mathcal{M}^{T^0_\perp}_\perp(\mathbf{v}_\perp)\,, \tag{3.3.9}$$

which is exactly (3.2.2a).

Step 2: Equation for the reduced distribution function g^0. We plug (3.3.9) into the second equation (3.3.8b) and then integrate with respect to $\mathbf{v}_\perp$. Using the conservation properties given in Lemma 7, one finds

$$\partial_t g^0 + v_\parallel\,\partial_z g^0 + \nabla_{\mathbf{x}_\perp}\cdot\left\langle \mathbf{v}_\perp f^0\right\rangle_\perp + E_\parallel \partial_{v_\parallel} g^0 = \nu_{\mathrm{r}}\,\partial_{v_\parallel}\left[(v_\parallel - u^0_\parallel)\,g^0 + T^0\,\partial_{v_\parallel} g^0_\parallel\right]\,. \tag{3.3.10}$$

It remains to compute the flux term, thanks to ansatz (3.3.9). We find that

$$\left\langle \mathbf{v}_\perp f^0\right\rangle_\perp = g^0 \int_{\mathbb{R}^2_v} \mathbf{v}_\perp\,\mathcal{M}^{T^0_\perp}_\perp\,\mathrm{d}\mathbf{v}_\perp = 0\,,$$

by imparity. Plugging this last equality into (3.3.10) yields exactly the kinetic equation on g^0.

Step 3: Equation for the perpendicular temperature $T^0_\perp$. Firstly, integrating (3.3.9) against $\frac{|\mathbf{v}_\perp|^2}{2}\,\mathrm{d}\mathbf{v}$ yields

$$n^0\,T^0_\perp = \left\langle \frac{|\mathbf{v}_\perp|^2}{2}\,f^0\right\rangle,$$

thanks to $n^0 = \langle g^0\rangle_\parallel$ (defined in (3.2.3)), and standard Gaussian moment computations. Now, let us integrate (3.3.8b) against $\frac{|\mathbf{v}_\perp|}{2}\,\mathrm{d}\mathbf{v}$. Using the conservation properties of $\mathbb{A}^{\mathrm{lin}}_{f^0}$ (given in Lemma 7) along with property (3.1.10) on Q_{r} ($\frac{k_B}{m}$ is now set to 1), one finds

$$\partial_t(n^0\,T^0_\perp) + \nabla_{\mathbf{x}_\perp}\cdot\mathbb{Q}^0_\perp + \partial_z\mathbb{Q}^0_\times = n^0\,\mathbf{u}^0_\perp\cdot\mathbf{E}_\perp + \frac{2}{3}\,\nu_{\mathrm{r}}\,n^0\,(T^0_\parallel - T^0_\perp)\,, \tag{3.3.11}$$

with the following definitions for the energy fluxes $\mathbb{Q}^0_\perp$ and $\mathbb{Q}^0_\times$

$$\mathbb{Q}^0_\perp := \left\langle \mathbf{v}_\perp \frac{|\mathbf{v}_\perp|^2}{2} f^0 \right\rangle, \qquad \mathbb{Q}^0_\times := \left\langle v_\parallel \frac{|\mathbf{v}_\perp|^2}{2} f^0 \right\rangle.$$

Let us now compute each of the terms in (3.3.11):

$$\begin{aligned}
\mathbb{Q}^0_\perp &= \left\langle \mathbf{v}_\perp \frac{|\mathbf{v}_\perp|^2}{2} f^0 \right\rangle = \int_{\mathbb{R}_v} g^0 \,\mathrm{d}v_\parallel \int_{\mathbb{R}^2_v} \mathbf{v}_\perp \frac{|\mathbf{v}_\perp|^2}{2} \mathcal{M}^{T^0_\perp}_\perp \,\mathrm{d}\mathbf{v}_\perp = 0\,, \\
\mathbb{Q}^0_\times &= \left\langle v_\parallel \frac{|\mathbf{v}_\perp|^2}{2} f^0 \right\rangle = \int_{\mathbb{R}_v} v_\parallel g^0 \,\mathrm{d}v_\parallel \int_{\mathbb{R}^2_v} \frac{|\mathbf{v}_\perp|^2}{2} \mathcal{M}^{T^0_\perp}_\perp \,\mathrm{d}\mathbf{v}_\perp = n^0\, u^0_\parallel\, T^0_\perp\,, \\
n^0\, \mathbf{u}^0_\perp &= \langle \mathbf{v}_\perp f^0 \rangle = \int_{\mathbb{R}_v} g^0 \,\mathrm{d}v_\parallel \int_{\mathbb{R}^2_v} \mathbf{v}_\perp\, \mathcal{M}^{T^0_\perp}_\perp \,\mathrm{d}\mathbf{v}_\perp = 0\,,
\end{aligned}$$

where the first and third equalities come from imparity. We also used the definition of parallel moments (3.2.3) for the second equality. Plugging these equalities into (3.3.11) yields exactly the required equation on $T^0_\perp$, thus concluding the proof.

3.4 First order correction

This section contains the analysis for obtaining first-order corrections to the limit model of Theorem 4. After stating the problem in the prelminaries of section 3.4.1, we proceed with the analysis of the dominant operators in section 3.4.2; this will permit the computation of the distribution function f^1, carried out in sections 3.4.3 and 3.4.4. Eventually this will lead to the proof of Theorem 5 in section 3.4.7.

3.4.1 Preliminaries

Let us now proceed to the computation of the first order correction model, investigating the following two equations of the Hilbert hierarchy (3.2.12):

$$O(1): \qquad \partial_t f^0 + \mathbf{v}\cdot\nabla_{\mathbf{x}} f^0 + \mathbf{E}\cdot\nabla_{\mathbf{v}} f^0 + \mathbb{A}^{\mathrm{lin}}_{f^0}(f^1) = \nu_{\mathrm{r}}\, Q_{\mathrm{r}}(f^0)\,, \tag{3.4.1a}$$

$$O(\varepsilon): \qquad \partial_t f^1 + \mathbf{v}\cdot\nabla_{\mathbf{x}} f^1 + \mathbf{E}\cdot\nabla_{\mathbf{v}} f^1 + \mathbb{A}^{\mathrm{lin}}_{f^0}(f^2) - \nu_\perp\, \delta^2 Q_\perp(f^1) = \nu_{\mathrm{r}}\, \delta Q_{\mathrm{r}}[f^0](f^1)\,. \tag{3.4.1b}$$

Here, $\mathbb{A}^{\mathrm{lin}}_{f^0}$ was given in (3.2.14) with the linearized operator $\delta Q_\perp[f^0]$ derived from the definition (3.2.13),

$$\delta Q_\perp[f^0](\delta f) = \nabla_{\mathbf{v}_\perp}\cdot\left[\mathbf{v}_\perp \delta f - \delta \mathbf{u}_\perp f^0 - \delta T_\perp \frac{\mathbf{v}_\perp}{T^0_\perp} f^0 + T^0_\perp \nabla_{\mathbf{v}_\perp}\delta f\right], \tag{3.4.2}$$

where we used $\mathbf{u}^0_\perp = 0$ (as seen in the proof of Theorem 4), and the following definitions:

$$n^0\, \delta \mathbf{u}_\perp = \int_{\mathbb{R}^3_v} \mathbf{v}_\perp \delta f \,\mathrm{d}\mathbf{v}\,, \tag{3.4.3}$$

$$n^0\, \frac{\delta T_\perp}{T^0_\perp} = \int_{\mathbb{R}^3_v} \left(\frac{|\mathbf{v}_\perp|^2}{2\, T^0_\perp} - 1\right) \delta f \,\mathrm{d}\mathbf{v}\,. \tag{3.4.4}$$

This last line can also be rewritten as

$$n^0\,\delta T_\perp + \delta n\, T_\perp^0 = \frac{1}{2}\int_{\mathbb{R}^3_v} |\mathbf{v}_\perp|^2\,\delta f\,\mathrm{d}\mathbf{v}\,, \qquad \text{where} \qquad \delta n := \int_{\mathbb{R}_v} \delta g\,\mathrm{d}v_\parallel = \int_{\mathbb{R}^3_v} \delta f\,\mathrm{d}\mathbf{v}\,.$$

The term $\delta^2 Q_\perp(f^1)$ is quadratic in f^1 and n^1, $\mathbf{u}_\perp^1, T_\perp^1$ defined as the first order terms in the expansions $X^\varepsilon = X^0 + \varepsilon\, X^1 + O(\varepsilon^2)$:

$$\delta^2 Q_\perp(f^1) = \nabla_{\mathbf{v}_\perp}\cdot\left[-\mathbf{u}_\perp^1\left\{f^1 - \frac{n^1\,f^0}{n^0}\right\} + T_\perp^1\nabla_{\mathbf{v}_\perp}\left\{f^1 - \frac{n^1\,f^0}{n^0}\right\} - \frac{1}{2}|\mathbf{u}_\perp^1|^2\,\nabla_{\mathbf{v}_\perp} f^0\right]. \tag{3.4.5}$$

This quantity inherits the following conservation properties from $Q_\perp$:

$$\int_{\mathbb{R}^3_v}\begin{pmatrix}1\\ \mathbf{v}_\perp\\ \frac{|\mathbf{v}_\perp|^2}{2}\end{pmatrix}\delta^2 Q_\perp(f^1)\,\mathrm{d}\mathbf{v} = 0\,, \qquad \text{and even} \qquad \int_{\mathbb{R}^2_v}\delta^2 Q_\perp(f^1)\,\mathrm{d}\mathbf{v}_\perp = 0\,. \tag{3.4.6}$$

To prove Theorem 5, we need firstly to characterize completely f^1. However, f^1 appears in both equations (3.4.1a) and (3.4.1b), and each of those equations characterizes a different part of f^1. We shall thus perform a so-called *micro-macro* decomposition of f^1 permitting to characterize each part of f^1 by an equation of its own. In order to explain more clearly how we shall do that, let us fix the functional setting in which we are going to work. In the following $(\mathbf{x}, t)$ are merely parameters, and thus shall be omitted, until subsection 3.4.3.

Let f^0 be the solution of the limit model (3.2.2). We define the Hilbert space

$$\mathcal{H} := \left\{f \;:\; \mathbb{R}^3_v \to \mathbb{R}, \quad \int_{\mathbb{R}^3_v} |f|^2\,(f^0)^{-1}\,\mathrm{d}\mathbf{v} < \infty\right\}, \tag{3.4.7}$$

which is associated with the following scalar product:

$$(f_1, f_2)_{\mathcal{H}} := \int_{\mathbb{R}^3_v} f_1 f_2 \frac{1}{f^0}\,\mathrm{d}\mathbf{v}\,, \qquad f_1, f_2 \in \mathcal{H}\,, \tag{3.4.8}$$

with norm denoted by $\|\cdot\|_{\mathcal{H}}$. We have $f^0 \in \mathcal{H}$ and

$$\|f^0\|_{\mathcal{H}}^2 = \int_{\mathbb{R}^3_v} f^0\,\mathrm{d}\mathbf{v} = n^0\,.$$

In this space we shall define for any unbounded linear operator $\mathcal{O}$ its associated definition domain by:

$$\mathcal{D}(\mathcal{O}) := \{f \in \mathcal{H}, \quad \mathcal{O}f \in \mathcal{H}\}. \tag{3.4.9}$$

Let us denote by $\Pi : \mathcal{H} \to \ker \mathbb{A}^{\mathrm{lin}}_{f^0}$ the orthogonal projection onto the kernel of $\mathbb{A}^{\mathrm{lin}}_{f^0}$. With this notation in mind, we shall decompose $f^1 \in \mathcal{D}(\mathbb{A}^{\mathrm{lin}}_{f^0})$ in its macroscopic and microscopic parts, respectively:

$$f^1 = \bar{f}^1 + \widetilde{f}^1\,, \qquad \bar{f}^1 = \Pi f^1 \in \ker \mathbb{A}^{\mathrm{lin}}_{f^0}\,, \qquad \widetilde{f}^1 = (\mathbb{I}\mathrm{d} - \Pi) f^1 \in \ker^\perp \mathbb{A}^{\mathrm{lin}}_{f^0}\,. \tag{3.4.10}$$

Our goal is to compute both the macroscopic part $\bar{f}^1$ and the microscopic part $\widetilde{f}^1$. The macroscopic part $\bar{f}^1$ shall be characterized by taking the projection Π of equation (3.4.1b) (subsection 3.4.3). The microscopic part $\widetilde{f}^1$ will be characterized by taking $(\mathbb{I}\mathrm{d} - \Pi)$ of equation (3.4.1a) (subsection 3.4.4). The proof of Theorem 5 shall be concluded in subsection 3.4.7 from the complete characterization of f^0 and f^1.

3.4.2 Study of $\delta Q_\perp[f^0]$ and $\mathbb{A}^{\mathrm{lin}}_{f^0}$

In order to carry out this program let us firstly state several properties of $\delta Q_\perp[f^0]$ and $\mathbb{A}^{\mathrm{lin}}_{f^0}$. All of these properties are proven in Appendix 3.B. The normed space $\mathcal{H}$ defined in (3.4.7) is convenient for the study of the operator $\mathbb{A}^{\mathrm{lin}}_{f^0}$. Indeed, $\mathbb{A}^{\mathrm{lin}}_{f^0}$ is naturally decomposed as the sum of the skew-adjoint operator

$$((\mathbf{v}\times\mathbf{B})\cdot\nabla_{\mathbf{v}}\,\chi,\chi)_{\mathcal{H}} = 0, \quad \forall\,\chi\,, \tag{3.4.11}$$

and the self-adjoint operator $\delta Q_\perp[f^0]$ given in (3.4.2), the properties of which are stated in the following proposition.

Proposition 3.4.1 (**Properties of** $\delta Q_\perp[f^0]$**).** In the space $\mathcal{H}$ endowed with the scalar product $(\cdot,\cdot)_{\mathcal{H}}$, the operator $\delta Q_\perp[f^0]$ given in (3.4.2) satisfies the following properties:

— It is self-adjoint, namely

$$(-\delta Q_\perp[f^0]\xi,\chi)_{\mathcal{H}} = (\xi,-\delta Q_\perp[f^0]\chi)_{\mathcal{H}}, \quad \forall\xi,\,\chi\,, \tag{3.4.12}$$

and satisfies more specifically

$$\begin{aligned}(-\delta Q_\perp[f^0]\xi,\chi)_{\mathcal{H}} = \int_{\mathbb{R}^3_v} T^0_\perp\, f^0\,\nabla_{\mathbf{v}_\perp}\left(\frac{\xi}{f^0}\right)\cdot\nabla_{\mathbf{v}_\perp}\left(\frac{\chi}{f^0}\right)\mathrm{d}\mathbf{v}\\ - \frac{n^0}{T^0_\perp}\,\delta\mathbf{u}_{\perp,\xi}\cdot\delta\mathbf{u}_{\perp,\chi} - 2\,\frac{n^0}{(T^0_\perp)^2}\delta T_{\perp,\xi}\,\delta T_{\perp,\chi}, \quad \forall\xi,\chi\,,\end{aligned} \tag{3.4.13}$$

where we denoted by $\delta\mathbf{u}_{\perp,\xi}, \delta T_{\perp,\xi}$ (respectively $\delta\mathbf{u}_{\perp,\chi}, \delta T_{\perp,\chi}$) the bulk velocity and temperature defined in (3.4.3) and (3.4.4) associated with the function ξ (respectively χ).

— It inherits from $Q_\perp$ the conservation properties (3.3.2), namely

$$\int_{\mathbb{R}^3_v}\begin{pmatrix}1\\ \mathbf{v}_\perp\\ \frac{|\mathbf{v}_\perp|^2}{2}\end{pmatrix}\delta Q_\perp[f^0](\xi)\,\mathrm{d}\mathbf{v} = 0 \qquad \text{and even} \qquad \int_{\mathbb{R}^2_v}\delta Q_\perp[f^0](\xi)\,\mathrm{d}\mathbf{v}_\perp = 0\,. \tag{3.4.14}$$

— The kernel of $\delta Q_\perp[f^0]$ writes

$$\begin{aligned}\ker(\delta Q_\perp[f^0]) = \left\{\xi\in\mathcal{H},\quad \xi = \alpha(v_\parallel)\,f^0(\mathbf{v})\right\}\\ \oplus\left\{\xi\in\mathcal{H},\quad \xi = \beta(\mathbf{v}_\perp)\,f^0(\mathbf{v}),\quad \beta(\mathbf{v}_\perp)\in\mathrm{Span}\,\{v_x, v_y, |\mathbf{v}_\perp|^2\}\right\}.\end{aligned} \tag{3.4.15}$$

Proof of Proposition 3.4.1. The two first points follow from a straightforward computation, while the third point is proven in Appendix 3.B, subsection 3.B.1. □

As a consequence of this characterization of $\ker \delta Q_\perp[f^0]$, one shall define an orthogonal projection onto that kernel.

Lemma 8. The projection on $\ker \delta Q_\perp[f^0]$ reads

$$\begin{aligned} \pi \,:\, \mathcal{H} &\longrightarrow \ker \delta Q_\perp[f^0] \\ \chi &\mapsto \left\langle \varphi^0\, \chi(v_\parallel) \right\rangle_\perp \Phi^0(\mathbf{v}) + \sum_{k=x,y} \left\langle \varphi^1_k\, \chi \right\rangle \Phi^1_k(\mathbf{v}) + \left\langle \varphi^2\, \chi \right\rangle \Phi^2(\mathbf{v}), \end{aligned} \tag{3.4.16}$$

where we introduce the following polynomial expressions $(\varphi^0, \varphi^1_x, \varphi^1_y, \varphi^2)$ in the velocity variable $\mathbf{v}_\perp$, and an orthonormal family $(\Phi^0, \Phi^1_x, \Phi^1_y, \Phi^2)$ of $\mathcal{H}$:

$$\begin{aligned} \varphi^0(v_\parallel) &:= \frac{\sqrt{n^0}}{g^0(v_\parallel)}, & \Phi^0(\mathbf{v}) &:= \frac{1}{\sqrt{n^0}}\, f^0(\mathbf{v}), \\ \varphi^1_x(\mathbf{v}_\perp) &:= \frac{1}{\sqrt{n^0\, T^0_\perp}}\, v_x, & \Phi^1_x(\mathbf{v}) &:= \varphi^1_x(\mathbf{v}_\perp)\, f^0(\mathbf{v}), \\ \varphi^1_y(\mathbf{v}_\perp) &:= \frac{1}{\sqrt{n^0\, T^0_\perp}}\, v_y, & \Phi^1_y(\mathbf{v}) &:= \varphi^1_y(\mathbf{v}_\perp)\, f^0(\mathbf{v}), \\ \varphi^2(\mathbf{v}_\perp) &:= \frac{1}{\sqrt{n^0}} \left(\frac{|\mathbf{v}_\perp|^2}{2T^0_\perp} - 1 \right), & \Phi^2(\mathbf{v}) &:= \varphi^2(\mathbf{v}_\perp)\, f^0(\mathbf{v}). \end{aligned} \tag{3.4.17}$$

One underlines that in the expression of π (3.4.16) the first term does not play exactly the same role as the others. Indeed, for instance $\langle \varphi^0\, \chi \rangle_\perp$ is a function of the variable $v_\parallel$, and is not a scalar.

The family $(\Phi^1_x, \Phi^1_y, \Phi^2)$ also permit to express the quantities $\delta \mathbf{u}_{\perp,\xi}$ and $\delta T_{\perp,\xi}$, defined in (3.4.3)-(3.4.4) and associated to an arbitrary function $\xi \in \mathcal{H}$. Indeed, one has for $\xi \in \mathcal{H}$:

$$\begin{aligned} (\xi,\, \Phi^1_x)_{\mathcal{H}} &= \langle \varphi^1_x\, \xi \rangle = \sqrt{\frac{n^0}{T^0_\perp}} (\delta \mathbf{u}_{\perp,\xi})_x, \\ (\xi,\, \Phi^1_y)_{\mathcal{H}} &= \langle \varphi^1_y\, \xi \rangle = \sqrt{\frac{n^0}{T^0_\perp}} (\delta \mathbf{u}_{\perp,\xi})_y, \\ (\xi,\, \Phi^2)_{\mathcal{H}} &= \langle \varphi^2\, \xi \rangle = \sqrt{n^0}\, \frac{\delta T_{\perp,\xi}}{T^0_\perp}. \end{aligned}$$

With these notations, $\ker \delta Q_\perp[f^0]$ rewrites

$$\ker(\delta Q_\perp[f^0]) = \left\{ \xi = \beta(v_\parallel)\, \Phi^0(\mathbf{v}), \quad \xi \in \mathcal{H} \right\} \oplus \mathrm{Span}\{\Phi^1_x,\, \Phi^1_y,\, \Phi^2\}.$$

Now, thanks to the definition of that projection π, one can write the following coercivity property of the collision operator.

Proposition 3.4.2. **(Coercivity property of $\delta Q_\perp[f^0]$).** The following coercivity estimate for the linearized collision operator holds:

$$(-\delta Q_\perp[f^0]\chi,\chi)_{\mathcal{H}} = \int_{\mathbb{R}^3_v} T^0_\perp f^0 \left|\nabla_{\mathbf{v}_\perp}\left(\frac{\chi-\pi\chi}{f^0}\right)\right|^2 \mathrm{d}\mathbf{v} \geqslant \|\chi-\pi\chi\|^2_{\mathcal{H}} \qquad \forall \chi\,. \tag{3.4.18}$$

Proof. The proof can be found in Appendix 3.B.2 □

This property guarantees the positivity of $-\delta Q_\perp[f^0]$, and is useful in the proof of the next property, where we characterize the kernel of $\mathbb{A}^{\mathrm{lin}}_{f^0}$ and state its closed range property.

Proposition 3.4.3 (**Properties of the operator $\mathbb{A}^{\mathrm{lin}}_{f^0}$**). The operator $\mathbb{A}^{\mathrm{lin}}_{f^0}$ defined on $\mathcal{H}$ by (3.2.14) has the following properties:

— The kernel of $\mathbb{A}^{\mathrm{lin}}_{f^0}$ is given by

$$\ker\,\mathbb{A}^{\mathrm{lin}}_{f^0} = \left\{\xi\in\mathcal{H},\quad \xi=\alpha(v_\parallel)\,f^0(\mathbf{v})\right\}\oplus\{\xi\in\mathcal{H},\quad \xi=\beta|\mathbf{v}_\perp|^2\,f^0(\mathbf{v}),\quad \beta\in\mathbb{R}\}. \tag{3.4.19}$$

As a consequence, the orthogonal of $\ker\mathbb{A}^{\mathrm{lin}}_{f^0}$ in $\mathcal{H}$ is given by

$$\ker^\perp\mathbb{A}^{\mathrm{lin}}_{f^0} = \left\{\chi\in\mathcal{H}\,,\qquad \langle\chi\rangle_\perp = 0,\quad \left\langle\left(\frac{|\mathbf{v}_\perp|^2}{2\,T^0_\perp}-1\right)\chi\right\rangle = 0\right\}. \tag{3.4.20}$$

— The projection on $\ker\mathbb{A}^{\mathrm{lin}}_{f^0}$ is given by

$$\begin{array}{rccl}\Pi : & \mathcal{H} & \longrightarrow & \ker\mathbb{A}^{\mathrm{lin}}_{f^0}\\ & \xi & \mapsto & \langle\varphi^0\,\xi\rangle_\perp(v_\parallel)\,\Phi^0(\mathbf{v}) + \langle\varphi^2\,\xi\rangle\;\Phi^2(\mathbf{v})\end{array}. \tag{3.4.21}$$

— The operator $\mathbb{A}^{\mathrm{lin}}_{f^0}$ satisfies the following Poincaré-type inequality: there exists an explicit constant $C_A>0$, depending on B and $v_\perp$ only, such that

$$\|\xi\|_{\mathcal{H}} \leqslant C_A\|\mathbb{A}^{\mathrm{lin}}_{f^0}\xi\|_{\mathcal{H}}, \qquad \forall\xi\in\ker^\perp\mathbb{A}^{\mathrm{lin}}_{f^0}\cap\mathcal{D}(\mathbb{A}^{\mathrm{lin}}_{f^0}). \tag{3.4.22}$$

As a consequence, the operator $\mathbb{A}^{\mathrm{lin}}_{f^0}$ has closed range, which implies $\mathcal{R}(\mathbb{A}^{\mathrm{lin}}_{f^0}) = \ker^\perp\mathbb{A}^{\mathrm{lin}}_{f^0}$.

— The operator $\mathbb{A}^{\mathrm{lin}}_{f^0}$ can be restricted to the space $\ker^\perp\mathbb{A}^{\mathrm{lin}}_{f^0}$, such that the restriction (which we still denote as $\mathbb{A}^{\mathrm{lin}}_{f^0}$)

$$\mathbb{A}^{\mathrm{lin}}_{f^0} \;:\quad \ker^\perp\mathbb{A}^{\mathrm{lin}}_{f^0}\to\ker^\perp\mathbb{A}^{\mathrm{lin}}_{f^0},$$

is well defined, and is a bijection.

Let us now state a few remarks on this Proposition.

— As one can see, $\ker\mathbb{A}^{\mathrm{lin}}_{f^0}$ is smaller than $\ker\delta Q_\perp[f^0]$, as it contains only functions that are invariant by rotation with respect to $\mathbf{v}_\perp$. This is due to the fact that $\mathbb{A}^{\mathrm{lin}}_{f^0}$ contains the term $(\mathbf{v}\times\mathbf{B})\cdot\nabla_{\mathbf{v}}$. The projection Π reflects this fact, and its expression resembles that of π (equation (3.4.16)), but without the functions of type Φ^1_k, which are not invariant by rotation in $\mathbf{v}_\perp$.

— The closed range property comes from the Poincaré-type inequality (3.4.22) (see for reference [Bré20]). The inequality (3.4.22) holds with an explicit constant $C_A = \frac{1}{\nu_\perp} + \frac{\sqrt{2}}{|B|}$.
— Let us recall that these properties are stated for a fixed set of parameters $(t, \mathbf{x})$ such that $\nu_\perp > 0$, $B(t, \mathbf{x}) > 0$. If one works in a time-space dependent setting, one can obtain for instance such a Poincaré-type inequality in $L^2((0, T) \times \mathbb{T}^3_x ; \mathcal{H})$ by assuming a uniform lower bound condition on B, for instance assuming the existence of a constant γ such that

$$|B(t, \mathbf{x})| \geqslant \gamma > 0 \qquad \forall (t, \mathbf{x}) \in \mathbb{R}_+ \times \mathbb{T}^3_x \,. \tag{3.4.23}$$

With that previous property in mind, we are now able to completely characterize f^1. Firstly, let us focus on its macroscopic part $\bar{f}^1$.

3.4.3 Macroscopic part of f^1

Using the form of the orthogonal projection Π onto $\ker \mathbb{A}^{\mathrm{lin}}_{f^0}$, given in equation (3.4.21)), we know that the macroscopic part of f^1, namely $\bar{f}^1$, is given by the following equation:

$$\bar{f}^1 = \Pi f^1 = \langle \varphi^0 f^1 \rangle_\perp \Phi^0 + \langle \varphi^2 f^1 \rangle \Phi^2 = g^1 \mathcal{M}^{T^0_\perp}_\perp + \frac{r^1_\perp}{n^0} \left(\frac{|\mathbf{v}_\perp|^2}{2\, T^0_\perp} - 1 \right) f^0 \,, \tag{3.4.24}$$

where

$$g^1 := \left\langle f^1 \right\rangle_\perp = \left\langle \bar{f}^1 \right\rangle_\perp \,, \qquad \text{as} \quad \left\langle \widetilde{f}^1 \right\rangle_\perp = 0 \,, \tag{3.4.25}$$

$$r^1_\perp := n^0 \, \frac{T^1_\perp}{T^0_\perp} = \left\langle \left(\frac{|\mathbf{v}_\perp|^2}{2\, T^0_\perp} - 1 \right) f^1 \right\rangle = \left\langle \left(\frac{|\mathbf{v}_\perp|^2}{2\, T^0_\perp} - 1 \right) \bar{f}^1 \right\rangle \quad \text{as} \quad \left\langle \left(\frac{|\mathbf{v}_\perp|^2}{2\, T^0_\perp} - 1 \right) \widetilde{f}^1 \right\rangle = 0 \,. \tag{3.4.26}$$

The equation for g^1 can be derived integrating equation (3.4.1b) against $\mathrm{d}\mathbf{v}_\perp$, yielding thus

$$\partial_t g^1 + v_\parallel \partial_z g^1 + \nabla_{\mathbf{x}_\perp} \cdot \left\langle \mathbf{v}_\perp \widetilde{f}^1 \right\rangle_\perp + E_\parallel \partial_{v_\parallel} g^1 = \nu_{\mathrm{r}} \, \partial_{v_\parallel} \left((v_\parallel - u^0_\parallel)\, g^1 - u^1_\parallel \, g^0 + T^1 \partial_{v_\parallel} g^0 + T^0 \partial_{v_\parallel} g^1 \right) \right) , \tag{3.4.27}$$

where the macroscopic quantities $u^1_\parallel$ and T^1 are depending on g^1 and $T^1_\perp$ only, and are the first order terms in the expansion of $u^\varepsilon_\parallel$ and T^ε defined in (3.1.15). We also used that

$$\left\langle \mathbf{v}_\perp f^1 \right\rangle_\perp = \left\langle \mathbf{v}_\perp \widetilde{f}^1 \right\rangle_\perp \,.$$

As one can see, this equation (3.4.27) is not closed, as the flux term still depends on the microscopic function $\widetilde{f}^1$.

Rather than computing the equation on $r_\perp^1$, in order to simplify the computations, we shall compute the equation on

$$w_\perp^1 := (n\, T_\perp)^1 = n^0\, T_\perp^1 + n^1\, T_\perp^0 = \left\langle \frac{|\mathbf{v}_\perp|^2}{2} f^1 \right\rangle ,$$

which is completely equivalent, with the knowledge of the equation on g^1. Integrating (3.4.1b) with respect to $\frac{|\mathbf{v}_\perp|^2}{2}\,\mathrm{d}\mathbf{v}$ yields

$$\partial_t w_\perp^1 + \nabla_{\mathbf{x}_\perp} \cdot \mathbb{Q}_\perp^1 + \partial_z \mathbb{Q}_\times^1 = n^0 \mathbf{u}_\perp^1 \cdot \mathbf{E}_\perp + \frac{2}{3}\, \nu_{\mathrm{r}}\, (n\,(T_\parallel - T_\perp))^1, \tag{3.4.28}$$

where we define

$$\mathbb{Q}_\perp^1 := \left\langle \mathbf{v}_\perp \frac{|\mathbf{v}_\perp|^2}{2} f^1 \right\rangle = \left\langle \mathbf{v}_\perp \frac{|\mathbf{v}_\perp|^2}{2} \widetilde{f}^1 \right\rangle , \qquad \mathbb{Q}_\times^1 := \left\langle v_\parallel \frac{|\mathbf{v}_\perp|}{2} f^1 \right\rangle .$$

This time again, this equation is not closed and we need more information of $\widetilde{f}^1$.

Altogether, we need to close equations (3.4.27)-(3.4.28) which depend on f^1, and in particular $\widetilde{f}^1$. In fact, we shall fully compute $\widetilde{f}^1$, and this is the purpose of the next subsection.

3.4.4 Microscopic part of f^1

In order to completely characterize the first order microscopic correction distribution $\widetilde{f}^1$, let us rearrange the terms of (3.4.1a), as

$$\mathbb{A}_{f^0}^{\mathrm{lin}}(\widetilde{f}^1) = \nu_{\mathrm{r}}\, Q_{\mathrm{r}}(f^0) - \partial_t f^0 - \mathbf{v} \cdot \nabla_{\mathbf{x}} f^0 - \mathbf{E} \cdot \nabla_{\mathbf{v}} f^0 =: \mathcal{R}^0 . \tag{3.4.29}$$

Using that $\mathcal{R}(\mathbb{A}_{f^0}^{\mathrm{lin}}) = \ker^\perp \mathbb{A}_{f^0}^{\mathrm{lin}}$, we deduce the following implicit definition for $\widetilde{f}^1$, namely

$$\widetilde{f}^1 = \mathbb{A}_{f^0}^{\mathrm{lin}\,-1}(\mathcal{R}^0) . \tag{3.4.30}$$

There only remains to compute explicitly $\mathcal{R}^0$, and then to find its preimage. The following property sums up the result of this analysis.

Proposition 3.4.4. The remainder term $\mathcal{R}^0$ defined in (3.4.29) belongs to $\mathcal{R}(\mathbb{A}_{f^0}^{\mathrm{lin}})$, and simplifies as

$$\mathcal{R}^0 = \left\{ \frac{\mathbf{E}_\perp \cdot \mathbf{v}_\perp}{T_\perp^0} - \frac{\left(\mathbf{v}_\perp \cdot \nabla_{\mathbf{x}_\perp} T_\perp^0\right)}{T_\perp^0} \left[\frac{|\mathbf{v}_\perp|^2}{2T_\perp^0} - 1 \right] + \frac{\partial_z T_\perp^0}{T_\perp^0} \left(u_\parallel^0 - v_\parallel\right) \left(\frac{|\mathbf{v}_\perp|^2}{2\, T_\perp^0} - 1 \right) \right\} f^0$$

$$- \mathbf{v}_\perp \cdot (\nabla_{\mathbf{x}_\perp} g^0) \mathcal{M}_\perp . \tag{3.4.31}$$

As a consequence, the microscopic density $\widetilde{f}^1$ defined through

$$\widetilde{f}^1 = \mathbb{A}_{f^0}^{\mathrm{lin}\,-1}(\mathcal{R}^0) ,$$

reads

$$\begin{aligned}\widetilde{f}^1 = &\left(g^0 \frac{\mathbf{E}_\perp \times \mathbf{B}}{|B|^2} - \frac{\nabla_{\mathbf{x}_\perp}(g^0\, T^0_\perp) \times \mathbf{B}}{|B|^2} \right) \cdot \frac{\mathbf{v}_\perp}{T^0_\perp} \mathcal{M}_\perp - \left(\mathbb{D}_1 \frac{\nabla_{\mathbf{x}_\perp} T^0_\perp}{T^0_\perp} \right) \cdot \mathbf{v}_\perp \left[\frac{|\mathbf{v}_\perp|^2}{2\, T^0_\perp} - 2 \right] f^0 \\ &+ \frac{\partial_z T^0_\perp}{T^0_\perp} \frac{u^0_\parallel - v_\parallel}{2\, v_\perp} \left[\frac{|\mathbf{v}_\perp|^2}{2\, T^0_\perp} - 1 \right] f^0 - n^0 \left\{ \mathbb{D}_2 \nabla_{\mathbf{x}_\perp} \left(\frac{g^0}{n^0} \right) \right\} \cdot \mathbf{v}_\perp \mathcal{M}_\perp,\end{aligned} \tag{3.4.32}$$

where the definite positive matrices $\mathbb{D}_1$, $\mathbb{D}_2$ are given by

$$\mathbb{D}_1 = \frac{1}{B^2 + 9\, v_\perp^2} \begin{bmatrix} 3\, v_\perp & B \\ -B & 3\, v_\perp \end{bmatrix}, \qquad \mathbb{D}_2 = \frac{v_\perp}{B} \frac{1}{B^2 + v_\perp^2} \begin{bmatrix} B & -v_\perp \\ v_\perp & B \end{bmatrix}. \tag{3.4.33}$$

Proof. The proof of this property is technical and is postponed in Appendix C. □

Thanks to this property, we can compute the moments of $\widetilde{f}^1$, which shall permit to close the macroscopic system (3.4.27)-(3.4.28).

3.4.5 Closure of the macroscopic system

Let us start by the closure of the equation on g^1 (3.4.27), in particular by giving an explicit form to the flux term. Using formula (3.4.32), one gets

$$\left\langle \mathbf{v}_\perp \widetilde{f}^1 \right\rangle_\perp = \frac{g^0\, \mathbf{E}_\perp \times \mathbf{B} - \nabla_{\mathbf{x}_\perp}(g^0\, T^0_\perp) \times \mathbf{B}}{|B|^2} - n^0\, T^0_\perp\, \mathbb{D}_2 \cdot \nabla_{\mathbf{x}_\perp} \left(\frac{g^0}{n^0} \right). \tag{3.4.34}$$

As one can see, the right-hand side of (3.4.34) is decomposed into two terms playing different roles. Let us focus on the first one, and introduce the electric field drift

$$\mathbf{u}_E := \frac{\mathbf{E}_\perp \times \mathbf{B}}{|B|^2},$$

along with

$$\mathbf{u}_D^{\mathrm{K}} := -\frac{\nabla_{\mathbf{x}_\perp}(g^0\, T^0) \times \mathbf{B}}{g^0\, |B|^2}.$$

This quantity, which we call the "*kinetic diamagnetic drift*", is related to the classical diamagnetic drift

$$\mathbf{u}_D := -\frac{\nabla_{\mathbf{x}_\perp}(n^0\, T^0) \times \mathbf{B}}{n^0\, |B|^2},$$

through to the formula

$$\langle g^0\, \mathbf{u}_D^{\mathrm{K}} \rangle_\parallel = n^0\, \mathbf{u}_D\,.$$

Defining further

$$\mathbf{u}_{drift} := \mathbf{u}_E + \mathbf{u}_D\,, \qquad \mathbf{u}^{\mathrm{K}}_{drift} := \mathbf{u}_E + \mathbf{u}^{\mathrm{K}}_D\,,$$

the flux computed in (3.4.34) rewrites

$$\left\langle \mathbf{v}_\perp \widetilde{f}^1 \right\rangle_\perp = g^0\, \mathbf{u}^{\mathrm{K}}_{drift} - n^0\, T^0_\perp\, \mathbb{D}_2 \cdot \nabla_{\mathbf{x}_\perp} \left(\frac{g^0}{n^0} \right) .$$

The second term on the right-hand side of (3.4.34) is a diffusion-type correction, acting in the perpendicular plane direction, and is a novelty.

With these computations in mind, one finds the following equation on g^1:

$$\begin{aligned} \partial_t g^1 + v_\parallel \partial_z g^1 + E_\parallel \partial_{v_\parallel} g^1 + \nabla_{\mathbf{x}_\perp} \cdot \left(g^0\, \mathbf{u}^{\mathrm{K}}_{drift} \right) - \nabla_{\mathbf{x}_\perp} \cdot \left(n^0\, T^0_\perp\, \mathbb{D}_2 \cdot \nabla_{\mathbf{x}_\perp} \left(\frac{g^0}{n^0} \right) \right) \\ = \nu_{\mathrm{r}}\, \partial_{v_\parallel} \left((v_\parallel - u^0_\parallel)\, g^1 - u^1_\parallel\, g^0 + T^1 \partial_{v_\parallel} g^0 + T^0 \partial_{v_\parallel} g^1 \right) \right) , \end{aligned}$$

which now does not depend on $\widetilde{f}^1$.

Let us now turn to the closure of equation (3.4.28). As we mentioned earlier, the first non-closed term in (3.4.28) is

$$\mathbb{Q}^1_\perp = \left\langle \mathbf{v}_\perp \frac{|\mathbf{v}_\perp|^2}{2} f^1 \right\rangle = \left\langle \mathbf{v}_\perp \frac{|\mathbf{v}_\perp|^2}{2} \widetilde{f}^1 \right\rangle . \tag{3.4.35}$$

Now, using Proposition 3.4.4 which gives the expression of $\widetilde{f}^1$, one computes

$$\mathbb{Q}^1_\perp = 2\, n^0\, T^0_\perp\, \mathbf{u}_{drift} - 2\, n^0\, T^0_\perp\, \mathbb{D}_1 \nabla_{\mathbf{x}_\perp} T^0_\perp . \tag{3.4.36}$$

In order to identify the role of each of these quantities, we shall use the following decomposition of $\mathbb{Q}^\varepsilon_\perp := \left\langle \mathbf{v}_\perp \frac{|\mathbf{v}_\perp|^2}{2} f^\varepsilon \right\rangle$:

$$\mathbb{Q}^\varepsilon_\perp = \mathbf{q}^\varepsilon_\perp + \mathbb{P}^\varepsilon_\perp \cdot \mathbf{u}^\varepsilon_\perp + p^\varepsilon_\perp\, \mathbf{u}^\varepsilon_\perp - \frac{1}{2}\, n^\varepsilon\, |\mathbf{u}^\varepsilon_\perp|^2\, \mathbf{u}^\varepsilon_\perp , \tag{3.4.37}$$

where the *perpendicular heat flux* $\mathbf{q}^\varepsilon_\perp$, the *perpendicular stress tensor* $\mathbb{P}^\varepsilon_\perp$ and the *perpendicular scalar pressure* $p^\varepsilon_\perp$ are defined through

$$\mathbf{q}^\varepsilon_\perp = \frac{1}{2} \int_{\mathbb{R}^3_v} |\mathbf{v}_\perp - \mathbf{u}^\varepsilon_\perp|^2\, (\mathbf{v}_\perp - \mathbf{u}^\varepsilon_\perp)\, f^\varepsilon\, \mathrm{d}\mathbf{v}\,, \qquad \mathbb{P}^\varepsilon_\perp := \int_{\mathbb{R}^3_v} (\mathbf{v}_\perp \otimes \mathbf{v}_\perp)\, f^\varepsilon\, \mathrm{d}\mathbf{v}\,, \qquad p^\varepsilon_\perp := n^\varepsilon\, T^\varepsilon_\perp . \tag{3.4.38}$$

At order one in ε, $\mathbb{Q}^\varepsilon_\perp$ writes

$$\mathcal{O}(\varepsilon)\,: \qquad \mathbb{Q}^1_\perp = \mathbf{q}^1_\perp + \mathbb{P}^0_\perp \cdot \mathbf{u}^1_\perp + p^0_\perp\, \mathbf{u}^1_\perp = \mathbf{q}^1_\perp + 2\, n^0\, T^0_\perp\, \mathbf{u}^1_\perp . \tag{3.4.39}$$

Comparing this last equation with (3.4.36) permits to find the following expression for the order one perpendicular heat flux

$$\mathbf{q}_\perp^1 = -2\, n^0\, T_\perp^0\, \mathbb{D}_1 \nabla_{\mathbf{x}_\perp} T_\perp^0 \,. \tag{3.4.40}$$

This is a Fourier law of Bragiinski-type, with gyroviscous (antidiagonal) and viscous (diagonal) terms [NP16; Bra65].

Now, we compute the second non-closed term in (3.4.28). It can be decomposed as follows into two parts, coming respectively from the microscopic and macroscopic part of f^1:

$$\mathbb{Q}_\times^1 = \left\langle v_\parallel \frac{|\mathbf{v}_\perp|^2}{2} f^1 \right\rangle = \left\langle v_\parallel \frac{|\mathbf{v}_\perp|^2}{2} \widetilde{f}^1 \right\rangle + \left\langle v_\parallel \frac{|\mathbf{v}_\perp|^2}{2} \bar{f}^1 \right\rangle \tag{3.4.41}$$

$$= -\frac{1}{2\,\nu_\perp} n^0\, T_\parallel^0\, \partial_z T_\perp^0 + n^0\, u_\parallel^0\, T_\perp^1 + (n\, u_\parallel)^1\, T_\perp^0 \tag{3.4.42}$$

$$= -\frac{1}{2\,\nu_\perp} n^0\, T_\parallel^0\, \partial_z T_\perp^0 + (n\, u_\parallel\, T_\perp)^1 \,. \tag{3.4.43}$$

This time again, the different terms carry some physical meaning. Defining the "*heat flux in the parallel direction*" $q_\times^\varepsilon$ as follows

$$q_\times^\varepsilon := \frac{1}{2} \int_{\mathbb{R}_v^3} (v_\parallel - u_\parallel^\varepsilon)\, |\mathbf{v}_\perp - \mathbf{u}_\perp^\varepsilon|^2 f^\varepsilon \, \mathrm{d}\mathbf{v} \,, \tag{3.4.44}$$

permits to show, similarly as before, the following Fourier law

$$q_\times^1 = -\frac{1}{2\,\nu_\perp}\, n^0\, T_\parallel^0\, \partial_z T_\perp^0 \,. \tag{3.4.45}$$

3.4.6 Recap: Order one Hilbert expansion of (3.2.11)

Let us summarize in this paragraph what we have proven in subsections 3.4.3, 3.4.4 and 3.4.5. Assuming our distribution function f^ε has the following Hilbert decomposition:

$$f^\varepsilon = f^0 + \varepsilon\, f^1 + \mathcal{O}(\varepsilon^2) \,,$$

the distribution f^0 is given by the limit model (3.2.2). The first order correction $f^1 \in \mathcal{D}(\mathbb{A}_{f^0}^{\mathrm{lin}})$ writes:

$$f^1 = \widetilde{f}^1 + \bar{f}^1, \tag{3.4.46}$$

where the microscopic part $\widetilde{f}^1 \in \ker^\perp \mathbb{A}_{f^0}^{\mathrm{lin}}$ is written (see Proposition 3.4.4):

$$\begin{aligned} \widetilde{f}^1 = {} & \frac{\mathbf{u}_{drift}^{\mathrm{K}} \cdot \mathbf{v}_\perp}{T_\perp^0} f^0 - \left(\mathbb{D}_1 \frac{\nabla_{\mathbf{x}_\perp} T_\perp^0}{T_\perp^0} \right) \cdot \mathbf{v}_\perp \left[\frac{|\mathbf{v}_\perp|^2}{2\, T_\perp^0} - 2 \right] f^0 \\ & + \frac{\partial_z T_\perp^0}{T_\perp^0} \frac{u_\parallel^0 - v_\parallel}{2\,\nu_\perp} \left[\frac{|\mathbf{v}_\perp|^2}{2\, T_\perp^0} - 1 \right] f^0 - n^0 \left\{ \mathbb{D}_2 \nabla_{\mathbf{x}_\perp} \left(\frac{g^0}{n^0} \right) \right\} \cdot \mathbf{v}_\perp \mathcal{M}_\perp, \end{aligned} \tag{3.4.47}$$

with $\mathbb{D}_1$, $\mathbb{D}_2$ given by

$$\mathbb{D}_1 = \frac{1}{B^2 + 9\,\nu_\perp^2}\begin{bmatrix} 3\,\nu_\perp & B \\ -B & 3\,\nu_\perp \end{bmatrix}, \qquad \mathbb{D}_2 = \frac{\nu_\perp}{B}\frac{1}{B^2+\nu_\perp^2}\begin{bmatrix} B & -\nu_\perp \\ \nu_\perp & B \end{bmatrix}. \tag{3.4.48}$$

The macroscopic part $\bar{f}^1 \in \ker \mathbb{A}^{\rm lin}_{f^0}$ writes (see (3.4.24)) as follows

$$\bar{f}^1 = g^1 \mathcal{M}_\perp^{T_\perp^0} + \frac{T_\perp^1}{T_\perp^0}\left(\frac{|\mathbf{v}_\perp|^2}{2\,T_\perp^0} - 1\right) f^0\,, \tag{3.4.49}$$

with the order one quantities $(g^1, T_\perp^1)$ given by (see subsection 3.4.3 for the equations and 3.4.5 for the closure):

$$\begin{cases} \partial_t g^1 + v_\parallel \partial_z g^1 + E_\parallel \partial_{v_\parallel} g^1 + \nabla_{\mathbf{x}_\perp}\cdot\left(g^0\,\mathbf{u}^{\rm K}_{drift}\right) - \nabla_{\mathbf{x}_\perp}\cdot\left(n^0\,T_\perp^0\,\mathbb{D}_2\cdot\nabla_{\mathbf{x}_\perp}\left(\dfrac{g^0}{n^0}\right)\right) \\ \qquad = \nu_{\rm r}\,\partial_{v_\parallel}\left((v_\parallel - u_\parallel^0)\,g^1 - u_\parallel^1\,g^0 + T^1\partial_{v_\parallel} g^0 + T^0\partial_{v_\parallel} g^1)\right)\,, \\ \partial_t (n\,T_\perp)^1 + \partial_z (n\,u_\parallel\,T_\perp)^1 + \nabla_{\mathbf{x}_\perp}\cdot\left(2\,n^0\,T_\perp^0\,\mathbf{u}_{drift}\right) + \nabla_{\mathbf{x}_\perp}\cdot\mathbf{q}_\perp^1 + \partial_z q_\times^1 \\ \qquad = n^0\,\mathbf{u}_{drift}\cdot\mathbf{E}_\perp + \dfrac{2}{3}\,\nu_{\rm r}(n(T_\parallel - T_\perp))^1\,, \end{cases} \tag{3.4.50}$$

where

$$\mathbf{q}_\perp^1 = -2\,n^0\,T_\perp^0\,\mathbb{D}_1\,\nabla_{\mathbf{x}_\perp} T_\perp^0\,, \qquad q_\times^1 = -\frac{1}{2\,\nu_\perp} n^0\,T_\parallel^0\,\partial_z T_\perp^0\,. \tag{3.4.51}$$

With this in mind, we are now ready to deal with the proof of Theorem 5.

3.4.7 Proof of Theorem 5

In this proof, we shall denote

$$\breve{f} = f^0 + \varepsilon\, f^1\,,$$

and all quantities with a check symbol $\breve{}$ on top shall be associated with $f^0 + \varepsilon\, f^1$. The proof is based on the fact that, due to the Hilbert expansion, one has

$$f^\varepsilon - \breve{f} = \mathcal{O}(\varepsilon^2)\,, \qquad \text{as } \varepsilon \to 0\,.$$

As a consequence, it is enough to show that the function $\widehat{f}$, constructed in Theorem 5 and solution of our truncated model, is such that

$$\widehat{f} - \breve{f} = \mathcal{O}(\varepsilon^2)\,, \qquad \text{as } \varepsilon \to 0\,. \tag{3.4.52}$$

Firstly, we show that $\breve{f}$ satisfies the following development.

$$\breve{f} = \breve{g}\,\mathcal{M}_\perp^{\breve{T}_\perp}(1 + \varepsilon\,\Lambda_{\breve{g},\breve{T}_\perp}) + \mathcal{O}(\varepsilon^2)\,, \tag{3.4.53}$$

where Λ is defined in (3.2.7f). We recognize a decomposition analogous to that of $\widehat{f}$ (3.2.7a), namely

$$\widehat{f} = \widehat{g}\,\mathcal{M}_{\perp}^{\widehat{T}_\perp}(1+\varepsilon\,\Lambda_{\widehat{g},\,\widehat{T}_\perp})\,. \tag{3.4.54}$$

As a consequence, we shall prove in a second time that

$$(\widehat{g},\ \widehat{T}_\perp) - (\breve{g},\ \breve{T}_\perp) = \mathcal{O}(\varepsilon^2)\,, \qquad \text{as } \varepsilon \to 0\,. \tag{3.4.55}$$

This shall finish the proof, as injecting expansion (3.4.55) into (3.4.53) leads to (3.4.52).

Step 1: Form of $\breve{f}$. Let us start with the decomposition

$$\breve{f} = (f^0 + \varepsilon\,\bar{f}^1) + \varepsilon\,\widetilde{f}^1.$$

Developing in powers of ε the term $\breve{g}\,\mathcal{M}_{\perp}^{\breve{T}_\perp}$ permits to find, with the help of (3.4.49), the first term of the previous decomposition:

$$f^0 + \varepsilon\,\bar{f}^1 = \breve{g}\,\mathcal{M}_{\perp}^{\breve{T}_\perp} + \mathcal{O}(\varepsilon^2)\,, \qquad \text{as } \varepsilon \to 0\,. \tag{3.4.56}$$

Then, one can focus on rewriting $\widetilde{f}^1$ given in (3.4.47): thanks to definition of Λ in (3.2.7f), one finds

$$\widetilde{f}^1 = g^0\,\mathcal{M}_{\perp}^{T_\perp^0}\Lambda_{g^0,T_\perp^0} = \breve{g}\,\mathcal{M}_{\perp}^{\breve{T}_\perp}\Lambda_{\breve{g},\breve{T}_\perp} + \mathcal{O}(\varepsilon)\,, \qquad \text{as } \varepsilon \to 0\,. \tag{3.4.57}$$

Taking (3.4.56) + ε (3.4.57) yields (3.4.53).

Step 2: First order PDE model. Summing the limit PDE model (3.2.2c) for $(g^0,\ T_\perp^0)$ with the system of equation (3.4.50) giving $\varepsilon\,(g^1,\ T_\perp^1)$ yields, after grouping terms of the same nature

$$\begin{cases} \partial_t\breve{g} + v_\parallel\partial_z\breve{g} + E_\parallel\partial_{v_\parallel}\breve{g} + \varepsilon\,\nabla_{\mathbf{x}_\perp}\cdot\left(g^0\,\mathbf{u}_{drift}^{\mathrm{K}}\right) - \varepsilon\,\nabla_{\mathbf{x}_\perp}\cdot\left(n^0\,T_\perp^0\,\mathbb{D}_2\cdot\nabla_{\mathbf{x}_\perp}\left(\dfrac{g^0}{n^0}\right)\right) \\ \qquad = \nu_{\mathrm{r}}\,\partial_{v_\parallel}\left((v_\parallel - u_\parallel^0)\,g^0 + T^0\partial_{v_\parallel}g^0 + \varepsilon\,\left((v_\parallel - u_\parallel^0)\,g^1 - u_\parallel^1\,g^0 + T^1\partial_{v_\parallel}g^0 + T^0\partial_{v_\parallel}g^1\right)\right), \\ \partial_t\left\{(n\,T_\perp)^0 + \varepsilon\,(n\,T_\perp)^1\right\} + \partial_z\left\{(n\,u_\parallel\,T_\perp)^0 + \varepsilon\,(n\,u_\parallel\,T_\perp)^1\right\} + \varepsilon\,\nabla_{\mathbf{x}_\perp}\cdot\left(2\,n^0\,T_\perp^0\,\mathbf{u}_{drift}\right) + \varepsilon\,\nabla_{\mathbf{x}}\cdot\breve{\mathbf{q}} \\ \qquad = \varepsilon\,n^0\,\mathbf{u}_{drift}\cdot\mathbf{E}_\perp + \dfrac{2}{3}\,\nu_{\mathrm{r}}\left\{(n(T_\parallel - T_\perp))^0 + \varepsilon\,(n(T_\parallel - T_\perp))^1\right\}. \end{cases}$$

Finally, adding several terms of order $\mathcal{O}(\varepsilon^2)$ permits to simplify the previous system:

$$\begin{cases} \partial_t\breve{g} + v_\parallel\,\partial_z\breve{g} + E_\parallel\,\partial_{v_\parallel}\breve{g} + \varepsilon\,\nabla_{\mathbf{x}_\perp}\cdot(\breve{\mathbf{u}}_{\mathrm{drift}}^{\mathrm{K}}\,\breve{g}) = \nu_{\mathrm{r}}\,\partial_{v_\parallel}\left[(v_\parallel - \breve{u}_\parallel)\,\breve{g} + \breve{T}\,\partial_{v_\parallel}\breve{g}\right] \\ \qquad\qquad + \varepsilon\,\nabla_{\mathbf{x}_\perp}\cdot\left(\breve{n}\,\breve{T}_\perp\,\mathbb{D}_2\nabla_{\mathbf{x}_\perp}\dfrac{\breve{g}}{\breve{n}}\right) + \mathcal{O}(\varepsilon^2)\,, \\ \partial_t(\breve{n}\,\breve{T}_\perp) + \partial_z(\breve{n}\,\breve{T}_\perp\,\breve{u}_\parallel) + \varepsilon\,\nabla_{\mathbf{x}_\perp}\cdot(2\,\breve{n}\,\breve{T}_\perp\,\breve{\mathbf{u}}_{\mathrm{drift}}) + \varepsilon\,\nabla_{\mathbf{x}}\cdot\breve{\mathbf{q}} = \varepsilon\,\breve{n}\,\breve{\mathbf{u}}_{\mathrm{drift}}\cdot\mathbf{E}_\perp \\ \qquad\qquad + \dfrac{2}{3}\,\nu_{\mathrm{r}}\,\breve{n}(\breve{T}_\parallel - \breve{T}_\perp) + \mathcal{O}(\varepsilon^2)\,, \\ \qquad\qquad \text{as } \varepsilon \to 0. \end{cases}$$

Therefore, in finite time, (3.4.55) holds. This concludes the proof.

3.5 Discussion and Conclusion

The main purpose of this work was to derive a reduced description of a plasma undergoing anisotropic collisions in a strong magnetic field. We started from a normalized kinetic equation featuring a small parameter $\varepsilon \in (0, 1)$ and performed a formal analysis, leading in the asymptotic regime $\varepsilon \ll 1$ to the factorization of the distribution function into a kinetic part in the parallel direction, and a macroscopic part in the plane perpendicular to the magnetic field. This new plasma model is an enhancement of the one used in [CHM16], as it includes plasma drifts and perpendicular diffusion terms. Classical Bragiinski-type closure terms were found for the perpendicular temperature, while new, fluid-like terms were discovered in the kinetic-parallel description. In particular we found in this kinetic equation a diamagnetic drift term. Such a term is usually not present in reduced kinetic models, for instance in gyrokinetic models, and points to the hybrid character of the newly derived model. This hybrid character of course arises because of the assumption of high collisionality perpendicular to $\mathbf{B}$. Moreover, a diffusion term occurs in the direction perpendicular to the magnetic field, which is responsible for the homogenisation of parallel moments in the perpendicular direction.

One can build upon this work in several directions. Firstly, one can investigate on the restrictions we made for this study: one can study the same regime in the context of a more complex geometry, with a curved magnetic field. We conjecture that such a modification will add several other terms to the drift velocity, such as a grad-B drift and a curved-B drift. It is also possible to remove the assumption of periodic boundary conditions in $\mathbf{x}$, to add the effects of multiple species, or to solve the electromagnetic fields in a self-consistent manner. Secondly, it would be interesting to consider numerical discretizations of the new model. Due to the fact that the dimensionality (4D) is lower than for instance in gyrokinetic descriptions (5D), a significant gain in performance can be expected. Thirdly, the range of validity of the new model should be investigated. For instance, one could try to reproduce the numerical experiments conducted in [CHM16] and then study the effect of the additional drift-/diffusion terms of the new model.

Acknowledgments. This work has been carried out within the framework of the EUROfusion Consortium, funded by the European Union via the Euratom Research and Training Programme (Grant Agreement No 101052200 — EUROfusion). Views and opinions expressed are however those of the author(s) only and do not necessarily reflect those of the European Union or the European Commission. Neither the European Union nor the European Commission can be held responsible for them. C. Negulescu would like to thank the TUM (Technical university of Munich) for the John von Neumann position, having permitted to conclude this work.

3.A Scaling assumptions and renormalization

In this section, we detail the scaling assumptions leading to the renormalized equation (3.1.13). We then rewrite the first order-model of Theorem 5 in physical units. This can be useful for the physics community.

3.A.1 Physical scaling

We start from (3.1.4)-(3.1.6), and express dependent variables in terms of a characteristic unit (denoted with a "bar") and a rescaled function (denoted with a "prime"), for instance

$$f = \bar{f}\, f' , \qquad \mathbf{E} = \bar{E}\, \mathbf{E}' , \qquad \mathbf{B} = \bar{B}\, \mathbf{B}' .$$

We normalize equations (3.1.4)-(3.1.6) by assuming characteristic scales for time and phase space,

$$t = \bar{t}\, t' , \qquad \mathbf{x} = \bar{x}\, \mathbf{x}' , \qquad \mathbf{v} = v_{\rm th} \mathbf{v}' ,$$

where the thermal speed v_{th} is defined as follows:

$$v_{th} := \sqrt{\frac{k_B\, \bar{T}}{m}} ,$$

with $\bar{T} = \bar{T}_\perp$ the characteristic temperature scale associated to f. We assume the relation $\bar{x} = \bar{t}\, v_{\rm th}$, as well as

$$\bar{n} = \bar{f} v_{\rm th}^3 , \qquad \bar{u} = v_{\rm th} , \qquad k_{\rm B}\, \bar{T} = m\, v_{\rm th}^2 = q\, \bar{\phi} , \qquad \bar{E} = \frac{\bar{\phi}}{\bar{x}} .$$

We also introduce the observation frequency, and the cyclotron frequency:

$$\bar{\omega} = \frac{1}{\bar{t}} , \qquad \Omega_c = \frac{q\, \bar{B}}{m} .$$

This leads to the normalized VFP model

$$\partial_{t'} f' + \mathbf{v}' \cdot \nabla_{\mathbf{x}'} f' + \frac{\Omega_{\rm c}}{\bar{\omega}} \left(\frac{\bar{E}}{v_{\rm th} \bar{B}} \mathbf{E}' + \mathbf{v}' \times B' \mathbf{e}_z \right) \cdot \nabla_{\mathbf{v}'} f' = \frac{\bar{\nu}_\perp}{\bar{\omega}}\, \nu'_\perp Q'_\perp(f') + \frac{\bar{\nu}_{\rm r}}{\bar{\omega}}\, \nu'_{\rm r}\, Q'_{\rm r}(f') , \quad (3.A.1)$$

where $Q'_\perp$ and $Q'_{\rm r}$ are defined as in (3.1.5)-(3.1.7), but setting the constants k_B and m to 1. The physical regime is now determined by four quantities:

i) $\Omega_{\rm c}/\bar{\omega}$, the ratio between the cyclotron frequency and the chosen frequency scale,

ii) $\bar{E}/(v_{\rm th}\bar{B})$, the ratio between the $E \times B$ drift velocity and the thermal velocity,

iii) $\bar{\nu}_\perp/\bar{\omega}$, the ratio between the perpendicular collision frequency and the chosen frequency scale,

iv) $\bar{\nu}_{\mathrm{r}}/\bar{\nu}_{\perp}$, the anisotropic collision parameter, defined as the ratio between the two collision frequencies.

One assumes firstly that the cyclotron frequency is much larger than the chosen frequency scale, due to the strong magnetic field. This assumption can be formulated as follows:

$$\frac{\Omega_{\mathrm{c}}}{\bar{\omega}} = \frac{1}{\varepsilon} \gg 1\,, \tag{3.A.2}$$

where ε is the small asymptotic parameter. This choice constraints the next quantity ii):

$$\frac{\bar{E}}{v_{\mathrm{th}}\bar{B}} = \frac{q\,\varepsilon\,\bar{E}}{m\,v_{\mathrm{th}}\,\bar{\omega}} = \frac{q\,\varepsilon\,\bar{\phi}}{m\,v_{\mathrm{th}}\,\bar{\omega}\,\bar{x}} = \frac{q\,\varepsilon\,\bar{\phi}}{m\,v_{\mathrm{th}}^2} = \frac{\varepsilon\,k_B\,\bar{T}}{m\,v_{\mathrm{th}}^2} = \varepsilon\,. \tag{3.A.3}$$

Next, we assume strong collisions in the perpendicular direction. In particular, we assume that the $\mathbf{v}\times\mathbf{B}\cdot\nabla_{\mathbf{v}}$ operator and the collision operator appear on the same order in the Vlasov equation, meaning

$$\frac{\bar{\nu}_{\perp}}{\bar{\omega}} = \frac{1}{\varepsilon} \gg 1\,. \tag{3.A.4}$$

The main novelty in this work is the assumption of anisotropic collisions, namely

$$\bar{\nu}_{\mathrm{r}}/\bar{\nu}_{\perp} = \varepsilon \ll 1\,. \tag{3.A.5}$$

One can now rewrite our rescaled Vlasov equation as follows, (the primes were omitted, for simplicity)

$$\partial_t f^{\varepsilon} + \mathbf{v}\cdot\nabla_{\mathbf{x}} f^{\varepsilon} + \mathbf{E}\cdot\nabla_{\mathbf{v}} f^{\varepsilon} + \frac{1}{\varepsilon}(\mathbf{v}\times B\mathbf{e}_z)\cdot\nabla_{\mathbf{v}} f^{\varepsilon} = \frac{\nu_{\perp}}{\varepsilon} Q_{\perp}(f^{\varepsilon}) + \nu_{\mathrm{r}}\, Q_{\mathrm{r}}(f^{\varepsilon})\,, \tag{3.A.6}$$

where $Q_{\perp}$ and Q_{r} are defined in (3.1.14).

3.A.2 Truncated system in physical units

For physical and implementation purposes, we give here the first order correction model of Theorem 5 in physical units. The distribution function f is given in the considered regime by

$$f(t,\mathbf{x},\mathbf{v}) = g(t,\,\mathbf{x},\,v_{\parallel})\;\mathcal{M}_{\perp}^{k_B\,T_{\perp}(t,\mathbf{x})/m}(\mathbf{v}_{\perp})\left(1+\,\Lambda_{g,T_{\perp}}\right)\,, \tag{3.A.7a}$$

where the Maxwellian distribution $\mathcal{M}_{\perp}^{k_B\,T_{\perp}(t,\mathbf{x})/m}$ is defined as

$$\mathcal{M}_{\perp}^{k_B\,T_{\perp}(t,\mathbf{x})/m}(\mathbf{v}_{\perp}) := \frac{m}{2\,\pi\,k_B\,T_{\perp}(t,\mathbf{x})}\,e^{-\frac{m|\mathbf{v}_{\perp}|^2}{2\,k_B\,T_{\perp}(t,\mathbf{x})}}.$$

The "reduced kinetic distribution g" and the perpendicular temperature $T_\perp$ satisfy the coupled system

$$\begin{cases} \partial_t g + v_\parallel\, \partial_z g + \dfrac{q}{m} E_\parallel\, \partial_{v_\parallel} g + \nabla_{\mathbf{x}_\perp} \cdot (\mathbf{u}^{\mathrm{K}}_{\mathrm{drift}}\, g) = \nu_{\mathrm{r}}\, \partial_{v_\parallel} \left[(v_\parallel - u_\parallel)\, g + \dfrac{k_B\, T}{m} \partial_{v_\parallel} g \right] \\ \qquad\qquad + \nabla_{\mathbf{x}_\perp} \cdot \left(n\, \dfrac{k_B\, T_\perp}{m}\, \mathbb{D}_2 \nabla_{\mathbf{x}_\perp} \dfrac{g}{n} \right), \\ \partial_t (n\, T_\perp) + \partial_z (n\, T_\perp\, u_\parallel) + \nabla_{\mathbf{x}_\perp} \cdot (2\, n\, T_\perp\, \mathbf{u}_{\mathrm{drift}}) + \nabla_{\mathbf{x}} \cdot \mathbf{q} = n\, \dfrac{q}{k_B} \mathbf{u}_{\mathrm{drift}} \cdot \mathbf{E}_\perp \\ \qquad\qquad + \dfrac{2}{3}\, \nu_{\mathrm{r}}\, n\, (T_\parallel - T_\perp). \end{cases} \tag{3.A.7b}$$

Here, the drift velocities are given by

$$\mathbf{u}^{\mathrm{K}}_{\mathrm{drift}} := \frac{\mathbf{E}_\perp \times \mathbf{B}}{|B|^2} - \frac{k_B}{q} \frac{\nabla_{\mathbf{x}_\perp} (g\, T_\perp) \times \mathbf{B}}{g\, |B|^2}, \qquad \mathbf{u}_{\mathrm{drift}} := \frac{\mathbf{E}_\perp \times \mathbf{B}}{|B|^2} - \frac{k_B}{q} \frac{\nabla_{\mathbf{x}_\perp} (n\, T_\perp) \times \mathbf{B}}{n\, |B|^2}, \tag{3.A.7c}$$

the temperature T is computed through the directional temperatures via $T = (2\, T_\perp + T_\parallel)/3$, the macroscopic quantities $(n,\ u_\parallel,\ T_\parallel)$ are defined through

$$n = \langle g \rangle_\parallel, \qquad n\, u_\parallel = \langle v_\parallel g \rangle_\parallel, \qquad \frac{1}{2} n\, k_B\, T_\parallel = \frac{m}{2} \left\langle (v_\parallel - u_\parallel)^2\, g \right\rangle_\parallel, \tag{3.A.7d}$$

and the heat flux is given by

$$\mathbf{q} = \begin{pmatrix} \mathbf{q}_\perp \\ q_\times \end{pmatrix}, \qquad \mathbf{q}_\perp = -\frac{2\, k_B}{m} n\, T_\perp\, \mathbb{D}_1\, \nabla_{\mathbf{x}_\perp} T_\perp, \qquad q_\times = -\frac{k_B}{2\, m\, \nu_\perp} n\, T_\parallel\, \partial_z T_\perp. \tag{3.A.7e}$$

The quantity $\Lambda_{g,T_\perp}$ is a correction term, polynomial in $\mathbf{v}_\perp$, and entirely defined in terms of the quantities g and $T_\perp$, through

$$\begin{aligned} \Lambda_{g,T_\perp}(\mathbf{v}) :=& \frac{\mathbf{u}^{\mathrm{K}}_{\mathrm{drift}} \cdot \mathbf{v}_\perp}{T_\perp} - \left(\mathbb{D}_1 \frac{\nabla_{\mathbf{x}_\perp} T_\perp}{T_\perp} \right) \cdot \mathbf{v}_\perp \left[\frac{m\, |\mathbf{v}_\perp|^2}{2\, k_B\, T_\perp} - 2 \right] + \frac{\partial_z T_\perp}{T_\perp} \frac{u_\parallel - v_\parallel}{2\, \nu_\perp} \left[\frac{m\, |\mathbf{v}_\perp|^2}{2\, k_B\, T_\perp} - 1 \right] \\ & - \left(\mathbb{D}_2 \frac{\nabla_{\mathbf{x}_\perp} (g/n)}{(g/n)} \right) \cdot \mathbf{v}_\perp. \end{aligned} \tag{3.A.7f}$$

Finally, the positive diffusion matrices are given by

$$\mathbb{D}_1 = \frac{1}{(\frac{q\,B}{m})^2 + 9\, \nu_\perp^2} \begin{bmatrix} 3\, \nu_\perp & \frac{q\,B}{m} \\ -\frac{q\,B}{m} & 3\, \nu_\perp \end{bmatrix}, \qquad \mathbb{D}_2 = \frac{m\, \nu_\perp}{q\, B} \frac{1}{(\frac{q\,B}{m})^2 + \nu_\perp^2} \begin{bmatrix} \frac{q\,B}{m} & -\nu_\perp \\ \nu_\perp & \frac{q\,B}{m} \end{bmatrix}. \tag{3.A.7g}$$

3.B Proof of the properties stated in Subsection 3.4.2

3.B.1 Proof of Proposition 3.4.1

In this subsection, we give a proof of the last point of Proposition 3.4.1, namely of (3.4.15). The first step is to state one of the inclusion of (3.4.15) in the following Lemma.

Lemma 9. Let $\delta Q_\perp[f^0]$ be the operator defined in (3.4.2) and define the set

$$\mathcal{S}_1 := \left\{ \xi = \alpha(v_\parallel)\, f^0(\mathbf{v}),\ \xi \in \mathcal{H} \right\} \oplus \left\{ \xi = \beta(\mathbf{v}_\perp)\, f^0(\mathbf{v}),\ \beta \in \mathrm{Span}\{v_x, v_y, |\mathbf{v}_\perp|^2\} \right\} .$$

Then one has

$$\mathcal{S}_1 \subset \ker(\delta Q_\perp[f^0]) . \tag{3.B.1}$$

Proof of Lemma 9. By direct computation (apply $\delta Q_\perp[f^0]$ to an element of $\mathcal{S}_1$).

□

Let us show now the reciprocal inclusion, using the coercivity inequality (3.4.18). For this, let us investigate the mapping π

$$\begin{aligned} \pi \,:\, \mathcal{H} &\longrightarrow \mathcal{H} \\ \chi &\mapsto \left\langle \varphi^0\, \chi(v_\parallel) \right\rangle_\perp \Phi^0(\mathbf{v}) + \sum_{k=x,y} \left\langle \varphi^1_k\, \chi \right\rangle \Phi^1_k(\mathbf{v}) + \left\langle \varphi^2\, \chi \right\rangle \Phi^2(\mathbf{v}) , \end{aligned} \tag{3.B.2}$$

defined in (3.4.16). Let us show that it is well defined. For this, it is enough to notice that if $\chi \in \mathcal{H}$, then $\langle \chi \varphi^0 \rangle_\perp \Phi^0 \in \mathcal{H}$. Indeed,

$$\begin{aligned} \left\| \langle \chi \varphi^0 \rangle_\perp \Phi^0 \right\|^2_{\mathcal{H}} = \left\| \langle \chi \rangle_\perp \mathcal{M}_\perp^{T^0_\perp} \right\|^2_{\mathcal{H}} &= \int_{\mathbb{R}_v} \langle \chi \rangle_\perp^2 \frac{1}{g^0}\, \mathrm{d}v_\parallel \\ &= \int_{\mathbb{R}_v} \left(\int_{\mathbb{R}^2_v} \frac{\chi}{\sqrt{f^0}} \sqrt{f^0}\, \mathrm{d}\mathbf{v}_\perp \right)^2 \frac{1}{g^0}\, \mathrm{d}v_\parallel \\ &\leqslant \int_{\mathbb{R}_v} \left(\int_{\mathbb{R}^2_v} \frac{\chi^2}{f^0}\, \mathrm{d}\mathbf{v}_\perp \right) \underbrace{\left(\int_{\mathbb{R}^2_v} f^0\, \mathrm{d}\mathbf{v}_\perp \right)}_{=g^0} \frac{1}{g^0}\, \mathrm{d}v_\parallel \\ &= \|\chi\|^2_{\mathcal{H}} < \infty, \end{aligned}$$

using Cauchy-Schwarz inequality, leading to the well-definition.

Observe that $\mathcal{S}_1 = \mathcal{R}(\pi)$, where $\mathcal{R}(\pi)$ is the range of π. As a consequence, Lemma 9 shows

$$\mathcal{R}(\pi) \subset \ker \delta Q_\perp[f^0] . \tag{3.B.3}$$

Proving (3.4.15) is exactly proving that (3.B.3) is an equality. But the latter fact is a direct consequence of the coercivity inequality [2] (3.4.18). Indeed, taking $\chi \in \ker \delta Q_\perp[f^0]$ we obtain

$$0 = (-\delta Q_\perp[f^0]\chi, \chi)_{\mathcal{H}} \geqslant \|\chi - \pi\chi\|^2_{\mathcal{H}} . \tag{3.B.4}$$

We quickly sketch the proof of this inequality. It shall finish the proof of Proposition 3.4.1.

2. At this point we do not know that the mapping π is the orthogonal projection onto $\ker \delta Q_\perp[f^0]$. However, the coercivity relation from Proposition 3.4.2 still holds, which can be verified by direct computation, or from the proof of Proposition 3.4.2 in 3.B.2, where only (3.B.3) is used.

3.B.2 Proof of Proposition 3.4.2

Let us recall firstly that $(\Phi^1_x,\ \Phi^1_y, \Phi^2)$ permit to express the quantities $\delta \mathbf{u}_{\perp,\xi}$ and $\delta T_{\perp,\xi}$, defined in (3.4.3)-(3.4.4) and associated to a function $\xi \in \mathcal{H}$. Indeed, one has

$$\begin{aligned}
(\xi,\ \Phi^1_x)_{\mathcal{H}} &= \langle \varphi^1_x\ \xi\rangle = \sqrt{\frac{n^0}{T^0_\perp}}(\delta \mathbf{u}_{\perp,\xi})_x\,,\\
(\xi,\ \Phi^1_y)_{\mathcal{H}} &= \langle \varphi^1_y\ \xi\rangle = \sqrt{\frac{n^0}{T^0_\perp}}(\delta \mathbf{u}_{\perp,\xi})_y\,,\\
(\xi,\ \Phi^2)_{\mathcal{H}} &= \langle \varphi^2\ \xi\rangle = \sqrt{n^0}\,\frac{\delta T_{\perp,\xi}}{T^0_\perp}\,.
\end{aligned}$$

With this in mind, we state that

$$(-\delta Q_\perp[f^0]\chi,\chi)_{\mathcal{H}} = (-\delta Q_\perp[f^0](\chi-\pi\chi),\chi-\pi\chi)_{\mathcal{H}} = \int_{\mathbb{R}^3_v} T^0_\perp f^0 \left|\nabla_{\mathbf{v}_\perp}\left(\frac{\chi-\pi\chi}{f^0}\right)\right|^2 \mathrm{d}\mathbf{v} + 0\,.$$

For the first equality, we used inclusion (3.B.3) and the self-adjointness of $\delta Q_\perp[f^0]$. For the second one, we used (3.4.13), along with the fact that

$$\delta \mathbf{u}_{\perp,\,\chi-\pi\chi} = \sqrt{\frac{T^0_\perp}{n^0}}\left(\chi-\pi\chi,\ \begin{pmatrix}\Phi^1_x\\ \Phi^1_y\end{pmatrix}\right)_{\mathcal{H}} = 0\,, \qquad \delta T_{\perp,\,\chi-\pi\chi} = \frac{T^0_\perp}{\sqrt{n^0}}(\chi-\pi\chi,\Phi^2)_{\mathcal{H}} = 0\,,$$

which can be seen using the orthonormality of the family $(\Phi^0,\ \Phi^1_x,\ \Phi^1_y,\ \Phi^2)$. Finally, the proof is ended by the following inequality

$$(-\delta Q_\perp[f^0]\chi,\chi)_{\mathcal{H}} = \int_{\mathbb{R}^3_v} T^0_\perp f^0 \left|\nabla_{\mathbf{v}_\perp}\left(\frac{\chi-\pi\chi}{f^0}\right)\right|^2 \mathrm{d}\mathbf{v} \geqslant \|\chi-\pi\chi\|^2_{\mathcal{H}}\,,$$

which is a consequence of the Gaussian Poincaré inequality. Such an inequality can be proven using well scaled Hermite functions (see for instance [Bog98]).

3.B.3 Proof of Proposition 3.4.3

Let us turn to the proof of Proposition 3.4.3. Let us firstly give a proof of the first point, giving the form of $\ker \mathbb{A}^{\mathrm{lin}}_{f^0}$. In other terms we prove the following lemma.

Lemma 10. Let $\mathbb{A}^{\mathrm{lin}}_{f^0}$ be the operator defined in (3.2.14) and define the set

$$\mathcal{S}_2 := \left\{\xi\in\mathcal{H},\quad \xi = \alpha(v_\parallel)\,f^0(\mathbf{v})\right\} \oplus \{\xi\in\mathcal{H},\quad \xi = \beta|\mathbf{v}_\perp|^2\,f^0(\mathbf{v}),\quad \beta\in\mathbb{R}\}\,. \tag{3.B.5}$$

Then one has

$$\mathcal{S}_2 = \ker\,\mathbb{A}^{\mathrm{lin}}_{f^0}\,. \tag{3.B.6}$$

Proof of Lemma 10. Let us prove it by double inclusion. Firstly, every function of $\mathcal{S}_2$ is rotation invariant with respect to $\mathbf{v}_\perp$, and $\mathcal{S}_2 \subset \mathcal{S}_1 = \ker \delta Q_\perp[f^0]$. Therefore

$$\mathcal{S}_2 \subset \ker \delta Q_\perp[f^0] \cap \ker(\mathbf{v} \times \mathbf{B} \cdot \nabla_{\mathbf{v}}) \subset \ker \mathbb{A}^{\mathrm{lin}}_{f^0}\,.$$

Let us now focus on the reciprocal inclusion of (3.B.6). To prove it, we are going to prove that

$$\ker \mathbb{A}^{\mathrm{lin}}_{f^0} \cap \mathcal{S}_2^\perp = \{0\}\,, \tag{3.B.7}$$

where $\mathcal{S}_2^\perp$ is the orthogonal of $\mathcal{S}_2$ in $\mathcal{H}$. This fact shall prove that $\mathcal{S}_2 = \ker \mathbb{A}^{\mathrm{lin}}_{f^0}$, as $\mathcal{S}_2$ is closed in $\mathcal{H}$.

In order to prove (3.B.7) we follow three steps. Firstly we show that if $\chi \in \ker \mathbb{A}^{\mathrm{lin}}_{f^0}$, then

$$\langle \varphi^1_x\, \chi\rangle_\perp = \langle \varphi^1_y\, \chi\rangle_\perp = 0\,,$$

directly from the definition of $\mathbb{A}^{\mathrm{lin}}_{f^0}$. Then, using the coercivity property (3.4.18), we shall show that $\chi = \pi\chi$. Finally assuming further that $\chi \in \ker \mathbb{A}^{\mathrm{lin}}_{f^0} \cap \mathcal{S}_2^\perp$, we shall prove that $\chi = 0$.

— Let $\chi \in \ker \mathbb{A}^{\mathrm{lin}}_{f^0}$. Firstly, integrating against $\mathbf{v}_\perp\, \mathrm{d}\mathbf{v}$ the equation

$$\mathbb{A}^{\mathrm{lin}}_{f^0}(\chi) = 0\,, \tag{3.B.8}$$

yields, after integrating by parts

$$-\langle \mathbf{v}_\perp\, \chi\rangle \times B\, \mathbf{e}_z = 0\,.$$

As a consequence, $\langle \mathbf{v}_\perp\, \chi\rangle = 0$, which reformulates as

$$\langle \varphi^1_x\, \chi\rangle = \langle \varphi^1_y\, \chi\rangle = 0\,. \tag{3.B.9}$$

— Then, testing (3.B.8) against χ in $\mathcal{H}$ yields, using the skew-symmetry of the magnetic transport term and the coercivity (3.4.18):

$$0 = (\mathbb{A}^{\mathrm{lin}}_{f^0}\chi, \chi)_{\mathcal{H}} = (-\nu_\perp\, \delta Q_\perp[f^0]\chi, \chi)_{\mathcal{H}} \geqslant \nu_\perp \|\chi - \pi\chi\|^2_{\mathcal{H}}\,.$$

Therefore $\chi = \pi\chi$.

— Finally, assume further that $\chi \in \ker \mathbb{A}^{\mathrm{lin}}_{f^0} \cap \mathcal{S}_2^\perp$. Let us denote by Π the orthogonal projection on the space $\mathcal{S}_2$ [3]. This projection writes

$$\Pi\,\chi := \left\langle \varphi^0 \chi \right\rangle_\perp \Phi^0 + \left\langle \varphi^2\, \chi \right\rangle \Phi^2(\mathbf{v})\,.$$

Since $\chi \in \mathcal{S}_2^\perp$, we have that $\Pi\chi = 0$, yielding

$$\pi\,\chi = \Pi\,\chi + \sum_{k=x,y} \langle \varphi^1_k\, \chi\rangle\, \Phi^1_k = 0 + \sum_{k=x,y} \langle \varphi^1_k\, \chi\rangle\, \Phi^1_k = 0\,, \tag{3.B.10}$$

using further (3.B.9) for the last equality.

We therefore conclude that $\chi = \pi\chi = 0$, thus concluding the proof.

3. At this stage, we still do not know that the projection Π defined in (3.4.21) is the projection onto $\ker \mathbb{A}^{\mathrm{lin}}_{f^0}$, but it is clear that it is the projection onto $\mathcal{S}_2$.

□

The second point of Proposition 3.4.3 is an easy consequence of the first one, as Π is the orthogonal projector on $\mathcal{S}_2$, and thus onto $\ker \mathbb{A}^{\mathrm{lin}}_{f^0}$. Let us now prove the third point of Proposition 3.4.3, namely the Poincaré-type inequality. From there, the closed range property (point 4) is an immediate consequence (see [Bré20] for instance).

Lemma 11. The operator $\mathbb{A}^{\mathrm{lin}}_{f^0}$ defined in (3.2.14) on $\mathcal{H}$ satisfies a Poincaré-type inequality. In other terms, there exists a constant $C_A > 0$, such that

$$\|\xi\|_{\mathcal{H}} \leqslant C_A \|\mathbb{A}^{\mathrm{lin}}_{f^0}\xi\|_{\mathcal{H}}, \qquad \forall \xi \in \ker^{\perp}\mathbb{A}^{\mathrm{lin}}_{f^0} \cap \mathcal{D}(\mathbb{A}^{\mathrm{lin}}_{f^0})\,. \tag{3.B.11}$$

Proof. Let us fix $\xi \in \ker^{\perp} \mathbb{A}^{\mathrm{lin}}_{f^0}$, and decompose the left-hand side of (3.B.11) as follows,

$$\|\xi\|^2_{\mathcal{H}} = \|\xi - \pi\xi\|^2_{\mathcal{H}} + \|\pi\xi\|^2_{\mathcal{H}} \tag{3.B.12}$$

$$= \|\xi - \pi\xi\|^2_{\mathcal{H}} + \left|\left\langle \varphi^1 \, \xi \right\rangle\right|^2, \tag{3.B.13}$$

with

$$\varphi^1(\mathbf{v}_\perp) = \begin{pmatrix} \varphi^1_x \\ \varphi^1_y \end{pmatrix}, \quad \Phi^1 = \varphi^1 \, f^0.$$

Indeed, the projection (3.4.16), together with $\xi \in \ker^{\perp}\mathbb{A}^{\mathrm{lin}}_{f^0}$, yields

$$\pi(\xi) = \Pi\xi + \langle \xi \, \varphi^1 \rangle \cdot \Phi^1 = \langle \xi \, \varphi^1 \rangle \cdot \Phi^1\,. \tag{3.B.14}$$

Let us now estimate the two terms arising in (3.B.13). To simplify notation, let us denote

$$\chi := \mathbb{A}^{\mathrm{lin}}_{f^0}(\xi)\,. \tag{3.B.15}$$

— For the first term in (3.B.13), we test (3.B.15) against ξ. Using the coercivity inequality (3.4.18) and the skew-adjointness of the $(\mathbf{v}\times\mathbf{B})\cdot\nabla_{\mathbf{v}}$ operator yields

$$\nu_\perp \|\xi - \pi\xi\|^2_{\mathcal{H}} \leqslant \left(-\nu_\perp \, \delta Q_\perp[f^0]\xi, \xi\right)_{\mathcal{H}} = \left(\mathbb{A}^{\mathrm{lin}}_{f^0}\xi, \xi\right)_{\mathcal{H}} = (\chi, \xi)_{\mathcal{H}} \leqslant \|\chi\|_{\mathcal{H}} \, \|\xi\|_{\mathcal{H}}. \tag{3.B.16}$$

— Now, to control the second term of (3.B.13), we test (3.B.15) against $-\frac{1}{B}\langle \varphi^1 \xi \rangle^{\top} \cdot (\Phi^1)$,

and get on the one hand the following sequence of inequalities

$$\begin{aligned}
\left|\left(\mathbb{A}^{\mathrm{lin}}_{f^0}(\xi), \frac{1}{B}\left\langle\varphi^1\xi\right\rangle^\top\cdot(\Phi^1)\right)_{\mathcal{H}}\right| &= \left|\frac{1}{B}\left(\chi, \left\langle\varphi^1\xi\right\rangle^\top\cdot(\Phi^1)\right)_{\mathcal{H}}\right| \\
&\leqslant \frac{1}{B}\left(\left|\left(\chi, \left\langle\varphi^1_x\xi\right\rangle(\Phi^1_y)\right)_{\mathcal{H}}\right| + \left|\left(\chi, \left\langle\varphi^1_y\xi\right\rangle(\Phi^1_x)\right)_{\mathcal{H}}\right|\right) \\
&\leqslant \frac{1}{|B|}\|\chi\|_{\mathcal{H}}\left\{\left|\left\langle\varphi^1_x\xi\right\rangle\right| + \left|\left\langle\varphi^1_y\xi\right\rangle\right|\right\} \\
&\leqslant \frac{\sqrt{2}}{|B|}\|\chi\|_{\mathcal{H}}\sqrt{|\langle\varphi^1_x\xi\rangle|^2 + \left|\left\langle\varphi^1_y\xi\right\rangle\right|^2} \\
&\leqslant \frac{\sqrt{2}}{|B|}\|\chi\|_{\mathcal{H}}\,\|\pi\xi\|_{\mathcal{H}} \\
&\leqslant \frac{\sqrt{2}}{|B|}\|\chi\|_{\mathcal{H}}\,\|\xi\|_{\mathcal{H}}\,,
\end{aligned}$$

where we used Cauchy-Schwarz for the third line and Parceval's theorem for the fifth line. On the other hand, using that $\Phi^1_x,\ \Phi^1_y \in \ker \delta Q_\perp[f^0] = \mathcal{R}(\delta Q_\perp[f^0])^\perp$, one computes

$$\begin{aligned}
\left(\mathbb{A}^{\mathrm{lin}}_{f^0}(\xi), -\frac{1}{B}\left\langle\varphi^1\xi\right\rangle^\top\cdot(\Phi^1)\right)_{\mathcal{H}} &= -\left(B(\mathbf{v}\times\mathbf{e}_z)\cdot\nabla_{\mathbf{v}}\xi, \frac{1}{B}\left\langle\varphi^1\xi\right\rangle^\top\cdot(\Phi^1)\right)_{\mathcal{H}} + 0 \\
&= -\int_{\mathbb{R}^3_v}\left[\nabla_{\mathbf{v}_\perp}\cdot((\mathbf{v}_\perp)^\top\xi)\right]\,\langle\varphi^1\,\xi\rangle^\top\cdot(\varphi^1)\,\mathrm{d}\mathbf{v} \\
&= \int_{\mathbb{R}^3_v}\left[(\mathbf{v}_\perp)^\top\xi\right]\cdot\nabla_{\mathbf{v}_\perp}\left[\langle\varphi^1\,\xi\rangle^\top\cdot(\varphi^1)\right]\,\mathrm{d}\mathbf{v} \\
&= \int_{\mathbb{R}^3_v}\frac{\left[(\mathbf{v}_\perp)^\top\xi\right]\cdot\nabla_{\mathbf{v}_\perp}\left[\langle\varphi^1\,\xi\rangle^\top\cdot(\mathbf{v}_\perp)\right]}{\sqrt{n^0\,T^0_\perp}}\,\mathrm{d}\mathbf{v} \\
&= \int_{\mathbb{R}^3_v}\left[(\varphi^1)^\top\xi\right]\cdot\nabla_{\mathbf{v}_\perp}\left[\langle\varphi^1\,\xi\rangle^\top\cdot(\mathbf{v}_\perp)\right]\,\mathrm{d}\mathbf{v} \\
&= \int_{\mathbb{R}^3_v}\left[(\varphi^1)^\top\xi\right]\,\mathrm{d}\mathbf{v}\cdot\langle\varphi^1\,\xi\rangle^\top \\
&= \left|\langle\varphi^1\xi\rangle\right|^2.
\end{aligned}$$

Assembling the two previous sequence of equalities/inequalities, we get

$$\left|\langle\varphi^1\xi\rangle\right|^2 \leqslant \frac{\sqrt{2}}{|B|}\|\chi\|_{\mathcal{H}}\|\xi\|_{\mathcal{H}}. \tag{3.B.17}$$

The result follows, summing (3.B.16) with (3.B.17), and taking $C_A = \frac{1}{\nu_\perp} + \frac{\sqrt{2}}{|B|}$. □

3.C Proof of the properties stated during the Hilbert expansion

3.C.1 Proof of Proposition 3.4.4

The goal of this subsection is to prove Proposition 3.4.4 characterizing the microscopic density $\widetilde{f}^1$. The first part of the proof will be dedicated to the rearrangement and computation of the term $\mathcal{R}^0$, using the limit model (3.2.2). The second step is dedicated to the computation of the preimage of this term $\mathcal{R}^0$.

Step 1: Computation of $\mathcal{R}^0$. Let us firstly recall the equations on the quantities $(g^0, T_\perp^0)$ (3.2.2):

$$\begin{cases} \partial_t g^0 + v_\parallel\, \partial_z g^0 + E_\parallel\, \partial_{v_\parallel} g^0 = \nu_{\mathrm{r}}\, \partial_{v_\parallel} \left[(v_\parallel - u_\parallel^0) g^0 + T^0\, \partial_{v_\parallel} g^0 \right] , \\ \partial_t T_\perp^0 + u_\parallel^0\, \partial_z T_\perp^0 = \dfrac{2}{3}\, \nu_{\mathrm{r}}\, \left(T_\parallel^0 - T_\perp^0 \right) . \end{cases}$$

The computation of $\mathcal{R}^0$ shall be a consequence of the previous system of equations. One decomposes as follows each of the terms composing $\mathcal{R}^0$:

$$\begin{aligned} \partial_t f^0 &= \partial_t g^0\, \mathcal{M}_\perp^{T_\perp^0} + g^0\, \partial_t \mathcal{M}_\perp^{T_\perp^0}, \\ \mathbf{v}\cdot\nabla_{\mathbf{x}} f^0 &= \mathbf{v}_\perp \cdot (\nabla_{\mathbf{x}_\perp} g^0) \mathcal{M}_\perp^{T_\perp^0} + \mathbf{v}_\perp \cdot (\nabla_{\mathbf{x}_\perp} \mathcal{M}_\perp^{T_\perp^0}) g^0 + v_\parallel (\partial_z \mathcal{M}_\perp^{T_\perp^0}) g^0 + (v_\parallel \partial_z g^0)\, \mathcal{M}_\perp^{T_\perp^0}, \\ \mathbf{E}\cdot\nabla_{\mathbf{v}} f^0 &= \mathbf{E}_\perp \cdot \nabla_{\mathbf{v}_\perp} f^0 + (E_\parallel \partial_{v_\parallel} g^0) \mathcal{M}_\perp^{T_\perp^0}, \\ Q_{\mathrm{r}}(f^0) &= \partial_{v_\parallel} \left[(v_\parallel - u_\parallel^0) g^0 + T^0\, \partial_{v_\parallel} g^0 \right]\, \mathcal{M}_\perp^{T_\perp^0} + \nabla_{\mathbf{v}_\perp} \cdot \left[\mathbf{v}_\perp\, f^0 + T^0\, \nabla_{\mathbf{v}_\perp} f^0 \right] , \\ &= \partial_{v_\parallel} \left[(v_\parallel - u_\parallel^0) g^0 + T^0\, \partial_{v_\parallel} g^0 \right]\, \mathcal{M}_\perp^{T_\perp^0} + \frac{2}{3\, T_\perp^0} \left(T_\parallel^0 - T_\perp^0 \right) \left[\frac{|\mathbf{v}_\perp|^2}{2\, T_\perp^0} - 1 \right] f^0 . \end{aligned}$$

Using those decompositions yields, after a rearrangement of the terms of $\mathcal{R}^0$,

$$\begin{aligned} \mathcal{R}^0 = &\left[-\mathbf{v}_\perp \cdot (\nabla_{\mathbf{x}_\perp} g^0) \mathcal{M}_\perp^{T_\perp^0} - \mathbf{v}_\perp \cdot (\nabla_{\mathbf{x}_\perp} \mathcal{M}_\perp^{T_\perp^0}) g^0 - \mathbf{E}_\perp \cdot \nabla_{\mathbf{v}_\perp} f^0 \right] \\ &- g^0 \partial_t \mathcal{M}_\perp^{T_\perp^0} - v_\parallel (\partial_z \mathcal{M}_\perp^{T_\perp^0}) g^0 + \frac{2}{3\, T_\perp^0}\, \nu_{\mathrm{r}} \left(T_\parallel^0 - T_\perp^0 \right) \left[\frac{|\mathbf{v}_\perp|^2}{2\, T_\perp^0} - 1 \right] f^0 \\ &- \left[\partial_t g^0 + v_\parallel\, \partial_z g^0 + E_\parallel\, \partial_{v_\parallel} g^0 - \nu_{\mathrm{r}}\, \partial_{v_\parallel} \left[(v_\parallel - u_\parallel^0) g^0 + T^0\, \partial_{v_\parallel} g^0 \right] \right]\, \mathcal{M}_\perp^{T_\perp^0} . \end{aligned}$$

The third line is zero, in view of the limit model equation on g^0 (3.2.2c). Let us now simplify the other terms.

- $$\left(-\mathbf{v}_\perp \cdot (\nabla_{\mathbf{x}_\perp} \mathcal{M}_\perp^{T_\perp^0})\, g^0\right) = -\frac{\left(\mathbf{v}_\perp \cdot \nabla_{\mathbf{x}_\perp} T_\perp^0\right)}{T_\perp^0} \left[\frac{|\mathbf{v}_\perp|^2}{2T_\perp^0} - 1\right] f^0,$$
- $$\left(-\mathbf{E}_\perp \cdot \nabla_{\mathbf{v}_\perp} f^0\right) = \mathbf{E}_\perp \cdot \frac{\mathbf{v}_\perp}{T_\perp^0} f^0,$$
- $$\begin{aligned} -g^0 \partial_t \mathcal{M}_\perp^{T_\perp^0} - v_\parallel (\partial_z \mathcal{M}_\perp^{T_\perp^0}) g^0 &= \frac{-\partial_t T_\perp^0 - v_\parallel \partial_z T_\perp^0}{T_\perp^0} \left[\frac{|\mathbf{v}_\perp|^2}{2\, T_\perp^0} - 1\right] f^0 \\ &= \frac{(u_\parallel^0 - v_\parallel)\, \partial_z T_\perp^0}{T_\perp^0} \left[\frac{|\mathbf{v}_\perp|^2}{2\, T_\perp^0} - 1\right] f^0 \\ &\quad - \frac{2}{3\, T_\perp^0} \nu_{\mathrm{r}} (T_\parallel^0 - T_\perp^0) \left[\frac{|\mathbf{v}_\perp|^2}{2\, T_\perp^0} - 1\right] f^0, \end{aligned}$$

the very last equality being given thanks to the equation on the temperature $T_\perp^0$ (3.2.5). In view of the last three equalities, $\mathcal{R}^0$ rewrites in the following way

$$\begin{aligned} \mathcal{R}^0 = \left\{ \frac{\mathbf{E}_\perp \cdot \mathbf{v}_\perp}{T_\perp^0} - \frac{\left(\mathbf{v}_\perp \cdot \nabla_{\mathbf{x}_\perp} T_\perp^0\right)}{T_\perp^0} \left[\frac{|\mathbf{v}_\perp|^2}{2T_\perp^0} - 1\right] + \frac{\partial_z T_\perp^0}{T_\perp^0} (u_\parallel^0 - v_\parallel) \left[\frac{|\mathbf{v}_\perp|^2}{2\, T_\perp^0} - 1\right] \right\} f^0 \\ - \mathbf{v}_\perp \cdot \left(\nabla_{\mathbf{x}_\perp} g^0\right) \mathcal{M}_\perp^{T_\perp^0}. \end{aligned}$$

One notices that $\Pi\, \mathcal{R}^0 = 0$, thus yielding that $\mathcal{R}^0 \in \ker^\perp \mathbb{A}_{f^0}^{\mathrm{lin}} = \mathcal{R}(\mathbb{A}_{f^0}^{\mathrm{lin}})$. It therefore makes sense to solve $\widetilde{f}^1 = \mathbb{A}_{f^0}^{\mathrm{lin}\,-1}(\mathcal{R}^0)$. This ends the first part of the proof. Let us now turn to the computation of the microscopic density $\widetilde{f}^1$.

Step 2: Computation of $\widetilde{f}^1$. One can separate this equality into several key terms:

$$\begin{aligned} \mathcal{R}^0 = \left\{ \left(\mathbf{E}_\perp + \nabla_{\mathbf{x}_\perp} T_\perp^0\right) \cdot \frac{\mathbf{v}_\perp}{T_\perp^0} - \frac{\nabla_{\mathbf{x}_\perp} T_\perp^0}{2\,(T_\perp^0)^2} \cdot \left(\mathbf{v}_\perp |\mathbf{v}_\perp|^2\right) + \frac{\partial_z T_\perp^0}{T_\perp^0} (u_\parallel^0 - v_\parallel) \left[\frac{|\mathbf{v}_\perp|^2}{2T_\perp^0} - 1\right] \right\} f^0 \\ - \mathbf{v}_\perp \cdot \left(\nabla_{\mathbf{x}_\perp} g^0\right) \mathcal{M}_\perp^{T_\perp^0}. \end{aligned}$$

It is therefore enough to find a preimage by $\mathbb{A}_{f^0}^{\mathrm{lin}}$ for each of those terms, by linearity. One however needs to notice that $\nabla_{\mathbf{x}_\perp} g^0$ depends on $v_\parallel$, therefore the associated term needs a special treatment.

The goal of the following Lemma is to compute those preimages. This Lemma is technical, so we shall firstly admit it to finish the computation, its proof is postponed in the next subsection of the Appendix.

Lemma 12. One gathers in this lemma the preimages in $\ker^{\perp} \mathbb{A}^{\mathrm{lin}}_{f^0}$ of some specific functions.

$$\mathbb{A}^{\mathrm{lin}}_{f^0}\left(\frac{-(\mathbf{v}_\perp)^\top}{B} f^0\right) = \mathbf{v}_\perp f^0, \tag{3.C.1}$$

$$\mathbb{A}^{\mathrm{lin}}_{f^0}\left(\frac{u^0_\parallel - v_\parallel}{2\,\nu_\perp}\left[\frac{|\mathbf{v}_\perp|^2}{2\,T^0_\perp} - 1\right] f^0\right) = (u^0_\parallel - v_\parallel)\left[\frac{|\mathbf{v}_\perp|^2}{2\,T^0_\perp} - 1\right] f^0, \tag{3.C.2}$$

$$\mathbb{A}^{\mathrm{lin}}_{f^0}\left(n^0\left[\mathbb{D}_2\nabla_{\mathbf{x}_\perp}\left(\frac{g^0}{n^0}\right)\right]\cdot\mathbf{v}_\perp\mathcal{M}^{T^0_\perp}_\perp - \frac{1}{B}\nabla_{\mathbf{x}_\perp}g^0\cdot(\mathbf{v}_\perp)^\top\mathcal{M}^{T^0_\perp}_\perp\right) = \mathbf{v}_\perp\cdot[\nabla_{\mathbf{x}_\perp}g^0]\mathcal{M}^{T^0_\perp}_\perp, \tag{3.C.3}$$

$$\mathbb{A}^{\mathrm{lin}}_{f^0}\left(2T^0_\perp\,\mathbb{D}^t_1\,\mathbf{v}_\perp\left[\frac{|\mathbf{v}_\perp|^2}{2\,T^0_\perp} - 2\right] f^0 - 4\,T^0_\perp\frac{(\mathbf{v}_\perp)^\top}{B} f^0\right) = \mathbf{v}_\perp\,|\mathbf{v}_\perp|^2\,f^0. \tag{3.C.4}$$

where the exponent t is the transposition of matrices, and $\mathbb{D}_1$, $\mathbb{D}_2$ are given by

$$\mathbb{D}_1 = \frac{1}{B^2 + 9\,\nu_\perp^2}\begin{bmatrix} 3\,\nu_\perp & B \\ -B & 3\,\nu_\perp\end{bmatrix}, \qquad \mathbb{D}_2 = \frac{\nu_\perp}{B}\frac{1}{B^2+\nu_\perp^2}\begin{bmatrix} B & -\nu_\perp \\ \nu_\perp & B\end{bmatrix}. \tag{3.C.5}$$

One checks easily that the preimages are in $\ker^{\perp}\mathbb{A}^{\mathrm{lin}}_{f^0}$. The proof of this Lemma is quite technical, and is delayed in the next subsection, for the sake of clarity.

Using this Lemma permits thus to explicit the microscopic part of the first order correction: using repeatedly that $X\cdot Y^\top = -X^\top\cdot Y$, we find

$$\widetilde{f}^1 = (\mathbb{A}^{\mathrm{lin}}_{f^0})^{-1}(\mathcal{R}^0) \tag{3.C.6}$$

$$= \left(g^0\,\mathbf{E}^\top_\perp + g^0\,\nabla^\top_{\mathbf{x}_\perp}T^0_\perp\right)\cdot\frac{\mathbf{v}_\perp}{B\,T^0_\perp}\mathcal{M}^{T^0_\perp}_\perp \tag{3.C.7}$$

$$- \left(\mathbb{D}_1\frac{\nabla_{\mathbf{x}_\perp}T^0_\perp}{T^0_\perp}\right)\cdot\mathbf{v}_\perp\left[\frac{|\mathbf{v}_\perp|^2}{2\,T^0_\perp} - 2\right] f^0 - 2\,\nabla^\top_{\mathbf{x}_\perp}T^0_\perp\cdot\frac{\mathbf{v}_\perp}{B\,T^0_\perp}f^0 \tag{3.C.8}$$

$$+ \frac{\partial_z T^0_\perp}{T^0_\perp}\frac{u^0_\parallel - v_\parallel}{2\,\nu_\perp}\left[\frac{|\mathbf{v}_\perp|^2}{2\,T^0_\perp} - 1\right] f^0 \tag{3.C.9}$$

$$- n^0\left\{\mathbb{D}_2\nabla_{\mathbf{x}_\perp}\left(\frac{g^0}{n^0}\right)\right\}\cdot\mathbf{v}_\perp\mathcal{M}^{T^0_\perp}_\perp - \frac{1}{B}\nabla^\top_{\mathbf{x}_\perp}g^0\cdot\mathbf{v}_\perp\,\mathcal{M}^{T^0_\perp}_\perp. \tag{3.C.10}$$

Arranging the last terms in the first, second, and last line in the right-hand side of the previous equality gives,

$$\begin{aligned}\widetilde{f}^1 = {} & \left(g^0\,\mathbf{E}^\top_\perp - \nabla^\top_{\mathbf{x}_\perp}(g^0\,T^0_\perp)\right)\cdot\frac{\mathbf{v}_\perp}{B\,T^0_\perp}\mathcal{M}_\perp \\ & - \left(\mathbb{D}_1\frac{\nabla_{\mathbf{x}_\perp}T^0_\perp}{T^0_\perp}\right)\cdot\mathbf{v}_\perp\left[\frac{|\mathbf{v}_\perp|^2}{2\,T^0_\perp} - 2\right] f^0 \\ & + \frac{\partial_z T^0_\perp}{T^0_\perp}\frac{u^0_\parallel - v_\parallel}{2\,\nu_\perp}\left[\frac{|\mathbf{v}_\perp|^2}{2\,T^0_\perp} - 1\right] f^0 \\ & - n^0\left\{\mathbb{D}_2\nabla_{\mathbf{x}_\perp}\left(\frac{g^0}{n^0}\right)\right\}\cdot\mathbf{v}_\perp\mathcal{M}_\perp\,,\end{aligned}$$

which is exactly (3.4.32). Therefore, it remains only to prove Lemma 12.

3.C.2 Proof of Lemma 12

The first equality (3.C.1) follows from a simple computation, and we skip it for the sake of shortness.

Proof of (3.C.2)**.** One firstly notices that

$$\mathbb{A}^{\mathrm{lin}}_{f^0}\left(\frac{u^0_\parallel - v_\parallel}{2}\left[\frac{|\mathbf{v}_\perp|^2}{2\,T^0_\perp}-1\right]f^0\right) = -\mathbb{A}^{\mathrm{lin}}_{f^0}\left(v_\parallel\,\frac{|\mathbf{v}_\perp|^2}{4\,T^0_\perp}\,f^0\right). \tag{3.C.11}$$

Then, the computation goes as follows:

$$\begin{aligned}
\mathbb{A}^{\mathrm{lin}}_{f^0}\left(\frac{u^0_\parallel - v_\parallel}{2}\left[\frac{|\mathbf{v}_\perp|^2}{2\,T^0_\perp}-1\right]f^0\right) &= -\mathbb{A}^{\mathrm{lin}}_{f^0}\left(v_\parallel\,\frac{|\mathbf{v}_\perp|^2}{4\,T^0_\perp}\,f^0\right)\\
&= \nu_\perp\,\delta Q_\perp[f^0]\left(v_\parallel\frac{|\mathbf{v}_\perp|^2}{4\,T^0_\perp}\,f^0\right)\\
&= \nu_\perp\,\nabla_{\mathbf{v}_\perp}\cdot\left[v_\parallel\,\mathbf{v}_\perp\frac{|\mathbf{v}_\perp|^2}{4\,T^0_\perp}\,f^0 - \frac{1}{2}u^0_\parallel\,\mathbf{v}_\perp\,f^0 + T^0_\perp\,\nabla_{\mathbf{v}_\perp}\left(v_\parallel\frac{|\mathbf{v}_\perp|^2}{4\,T^0_\perp}\,f^0\right)\right]\\
&= \nu_\perp\,\frac{(v_\parallel - u^0_\parallel)}{2}\,\nabla_{\mathbf{v}_\perp}\cdot\left[\mathbf{v}_\perp\,f^0\right]\\
&= \nu_\perp\,\frac{(v_\parallel - u^0_\parallel)}{2}\left(2-\frac{|\mathbf{v}_\perp|^2}{T^0_\perp}\right)f^0\\
&= \nu_\perp\,(u^0_\parallel - v_\parallel)\left(\frac{|\mathbf{v}_\perp|^2}{2T^0_\perp}-1\right)f^0.
\end{aligned}$$

Proof of (3.C.3)**.** In this proof, $\chi(v_\parallel)$ will denote a function of the parallel variable $v_\parallel$ only. One computes the following equality:

$$\mathbb{A}^{\mathrm{lin}}_{f^0}(\mathbf{v}_\perp\,\chi(v_\parallel)\,\mathcal{M}^{T^0_\perp}_\perp) = \begin{pmatrix}\nu_\perp & B\\ -B & \nu_\perp\end{pmatrix}\mathbf{v}_\perp\,\chi(v_\parallel)\,\mathcal{M}^{T^0_\perp}_\perp - \nu_\perp\frac{\langle\chi\rangle_\parallel}{n^0}\mathbf{v}_\perp\,f^0. \tag{3.C.12}$$

Thus, multiplying by the inverse matrix

$$\begin{pmatrix}\nu_\perp & B\\ -B & \nu_\perp\end{pmatrix}^{-1} = \frac{1}{B^2+\nu_\perp^2}\begin{pmatrix}\nu_\perp & -B\\ B & \nu_\perp\end{pmatrix}, \tag{3.C.13}$$

using equation (3.C.1), and reordering the terms, one isolates $\mathbf{v}_\perp\,\chi(v_\parallel)\,\mathcal{M}^{T^0_\perp}_\perp$ and we find

$$\frac{1}{B^2+\nu_\perp^2}\mathbb{A}^{\mathrm{lin}}_{f^0}\left(\nu_\perp\,\mathbf{v}_\perp\chi\mathcal{M}^{T^0_\perp}_\perp - B\,(\mathbf{v}_\perp)^\top\chi\mathcal{M}^{T^0_\perp}_\perp - \nu_\perp^2\,\frac{\langle\chi\rangle_\parallel}{n^0}\frac{(\mathbf{v}_\perp)^\top}{B}\,f^0 - \nu_\perp\frac{\langle\chi\rangle_\parallel}{n^0}\mathbf{v}_\perp\,f^0\right) = \mathbf{v}_\perp\chi\mathcal{M}^{T^0_\perp}_\perp.$$

Now, let us take $\chi = \partial_x g^0$ and look at the first coordinate of the previous equality. Then take $\chi = \partial_y g^0$, and look at the second coordinate. Summing these two observations yields

$$\frac{1}{B^2+\nu_\perp^2}\mathbb{A}_{f^0}^{\mathrm{lin}}\Big(\nu_\perp\,\mathbf{v}_\perp\cdot[\nabla_{\mathbf{x}_\perp}g^0]\mathcal{M}_\perp^{T_\perp^0}-B\,(\mathbf{v}_\perp)^\top\cdot[\nabla_{\mathbf{x}_\perp}g^0]\mathcal{M}_\perp^{T_\perp^0}$$
$$-\nu_\perp^2\,\frac{\langle\nabla_{\mathbf{x}_\perp}g^0\rangle_\parallel}{n^0}\cdot\frac{(\mathbf{v}_\perp)^\top}{B}\,f^0-\nu_\perp\,\frac{\langle\nabla_{\mathbf{x}_\perp}g^0\rangle_\parallel}{n^0}\cdot\mathbf{v}_\perp\,f^0\Big)=\mathbf{v}_\perp\cdot[\nabla_{\mathbf{x}_\perp}g^0]\mathcal{M}_\perp^{T_\perp^0}.$$

Now, getting the result is just a matter of presentation. Using that $\langle g^0\rangle_\parallel = n^0$, and performing a simple computation, the last equality rewrites

$$\mathbb{A}_{f^0}^{\mathrm{lin}}\left(n^0\left[\mathbb{D}_2\,\nabla_{\mathbf{x}_\perp}\left(\frac{g^0}{n^0}\right)\right]\cdot\mathbf{v}_\perp\mathcal{M}_\perp^{T_\perp^0}-\frac{1}{B}\nabla_{\mathbf{x}_\perp}g^0\cdot(\mathbf{v}_\perp)^\top\mathcal{M}_\perp^{T_\perp^0}\right)=\mathbf{v}_\perp\cdot[\nabla_{\mathbf{x}_\perp}g^0]\mathcal{M}_\perp^{T_\perp^0},$$

thus finishing the proof.

Proof of (3.C.4)**.** One computes:

$$\mathbb{A}_{f^0}^{\mathrm{lin}}\left(\mathbf{v}_\perp|\mathbf{v}_\perp|^2f^0\right)=M_3^{\mathbb{A}_{f^0}^{\mathrm{lin}}}\mathbf{v}_\perp|\mathbf{v}_\perp|^2f^0\;-12\;\nu_\perp\;T_\perp^0\mathbf{v}_\perp\,f^0,\tag{3.C.14}$$

where we denoted by $M_3^{\mathbb{A}_{f^0}^{\mathrm{lin}}}$ the matrix

$$M_3^{\mathbb{A}_{f^0}^{\mathrm{lin}}}:=\begin{pmatrix}3\,\nu_\perp & B\\ -B & 3\,\nu_\perp\end{pmatrix},$$

which is invertible with inverse

$$(M_3^{\mathbb{A}_{f^0}^{\mathrm{lin}}})^{-1}=\frac{1}{B^2+9\,\nu_\perp^2}\begin{pmatrix}3\,\nu_\perp & -B\\ B & 3\,\nu_\perp\end{pmatrix}=\mathbb{D}_1^t\,.$$

Therefore one gets, after multiplication by $\mathbb{D}_1^t$, and reordering the terms

$$\begin{aligned}\mathbf{v}_\perp\;|\mathbf{v}_\perp|^2\;f^0&=\frac{36\;T_\perp^0\;\nu_\perp^2}{B^2+9\;\nu_\perp^2}\,\mathbf{v}_\perp\,f^0-\frac{12\;T_\perp^0\;B\;\nu_\perp}{B^2+9\;\nu_\perp^2}\,(\mathbf{v}_\perp)^\top\,f^0+\mathbb{A}_{f^0}^{\mathrm{lin}}\left(\mathbb{D}_1^t\,\mathbf{v}_\perp\;|\mathbf{v}_\perp|^2\;f^0\right)\\&=\mathbb{A}_{f^0}^{\mathrm{lin}}\left(-\frac{36\;T_\perp^0\;\nu_\perp^2}{B^3+9\,B\;\nu_\perp^2}\,(\mathbf{v}_\perp)^\top\,f^0-\frac{12\;T_\perp^0\;\nu_\perp}{B^2+9\;\nu_\perp^2}\,(\mathbf{v}_\perp)\,f^0+\mathbb{D}_1^t\,\mathbf{v}_\perp\;|\mathbf{v}_\perp|^2\;f^0\right)\\&=\mathbb{A}_{f^0}^{\mathrm{lin}}\left(-4\frac{T_\perp^0}{B}\,(\mathbf{v}_\perp)^\top\,f^0+2\;T_\perp^0\,\mathbb{D}_1^t\mathbf{v}_\perp\left[\frac{|\mathbf{v}_\perp|^2}{2\;T_\perp^0}-2\right]\;f^0\right).\end{aligned}$$

For the second equality, we used equality (3.C.1). The last equality comes after simple computation using the definition of $\mathbb{D}_1^t$.

CHAPTER 4

FOKKER-PLANCK EQUATION FOR ENERGETIC PARTICLES. THE κ-DISTRIBUTION FUNCTION.

Le contenu de ce chapitre est en anglais, et est tiré de l'article suivant :

- Etienne Lehman, Claudia Negulescu. "Fokker-Planck equation for energetic particles. The κ-distribution function", soumis pour publication.

Abstract: The first concern of the present paper is the mathematical study of a specific Fokker-Planck equation describing the dynamics of energetic particles (runaway electrons for example) occurring in thermonuclear fusion plasmas or astrophysics. In the long-time limit, the velocity distribution function of these particles tends towards a (thermal) non-equilibrium distribution, namely a κ-distribution function which is a steady-state of the considered Fokker-Planck equation. Our aim is firstly to investigate the convergence rate of the velocity distributions towards these stationary states as $t \to \infty$, as well as in a second step to design an efficient spectral scheme, permitting to cope with this long-time asymptotics, without too much numerical costs. Non-equilibrium (or non-Maxwellian) distributions need to be considered properly enough in fusion or astrophysical plasmas in order to accurately reproduce the plasma dynamics and to understand the impact of the runaway electrons on the whole thermal plasma bulk as well as for issues like astonaut safety in astrophysics.

Contents

4.1 Introduction

Stationary states out of thermal equilibrium, are often observed in a large number of fields, such as laboratory (tokamak) plasmas [HMD85], astrophysical plasmas [Bia+14; Liv14; ST91], molecular dynamics [BG06], economy [DT07] and so on. In magnetically confined fusion plasmas a lot of mechanisms keep the particle distribution function far from a thermal equilibrium (Maxwellian distribution), mechanisms such as radio-frequency heating and neutral beam injection used for ignition, production of highly energetic α-particles through fusion reactions, non-thermal acceleration processes via electric fields (runaway electrons) and so on. The physical reason for the departure from Maxwellian distributions is linked to the fact that while low-energy particles are often collisional, faster ones are generally not any more (or less collisional), being thus easily driven out of the equilibrium and escaping to large distances. This comes from the fact that fast particles spend less time in the neighbourhood of each particle it collides with, when compared to slower particles. The question is now, how to model such energetic particle distribution functions (in the velocity space), keeping the Maxwellian distributions as a limiting case.
It is important to understand that an accurate description of the energetic particle dynamics is of crucial importance for fusion reactor performances, in particular to predict confinement. Indeed, the success of magnetically confined fusion reactors relies upon a proper confinement of the energetic fusion products (*α-particles*), and this for sufficiently long times, such that they can transfer enough energy to the fuel ions in order to permit the fusion reaction to take place in a self-sustained manner. Furthermore, *runaway electrons* can have an essential impact on the global stability of the fusion bulk plasma, their control being thus an essential point. In astrophysics a good understanding of runaway dynamics is essential for issues like astronaut safety or for more fundamental reasons, such as the understanding of solar flares. For more physical details about all these phenomena we refer to [Che12; HM03].

Different mathematical approaches can be now considered to describe a plasma gas. A fully kinetic description of the whole electron-ion plasma is a very precise approach, however for the moment still numerically out of reach in the full coupled $6D$ phase-space. Fluid approximations become questionable when the velocity distribution functions have suprathermal tails, as they assume the plasma to be in a local thermodynamic equilibrium. Thus, different strategies have been introduced in literature, trying to keep a balance between physical precision and computational costs. One of these approaches is based on the introduction of analytic non-Maxwellian distribution functions, permitting to reduce the degrees of freedom of the full kinetic distribution $f(t, \mathbf{x}, \mathbf{v})$ to the computation of a small amount of macroscopic quantities, such as the particle density $n(t, \mathbf{x})$, the mean velocity $\mathbf{u}(t, \mathbf{x})$, the temperature $T(t, \mathbf{x})$ *etc.* For example *beam-distributions* of the type

$$f(t, \mathbf{x}, \mathbf{v}) := n_b \left(\frac{m_b}{2\,\pi\, k_B\, T_b} \right)^{3/2} e^{-m_b \frac{|\mathbf{v}-\mathbf{u}_b|^2}{2\, k_B\, T_b}} + n_f \left(\frac{m_f}{2\,\pi\, k_B\, T_f} \right)^{3/2} e^{-m_f \frac{|\mathbf{v}-\mathbf{u}_f|^2}{2\, k_B\, T_f}}, \tag{4.1.1}$$

are a good approximation for plasmas comprising also fast particles, and this in the case there is no interaction between the bulk plasma (main Gaussian bump, described by $(n_b, \mathbf{u}_b, T_b)$) and the fast particles (secondary Gaussian bump, described by $(n_f, \mathbf{u}_f, T_f)$). The generalization to a sum of more than two Maxwellians is also possible.

κ-distribution functions are commonly encountered in astrophysics to describe particle distributions having a core Maxwellian and a power-law (and not exponential) decrease in the large velocity ranges. This means, κ-distributions describe an over-population of particles at high speeds, when compared to Maxwellian distributions, however the fast particles are not any more localized around some specific velocity as in the bump-distribution case (4.1.1). Several definitions of κ-distributions exist in literature, characterizing the power-law nature of the energetic tails in different manners. The κ-distribution of first kind is given by the formula

$$f_\kappa(t,\mathbf{x},\mathbf{v}) = A_\kappa\, n(t,\mathbf{x}) \left(1 + \frac{|\mathbf{v}|^2}{\kappa\, v_{th}^2}\right)^{-\kappa}, \qquad A_\kappa := \frac{1}{(\pi\,\kappa\, v_{th}^2)^{3/2}}\, \frac{\Gamma(\kappa)}{\Gamma(\kappa - 3/2)}, \tag{4.1.2}$$

where the thermal speed $v_{th} := \sqrt{\frac{2\,k_B\,T}{m}}$ and the particle density n are fixed by the associated Maxwellian $\mathcal{M}$, given by

$$\mathcal{M}(t,\mathbf{x},\mathbf{v}) := \frac{n(t,\mathbf{x})}{(\pi\, v_{th}^2)^{3/2}}\, e^{-\frac{|\mathbf{v}|^2}{v_{th}^2}}, \quad n := \int_{\mathbb{R}^3} \mathcal{M}\, d\mathbf{v} = \int_{\mathbb{R}^3} f_\kappa\, d\mathbf{v}, \quad \frac{3}{2}\, n\, k_B\, T := \frac{m}{2} \int_{\mathbb{R}^3} |\mathbf{v}|^2\, \mathcal{M}\, d\mathbf{v}.$$

Let us recall here for simplicity the Euler Gamma function Γ, defined for $r \in \mathbb{R}_*^+$ by

$$\Gamma(r) := \int_0^\infty s^{r-1}\, e^{-s}\, ds, \qquad \Gamma(1) = 1, \;\; \Gamma(1/2) = \sqrt{\pi}, \;\; \Gamma(r+1) = r\,\Gamma(r),$$

and satisfying $\Gamma(r+\alpha) \sim_{r\to\infty} \Gamma(r)\, r^\alpha$ for all $\alpha \in \mathbb{R}^+$, where the symbol $\sim$ stands for the asymptotic equivalence. Remark now that f_κ contains three parameters, v_{th} and n which are linked to the associated Maxwellian, and $3/2 < \kappa < \infty$ which is the only free parameter and determines the distance away from the Maxwellian, in particular the lower the κ, the more pronounced are the tails. One can introduce a temperature T_κ (for $\kappa > 5/2$) corresponding to this κ-distribution function

$$\frac{3}{2}\, n\, k_B\, T_\kappa(t,\mathbf{x}) := \frac{m}{2} \int_{\mathbb{R}^3} |\mathbf{v}|^2\, f_\kappa(t,\mathbf{x},\mathbf{v}) d\mathbf{v},$$

which is however different from the Maxwellian temperature T. Note that temperature definitions are appropriate for thermal equilibrium (Maxwellian) distributions, thus not rigorously valid for a κ-distribution function, but there are practical reasons for using such kinetic temperature definitions.

We represented on the left of Figure 4.1 a comparison between the different κ-distributions and the associated Maxwellian. What one observes is that the κ-distribution function has an asymptotic power law decrease for large v and joints smoothly with a Maxwellian core at

low speeds. Furthermore, remark that one recovers the associated Maxwellian distribution function for $\kappa \to \infty$, in particular one has $T_\kappa \to_{\kappa\to\infty} T$. All this can be simply shown, using

$$e^{-\xi} = \lim_{\kappa\to\infty}\left(1+\frac{\xi}{\kappa}\right)^{-\kappa}, \quad \lim_{\kappa\to\infty} A_\kappa = \frac{1}{(\pi\, v_{th}^2)^{3/2}} \qquad \Rightarrow \qquad f_\kappa(\mathbf{v}) \to_{\kappa\to\infty} \frac{1}{(\pi\, v_{th}^2)^{3/2}}\, e^{-\frac{|\mathbf{v}|^2}{v_{th}^2}},$$

as well as

$$f_\kappa(\mathbf{v}) \propto_{|\mathbf{v}|\ll 1} \left(1-\frac{|\mathbf{v}|^2}{v_{th}^2}\right), \qquad f_\kappa(\mathbf{v}) \propto_{|\mathbf{v}|\gg 1} |\mathbf{v}|^{-2\,\kappa},$$

where the symbol $\propto$ shall stand in the following for the proportionality relation, to be distinguished from the asymptotic equivalence symbol $\sim$. Finally, let us finish with mentioning that the moments of the κ-distribution function are bounded only for a finite number of $l \in \mathbb{N}$, as the distributions are not exponentially decaying in $|\mathbf{v}|$, but polynomially. One can show indeed that

$$\int_{\mathbb{R}^3} |\mathbf{v}|^l\, f_\kappa(t,\mathbf{x},\mathbf{v}) d\mathbf{v} = \frac{n(t,\mathbf{x})}{\pi^{3/2}}\, \left(\kappa\, v_{th}^2\right)^{l/2}\, \frac{\Gamma\left(\frac{l+3}{2}\right)\,\Gamma\left(\kappa-\frac{l+3}{2}\right)}{\Gamma\left(\kappa-\frac{3}{2}\right)}, \quad \forall 0 \leqslant l < 2\,\kappa-3\,. \tag{4.1.3}$$

The fact that higher moments are unbounded excludes the design of spectral methods based on orthogonal polynomials as basis-sets (orthogonal with respect to the weight-function f_κ), such as the Hermite-polynomials for the Maxwellian weights. Finally, integrating (4.1.2) over two velocity space dimensions yields the 1D κ-distribution function of first kind

$$f_\kappa^{1D}(t,\mathbf{x},v) = A_\kappa^{1D}\, n(t,\mathbf{x}) \left(1+\frac{v^2}{\kappa\, v_{th}^2}\right)^{-(\kappa-1)}, \qquad A_\kappa^{1D} := \frac{1}{(\pi\,\kappa\, v_{th}^2)^{1/2}}\, \frac{\Gamma(\kappa-1)}{\Gamma(\kappa-3/2)}\,. \tag{4.1.4}$$

Remark 8. The more conventional form of the κ-distribution function is the so-called κ-distribution of second kind (see Fig. 4.1, for a comparison with the first kind)

$$g_k(t,\mathbf{x},\mathbf{v}) = N_k \left(1+\frac{|\mathbf{v}|^2}{k\, v_{th,k}^2}\right)^{-(k+1)}, \qquad N_k := \frac{n(t,\mathbf{x})}{(\pi\, k\, v_{th,k}^2)^{3/2}}\, \frac{\Gamma(k+1)}{\Gamma(k-1/2)}, \tag{4.1.5}$$

with $k > 3/2$ and $v_{th,k}$ the k-dependent effective thermal velocity $v_{th,k} := \sqrt{\frac{(k-3/2)}{k}}\,\sqrt{\frac{2\,k_B\,T}{m}}$. The particle density and temperature of this distribution function

$$n(t,\mathbf{x}) := \int_{\mathbb{R}^3} g_k(t,\mathbf{x},\mathbf{v}) d\mathbf{v}\,, \qquad \frac{3}{2}\, k_B\, n\, T(t,\mathbf{x}) := \frac{m}{2} \int_{\mathbb{R}^3} |\mathbf{v}|^2\, g_k(t,\mathbf{x},\mathbf{v}) d\mathbf{v}\,,$$

are the same as for the associated Maxwellian

$$\mathcal{M}(t,\mathbf{x},\mathbf{v}) := \frac{n(t,\mathbf{x})}{(\pi\, v_{th}^2)^{3/2}}\, e^{-\frac{|\mathbf{v}|^2}{v_{th}^2}}, \qquad \text{where} \quad v_{th} := \sqrt{\frac{2\,k_B\,T}{m}}\,.$$

Remark that this time, the effective thermal velocity $v_{th,k}$ is a reference speed and not the usual thermal speed of the Maxwellian, but linked to it through $v_{th,k} \to_{k\to\infty} v_{th} := \sqrt{\frac{2\,k_B\,T}{m}}$.

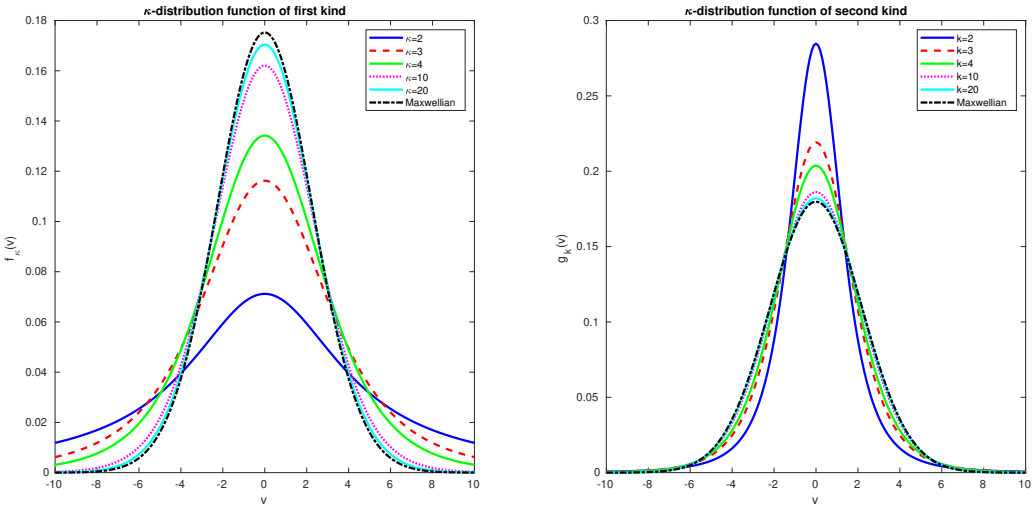

Figure 4.1 – $1D$ κ-distribution functions for several κ-values and associated Maxwellian distributions, recovered for $\kappa \to \infty$. Left: κ-distribution function of first kind, given in (4.1.4). Right: κ-distribution function of second kind, given by integrating (4.1.5) over 2 velocity degrees of freedom.

4.1.1 Physical motivation

Let us say some words in this subsection, about the manner how κ-distributions arise. We shall restrict here, for simplicity reasons, to the one-dimensional case $v \in \mathbb{R}$. κ-distribution functions are steady state solutions of specific Fokker-Planck equations, where the drift and diffusion coefficients are velocity dependent and are linked through a specific ratio-relation. It is a non-equilibrium effect which leads to κ-distributions, where the driving (drift) and the compensation via diffusion give rise to a stationary state that does not satisfy the fluctuation-dissipation theorem (Einstein's relation is violated).

Let us precise this in more details and consider first the general one-dimensional Fokker-Planck equation

$$\partial_t f = \nu\, \partial_v \left[D(v) \left(U'(v)\, f + \partial_v f \right) \right] , \qquad \forall (t,v) \in \mathbb{R}^+ \times \mathbb{R} , \tag{4.1.6}$$

where $\nu > 0$ is the collisional frequency, $D(v) \geq 0$ is the velocity dependent diffusion coefficient and $U(v)$ a potential function describing the drift mechanism. Remark that we have omitted in this paper the usual transport term in the kinetic equation, in order to concentrate only on the Fokker-Planck collision operator. In plasma physics the diffusion coefficient is usually decaying for $v \to \pm\infty$, for example we have the proportionality relation $D(v) \propto_{v \gg 1} v^{-3}$ in the case of Coulomb collisions. In the work [CN] of one of the authors, it is more precisely

explained that one has indeed $D(v) := \frac{G(v/v_{th})}{v/v_{th}}$, with $v_{th} := \sqrt{\frac{2\,k_B\,T}{m}}$ the thermal speed and where the Chandrasekhar function G is defined via the error function ϕ as follows

$$G(x) := \frac{\phi(x) - x\,\phi'(x)}{2\,x^2}\,, \qquad \phi(x) := \frac{2}{\sqrt{\pi}} \int_0^x e^{-y^2}\,dy\,. \tag{4.1.7}$$

The stationary solutions of (4.1.6) are given by

$$f_\infty(v) := \alpha\, e^{-U(v)}\,, \qquad \forall v \in \mathbb{R}\,,$$

with $\alpha > 0$ determined by the initial condition f_{in}. The first observation is that a quadratic potential $U(v) := \frac{v^2}{v_{th}^2}$ yields the standard Fokker-Planck equation

$$\partial_t f = \nu\,\partial_v \left[\frac{2\,D(v)}{v_{th}^2} \left(v\,f + \frac{v_{th}^2}{2}\,\partial_v f \right) \right], \qquad \forall (t,v) \in \mathbb{R}^+ \times \mathbb{R}\,,$$

with the usual Maxwellian equilibrium $\frac{n}{\sqrt{\pi\,v_{th}^2}}\,e^{-v^2/v_{th}^2}$.

The question now is how κ-distributions can arise. Consider thus in a second step the following specific Fokker-Planck equation

$$\partial_t f = \nu\,\partial_v \left\{ \gamma(v) \left[v\,f + \left(\frac{v_{th}^2}{2} + D_{turb}(v) \right) \partial_v f \right] \right\}, \qquad \forall (t,v) \in \mathbb{R}^+ \times \mathbb{R}\,, \tag{4.1.8}$$

which includes the combined effects of Coulomb collisions with a dense plasma background and a turbulent acceleration mechanism described by $D_{turb}(v)$. Here $v_{th} := \sqrt{\frac{2\,k_B\,T}{m}}$ is again the thermal speed and $\gamma(v)$ is the friction coefficient. One can put this Fokker-Planck equation under the form (4.1.6) with $D(v) = \gamma(v) \left(\frac{v_{th}^2}{2} + D_{turb}(v) \right)$ and $U'(v) = v \left(\frac{v_{th}^2}{2} + D_{turb}(v) \right)^{-1}$. Hence, one observes immediately that for $D_{turb}(v) \equiv cst.$, meaning $\gamma(v)$ proportional to $D(v)$ (Einstein's relation), one gets standard Maxwellian steady states. However for large $D_{turb}(v)$, for example if $D_{turb}(v) \propto v^2$, one gets a potential of logarithmic type. In particular, taking $D_{turb}(v) = D_0\,v^2$, which leads to $U(v) = \kappa \ln\left(1 + \frac{|v|^2}{\kappa\,v_{th}^2}\right)$, yields the following κ-distribution function of first kind as a steady-state

$$f_\kappa(v) = C_\kappa \left(1 + \frac{v^2}{\kappa\,v_{th}^2} \right)^{-\kappa}, \qquad \kappa := \frac{1}{2\,D_0}\,, \quad v_{th} := \sqrt{\frac{2\,k_B\,T}{m}}\,, \tag{4.1.9}$$

with $C_\kappa > 0$ a normalization factor. More generally, the shape of the distribution function is obtained by examining the exponent in the ratio between the friction coefficient and the diffusion coefficient $\gamma(v)/D(v) = \left(\frac{v_{th}^2}{2} + D_{turb}(v) \right)^{-1}$ in the high-velocity regime. In particular, if this ratio behaves for large velocities as $v^{\beta-1}$ with some $\beta \in (-1, 1)$, then we have to cope with different types of suprathermal tails. Einstein's relation is recovered for $\beta = 1$ and the

κ-distributions are recovered for $\beta = -1$. The addition of the turbulent term D_{turb} is only empirical. This diffusion term describes on a mesoscopic level the effect on the particles of force-fields which arise from turbulent phenomena not including the usual stochastic Brownian motion. This extra term injects energy into the system, which combined with the friction force, determines the steady-state distribution function.

4.1.2 Outline of this paper and main results

The relaxation of an initial distribution function towards the steady-state solution of the Fokker-Planck equation is a classical problem in plasma kinetic theory. The knowledge of the asymptotic behaviour of the solution as well as of the convergence rate towards this steady-state function is of crucial importance for experiments and numerical simulations. Several studies have been performed for the standard (constant coefficient) Fokker-Planck collision operator, investigating via coercivity techniques the convergence rate towards Maxwellian distribution functions [Bak+08; Bla+09; DT11]. The first aim of the present work is to adapt these techniques to the more general Fokker-Planck collision operator of the type (4.1.6) (with velocity dependent drift and diffusion coefficients), in order to study the convergence towards the corresponding κ-distribution function. The particularity of this operator is that it features a gapless, continuous spectrum, thus the usual exponential decay in time is now replaced by an algebraic time-decay rate towards the steady state. Secondly Hermite spectral numerical schemes have been proposed in literature [FN22] to efficiently discretize standard Fokker-Planck equations in the velocity space, permitting among others to get, without too much numerical burden, the limiting Maxwellian distribution function as $t \to \infty$. Our second aim in this work is hence to propose an efficient numerical, scheme adapted to the here treated specific Fokker-Planck operators and their κ-distribution steady-states. The problem is now more challenging than in the standard Fokker-Planck case, the gapless continuous spectrum leading to numerical difficulties. Spectral techniques will be used in this paper to render an accurate treatment of the small λ-modes (small energy-modes) of the solution, which are essential for a correct handling of the long-time asymptotic behaviour of the solutions. Given these characteristics of our scheme, we shall call it *Low Energy Accurate Scheme* (LEAS). Finally, we would like to refer here to the related works [BMP11; CMT12; Mel02; MMM11], which deal with the diffusion limit of Vlasov-Lévy-Fokker-Planck or linear Boltzmann equations. The equilibria in these equations are also heavy-tail distribution functions, the long-time/mean-free path limit leading to fractional diffusion equations. A more recent work [Fur+22] studies functional inequalities for such type of heavy-tail distributions.

The outline of this paper is the following. Section 4.2 reviews the mathematical and numerical results of the standard Fokker-Planck operator. Section 4.3 and 4.4 focus on the mathematical study of the more general Fokker-Planck operator (4.1.6), which can be also

rewritten, with a well-defined equilibrium function $f_{eq} = \alpha\, e^{-U}$, $\alpha \in \mathbb{R}^+$, as

$$\partial_t f = \nu\, \partial_v \left[D(v)\, f_{eq}\, \partial_v \left(\frac{f}{f_{eq}} \right) \right], \qquad \forall (t,v) \in \mathbb{R}^+ \times \mathbb{R}\,. \tag{4.1.10}$$

Section 4.3 investigates the long-time asymptotics and the (algebraic) convergence rate of the solutions to (4.1.10) towards the stationary states (Theorems 6, 7 and 8). Section 4.4 focuses on the spectral analysis of these Fokker-Planck operators, in particular we are interested to express the solution in terms of generalized eigenfunctions and density functions (Proposition 4.4.2), in order to prepare the design of the LEAS scheme. Based on these mathematical results, Section 4.5 presents an efficient numerical scheme (LEAS), permitting to compute without too much numerical burden, the solutions of the corresponding Fokker-Planck equation, even for long simulation times. In order not to render the lecture too heavy, we preferred to postpone to the Appendix the proof of the continuous spectral theorem.

4.2 Study of the Fokker-Planck collision operator

The main objective of this paper is the mathematical and numerical study of the following $1D$ evolution problem

$$\partial_t f = \partial_v \left[D(v)\, f_{eq}\, \partial_v \left(\frac{f}{f_{eq}} \right) \right], \qquad \forall (t,v) \in \mathbb{R}^+ \times \mathbb{R}\,, \tag{4.2.1}$$

associated with some initial condition f_{in}, and we shall focus on four particular cases, namely

(I) $D(v) \equiv 1$ and $f_{eq} = \mathcal{M}(v)$;
(II) $D(v) \equiv 1$ and $f_{eq} = f_\kappa(v)$;
(III) $D(v) = G(v)/v$ and $f_{eq} = \mathcal{M}(v)$;
(IV) $D(v) = G(v)/v$ and $f_{eq} = f_\kappa(v)$.

Here the Maxwellian equilibrium is defined as

$$\mathcal{M}(v) := \frac{1}{\sqrt{2\,\pi}}\, e^{-v^2/2}, \qquad \forall v \in \mathbb{R}\,, \tag{4.2.2}$$

whereas the κ-equlibria are given for $\kappa > 1/2$ and $v \in \mathbb{R}$ by the formula

$$f_\kappa(v) := \alpha_\kappa \left(1 + \frac{v^2}{\kappa} \right)^{-\kappa}, \qquad \text{where} \quad \alpha_\kappa := \frac{1}{(\pi\,\kappa)^{1/2}}\, \frac{\Gamma(\kappa)}{\Gamma(\kappa - 1/2)}\,.$$

Let us recall here the definitions of the error function $\phi \in C^\infty(\mathbb{R})$ and the Chandrasekhar function $G \in C^\infty(\mathbb{R})$

$$\phi(x) := \frac{2}{\sqrt{\pi}} \int_0^x e^{-y^2}\, dy\,, \qquad G(x) := \frac{\phi(x) - x\,\phi'(x)}{2\,x^2} \quad \text{and} \quad G(0) := 0\,, \tag{4.2.3}$$

as well as their asymptotic developments for small and large arguments, given by

$$\phi(x) \sim_{x\ll 1} \frac{2x}{\sqrt{\pi}}\left(1-\frac{x^2}{3}+\frac{x^4}{10}\cdots\right) \quad ; \quad \phi(x) \sim_{x\gg 1} 1-\frac{e^{-x^2}}{\sqrt{\pi}\,x}\left(1-\frac{1}{2x^2}+\frac{3}{4\,x^4}\cdots\right),$$
$$G(x) \sim_{x\ll 1} \frac{2x}{3\sqrt{\pi}}-\frac{2x^3}{5\sqrt{\pi}}\cdots \quad ; \quad G(x) \sim_{x\gg 1} \frac{1}{2x^2}-\frac{e^{-x^2}}{\sqrt{\pi}\,x}\left(1+\frac{1}{2x^2}-\frac{1}{4\,x^4}\cdots\right).$$

The degeneracy of the Fokker-Planck collision operator (4.2.1) can be understood, when taking a look at Figure 4.2, where $D(\cdot) \in C^\infty(\mathbb{R})$ is plotted. Observe thus that the collision operator becomes negligible for high velocities of the energetic particles, due to $D(v) \to_{v\to\infty} 0$.

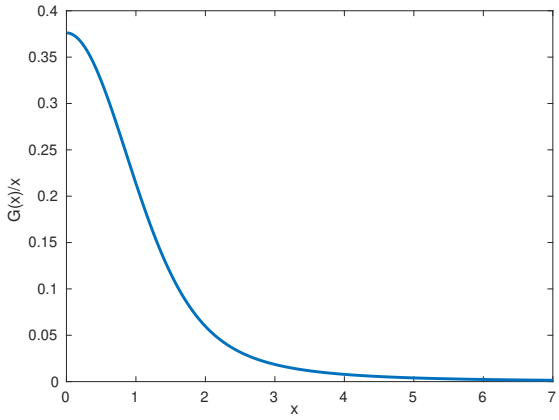

Figure 4.2 – Plot of the symmetric, smooth diffusion term $D(v) := G(v)/v$.

Our aim is to investigate in more details the convergence of the solution f of (4.2.1) towards the corresponding stationary solution f_∞ and to understand the influence of the diffusion coefficient $D(v)$ on the convergence rate. This shall be done via spectral analysis, with the specificity that cases (II)-(IV) are not standard, featuring a gapless, continuous spectrum.

When considering the time decay of the solutions towards the corresponding stationary states, we shall adopt in each of these four cases the following functional transformation $f = h\, f_{eq}$, leading to the evolution problem

$$\partial_t h = \frac{1}{f_{eq}(v)}\,\partial_v\left[D(v)\, f_{eq}(v)\,\partial_v h\right], \tag{4.2.4}$$

associated with an initial condition h_{in} and with the corresponding stationary state $h_\infty \equiv \bar{h}_{in} = \int_{\mathbb{R}} h_{in}(v)\, f_{eq}(v)\, \mathrm{d}v$, which is obtained from the conservation of mass property of the equation, namely $\partial_t \bar{h} = 0$.

Proposition 4.2.1. **(Existence/uniqueness of a solution)** Let us denote the second order differential operator occurring in (4.2.4) by

$$\mathcal{L}_{D,eq}(h) := -\frac{1}{f_{eq}}\,\partial_v\left[D\, f_{eq}\,\partial_v h\right].$$

Then one can show that $\mathcal{L}_{D,eq}(h) : \mathcal{D}(\mathcal{L}_{D,eq}) \subset L^2_{eq} \to L^2_{eq}$ is a linear, unbounded, self-adjoint and positive operator on the Hilbert-space

$$L^2_{eq} := \left\{ h : \mathbb{R} \to \mathbb{R} \ \text{ measurable}, \quad \int_{\mathbb{R}} |h|^2 \, f_{eq} \, \mathrm{d}v < \infty \right\}, \qquad \|h\|^2_{L^2_{eq}} := \int_{\mathbb{R}} |h|^2 \, f_{eq} \, \mathrm{d}v, \tag{4.2.5}$$

and with domain

$$\mathcal{D}(\mathcal{L}_{D,eq}) = \{ h \in L^2_{eq}, \quad \mathcal{L}_{D,eq}(h) \in L^2_{eq} \}. \tag{4.2.6}$$

Furthermore, for each $h_{in} \in \mathcal{D}(\mathcal{L}_{D,eq})$ there exists a unique solution $h \in C^1([0,\infty); L^2_{eq}) \cap C([0,\infty); \mathcal{D}(\mathcal{L}_{D,eq}))$ of the Fokker-Planck equation (4.2.4). For less regular initial conditions $h_{in} \in L^2_{eq}$ and each $T > 0$, one has nonetheless a unique weak solution $h \in W^1_2(0,T; H^1_{eq}, L^2_{eq}) \subset C([0,T]; L^2_{eq})$, where

$$H^1_{eq} := \{ u \in L^2_{eq} \ / \ \sqrt{D(v)}\, \partial_v u \in L^2_{eq} \}.$$

Finally one has also a maximum principle, meaning that if furthermore $h_{in} \in L^\infty(\mathbb{R}_v)$, then

$$\|h(t,\cdot)\|_{L^\infty(\mathbb{R}_v)} \leqslant \|h_{in}\|_{L^\infty(\mathbb{R}_v)}, \quad \forall t \geqslant 0.$$

Proof. The proof is a simple consequence of Weyl's theory for second order differential operators [CL55], the unbounded operator $\mathcal{L}_{D,eq}$ being in the limit-point case in $v = \pm\infty$, and hence it is not necessary to implement additional boundary conditions at infinity. Furthermore standard arguments, such as Hille Yosida theorem respectively Lions theorem, permit to show the existence and uniqueness of a solution to the Fokker-Planck equation (4.2.4). □

We shall denote in the following the Hilbert-space (4.2.5) simply by L^2_κ in cases (II) and (IV), with $\|\cdot\|_\kappa$ its associated norm, and $L^2_{\mathcal{M}}$ in cases (I) and (III), with $\|\cdot\|_{\mathcal{M}}$ the associated norm.

The aim of the rest of this paper will be to investigate the decay of the solutions to (4.2.4) towards the stationary state h_∞, to say more about the spectrum of $\mathcal{L}_{D,eq}$ and the spectral representation of the solutions, all this in the aim to design an efficient numerical scheme for the resolution of (4.2.4). Let us however start with the standard case.

4.2.1 Spectral analysis of case (I) with $D \equiv 1$ and $f_{eq} = \mathcal{M}$.

This case is very well documented, we recall here the results only for the sake of completeness. In this situation, the space L^2_{eq} rewrites

$$L^2_{\mathcal{M}} := \left\{ h : \mathbb{R} \to \mathbb{R} \ \text{ measurable}, \quad \int_{\mathbb{R}} |h|^2 \, \mathcal{M}(v) \, \mathrm{d}v < \infty \right\}, \tag{4.2.7}$$

while the operator is the standard linear Fokker-Planck operator

$$\mathcal{L}_{1,\mathcal{M}}(h) = -\frac{1}{\mathcal{M}}\partial_v[\mathcal{M}\,\partial_v h] = -\partial_{vv}h + v\partial_v h\,. \tag{4.2.8}$$

This operator is well studied, and one has the following standard result.

Proposition 4.2.2. [SA14] **(Spectrum of $\mathcal{L}_{1,\mathcal{M}}$)** The operator (4.2.8) is self-adjoint, positive and with compact resolvant, such that its spectrum is discrete, real, positive and consists of a sequence of eigenvalues $(\lambda_k)_{k\in\mathbb{N}} \subset \mathbb{R}$ with $\lambda_k \to \infty$ as $k \to \infty$. In particular one has for all $k \in \mathbb{N}$

$$\mathcal{L}_{1,\mathcal{M}}\,H_k(v) = \lambda_k\,H_k(v)\,, \qquad \forall v \in \mathbb{R}\,, \quad \text{with eigenvalue } \lambda_k := k\,,$$

and the associated eigenvectors are the Hermite polynomials, defined recursively via $H_0 \equiv 1$, $H_1(v) \equiv v$ and for all $k \geqslant 1$ by the formulae

$$\sqrt{k+1}\,H_{k+1}(v) = v\,H_k(v) - \sqrt{k}\,H_{k-1}(v)\,, \quad \forall v \in \mathbb{R}\,. \tag{4.2.9}$$

Remark that $H_k'(v) = \sqrt{k}\,H_{k-1}(v)$ and that $\{H_k\}_{k\in\mathbb{N}}$ form a complete orthonormal basis set of the space $L^2_{\mathcal{M}}$.

This property is useful both from an analytic point of view, permitting to study the decay rate towards the equilibrium, but also from a numerical perspective, permitting the construction of a spectral method. We shall illustrate this fact in the two following subsections.

4.2.1.1 Time decay

The first consequence of the discrete spectrum of the operator $\mathcal{L}_{1,\mathcal{M}}$ is the existence of a spectral gap between the smallest two eigenvalues $\lambda_0 = 0$ and $\lambda_1 = 1$. This leads to the following Poincaré-Wirtinger inequality (with constant $C = \lambda_1 = 1$)

$$\int_{\mathbb{R}} |h(v) - \bar{h}|^2\,\mathcal{M}(v)\,\mathrm{d}v \leqslant \int_{\mathbb{R}} |\partial_v h(v)|^2 \mathcal{M}(v)\,\mathrm{d}v\,, \qquad \forall h \in H^1(\mathbb{R}, \mathcal{M}dv)\,, \tag{4.2.10}$$

where $\bar{h} := \int_{\mathbb{R}} h(v)\,\mathcal{M}(v)\,\mathrm{d}v$. This equality permits to show the convergence for $t \to \infty$ of the solution of the evolution problem

$$\begin{cases} \partial_t h = \partial_{vv}h - v\partial_v h = \frac{1}{\mathcal{M}}\partial_v[\mathcal{M}\,\partial_v h]\,, & \forall (t,v) \in \mathbb{R}^+ \times \mathbb{R} \\ h(0,\cdot) = h_{in}\,, \end{cases} \tag{4.2.11}$$

towards its stationary solution $h_\infty \equiv \bar{h}_{in}$. Indeed, multiplying (4.2.11) by $h\,\mathcal{M}$ and integrating in v, remarking besides that $\partial_t \bar{h} = 0$ and using Poincaré-Wirtinger's inequality (4.2.10), yields

$$\frac{1}{2}\frac{\mathrm{d}}{\mathrm{d}t}\|h(t) - \bar{h}\|^2_{\mathcal{M}} = -\int_{\mathbb{R}} |\partial_v h(t,v)|^2 \mathcal{M}(v)\,\mathrm{d}v \leqslant -\int_{\mathbb{R}} |h(t,v) - \bar{h}|^2\,\mathcal{M}(v)\,\mathrm{d}v = -\|h(t) - \bar{h}\|^2_{\mathcal{M}}\,. \tag{4.2.12}$$

Gronwall's inequality implies then immediately the following exponential decay of the solution towards its equilibrium

$$\|h(t) - h_\infty\|_{\mathcal{M}} \leqslant \|h_{in} - \bar{h}_{in}\|_{\mathcal{M}}\, e^{-t}\,, \quad \forall t \geq 0\,. \tag{4.2.13}$$

The rate of convergence is directly given by the spectral gap between the eigenvalue $\lambda_0 = 0$ and the eigenvalue $\lambda_1 = 1$. The spectral gap is indeed an essential quantity which gives important physical information about the system under study, in particular it determines the low-energy physics.

4.2.1.2 Spectral representation

Now, one can make use of the orthonormal basis of eigenvectors $\{H_k\}_{k\in\mathbb{N}} \subset L^2_{\mathcal{M}}$ to expand the solution of the evolution problem (4.2.11).

Proposition 4.2.3. **(Spectral representation in the discrete case)** The solution of (4.2.11) can be expressed in terms of the Hermite polynomials introduced in Proposition 4.2.2, *i.e.*

$$h(t,v) = \sum_{k=0}^{\infty} \alpha_k(t)\, H_k(v) \qquad \text{with} \quad \alpha_k(t) = (h(t), H_k)_{\mathcal{M}} = \int_{\mathbb{R}} h(t,v)\, H_k(v)\, \mathcal{M}(v)\, \mathrm{d}v\,. \tag{4.2.14}$$

Inserting this expression in (4.2.11) yields an equation to be solved for the expansion coefficients $\alpha_k(t)$, leading for all $t \geq 0$ and $k \in \mathbb{N}$ to

$$\alpha_k'(t) + \lambda_k\, \alpha_k(t) = 0 \quad \Rightarrow \quad \alpha_k(t) = e^{-kt}\, \alpha_{\mathrm{in},k}\,, \quad \alpha_{\mathrm{in},k} := \int_{\mathbb{R}} h_{in}(v)\, H_k(v)\, \mathcal{M}(v)\, \mathrm{d}v\,. \tag{4.2.15}$$

This proposition is the starting point of numerical spectral methods. To prepare the continuous case (Proposition 4.4.2), let us remark that the expansion (4.2.14) may be written also in the equivalent Riemann-Stieltjes form

$$h(t,v) = \int_{-\infty}^{\infty} \alpha(t,\lambda)\, H_\lambda(v)\ \mathrm{d}\rho_d(\lambda)\,, \qquad \alpha(t,\lambda) = (h(t), H_\lambda)_{\mathcal{M}} = \int_{\mathbb{R}} h(t,v)\, H_\lambda(v)\, \mathcal{M}(v)\, \mathrm{d}v\,, \tag{4.2.16}$$

where ρ_d is the spectral function defined as

$$\rho_d(\lambda) := \sum_{\substack{k=0 \\ k\leqslant\lambda}}^{\infty} \frac{1}{\|H_k\|^2_{\mathcal{M}}}\,, \qquad \forall \lambda \in \mathbb{R}\,,$$

and where H_λ are defined only for $\lambda = \lambda_k$, thus almost everywhere for the measure $\mathrm{d}\rho_d(\lambda)$. The spectral function ρ_d is a step-function (*"d"* standing for discontinuous or discrete), monotonically increasing and right-continuous at the eigenvalues $\lambda_k = k$ (see Figure 4.5 for an example). The magnitude of the jumps is fixed by the normalization of the eigenvectors. The spectral function ρ_d encapsulates somehow the scaling factors of the eigenvectors, when λ is an eigenvalue.

4.2.2 Some numerical observations on the Hermite spectral scheme for case (I)

In order to construct a spectral method based on the spectral representation (4.2.14), it is obvious that one would like to have a basis set which, apart of being orthogonal and easy to compute, also yields a rapid convergence. Thus, firstly one needs to transform the Hermite polynomials in Hermite functions, as the Hermite polynomials are not convenient in practice due to their non-vanishing asymptotic behaviour at infinity. Hermite functions, defined as $\psi_k(v) := \frac{1}{\sqrt{2\,\pi}} H_k(v)\, e^{-v^2/2}$, are therefore used in numerical schemes, forming an orthonormal basis in $L^2(\mathbb{R}; \mathcal{M}^{-1}\, dv)$. Secondly, the rapid convergence can be handled with, via the introduction of a scaling parameter $\alpha \in \mathbb{R}$, which is closely related to the physical phenomenon one is studying. It is usually chosen such that in the long-time limit $t \to \infty$ lesser and lesser Hermite-basis functions are necessary in the spectral decomposition, leading in this manner to an acceleration of the numerical scheme.

After having considered these last two points, the Hermite-spectral scheme for the resolution of the evolution problem (4.2.11) is very efficient, due mainly to two reasons. Firstly, the higher the mode in (4.2.14), the faster the decay (see (4.2.15)), justifying thus a truncation at a reasonable index $N \in \mathbb{N}$ (higher precision can be of course achieved by taking a bigger N). Secondly, the associated numerical decay rate matches the theoretical decay given in (4.2.13). In other words, if h^N is given by the truncated expansion of (4.2.14) up to an order $N \in \mathbb{N}$, then one can show, remarking that $\bar{H}_k = 0$ for all $k \neq 0$, that

$$\|h^N(t) - h_\infty\|^2_{\mathcal{M}} = \|h^N(t) - \alpha_{\mathrm{in},0}\|^2_{\mathcal{M}} = \sum_{k=1}^{N} |\alpha_{\mathrm{in},k}|^2\, e^{-2\,kt} \leqslant e^{-2\,t}\, \|h^N_{\mathrm{in}} - \bar{h}_{\mathrm{in}}\|^2_{\mathcal{M}}\,. \tag{4.2.17}$$

This method is therefore very accurate for approximating the evolution problem (4.2.11), especially in the long-time asymptotics.

The second advantage of this spectral method, namely the correspondence of the theoretical and the numerical (exponential) decay rate, relies on the existence of a spectral gap. We shall see in the following examples that in the cases (II)-(IV), the operator $\mathcal{L}_{D,eq}$ features a continuous spectrum and that there is no spectral gap, leading to a more challenging problem.

4.3 Time decay of the cases (II) to (IV)

Sections 4.3 and 4.4 will be now concerned with the study of the Fokker-Planck collision operator in the cases (II)-(IV), which have the particularity of possessing a continuous spectrum, with no spectral gap. Gapless systems exhibit very particular behaviours and are very challenging from a mathematical as well as numerical point of view. Before passing to the spectral analysis, let us start in this section with the investigation of the rate of convergence

of the solution to the evolution problem

$$\begin{cases} \partial_t h = \dfrac{1}{f_{eq}}\,\partial_v\left[D(v)\,f_{eq}\,\partial_v\,h\right] =: -\mathcal{L}_{D,eq}(h) \qquad \forall (t,v)\in\mathbb{R}^+\times\mathbb{R} \\ h(0,\cdot) = h_{in}\,, \end{cases} \tag{4.3.1}$$

towards the corresponding stationary solution $h_\infty = \bar{h} := \int_{\mathbb{R}_v} h\, f_{eq}\,\mathrm{d}v$, and this in the remaining three cases (II)-(IV). For simplicity reasons, let us introduce in the rest of this paper the following notation

$$\langle v\rangle_\kappa = \sqrt{1+v^2/\kappa}\,, \qquad \langle v\rangle_{\mathcal{M}} = \sqrt{1+v^2}\,.$$

4.3.1 Study of the operator in the case (II) with $D = 1$ and $f_{eq} = f_\kappa$.

We focus now on the following evolution problem

$$\partial_t h(t,v) = \frac{1}{f_\kappa}\,\partial_v\left[\, f_\kappa\,\partial_v h\,\right], \qquad \forall (t,v)\in\mathbb{R}^+\times\mathbb{R}\,, \tag{4.3.2}$$

and the decay of h, as $t\to\infty$, towards the stationary solution h_∞, which is indeed a quantity independent on time, due to the conservation of mass property of the evolution problem (4.3.2). The considered functional space is

$$L^2_\kappa := \left\{ h\,:\,\mathbb{R}\to\mathbb{R}\ \text{ measurable}\,, \quad \int_{\mathbb{R}} |h|^2\, f_\kappa\,\mathrm{d}v < \infty \right\}, \tag{4.3.3}$$

with associated norm $\|\cdot\|_\kappa$.

Theorem 6. [BDZ23] **(Time decay for case (II))** Let h be a solution of the evolution problem (4.3.2), with an initial condition $h_{in}\in L^\infty(\mathbb{R}_v)\subset L^2_\kappa$. Then for all $0<p<2\,\kappa-1$, with $\kappa>1$, the following estimate holds

$$\|h(t)-h_\infty\|^2_\kappa \leqslant \left[\|h_{in}-\bar{h}_{in}\|_\kappa^{-4/p} + K^{II}_{p,\kappa}\,\frac{4t}{p}\right]^{-p/2}, \qquad \forall t\geq 0\,, \tag{4.3.4}$$

with $h_\infty = \bar{h} := \int_{\mathbb{R}_v} h\, f_\kappa\,\mathrm{d}v = \bar{h}_{in}$ and $K^{II}_{p,\kappa}>0$ a constant given in (4.3.11).

The proof of this theorem follows [BDZ23], and is especially based on the following Hardy-Poincaré inequality.

Lemma 13. [Bla+09] **(Hardy-Poincaré)** Let us introduce the function $\Theta_\beta(v) := \left(1+|v|^2\right)^{-\beta}$ for some $\beta>1$ and define furthermore the two measures

$$\mathrm{d}\nu := \Theta_\beta\, dv\,, \qquad \mathrm{d}\mu = \Theta_{\beta+1}\,\mathrm{d}v = \frac{1}{1+|v|^2}\,\mathrm{d}\nu\,.$$

Then there exists a positive constant $C_\beta>0$ such that

$$\int_{\mathbb{R}} |g-\tilde{g}|^2\,\mathrm{d}\mu \leqslant C_\beta \int_{\mathbb{R}} |\partial_v g|^2\,\mathrm{d}\nu\,, \qquad \forall g\in H^1(\mathbb{R},\mathrm{d}\nu)\,, \quad \tilde{g} := \int_{\mathbb{R}} g\,\mathrm{d}\mu\,. \tag{4.3.5}$$

Hardy-Poincaré inequalities can be seen as "weak Poincaré inequalities" and occur often for unbounded domains, for measures that are "not confining enough". Adapting Lemma 13 for our case, yields the following inequality for all $r \geq 0$

$$\int_{\mathbb{R}} |h(v) - \tilde{h}_r|^2 \langle v \rangle_\kappa^{-r-2} f_\kappa(v)\,\mathrm{d}v \leqslant C_{r,\kappa} \int_{\mathbb{R}} |\partial_v h(v)|^2 \langle v \rangle_\kappa^{-r} f_\kappa(v)\,\mathrm{d}v\ . \tag{4.3.6}$$

with $\tilde{h}_r := \int_{\mathbb{R}} h \langle v \rangle_\kappa^{-r-2} f_\kappa(v)\,\mathrm{d}v$ and $C_{r,\kappa} > 0$ a constant. Indeed, we used Lemma 13 with $\beta := \kappa + r/2$ and $\kappa > 1$, $\Theta_\beta(v) := \langle v \rangle_\kappa^{-r} f_\kappa$, $\mathrm{d}\nu := \Theta_\beta(v)\ \mathrm{d}v$ and $\mathrm{d}\mu = \langle v \rangle_\kappa^{-2}\ \mathrm{d}\nu$, after a change of variables.

Proof of Theorem 6. Integrating equation (4.3.2) against $h(t,v)\, f_\kappa(v)\ \mathrm{d}v$ yields

$$\frac{1}{2}\frac{\mathrm{d}}{\mathrm{d}t}\int_{\mathbb{R}} |h - \bar{h}|^2 f_\kappa\,\mathrm{d}v = -\int_{\mathbb{R}} |\partial_v h|^2 f_\kappa\,\mathrm{d}v\,, \quad \forall t \geq 0\,. \tag{4.3.7}$$

Thanks to Hardy-Poincaré's inequality (4.3.6) with $r = 0$, we can estimate (Nash-type inequality [RW01])

$$\begin{aligned}
\int_{\mathbb{R}} |h - \bar{h}|^2 f_\kappa\,\mathrm{d}v &= \inf_{c\in\mathbb{R}} \int_{\mathbb{R}} |h - c|^2 f_\kappa\,\mathrm{d}v\,, && \bar{h} := \int_{\mathbb{R}} h\, f_\kappa\,\mathrm{d}v \\
&\leqslant \int_{\mathbb{R}} |h - \tilde{h}_0|^2 f_\kappa\,\mathrm{d}v\,, && \tilde{h}_0(t) := \int_{\mathbb{R}} h(t) \langle v \rangle_\kappa^{-2} f_\kappa(v)\,\mathrm{d}v \\
&\overset{\text{Hölder}}{\leqslant} \left(\int_{\mathbb{R}} |h - \tilde{h}_0|^2 \langle v \rangle_\kappa^{-2} f_\kappa\,\mathrm{d}v\right)^{\frac{p}{p+2}} \left(\int_{\mathbb{R}} |h - \tilde{h}_0|^2 \langle v \rangle_\kappa^{p} f_\kappa\,\mathrm{d}v\right)^{\frac{2}{p+2}} \\
&\overset{(4.3.6)}{\leqslant} C_{0,\kappa}^{\frac{p}{p+2}} \left(\int_{\mathbb{R}} |\partial_v h(v)|^2 f_\kappa(v)\,\mathrm{d}v\right)^{\frac{p}{p+2}} \left(\int_{\mathbb{R}} |h - \tilde{h}_0|^2 \langle v \rangle_\kappa^{p} f_\kappa\,\mathrm{d}v\right)^{\frac{2}{p+2}}\ .
\end{aligned}$$

Plugging this into (4.3.7) yields

$$\frac{1}{2}\frac{\mathrm{d}}{\mathrm{d}t}\int_{\mathbb{R}} |h - \bar{h}|^2 f_\kappa\,\mathrm{d}v \leqslant -\frac{1}{C_{0,\kappa}} \left(\int_{\mathbb{R}} |h - \bar{h}|^2 f_\kappa\,\mathrm{d}v\right)^{\frac{p+2}{p}} \left(\int_{\mathbb{R}} |h - \tilde{h}_0|^2 \langle v \rangle_\kappa^{p} f_\kappa\,\mathrm{d}v\right)^{-\frac{2}{p}}\ . \tag{4.3.8}$$

In order to conclude, it is enough to find one $p > 0$ such that

$$\int_{\mathbb{R}} |h - \tilde{h}_0(t)|^2 \langle v \rangle_\kappa^{p} f_\kappa\,\mathrm{d}v \leqslant K_{p,\kappa}, \tag{4.3.9}$$

with some constant $K_{p,\kappa} > 0$ to be determined. This would lead to

$$\frac{1}{2}\frac{\mathrm{d}}{\mathrm{d}t}\int_{\mathbb{R}} |h - \bar{h}|^2 f_\kappa\,\mathrm{d}v \leqslant -K_{p,\kappa}^{II} \left(\int_{\mathbb{R}} |h - \bar{h}|^2 f_\kappa\,\mathrm{d}v\right)^{\frac{p+2}{p}}\ , \tag{4.3.10}$$

with $K^{II}_{p,\kappa} = \frac{1}{C_{0,\kappa}} K^{-2/p}_{p,\kappa}$ and we can finally establish (4.3.4) thanks to Gronwall's inequality.

One way to show (4.3.9) is to prove some propagation of moments estimate, namely assume that the initial condition h_{in} has bounded velocity moments, and prove then that these moments stay bounded for all times (see [BDZ23] for more details). Here, we impose a much stronger assumption on the initial data h_{in}, namely $h_{in} \in L^\infty(\mathbb{R}_v)$. Starting thus from

$$\int_{\mathbb{R}} |h - \tilde{h}_0(t)|^2 \langle v\rangle^p_\kappa \, f_\kappa \, \mathrm{d}v \leqslant \left(\int_{\mathbb{R}} \langle v\rangle^p_\kappa \, f_\kappa \, \mathrm{d}v \right) \|h - \tilde{h}_0(t)\|^2_\infty \,,$$

we remark first that the maximum principle for diffusion equations implies $\|h(t)\|_\infty \leqslant \|h_{in}\|_\infty$ for all $t > 0$, yielding

$$\|h - \tilde{h}_0(t)\|_\infty \leqslant \left(1 + \int_{\mathbb{R}} \langle v\rangle^{-2}_\kappa \, f_\kappa \, \mathrm{d}v \right) \|h_{in}\|_\infty \,.$$

Secondly, denoting the moment by

$$M_{p,\kappa} := \int_{\mathbb{R}} \langle v\rangle^p_\kappa \, f_\kappa \, \mathrm{d}v \,,$$

we remark that it is bounded for $0 < p < 2\kappa - 1$. Altogether we have (4.3.9) with

$$K_{p,\kappa} := M_{p,\kappa} \left(1 + \int_{\mathbb{R}} \langle v\rangle^{-2}_\kappa \, f_\kappa \, \mathrm{d}v \right)^2 \|h_{in}\|^2_\infty \quad \text{and} \quad K^{II}_{p,\kappa} = \frac{1}{C_{0,\kappa}} K^{-2/p}_{p,\kappa} \,. \tag{4.3.11}$$

□

4.3.2 Convergence rate in the case (III) with $D = G(v)/v$ and $f_{eq} = \mathcal{M}$.

This section focuses on the evolution problem

$$\partial_t h = \frac{1}{\mathcal{M}(v)} \, \partial_v \left[D(v) \, \mathcal{M}(v) \, \partial_v h \right] , \qquad \forall (t, v) \in \mathbb{R}^+ \times \mathbb{R} \,, \tag{4.3.12}$$

with a diffusion coefficient $D(v) = G(v)/v$ which is this time vanishing as $v \to \infty$, and with a Maxwellian equilibrium. Remark however that this diffusion coefficient is such that there exists a constant $C_d > 0$ s.t. $D(v) \geq C_d \langle v\rangle^{-3}_{\mathcal{M}}$ for large v.

Theorem 7. **(Time decay for case (III))** Let h be a solution of the evolution problem (4.3.12), with an initial condition $h_{in} \in L^\infty(\mathbb{R}_v) \subset L^2_{\mathcal{M}}$. Then the following estimate holds

$$\|h(t) - h_\infty\|^2_{\mathcal{M}} \leqslant \left[\|h_{in} - \bar{h}_{in}\|^{-6/p}_{\mathcal{M}} + K^{III}_p \, \frac{6\,t}{p} \right]^{-p/3} , \quad \forall t \geq 0 \,, \tag{4.3.13}$$

for all $p > 0$ and where $h_\infty = \bar{h} = \int_{\mathbb{R}} h\mathcal{M} \, \mathrm{d}v = \bar{h}_{in}$ and $K^{III}_p > 0$ a constant given in (4.3.17).

We have this time only a "super-algebraic decay" rate, and not an exponential one as in the standard Fokker-Planck case (see (4.2.13)), because although the functional space we are working with enjoys a Poincaré-Wirtinger inequality, the operator on the right-hand side of (4.3.12) features a vanishing diffusion coefficient, such that we need a Nash-type inequality. Let us start with the following Poincaré inequality (weighted version of (4.2.10))

Lemma 14. **(Poincaré-Wirtinger inequality)** The following Poincaré inequality holds

$$\int_{\mathbb{R}} |h-\tilde{h}|^2 \langle v\rangle_{\mathcal{M}}^{-3}\mathcal{M}\,\mathrm{d}v \leqslant C_P \int_{\mathbb{R}} |\partial_v h(v)|^2 \langle v\rangle_{\mathcal{M}}^{-3}\mathcal{M}\,\mathrm{d}v\,, \qquad \forall h\in H^1(\mathbb{R};\,\mathcal{M}dv)\,, \tag{4.3.14}$$

where $\tilde{h} := \int_{\mathbb{R}} h\langle v\rangle_{\mathcal{M}}^{-3}\mathcal{M}\,\mathrm{d}v$ and $C_P>0$ is the Poincaré constant.

Proof. To prove this Lemma, we use [Bak+08], Corollary 1.6, with $V(v) := \frac{1}{2}|v|^2 + 3\,\ln\langle v\rangle_{\mathcal{M}} + \ln(\sqrt{2\,\pi})$. □

Proof of Theorem 7. The general idea is still the same, starting with

$$\frac{1}{2}\frac{\mathrm{d}}{\mathrm{d}t}\|h(t)-\bar{h}\|_{\mathcal{M}}^2 = -\int_{\mathbb{R}} D(v)(\partial_v h)^2\,\mathcal{M}\,\mathrm{d}v \leqslant -C_d\int_{\mathbb{R}} |\partial_v h|^2\langle v\rangle_{\mathcal{M}}^{-3}\mathcal{M}\,\mathrm{d}v\,. \tag{4.3.15}$$

Now, we conclude in the same fashion as in the previous subsection, namely via

$$\begin{aligned}
\int_{\mathbb{R}} |h(t)-\bar{h}|^2\,\mathcal{M}\,\mathrm{d}v &= \inf_{c\in\mathbb{R}}\int_{\mathbb{R}} |h-c|^2\,\mathcal{M}\,\mathrm{d}v\,, && \bar{h} := \int_{\mathbb{R}} h\,\mathcal{M}\,\mathrm{d}v\\
&\leqslant \int_{\mathbb{R}} |h-\tilde{h}|^2\,\mathcal{M}\,\mathrm{d}v\,, && \tilde{h}(t) := \int_{\mathbb{R}} h(t)\langle v\rangle_{\mathcal{M}}^{-3}\mathcal{M}\,\mathrm{d}v\\
&\overset{Hoelder}{\leqslant} \left(\int_{\mathbb{R}} |h-\tilde{h}|^2\langle v\rangle_{\mathcal{M}}^{-3}\mathcal{M}\,\mathrm{d}v\right)^{\frac{p}{p+3}}\left(\int_{\mathbb{R}} |h-\tilde{h}|^2\langle v\rangle_{\mathcal{M}}^{p}\mathcal{M}\,\mathrm{d}v\right)^{\frac{3}{p+3}}\\
&\overset{(4.3.14)}{\leqslant} C_P^{\frac{p}{p+3}}\left(\int_{\mathbb{R}} |\partial_v h(v)|^2\langle v\rangle_{\mathcal{M}}^{-3}\,\mathcal{M}\,\mathrm{d}v\right)^{\frac{p}{p+3}}\left(\int_{\mathbb{R}} |h-\tilde{h}|^2\langle v\rangle_{\mathcal{M}}^{p}\mathcal{M}\,\mathrm{d}v\right)^{\frac{3}{p+3}}.
\end{aligned}$$

Now, since this time we have bounded moments for all $p>0$ (advantage of the Maxwellian equilibria)

$$M_p := \int_{\mathbb{R}} \langle v\rangle_{\mathcal{M}}^{p}\,\mathcal{M}\,\mathrm{d}v < \infty\,, \tag{4.3.16}$$

one gets for all $p>0$

$$\frac{1}{2}\frac{\mathrm{d}}{\mathrm{d}t}\|h-\bar{h}\|_{\mathcal{M}}^2 \leqslant -K_p^{III}\left(\int_{\mathbb{R}} |h-\bar{h}|^2\,\mathcal{M}\,\mathrm{d}v\right)^{\frac{p+3}{p}},$$

with

$$K_p^{III} = \frac{C_d}{C_P}\,K_p^{-3/p}\,, \qquad K_p := M_p\left(1+\int_{\mathbb{R}}\langle v\rangle_{\mathcal{M}}^{-3}\,\mathcal{M}\,\mathrm{d}v\right)^2\|h_{in}\|_{\infty}^2\,. \tag{4.3.17}$$

We can conclude the proof with Gronwall's lemma. Let us remark that one can probably improve this result, by choosing an adequate $p>0$, in order to recover a better rate of convergence (like for instance e^{-t^σ} for some $\sigma>0$). □

4.3.3 Convergence rate in the case (IV) with $D = G(v)/v$ and $f_{eq} = f_\kappa$

Finally let us consider now the more physical evolution problem

$$\partial_t h = \frac{1}{f_\kappa}\,\partial_v\left[D(v)\,f_\kappa\,\partial_v h\right], \qquad \forall (t,v)\in\mathbb{R}^+\times\mathbb{R}, \tag{4.3.18}$$

where $D(v) = G(v)/v$ and a κ-equilibrium. Again we shall use the fact that this diffusion coefficient is such that there exists a constant $C_{d,\kappa} > 0$ s.t. $D(v) \geq C_{d,\kappa}\,\langle v\rangle_\kappa^{-3}$ for large v.

Theorem 8. **(Time decay for case (IV))** Let h be a solution of the evolution problem (4.3.18), with an initial condition $h_{in} \in L^\infty(\mathbb{R}_v) \subset L^2_\kappa$. Then for all $0 < p < 2\,\kappa - 1$, with $\kappa > 1/2$, the following estimate holds

$$\|h(t) - h_\infty\|_\kappa^2 \leqslant \left[\|h_{in} - \bar{h}_{in}\|_\kappa^{-10/p} + K^{IV}_{p,\kappa}\frac{10\,t}{p}\right]^{-p/5}, \quad \forall t \geq 0, \tag{4.3.19}$$

where $h_\infty = \bar{h} := \int_{\mathbb{R}} h\,f_\kappa\,\mathrm{d}v = \bar{h}_{in}$ and $K^{IV}_{p,\kappa} > 0$ a constant given in (4.3.21).

Proof of Theorem 8. The proof is given by the same technique as before. Starting again from the inequality

$$\frac{1}{2}\frac{\mathrm{d}}{\mathrm{d}t}\|h-\bar{h}\|_\kappa^2 = -\int_{\mathbb{R}} D(v)(\partial_v h)^2\,f_\kappa\,\mathrm{d}v \leqslant -C_{d,\kappa}\int_{\mathbb{R}}|\partial_v h|^2\,\langle v\rangle_\kappa^{-3}\,f_\kappa\,\mathrm{d}v, \tag{4.3.20}$$

and using Hardy-Poincare's inequality (4.3.6) with $r = 3$ ($\kappa > 1/2$ possible here), permits to conclude in the same fashion as in the previous subsection, via

$$\begin{aligned}
\int_{\mathbb{R}}|h-\bar{h}|^2\,f_\kappa\,\mathrm{d}v &= \inf_{c\in\mathbb{R}}\int_{\mathbb{R}}|h-c|^2\,f_\kappa\,\mathrm{d}v, && \bar{h} := \int_{\mathbb{R}} h\,f_\kappa\,\mathrm{d}v\\
&\leqslant \int_{\mathbb{R}}|h-\tilde{h}_3|^2\,f_\kappa\,\mathrm{d}v, && \tilde{h}_3(t) := \int_{\mathbb{R}} h(t)\,\langle v\rangle_\kappa^{-5}\,f_\kappa(v)\,\mathrm{d}v\\
&\overset{Hoelder}{\leqslant} \left(\int_{\mathbb{R}}|h-\tilde{h}_3|^2\,\langle v\rangle_\kappa^{-5}\,f_\kappa\,\mathrm{d}v\right)^{\frac{p}{p+5}}\left(\int_{\mathbb{R}}|h-\tilde{h}_3|^2\,\langle v\rangle_\kappa^{p}\,f_\kappa\,\mathrm{d}v\right)^{\frac{5}{p+5}}\\
&\overset{(4.3.6)}{\leqslant} C_{3,\kappa}^{\frac{p}{p+5}}\left(\int_{\mathbb{R}}|\partial_v h(v)|^2\,\langle v\rangle_\kappa^{-3}\,f_\kappa(v)\,\mathrm{d}v\right)^{\frac{p}{p+5}}\left(\int_{\mathbb{R}}|h-\tilde{h}_3|^2\,\langle v\rangle_\kappa^{p}\,f_\kappa\,\mathrm{d}v\right)^{\frac{5}{p+5}}.
\end{aligned}$$

Thus one gets

$$\frac{1}{2}\frac{\mathrm{d}}{\mathrm{d}t}\|h-\bar{h}\|_\kappa^2 \leqslant -K^{IV}_{p,\kappa}\left(\int_{\mathbb{R}}|h-\bar{h}|^2\,f_\kappa\,\mathrm{d}v\right)^{\frac{p+5}{p}},$$

with

$$K^{IV}_{p,\kappa} = \frac{C_{d,\kappa}}{C_{3,\kappa}}\,K_{p,\kappa}^{-5/p}, \qquad K_{p,\kappa} := M_{p,\kappa}\left(1+\int_{\mathbb{R}}\langle v\rangle_\kappa^{-5}\,f_\kappa\,\mathrm{d}v\right)^2\|h_{in}\|_\infty^2. \tag{4.3.21}$$

Gronwall's lemma permits then to get the desired decay rate. □

4.4 Spectral analysis of the cases (II) to (IV)

In this section, we show that the spectrum of the operator $\mathcal{L}_{D,eq}$ is continuous, with eigenvalue $\lambda = 0$ as an accumulation point. The spectral investigation is based on the transformation of the Fokker-Planck operator into an associated Schrödinger operator through a change of variable, so-called *Liouville transformation*. This transformation permits to reduce the number of parameters from two, namely the diffusion-coefficient and the drift-potential (D, U), to only one parameter, namely the potential Q. We deduce then the spectral properties of our operator, along with the associated spectral representation formula, from well-known Schrödinger-operator theory [CR21; Lav73; RS72].

4.4.1 Liouville transformation and Schrödinger form of the Fokker-Planck operator

Let us rewrite the equilibria for the four cases (I)-(IV) via a well-chosen potential U as follows

$$f_{eq} := \alpha\, e^{-U(v)}\,, \qquad \forall v \in \mathbb{R}\,,$$

with $\alpha > 0$ a normalization constant. Then the Fokker-Planck eigenvalue problem

$$-\partial_v \left[D(v)\, f_{eq}\, \partial_v \left(\frac{f}{f_{eq}} \right) \right] = \lambda\, f\,, \qquad \lambda \in \mathbb{C}\,, \qquad \forall v \in \mathbb{R}\,, \tag{4.4.1}$$

can be transformed into the following Schrödinger eigenvalue problem

$$-\partial_{ss} g + Q(v(s))\, g = \lambda\, g\,, \qquad \lambda \in \mathbb{C}\,, \qquad \forall s \in \mathbb{R}\,. \tag{4.4.2}$$

To do this, we performed the change of variable $v \leftrightarrow s$

$$v'(s) = \frac{\mathrm{d}}{\mathrm{d}s} v(s) = \sqrt{D(v(s))}\,, \tag{4.4.3}$$

along with the functional transformation $g(s) := \wp(s)\, h(v(s)) = \wp(s)\, f(v(s))/f_{eq}(v(s))$, where

$$\wp(s) := \{D(v(s))\}^{1/4} \{f_{eq}(v(s))\}^{1/2}\,, \quad \forall s \in \mathbb{R}\,. \tag{4.4.4}$$

The potential $Q(v(s)) := \frac{\wp''(s)}{\wp(s)}$ occurring in the Schrödinger eigenvalue problem (4.4.2) is given by

$$Q(v) := \frac{D''(v)}{4} - \frac{(D'(v))^2}{16\, D(v)} - \frac{1}{2} D'(v)\, U'(v) + D(v) \left[\frac{1}{4} (U'(v))^2 - \frac{1}{2} U''(v) \right]. \tag{4.4.5}$$

The next subsections summarize these transformations in the particular cases (II) to (IV).

4.4.1.1 Schrödinger form in case (II)

In the case $D \equiv 1$ and $f_{eq} = f_\kappa$, the previous transformations writes $f = g\sqrt{f_\kappa}$, where

$$U(v) = \kappa \ln\left(1 + \frac{|v|^2}{\kappa}\right), \tag{4.4.6}$$

$$D(v) = 1, \qquad v(s) = s. \tag{4.4.7}$$

The potential $Q(v)$ is given by

$$Q(v) := \frac{|U'(v)|^2}{4} - \frac{1}{2}U''(v) = \frac{1}{\langle v\rangle^4}\left(\left[\frac{1}{\kappa}+1\right]v^2 - 1\right). \tag{4.4.8}$$

As a consequence one has the asymptotic behaviour, where we recall that $\sim$ stands for the asymptotic equivalence

$$Q(v) \sim \kappa^2 \frac{(\frac{1}{\kappa}+1)}{v^2}, \qquad \text{as } v \to \pm\infty.$$

4.4.1.2 Schrödinger form in case (III)

In the case $D(v) = G(v)/v$ and $f_{eq} = \mathcal{M}$, the previous procedure leads to

$$U(v) = v^2/2, \tag{4.4.9}$$

$$v'(s) = \frac{\mathrm{d}}{\mathrm{d}s}v(s) = \sqrt{D(v(s))}, \qquad v(s) \sim \left(\frac{5}{2\sqrt{2}}\right)^{2/5} s^{2/5} \qquad \text{as } s \to +\infty. \tag{4.4.10}$$

Here the potential $Q(v)$ is given by

$$Q(v) := \frac{D''(v)}{4} - \frac{(D'(v))^2}{16\,D(v)} - \frac{1}{2}D'(v)\,v + D(v)\left[\frac{1}{4}v^2 - \frac{1}{2}\right], \tag{4.4.11}$$

and as a consequence, we have asymptotically

$$Q(v) \sim \frac{1}{8\,|v|}, \qquad \text{as } v \to \pm\infty,$$

and we plotted $Q(v(s))$ on Figure 4.3 to visualize the potential occurring in the Schrödinger operator.

4.4.1.3 Schrödinger form in case (IV)

In the case $D(v) = G(v)/v$ and $f_{eq} = f_\kappa$, the Liouville transformation leads to

$$U(v) = \kappa \ln\left(1 + \frac{|v|^2}{\kappa}\right), \tag{4.4.12}$$

$$v'(s) = \frac{\mathrm{d}}{\mathrm{d}s}v(s) = \sqrt{D(v(s))}, \qquad v(s) \sim \left(\frac{5}{2\sqrt{2}}\right)^{2/5} s^{2/5}, \qquad \text{as } s \to +\infty. \tag{4.4.13}$$

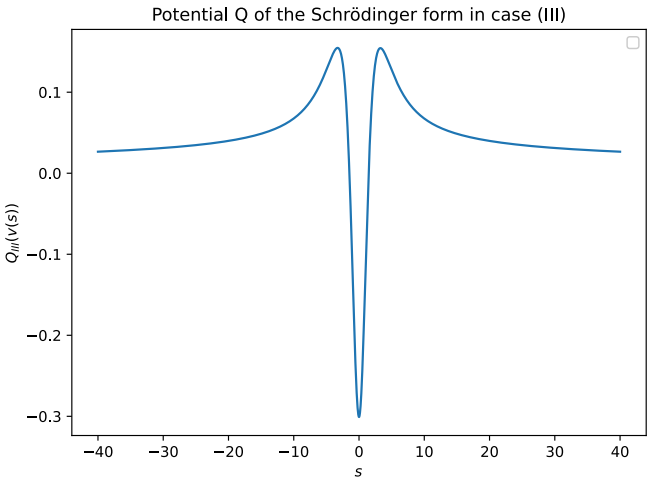

Figure 4.3 – Plot of the potential $Q(v(s))$ in case (III), with respect to the variable s.

Here the potential $Q(v)$ is given by

$$Q(v) := \frac{D''(v)}{4} - \frac{(D'(v))^2}{16\,D(v)} - \frac{v\,D'(v)}{\langle v\rangle^2} + \frac{D}{\langle v\rangle^4}\left(\left[\frac{1}{\kappa}+1\right]v^2 - 1\right). \tag{4.4.14}$$

As a consequence,

$$Q(v) \sim \frac{1}{|v|^5}\left[\frac{\kappa^2}{2}\left(\frac{1}{\kappa}+1\right) + \frac{3\,\kappa}{2} + \frac{39}{32}\right], \qquad \text{as } v \to \pm\infty,$$

with again a representation of $Q(v(s))$ given on Figure 4.4.

4.4.2 Spectrum and spectral representation

From this reduction to a Schrödinger form, one can deduce now information on the spectrum of the Fokker-Planck operator, applying the spectral theory of Quantum Mechanics. This shall permit in a second step to study in more details the evolution problem

$$\begin{cases} \partial_t h = \frac{1}{f_{eq}}\,\partial_v\left[D(v)\,f_{eq}\,\partial_v\,h\right] = -\mathcal{L}_{D,eq}(h) & \forall (t,v)\in\mathbb{R}^+\times\mathbb{R} \\ h(0,\cdot) = h_{in}\,. \end{cases} \tag{4.4.15}$$

Taking a look at the potentials plotted in Figures 4.3-4.4, one expects that the Fokker-Planck operator possesses a continuous spectrum $[0,\infty)$, as shown in the next proposition.

Proposition 4.4.1. **(Spectrum of $\mathcal{L}_{D,eq}$)** In each of the cases (II)-(IV), the operator $\mathcal{L}_{D,eq}$ is self-adjoint, positive and its spectrum consists of the set

$$\sigma(\mathcal{L}_{D,eq}) = \sigma_{ess}(\mathcal{L}_{D,eq}) = [0,+\infty)\,. \tag{4.4.16}$$

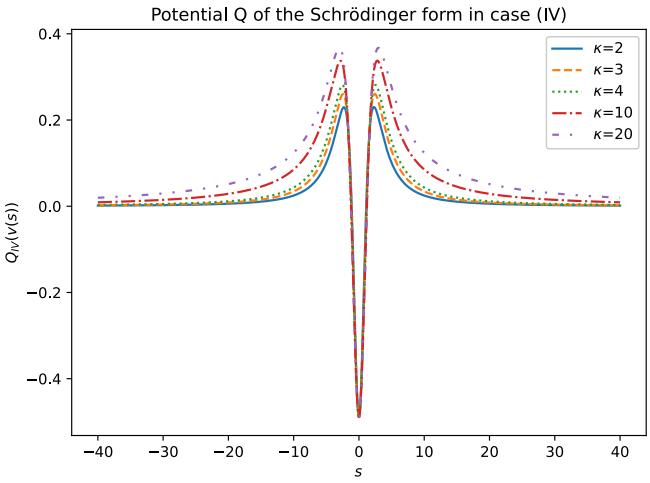

Figure 4.4 – Plot of the potential $Q(v(s))$ in case (IV), with respect to the variable s, and for several values of κ.

Furthermore, it comprises an eigenvalue $\lambda = 0$ and an absolute continuous part

$$\sigma_{pp}(\mathcal{L}_{D,eq}) = \{0\}\,, \qquad \sigma(\mathcal{L}_{D,eq}) = \sigma_{ac}(\mathcal{L}_{D,eq}) \cup \sigma_{pp}(\mathcal{L}_{D,eq}) = [0, +\infty)\,. \tag{4.4.17}$$

Proof. The proof of this theorem is based on standard arguments, scattered a little bit in literature. For completeness, we detailed this proof, but postponed it to the Appendix, in order not to interrupt the flow of the lecture. □

The spectral representation of the solution to (4.4.15) is more intricate in cases (II)-(IV) than the one of the standard case (I), (4.2.14), given the fact that the operators posses now a continuous spectrum. Points in the continuous spectrum can be associated with generalized eigenfunctions, which solve the corresponding Sturm-Liouville eigenvalue problem, however do not belong anymore to the considered Hilbert-space L^2_{eq}. However, similar to the Fourier-transform, one can give a spectral representation of solutions to (4.4.15) in terms of these generalized eigenfunctions and so-called *spectral functions* $\rho(\lambda)$, as mentioned in the next proposition. The interested reader can refer to [CL55; Pea88] for a complete introduction to this topic.

Proposition 4.4.2. [CL55] **(Spectral representation in the continuous cases)** The solution of the evolution problem (4.4.15) can be expanded for all $(t, v) \in \mathbb{R}^+ \times \mathbb{R}$ as follows

$$h(t,v) = \sum_{l,j=0}^{1} \int_{[0,\infty)} \mathfrak{A}_l(t,\lambda)\, \varphi_j(v,\lambda)\, \mathrm{d}\rho_{lj}(\lambda)\,, \qquad \mathfrak{A}_l(t,\lambda) := \int_{\mathbb{R}} h(t,v)\, \varphi_l(v,\lambda)\, f_{eq}(v)\, \mathrm{d}v\,, \tag{4.4.18}$$

where $\{\varphi_l(\cdot,\lambda)\}_{l=0}^1$ are two linearly independent, generalized eigenfunctions of $\mathcal{L}_{D,eq}$ (see (4.4.19)-(4.4.20)), belonging to $C^\infty(\mathbb{R}\times\mathbb{R}^+)$ and corresponding to the generalized eigenvalue $\lambda\in\mathbb{R}^+$, and $\{\rho_{lj}(\lambda)\}_{l,j=0}^1$ is a positive, symmetric spectral matrix, necessarily linked to the chosen generalized eigenfunctions. The coefficients $\mathfrak{A}(t,\lambda) := (\mathfrak{A}_0,\mathfrak{A}_1)^T(t,\lambda)$ are said to be the spectral transform of h, *i.e.*

$$h(t,\cdot)\in L^2_{eq} \longrightarrow \mathfrak{A}(t,\cdot)\in\mathcal{H}\,,\quad \forall t\geq 0\,,$$

where $\mathcal{H}$ is the Hilbert-space of vector-valued functions, measurable with respect to the Lebesgue-Stieltjies measure defined by ρ, and is given by

$$\mathcal{H} := \{(\zeta_1,\zeta_2)\,:\,\mathbb{R}^+\to\mathbb{R}^2\ /\ \sum_{l,j=0}^{1}\int_{[0,\infty)}\zeta_l(\lambda)\,\zeta_j(\lambda)\,\mathrm{d}\rho_{lj}(\lambda)<\infty\}\,.$$

This last Proposition deserves several remarks.

Remark 9. Let us underline that the integral in the decomposition of $h(t,v)$ in (4.4.18) has to be understood as a Lebesgue-Stieltjes integral, involving a Stieltjes measure $\mathrm{d}\rho$ which is obtained from an increasing, right-continuous function ρ which assigns to a half-open interval $(a,b]$ the measure $\mathrm{d}\rho((a,b]) = \rho(b)-\rho(a)$. The use of half-open integrals is significant here, because a Lebesgue-Stieltjes measure may allocate non-zero values to single points. Furthermore, let us also observe that in the case ρ is an absolute-continuous function, one has $\mathrm{d}\rho(\lambda) = \rho'(\lambda)\,\mathrm{d}\lambda$.

Remark 10. The decomposition (4.4.18) is very similar to a Fourier transformation. When compared to the discrete spectral decomposition (4.2.14), one remarks that the summation has been now replaced by an integration over the continuous spectrum, the eigenfunctions are now replaced by generalized eigenfunctions, which are not any more belonging to the Hilbert-space L^2_{eq} (in the Fourier case, these functions are trigonometric functions). Probably the main difference comes from the occurrence of the spectral density matrix, which accounts somehow for the normalization of the generalized eigenfunctions, and contains four terms, due to the fact that we are working on the whole velocity-space, thus with two singular end-points $v=\pm\infty$.

Remark 11. The expression of the spectral coefficients $\mathfrak{A}_l$ in (4.4.18) is simply obtained by introducing this decomposition into the evolution equation and solving the obtained equations for $\mathfrak{A}_l$, leading thus for all $t>0$ and $\lambda\geq 0$ to (compare with (4.2.15))

$$\mathfrak{A}_l(t,\lambda) = e^{-\lambda\,t}\,\mathfrak{A}_{in,l}(\lambda)\,,\qquad \mathfrak{A}_{in,l}(\lambda) = \int_{\mathbb{R}} h_{in}(v)\,\varphi_l(v,\lambda)\,f_{eq}(v)\,\mathrm{d}v\,.$$

The most difficult part in computing the solution $h(t,v)$ of (4.4.15) via the spectral representation (4.4.18), is the determination of the spectral density measures $\{\mathrm{d}\rho_{lj}(\lambda)\}_{l,j=0}^1$ and the corresponding generalized eigenfunctions $\{\varphi_l(\cdot,\lambda)\}_{l=0}^1$. Let us thus say now some more words about the delicate mathematical choice or numerical computation of these quantities. The following next two sections are rather technical, however important to understand the main idea of the LEAS numerical method proposed in this paper, Section 4.5.

4.4.2.1 Titchmarsh-Weyl approach [CL55]

The Titchmarsh-Weyl strategy is often used to evaluate the spectral function via a correct normalization of the generalized eigenfunctions. This is done in the following manner. Let us introduce two functions $\varphi_0(\cdot,\eta), \varphi_1(\cdot,\eta) \in C^\infty(\mathbb{R})$ as being the fundamental solution set of the following Sturm-Liouville problem

$$\mathcal{L}_{D,eq}\,\varphi = \eta\,\varphi\,, \qquad \forall \eta \in \mathbb{C}\,, \tag{4.4.19}$$

associated with the following conditions in $v = 0$

$$\begin{cases} \varphi_0(0,\eta) & = 1 \\ D(0)\,\varphi_0'(0,\eta) & = 0 \end{cases}, \qquad \begin{cases} \varphi_1(0,\eta) & = 0 \\ D(0)\,\varphi_1'(0,\eta) & = 1 \end{cases}, \quad \forall \eta \in \mathbb{C}\,. \tag{4.4.20}$$

We underline that these two linearly independent solutions are fixed through the specific condition in $v = 0$ and can be considered as weak or generalized eigenfunctions of the Sturm-Liouville problem.

Starting from these two functions, one can compute the so-called *Titchmarsh-Weyl m-function* of the problem at the infinite boundaries, namely for $v = \pm\infty$, as follows

$$m_{\pm\infty}(\lambda + i\varepsilon) := -\lim_{v\to\pm\infty} \frac{\varphi_0(v,\lambda+i\,\varepsilon)}{\varphi_1(v,\lambda+i\,\varepsilon)}, \qquad \forall \lambda \in \mathbb{R}\,, \quad \forall \varepsilon \in \mathbb{R}^*\,. \tag{4.4.21}$$

We want to emphasize that the previous definition only holds for complex, non-real numbers and that this limit exists because $\mathcal{L}_{D,eq}$ is in the limit-point case in $v = \pm\infty$ [CL55].

These complex coefficients $m_{\pm\infty}(\lambda + i\varepsilon)$ and their boundary values on the real axis (as $\varepsilon \to 0+$) are the main building blocks in the computation of the spectral matrix $\{\rho_{lj}(\lambda)\}_{l,j=0}^{1}$ occurring in Proposition 4.4.2. To see this, let us define the matrix $M(\eta) := \{M_{lj}(\eta)\}_{l,j\in\{0,1\}}$ in terms of $m_{\pm\infty}$ as follows

$$M(\eta) := \frac{1}{m_{-\infty}(\eta) - m_{+\infty}(\eta)} \begin{pmatrix} 1 & \dfrac{m_{-\infty}(\eta)+m_{+\infty}(\eta)}{2} \\ \dfrac{m_{-\infty}(\eta)+m_{+\infty}(\eta)}{2} & m_{-\infty}(\eta)\,m_{+\infty}(\eta) \end{pmatrix}, \qquad \forall \eta \in \mathbb{C}\setminus\mathbb{R}\,. \tag{4.4.22}$$

This matrix enables finally to define 4 real-valued Stieltjes measures $\mathrm{d}\rho_{lj}$, generated by some functions $\{\rho_{lj}\}_{l,j=0}^{1}$, which are right-continuous, defined up to an additive constant and of bounded total variation on every finite interval of $\mathbb{R}$ [CL55]. To be more precise, at all continuity points λ of ρ_{lj} (meaning λ is not eigenvalue of $\mathcal{L}_{D,eq}$), and for $\lambda > \mu$ one has

$$\mathrm{d}\rho_{lj}((\mu,\lambda]) = \rho_{lj}(\lambda) - \rho_{lj}(\mu) = \frac{1}{\pi}\lim_{\varepsilon\to 0+}\int_\mu^\lambda \mathrm{Im}\left(M_{lj}(\tau+i\,\varepsilon)\right)\,\mathrm{d}\tau\,, \quad \forall l,j = 0,1\,. \tag{4.4.23}$$

At eigenvalues $\lambda = \lambda_k$, the density function $\rho_{lj}(\lambda)$ is discontinuous, with a jump defined by

$$\mathrm{d}\rho_{lj}(\{\lambda_k\}) = \rho_{lj}(\lambda_k) - \rho_{lj}(\lambda_k^-) = r_{lk}\,r_{jk}\,, \qquad \forall l,j = 0,1\,,$$

where $\{r_{lk}\}_{k\in\mathbb{N},l\in\{0,1\}}$ are the coefficients of the decomposition of the eigenfunction $\phi_{\lambda_k}(v)$ in the fundamental basis, namely

$$\phi_{\lambda_k}(v) = r_{0k}\,\varphi_0(v,\lambda_k) + r_{1k}\,\varphi_1(v,\lambda_k)\,, \qquad \forall v\in\mathbb{R}\,.$$

Notice that $\mathrm{d}\rho_{0,1} = \mathrm{d}\rho_{1,0}$ because of the symmetry of the matrix M.

Remark 12. Since, in our case, both $D(v)$ and $f_{eq}(v)$ are even functions, we conclude that φ_0 is even and φ_1 is odd. Therefore, using (4.4.21), the following equality holds true

$$m_{-\infty}(\eta) = -m_{+\infty}(\eta)\,, \qquad \forall \eta\in\mathbb{C}\setminus\mathbb{R}\,. \tag{4.4.24}$$

This results in a diagonal matrix M, thus simplifying the computations. However, since we develop a general method for any Fokker-Planck equation (a priori with non-even coefficients), we do not assume M to be diagonal in the rest of the paper.

To separate the eigenvalue $\lambda = 0$ from the absolute continuous spectrum in (4.4.18), we recall that the Lebesgue decomposition theorem [CR21; RS72] permits to separate the Stieltjes measure $\mathrm{d}\rho_{lj}$ in a unique way as

$$\mathrm{d}\rho_{lj} = \mathrm{d}\rho_{lj,pp} + \mathrm{d}\rho_{lj,ac} + \mathrm{d}\rho_{lj,sc}\,,$$

these three measures corresponding to the pure point, absolute continuous and singular continuous spectrum. Now we know that:

- $\mathcal{L}_{D,eq}$ has no singular continuous spectrum (See Proposition 4.4.1);
- The pure point spectrum of $\mathcal{L}_{D,eq}$ contains the only eigenvalue $\lambda = 0$, associated with the eigenfunction $\varphi_0(0,v)\equiv 1$, which is of norm 1 in L^2_{eq}. Therefore, the pure point component of the measure $\mathrm{d}\rho_{lj}$ is given by

$$\mathrm{d}\rho_{lj,pp} = \begin{cases} \mathrm{d}\delta_0\,, & \text{if } l=j=0 \\ 0\,, & \text{else} \end{cases}\,, \qquad \mathrm{d}\delta_0 \text{ being the Dirac measure in } \lambda=0\,; \tag{4.4.25}$$

- Concerning the absolute continuous spectrum, we know from [Pea88] that for almost every $\lambda\in\mathbb{R}$, the limit $\lim_{\varepsilon\to 0^+} M(\lambda+i\varepsilon)$ exists and that the functions $\rho_{lj,ac}$ are differentiable at λ. Thus one has $\mathrm{d}\rho_{lj,ac} = \rho'_{lj,ac}\,\mathrm{d}\lambda$ and we can define the spectral density matrix

$$P(\lambda) := (\rho'_{lj}(\lambda))_{l,j\in\{0,1\}} = \frac{1}{\pi}\lim_{\varepsilon\to 0^+}\operatorname{Im} M(\lambda+i\,\varepsilon)\,, \quad \text{for a.e } \lambda>0\,. \tag{4.4.26}$$

With all these informations, let us introduce now the following vectors and matrices

$$\Phi(v,\lambda) = \begin{pmatrix}\varphi_0(v,\lambda)\\ \varphi_1(v,\lambda)\end{pmatrix}\,, \qquad \mathfrak{A}(t,\lambda) := \begin{pmatrix}\mathfrak{A}_0(t,\lambda)\\ \mathfrak{A}_1(t,\lambda)\end{pmatrix}\,, \qquad P(\lambda) := \left(\rho'_{lj}(\lambda)\right)_{l,j=0}^{1}\,, \tag{4.4.27}$$

which shall permit to write the spectral representation (4.4.18) in a more concise manner

$$h(t,v) = \mathfrak{A}_0(t,0) + \int_0^{+\infty} \mathfrak{A}(t,\lambda)^T\, P(\lambda)\, \Phi(v,\lambda)\, \mathrm{d}\lambda\,, \tag{4.4.28}$$

where again for all $t > 0$ and $\lambda \geq 0$ one has

$$\mathfrak{A}_l(t,\lambda) = e^{-\lambda\, t}\, \mathfrak{A}_{in,l}(\lambda)\,, \qquad \mathfrak{A}_{in,l}(\lambda) = \int_{\mathbb{R}} h_{in}(v)\, \varphi_l(v,\lambda)\, f_{eq}(v)\, \mathrm{d}v\,. \tag{4.4.29}$$

Let us underline that the first term on the right-hand side in (4.4.28) corresponds to the only eigenvalue $\lambda = 0$, whereas the integral term browses over the whole continuous spectrum. Notice that this integral term vanishes as $t \to \infty$, thus emphasizing the convergence of h towards the steady state $\bar{h}$. If there were a spectral gap, it would be apparent from (4.4.28)-(4.4.29) that this convergence of h is exponential as $t \to +\infty$, however this does not hold true in the cases (II)-(IV). The time decay (for $t \to \infty$) of the evolution semigroup is intimately connected to the asymptotics of $P(\lambda)$ in the limit $\lambda \to 0^+$, asymptotics which is widely studied in literature and shall be exploited in Section 4.5, in order to develop a numerical method that preserves the spectral structure of the Fokker-Planck operator in this $\lambda \to 0^+$ regime.

In practice it is rare to find explicit expressions for the fundamental solutions φ_0, φ_1 as well as for the spectral densities $\rho'_{lj}(\lambda)$ in order to use the spectral representation (4.4.18) in a simple manner, similar to a Fourier transform. There exist however papers in literature which use this Titchmarsh-Weyl theory in conjunction with a numerical computation of these quantities $(\varphi_0, \varphi_1, \rho'_{lj})$, see [WC15]. Our approach is different, similar to [PF93] and based rather on the truncation of the velocity domain and the introduction of a subsequent correction term.

4.4.2.2 Numerical approach

A numerical approach for the computation of the spectral function $\rho_{lj}(\lambda)$ and the subsequent resolution of (4.4.15) is based on the idea of truncating the domain at $v = \pm L$ for large $L \gg 1$, representing then the solution in terms of the corresponding orthonormal eigenfunctions (discrete spectral theorem), computing the step spectral functions $\rho^L_{lj}(\lambda)$ and passing finally to the limit $L \to \infty$. The passage to the limit is not so trivial, and is possible if the generalized eigenfunctions are chosen and normalized in a specific manner, given by Titchmarsh-Weyl's approach, presented above.

Let us first truncate the velocity domain and consider the following evolution problem

$$\begin{cases} \partial_t h^L = -\mathcal{L}_{D,eq}(h^L)\,, \qquad \forall (t,v) \in \mathbb{R}^+ \times (-L,L)\,, \\ \partial_v h^L(t,-L) = \partial_v h^L(t,L) = 0 \\ h^L(0,\cdot) = h^L_{in}\,, \end{cases} \tag{4.4.30}$$

where h_{in}^L is a regularization of the initial condition, such that it satisfies the homogeneous Neumann boundary conditions and that $h_{in}^L \to_{L\to\infty} h_{in}$ in a certain sense. Domain truncation regularizes the Sturm-Liouville problem (the resolvant of the self-adjoint operator becoming now compact) and renders the spectrum discrete. The discreteness of the spectrum enables then a simple expansion of the solution in the eigenfunction basis.

Let thus $\{\lambda_k^L\}_{k\in\mathbb{N}} \subset \mathbb{R}^+$ be the increasing sequence of eigenvalues of the following positive, self-adjoint Sturm-Liouville problem, considered in the Hilbert-space $L^2((-L,L); f_{eq}\ \mathrm{d}v)$:

$$\begin{cases} \mathcal{L}_{D,eq}(\phi) = \lambda\,\phi\,, & \forall v \in (-L,L)\,, \\ \phi'(-L) = \phi'(L) = 0\,, \end{cases} \tag{4.4.31}$$

and $\{\phi_k^L\}_{k\in\mathbb{N}} \subset L^2((-L,L); f_{eq}\ \mathrm{d}v))$ be the associated sequence of orthonormal eigenfunctions. Notice that the boundary conditions have been chosen so that $\lambda_0^L = 0$ is indeed an eigenvalue, associated with a constant solution ϕ_0^L of norm 1 in $L^2((-L,L); f_{eq}\ \mathrm{d}v))$. The general solution h^L of (4.4.30) can thus be represented via the discrete spectral theorem (compare with (4.2.14)) for all $(t,v) \in \mathbb{R}^+ \times \mathbb{R}$ as

$$h^L(t,v) = \alpha_0^L\,\phi_0^L + \sum_{k=1}^{\infty} \alpha_k^L(t)\,\phi_k^L(v)\,, \quad \alpha_k^L(t) = e^{-\lambda_k^L t}\,\alpha_{\mathrm{in},k}^L\,, \quad \alpha_{\mathrm{in},k}^L := \int_{-L}^{L} h_{in}^L(v)\,\phi_k^L(v)\,f_{eq}(v)\,\mathrm{d}v. \tag{4.4.32}$$

This representation is however not adapted to pass to the limit $L \to \infty$, as the normalized eigenfunctions $\phi_k^L(v)$ could not converge towards the non-normalized generalized eigenfunctions. To overcome this difficulty, one considers the fundamental basis functions $\varphi_0(\cdot,\lambda),\ \varphi_1(\cdot,\lambda) \in C^\infty(\mathbb{R})$ as defined in (4.4.19)-(4.4.20). Due to their linear independence, we decompose the eigenfunctions $\phi_k^L(v)$ in this basis set and find scalars $r_{0,k}^L,\ r_{1,k}^L \in \mathbb{R}$ verifying

$$\phi_k^L(\cdot) = r_{0,k}^L\,\varphi_0(\cdot,\lambda_k) + r_{1,k}^L\,\varphi_1(\cdot,\lambda_k)\,, \qquad \forall k \in \mathbb{N}, \quad \forall L > 0\,. \tag{4.4.33}$$

Inserting this expression of ϕ_k^L into (4.4.32) yields the following representation

$$h^L(t,v) = \alpha_0^L\,\phi_0^L + \sum_{l,j=0}^{1}\sum_{k=1}^{\infty} \mathfrak{A}_l^L(t,\lambda_k)\,\varphi_j(v,\lambda_k)\,r_{l,k}^L\,r_{j,k}^L\,,$$
$$\mathfrak{A}_l^L(t,\lambda) := \int_{-L}^{L} h^L(t,v)\,\varphi_l(v,\lambda)\,f_{eq}(v)\ \mathrm{d}v\,.$$

This expansion can be reformulated as follows

$$h^L(t,v) = \alpha_0^L\,\phi_0^L + \sum_{l,j=0}^{1} \int_{(0,+\infty)} \mathfrak{A}_l^L(t,\lambda)\,\varphi_j(v,\lambda)\ \mathrm{d}\rho_{lj}^L(\lambda)\,, \tag{4.4.34}$$

where $\rho_{lj}^L(\lambda)$ is simply defined by

$$\rho_{lj}^L(\lambda) := \sum_{\substack{k\in\mathbb{N} \\ \lambda_k \leqslant \lambda}} r_{l,k}^L\,r_{j,k}^L\,, \qquad \forall l,j = 0,1\,, \tag{4.4.35}$$

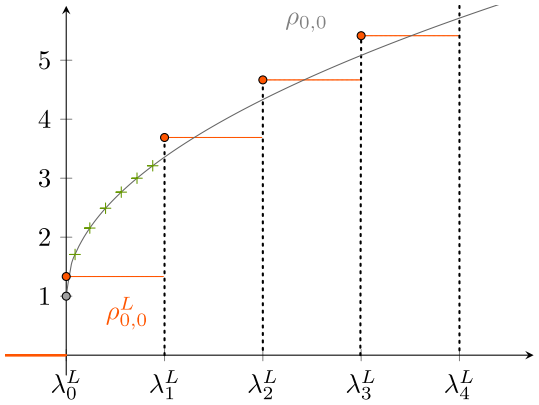

Figure 4.5 – Sketch of the behaviour of the spectral function $\rho_{0,0}$ (in grey) as a function of λ. The approached density $\rho^L_{0,0}$ (in orange) is right-continuous. In green (+) is the part of $\rho_{0,0}$ that is misrepresented, leading to a numerical spectral gap.

and is a right-continuous step-function, constant in the intervals $[\lambda_{k-1}, \lambda_k)$ and with a jump discontinuity at the eigenvalues λ_k.

The fact that we decomposed $h^L(t,v)$ in the non-normalized eigenfunctions $\{\varphi_0(\cdot,\lambda),\ \varphi_1(\cdot,\lambda)\}$, rather than in the more natural normalized basis-functions $\{\phi^L_k(v)\}_{k\in\mathbb{N}}$ shall permit, via Titchmarsh-Weyl's theory, to pass to the limit $L \to \infty$ and to derive the continuous representation framework. Indeed one can show the following convergence at points of continuity of $\rho_{lj}(\lambda)$ [CL55]

$$\rho^L_{lj}(\lambda) \longrightarrow_{L\to+\infty} \rho_{lj}(\lambda)\,, \qquad \forall l,j = 0,1\,, \tag{4.4.36}$$

where $\rho_{lj}(\lambda)$ was defined in (4.4.23). Sketches of $\rho_{0,0}$ and the approaching step function $\rho^L_{0,0}$ were represented in Figure 4.5. The discrete spectral representation (4.4.32) is a good approximation of the continuous spectral decomposition (4.4.18), for large domain truncations $L \gg 1$. However domain truncation always introduces a spectral gap, which governs the long-time behaviour of the solution and besides, from a practical point of view, taking too large $L \gg 1$ can be very time and memory consuming. The aim of the next section is to show how to cope with this new difficulty.

4.5 Low Energy Accurate numerical Scheme

We start this section by briefly reviewing the existent numerical methods for the resolution of an evolution problem of the type

$$\begin{cases} \partial_t h = \frac{1}{f_{eq}}\,\partial_v\left[D(v)\,f_{eq}\,\partial_v\,h\right] = -\mathcal{L}_{D,eq}(h)\,, \qquad \forall (t,v)\in\mathbb{R}^+\times\mathbb{R}\,, \\ h(0,\cdot) = h_{in}\,, \end{cases} \tag{4.5.1}$$

where the operator $\mathcal{L}_{D,eq}$ possesses a gapless, continuous spectrum. One of our main interests is to explore how standard methods fail to correctly describe the long-time behaviour of such problems. Indeed, when one is interested in accurately describing the long-time asymptotics, the behaviour of the small energy-modes is very important, as they dominate this long-time regime. Indeed, due to the fact that for long times the modes decay as $e^{-\lambda t}$, they are quickly damped for intermediate to large $\lambda > 0$. The aim of subsection 4.5.2 is thus to propose the addition of a new correction term to standard numerical methods, in order to accurately take into account for the small λ-modes and catch the right rate of relaxation towards the equilibrium (algebraic decay in our case).

4.5.1 Discussions on standard discretizations

Let us discuss first the difficulties encountered when trying to solve (4.5.1). The first immediately visible difficulty is related to the unboundedness of the velocity-domain, which leads to challenging numerical complications. Several possibilities are available to treat such problems, for example:

(a) *Spectral method*, based on basis functions intrinsic to unbounded domains, such as Hermite-basis functions or Sinc-functions;

(b) *Domain truncation*, approximating the unbounded interval $(-\infty, \infty)$ by a truncated one $(-L, L)$ with $L \gg 1$, and solving then the problem on the bounded domain, with appropriate artificial or transparent boundary conditions at $v = \pm L$;

(c) *Mapping techniques*, meaning mapping the unbounded interval $(-\infty, \infty)$ via a well-chosen change of variable (such as for ex. the algebraic mapping $v = \frac{w/a}{\sqrt{1-(w/a)^2}}$) to a bounded domain $(-a, a)$, and solving then the new problem on the bounded domain.

All these methods have their advantages and disadvantages and are well-adapted for specific situations. For example, Hermite spectral methods are usually used for solving Fokker-Planck equations of the type (4.2.1), case (I), which posses a discrete spectrum. These methods are however not appropriate for the cases (II)-(IV), which feature continuous spectra. Secondly, domain truncation with artificial boundary conditions is very well suited for exponentially decaying functions as $v \to \pm\infty$, but not for a slower decay in the velocity variable as in the case of energetic particles (κ-distributions). Constructing open (exact or transparent) boundary conditions or a well-suited mapping (c) is a very good idea in such situations, of gapless, continuous spectrum, however usually a very complex procedure from a mathematical and practical (numerical) point of view.

The approach we propose in this paper is based on the domain truncation procedure, supplied with artificial boundary conditions. The evolution problem on the truncated velocity domain (4.4.32) can be solved via standard methods, such as finite-differences, finite-elements or finite-volumes, we shall focus here rather on a spectral resolution, due to its bigger accuracy as compared to standard discretizations. As artificial boundary conditions introduce an artificial

gap into the problem, we shall introduce a correction term in our scheme, permitting to take into account more precisely for the small λ-modes, such that our numerical scheme shall reveal an algebraic time-decay rate as the theoretical results suggest (Theorems 6, 7, 8). This correction term shall be obtained via perturbation techniques.

4.5.2 Correction term

To understand how to redress the appearance of the artificial spectral gap, let us start from the spectral representation (4.4.28) of the solution, namely

$$h(t,v) = \mathfrak{A}_0(t,0) + \int_0^{+\infty} \mathfrak{A}(t,\lambda)^T\, P(\lambda)\, \Phi(v,\lambda)\, \mathrm{d}\lambda\,, \tag{4.5.2}$$

where the spectral coefficients $\mathfrak{A}(t,\lambda)$ are defined in (4.4.29). Recent works as [WC15] employed such a spectral representation to compute solutions for analogous Fokker-Planck type equations, by simply discretizing the integral term (hence the spectrum), leading finally to the introduction of a spectral gap. Such procedures are intimately linked to the truncation of the velocity domain at $v = \pm L$, which is the starting point of classical discretization methods, such as finite-differences, finite-elements or finite-volumes. In each of these discretization methods a spectral gap is artificially introduced into the problem and one only accurately approximates the term

$$h^{\varepsilon}_{st}(t,v) = \mathfrak{A}_0(t,0) + \int_{\varepsilon}^{+\infty} \mathfrak{A}(t,\lambda)^T\, P(\lambda)\, \Phi(v,\lambda)\, \mathrm{d}\lambda\,, \tag{4.5.3}$$

for some small ε, omitting the part

$$\mathcal{C}_{\varepsilon}(t,v) := \int_0^{\varepsilon} \mathfrak{A}(t,\lambda)^T\, P(\lambda)\, \Phi(v,\lambda)\, \mathrm{d}\lambda\,, \qquad \forall (t,v) \in \mathbb{R}^+ \times \mathbb{R}\,. \tag{4.5.4}$$

This last part is however the one carrying the information in the long-time limit and gives rise to the algebraic time-decay rate. We propose thus to carefully evaluate this small-energy term (4.5.4) (using perturbation techniques) and to introduce it in standard discretization methods as a correction term, as follows

$$h(t,v) = h^{\varepsilon}_{st}(t,v) + \mathcal{C}_{\varepsilon}(t,v)\,.$$

For the computation of $\mathcal{C}_{\varepsilon}$ we shall make use of the specific asymptotic behaviour close to $\lambda = 0$ of the functions $\mathfrak{A}(t,\lambda)$, $P(\lambda)$ and $\Phi(v,\lambda)$. More specifically, let us observe the following:

— *Spectral coefficients.* The regularity of the vector-valued function $\mathfrak{A}_{in}(\lambda)$ depends on the decay of the initial condition $h_{in}(v)$ as $v \to \pm\infty$, as it happens with Fourier coefficients. In particular, we shall assume $h_{in}(v)$ sufficiently decaying, such that the following asymptotic behaviour of the spectral coefficients holds

$$\mathfrak{A}(t,\lambda) = e^{-\lambda\, t}\, \mathfrak{A}_{in}(\lambda)\,, \qquad \mathfrak{A}_{in}(\lambda) = \mathfrak{A}^0_{in} + \lambda\, \tilde{\mathfrak{A}}_{in,\lambda}\,, \qquad \forall (t,\lambda) \in \mathbb{R}^+ \times \mathbb{R}^+\,, \tag{4.5.5}$$

where the 2×1 vector $\tilde{\mathfrak{A}}_{in,\lambda}$ is supposed to be bounded near $\lambda = 0$.

— *Spectral density.* We shall also assume the following development of the spectral density matrix

$$P(\lambda) = \lambda^{\alpha} P_0 + \lambda^{\alpha+\beta}\, \tilde{P}_\lambda\,, \qquad \forall \lambda > 0\,, \tag{4.5.6}$$

with $\beta > 0$, $\alpha > -1$ and $\tilde{P}_\lambda$ a bounded matrix near $\lambda = 0^+$.
It is common for spectral density matrices to take the specific form (4.5.6). It is especially the case when the potential in the Schrödinger eigenvalue problem (4.4.2) behaves like $o(1/s^2)$, for $s \to \pm\infty$, leading to $\alpha = -\frac{1}{2}$ and $\beta = \frac{1}{2}$, as discussed in works like [Cle97; Kla87; Sch07].
Concerning the cases considered in the present paper, due to the fact that the potential is decaying much slower than the one of the previous remark, being only of order $\mathcal{O}(1/s^2)$ (or even $\mathcal{O}(1/s^{2/5})$ for case (III)), one cannot apply the theory mentioned above. However, even if (4.5.6) is still not proven for the cases we are studying, there are indications suggesting that this Ansatz may hold true for case (II) and (IV). In [KTT16; KT14] the analysis is conducted solely on the half line $\mathbb{R}^+$, for potentials behaving like $\sim \frac{c}{s^2}$, with a constant $c \in \mathbb{R}$, and (4.5.6) is proven to be valid in this case. In [Miy08] the case of the whole line $\mathbb{R}$ is treated, with the specificity that the presence of the zero eigenvalue complicates the analysis; the author show that in this case one has $P(\lambda) = \mathcal{O}(\lambda^r)$ for some $r > 0$. Concerning case (III), the literature is very sparse, but there are some results suggesting a more rapid decay of the spectral density function (as $\lambda \to 0$) than (4.5.6) could suggest (see [Yaf82]). Our method could therefore be also adapted to this case in the same fashion as [Yaf82]. There are also hints of a very quickly decaying spectral density in this case when looking at [WC15] (Figure 3.1) .

— *Eigenfunctions.* Perturbation theory [Ben21] permits to show finally that one has the development

$$\Phi(v, \lambda) = \Phi(v, 0) + \lambda\, \tilde{\Phi}(v, \lambda)\,, \quad \forall (v, \lambda) \in \mathbb{R} \times \mathbb{R}^+\,, \tag{4.5.7}$$

with $\tilde{\Phi}(\cdot, \lambda)$ bounded near $\lambda = 0$, in the sense given later in (4.5.14).

Retaining now the main parts of the developments in (4.5.5), (4.5.6) and (4.5.7), we can approximate the low-energy term (4.5.4) for all $(t, v) \in \mathbb{R}^+ \times \mathbb{R}$ as follows

$$C_\varepsilon(t, v) = \int_0^\varepsilon e^{-\lambda t}\, \mathfrak{A}_{in}^T(\lambda)\, P(\lambda)\, \Phi(v, \lambda)\, \mathrm{d}\lambda \simeq \tilde{C}_{\varepsilon,\alpha}(t, v) := \left(\int_0^\varepsilon e^{-\lambda t}\, \lambda^\alpha \ \mathrm{d}\lambda \right) (\mathfrak{A}_{in}^0)^T\, P_0\, \Phi(v, 0)\,. \tag{4.5.8}$$

For simplicity reasons let us denote in the following the time-integral occurring in the expression of $\tilde{C}_{\varepsilon,\alpha}(t, v)$ simply by

$$\theta_\varepsilon^\alpha(t) := \int_0^\varepsilon e^{-\lambda t} \lambda^\alpha \ \mathrm{d}\lambda\,. \tag{4.5.9}$$

Let us comment a little bit on this correction term and its approximation (4.5.8). Firstly, the correction term $C_\varepsilon(t,v)$ brings the algebraic time-decay rate in our solution, and this rate is linked to the asymptotics of the spectral matrix $P(\lambda)$, as $\lambda \to 0^+$. Secondly, the approximation we propose for this term (4.5.8), is not destroying this decay rate, as the error done is smaller than the term itself, as shown in the next theorem.

Theorem 9. **(Low energy correction term)** Let Φ be computed as in (4.4.19),(4.4.20),(4.4.27). Assume furthermore that we can write for all $\lambda > 0$

$$\mathfrak{A}_{in}(\lambda) = \mathfrak{A}_{in}^0 + \lambda\, \tilde{\mathfrak{A}}_{in,\lambda}\,, \qquad P(\lambda) = \lambda^\alpha P_0 + \lambda^{\alpha+\beta}\, \tilde{P}_\lambda\,, \tag{4.5.10}$$

where $\beta > 0$, $\alpha > -1$, and $\tilde{\mathfrak{A}}_{in,\lambda}\,, \tilde{P}_\lambda$ are assumed to be bounded near $\lambda = 0^+$. Now, for each compact subset $K \subset \mathbb{R}$ and each $0 < \varepsilon < 1$, there exists a constant $C_{\varepsilon,K} > 0$ (bounded with respect to ε) such that

$$\begin{aligned} \mathfrak{E}_\varepsilon(t) &:= \sup_{v\in K} \left| C_\varepsilon(t,v) - \tilde{C}_{\varepsilon,\alpha}(t,v) \right| \\ &= \sup_{v\in K} \left| \int_0^\varepsilon e^{-\lambda t}\, \mathfrak{A}_{in}^T(\lambda)\, P(\lambda)\, \Phi(v,\lambda)\, \mathrm{d}\lambda - \left(\int_0^\varepsilon e^{-\lambda t}\, \lambda^\alpha \ \mathrm{d}\lambda \right) (\mathfrak{A}_{in}^0)^T\, P_0\, \Phi(v,0) \right| \\ &\leqslant C_{\varepsilon,K} \int_0^\varepsilon e^{-\lambda t}\, \lambda^{\alpha+\min\{1,\beta\}}\, \mathrm{d}\lambda\,. \end{aligned} \tag{4.5.11}$$

Remark 13. Let us make now some observations about the error term $\mathfrak{E}_\varepsilon(t)$ estimated in this theorem, in particular let us investigate its behaviour in two limiting regimes, namely:

— The case of fixed $t > 0$ and $\varepsilon \to 0$: Due to the simple estimate

$$\int_0^\varepsilon e^{-\lambda t}\, \lambda^{\alpha+\min\{1,\beta\}}\, \mathrm{d}\lambda \leqslant \varepsilon^{\min\{1,\beta\}} \int_0^\varepsilon e^{-\lambda t}\, \lambda^\alpha\, \mathrm{d}\lambda\,,$$

one concludes firstly that $\mathfrak{E}_\varepsilon(t) \to_{\varepsilon\to 0} 0$ and secondly that the error done, $\mathfrak{E}_\varepsilon(t)$, is smaller by a factor of $\varepsilon^{\min\{1,\beta\}}$ than the approximated correction term $\tilde{C}_{\varepsilon,\alpha}(t,v)$, justifying thus that $\tilde{C}_{\varepsilon,\alpha}(t,v)$ is a good approximation for $\varepsilon \ll 1$.

— The case of fixed $\varepsilon > 0$ and $t \to \infty$: One observes firstly that the change of variable $\eta = \lambda\, t$ leads to

$$\int_0^\varepsilon e^{-\lambda t}\, \lambda^\alpha \ \mathrm{d}\lambda = t^{-(\alpha+1)} \left(\int_0^{\varepsilon\, t} e^{-\eta}\, \eta^\alpha \ \mathrm{d}\eta \right) \sim_{t\to\infty} t^{-(\alpha+1)}\, \Gamma(\alpha+1) = \mathfrak{O}(t^{-(\alpha+1)})\,. \tag{4.5.12}$$

On the other hand the same change of variables yields

$$\begin{aligned} \int_0^\varepsilon e^{-\lambda t}\, \lambda^{\alpha+\min\{1,\beta\}}\, \mathrm{d}\lambda \ &= t^{-(\min\{1,\beta\}+\alpha+1)} \int_0^{\varepsilon\, t} e^{-\eta}\, \eta^{\alpha+\min\{1,\beta\}}\, \mathrm{d}\eta \\ &\sim_{t\to\infty} t^{-(\min\{1,\beta\}+\alpha+1)}\, \Gamma(\min\{1,\beta\}+\alpha+1) = \mathfrak{o}(t^{-(\alpha+1)})\,. \end{aligned}$$

Hence, the error term $\mathfrak{E}_\varepsilon(t)$ vanishes faster than the approximated correction term $\tilde{C}_{\varepsilon,\alpha}(t,v)$ by a factor of $t^{-\min\{1,\beta\}}$. This permits to understand that the incorporation of the correction term $C_\varepsilon(t,v)$ (via its approximation $\tilde{C}_\varepsilon(t,v)$) accurately renders the algebraic convergence rate of the evolution semigroup $e^{-t\mathcal{L}_{D,eq}}$, which is proportional to $t^{-(1+\alpha)}$ (compare with Theorems 6, 7, 8), instead of an artificial exponential decay rate, as obtained with standard methods.

Proof of Theorem 9. Let $K \subset \mathbb{R}$ be a compact set. Then the following development holds true [Ben21]

$$\Phi(v,\lambda) = \Phi(v,0) + \lambda\,\tilde{\Phi}(v,\lambda)\,, \quad \forall (v,\lambda) \in \mathbb{R}\times\mathbb{R}^+\,, \tag{4.5.13}$$

where the vector valued function $\tilde{\Phi}(v,\lambda)$ is uniformly bounded in $(v,\lambda) \in K \times [0,\varepsilon]$:

$$\sup_{(v,\lambda)\in K\times[0,\varepsilon]} \|\tilde{\Phi}(v,\lambda)\|_2 < \infty\,. \tag{4.5.14}$$

Developments (4.5.10) and (4.5.13) yield the following decomposition of the error term

$$\begin{aligned}
&\int_0^\varepsilon e^{-\lambda t}\,\mathfrak{A}_{in}^T(\lambda)\,P(\lambda)\,\Phi(v,\lambda)\,\mathrm{d}\lambda - \left(\int_0^\varepsilon e^{-\lambda t}\,\lambda^\alpha\ \mathrm{d}\lambda\right)(\mathfrak{A}_{in}^0)^T\,P_0\,\Phi(v,0)\\
&= \int_0^\varepsilon e^{-\lambda t}\,\lambda^{1+\alpha}\,\tilde{\mathfrak{A}}_{in,\lambda}^T\,(\lambda^{-\alpha}P(\lambda))\,\Phi(v,\lambda)\,\mathrm{d}\lambda\\
&\quad + \int_0^\varepsilon e^{-\lambda t}\lambda^{\alpha+\beta}\,\mathfrak{A}_{in}^T(\lambda)\,\tilde{P}_\lambda\,\Phi(v,\lambda)\,\mathrm{d}\lambda\\
&\quad + \int_0^\varepsilon e^{-\lambda t}\,\lambda^{1+\alpha}\,\mathfrak{A}_{in}^T(\lambda)\,(\lambda^{-\alpha}P(\lambda))\,\tilde{\Phi}(v,\lambda)\,\mathrm{d}\lambda\,.
\end{aligned}$$

Because of the boundedness of the first order terms $\tilde{\mathfrak{A}}_{in,\lambda}$, $\tilde{P}_\lambda$ and $\tilde{\Phi}(\cdot,\lambda)$ with respect to $\lambda > 0$, one can find constants $C_{\varepsilon,K}^i > 0$, $i \in \{1,2,3\}$, all bounded for ε close to 0^+, such that

$$\begin{aligned}
\sup_{(v,\lambda)\in K\times[0,\varepsilon]} |\tilde{\mathfrak{A}}_{in,\lambda}^T\,(\lambda^{-\alpha}P(\lambda))\,\Phi(v,\lambda)| &\leqslant C_{\varepsilon,K}^1\,,\\
\sup_{(v,\lambda)\in K\times[0,\varepsilon]} |\mathfrak{A}_{in}^T(\lambda)\,\tilde{P}_\lambda\,\Phi(v,\lambda)| &\leqslant C_{\varepsilon,K}^2\,,\\
\sup_{(v,\lambda)\in K\times[0,\varepsilon]} |\mathfrak{A}_{in}^T(\lambda)\,(\lambda^{-\alpha}P(\lambda))\,\tilde{\Phi}(v,\lambda)| &\leqslant C_{\varepsilon,K}^3\,.
\end{aligned}$$

As a consequence, the error term is bounded as follows

$$\sup_{v\in K}\left|\int_0^\varepsilon e^{-\lambda t}\,\mathfrak{A}_{in}^T(\lambda)\,P(\lambda)\,\Phi(v,\lambda)\,\mathrm{d}\lambda - \left(\int_0^\varepsilon e^{-\lambda t}\,\lambda^\alpha\ \mathrm{d}\lambda\right)(\mathfrak{A}_{in}^0)^T\,P_0\,\Phi(v,0)\right| \tag{4.5.15}$$

$$\leqslant (C_{\varepsilon,K}^1 + C_{\varepsilon,K}^3)\int_0^\varepsilon e^{-\lambda t}\,\lambda^{1+\alpha}\,\mathrm{d}\lambda + C_{\varepsilon,K}^2\int_0^\varepsilon e^{-\lambda t}\,\lambda^{\alpha+\beta}\,\mathrm{d}\lambda \tag{4.5.16}$$

$$\leqslant \left(C_{\varepsilon,K}^1 + C_{\varepsilon,K}^2 + C_{\varepsilon,K}^3\right)\int_0^\varepsilon e^{-\lambda t}\,\lambda^{\alpha+\min\{1,\beta\}}\,\mathrm{d}\lambda\,, \qquad (\text{since } \varepsilon < 1)\,. \tag{4.5.17}$$

The result follows immediately after taking $C_{\varepsilon,K} = C_{\varepsilon,K}^1 + C_{\varepsilon,K}^2 + C_{\varepsilon,K}^3$. □

4.5.3 LEAS numerical method

Let us summarize now the method we propose in this paper for the resolution of the Fokker-Planck equation (4.5.1), cases (II)-(IV). Remark however that this method can be applied to any parabolic evolution problem with gapless, continuous spectrum. Furthermore, remark also that a simplified version of this method can be designed for time evolution problems on the half-line $\mathbb{R}^+$, by simply changing the spectral matrix $(\rho'_{lj})_{l,j\in\{0,1\}}$ into a scalar valued spectral function $\rho'(\lambda)$.

We shall assume that the low energy asymptotics of the corresponding spectral density matrix $P(\lambda)$ is known and of the form

$$P(\lambda) \sim \lambda^{\alpha}\, P_0\,, \quad \text{when } \lambda \to 0^+\,, \tag{4.5.18}$$

for some real symmetric spectral matrix $P_0 = \{p_{l,j}\}_{l,j=0,1}$. This form can be obtained from theoretical results [Cle97; Kla87; KT14; Miy08], however it is also possible to determine numerically this asymptotic form through linear regressions, when a theoretical result has not yet been found.

LEAS algorithm:

(a) *Truncation:* First, let us truncate the velocity domain at $v = \pm L$ with fixed $L \gg 1$. The continuous problem (4.5.1) is hence approximated by

$$\begin{cases} \partial_t h^L = -\mathcal{L}_{D,eq}(h^L)\,, & \forall v \in (-L, L)\,, \\ \partial_v h^L(t,-L) = \partial_v h^L(t,L) = 0 \\ h^L(0,\cdot) = h^L_{in}\,. \end{cases} \tag{4.5.19}$$

This problem can be now solved either with classical schemes, such as finite-differences for example, leading to an approximation of $h^L(t_i, v_j)$, and one can pass then directly to step (c). We shall here focus rather on a spectral resolution, the corresponding spectral representation of the solution being given by (4.4.32), namely

$$h^L(t,v) = \alpha^L_0\, \phi^L_0 + \sum_{k=1}^{\infty} \alpha^L_k(t)\, \phi^L_k(v)\,, \qquad \alpha^L_k(t) := \int_{-L}^{L} h^L(t,v)\, \phi^L_k(v)\, f_{eq}(v)\, \mathrm{d}v\,. \tag{4.5.20}$$

(b) *Eigenvalue/function computation:* Compute then some approximations of a finite number N of eigenfunctions $\{\phi^L_k\}_{k=0}^{N-1}$ and eigenvalues $\{\lambda^L_k\}_{k=0}^{N-1}$. This permits to truncate the sum in (4.5.20) at $k = N-1$. Let us remark at this point the relations between the velocity space $v \in \mathbb{R}$ (truncation size L; discretization step $\mathrm{d}v$) and the spectral space $\lambda \in \mathbb{R}^+$ (discretization step $\mathrm{d}\lambda$; truncation index N).

(c) *Correction term:* Now, let us set

$$\varepsilon := \lambda_1^L ,$$

and compute the correction term obtained in (4.5.8) via

$$\tilde{\mathcal{C}}_{\lambda_1^L,\alpha}(t,v) = \left(\int_0^{\varepsilon} e^{-\lambda t}\, \lambda^{\alpha}\ \mathrm{d}\lambda \right) (\mathfrak{A}_{in}^0)^T\, P_0\, \Phi(v,0) , \tag{4.5.21}$$

where we recall

$$\Phi(v,0) = \begin{pmatrix} \varphi_0(v,0) \\ \varphi_1(v,0) \end{pmatrix} , \qquad \mathfrak{A}_{in}^0 = \int_{-\infty}^{+\infty} h_{in}^L(v)\, \Phi(v,0)\, f_{eq}(v)\, \mathrm{d}v , \tag{4.5.22}$$

with $\varphi_0(\cdot,\lambda)$, $\varphi_1(\cdot,\lambda)$ the *generalized eigenfunctions* defined in (4.4.19)-(4.4.20). Recalling (4.5.9), we remark that past a certain threshold-value for t (to be determined), it is better (for numerical reasons) to use the following formulae

$$\theta_{\varepsilon}^{\alpha}(t) = t^{-(\alpha+1)} \left(\int_0^{\varepsilon\, t} e^{-\eta}\, \eta^{\alpha}\ \mathrm{d}\eta \right) , \tag{4.5.23}$$

obtaiend via the change of variable $\eta = t\,\lambda$.

(d) *LEAS scheme:* As a result, the solution of the evolution problem (4.5.1) is well approximated, for $L \gg 1$ large enough, by the following eigenfunction expansion:

$$h^L(t,v) = \alpha_0^L\, \phi_0^L + \theta_{\varepsilon}^{\alpha}(t) \sum_{i=0}^{1} \left[p_{0,i}\, \mathfrak{A}_{in,0}^0 + p_{1,i}\, \mathfrak{A}_{in,1}^0 \right] \varphi_i(v,0) + \sum_{k=1}^{N-1} \alpha_k^L(t)\, \phi_k^L(v) , \tag{4.5.24}$$

where

$$\alpha_k^L(t) = e^{-\lambda_k^L\, t}\, \alpha_{\mathrm{in},k}^L , \qquad \alpha_{\mathrm{in},k}^L := \int_{-L}^{L} h_{in}^L(v)\, \phi_k^L(v)\, f_{eq}(v)\, \mathrm{d}v , \qquad \forall k = 0, \cdots, N-1 , \quad \forall t > 0 ,$$

and with $P_0 = \{p_{l,j}\}_{l,j=0,1}$ the main term in the asymptotic form of the spectral density, given in (4.5.18).

The second term on the right hand side of (4.5.24) is the correction term we propose in this paper in order to take into account for the specificities of the here considered Fokker-Planck equation, possessing a gapless, continuous spectrum which leads to an algebraic relaxation towards the steady states. A forthcoming paper shall compare this scheme with standard numerical methods in order to evaluate the importance of the introduction of the correction term in a real physical situation.

At the end we would like to remark that the big advantage of the LEAS-scheme, as compared to methods such as [PF93; WC15], is its simplicity (see (4.5.24)), and in particular the fact that it introduces a correction term, permitting to get the right algebraic time-decay rate for $t \to \infty$, and this in any standard discretization scheme, namely finite-difference, finite-element, finite-volume or spectral schemes.

4.6 Concluding remarks and perspectives

Let us conclude this paper by summarizing what was achieved in this work and what remains still to be done in future works. The main part of this work was concerned with the mathematical study of a specific Fokker-Planck equation, whose stationary states are given by κ-distribution functions, which are (thermal) non-equilibrium distributions and describe the energetic particle population in a fusion plasma gas. In particular we studied the (algebraic) decay rate as $t \to \infty$ of the velocity distribution function towards these steady-states and prepared the mathematical framework for the design of an efficient numerical method, based on the spectral representation theorem of the solutions to this Fokker-Planck operator. The here treated problem differs from standard Fokker-Planck equations, which posses Maxwellian steady-states (thus thermal equilibria) and feature an exponential relaxation rate in time. As the long-time behaviour of the solutions of our Fokker-Planck equation is dominated by the low-energy modes, a precise description of this $\lambda \ll 1$ modes is the basic ingredient of our scheme, called *Low Energy Accurate Scheme* (LEAS). For lengthy reasons of this paper, we postponed to a second paper the implementation of this LEAS-method in a physical realistic framework for fusion plasmas and the comparison of the results with those obtained via standard methods.

Acknowledgments. This work has been carried out within the framework of the EUROfusion Consortium, funded by the European Union via the Euratom Research and Training Programme (Grant Agreement No 101052200 — EUROfusion). Views and opinions expressed are however those of the author(s) only and do not necessarily reflect those of the European Union or the European Commission. Neither the European Union nor the European Commission can be held responsible for them. The authors would also like to thank Viviana Grasselli for fruitful discussions around spectral theory.

4.A Appendix

We postponed to this Appendix the proof of the Proposition 4.4.1 about the spectrum of the Fokker-Planck operator $\mathcal{L}_{D,eq}$ in cases (II)-(IV).

Proof. Before starting, let us recall that the spectrum of any self-adjoint operator is a subset of $\mathbb{R}$.

— *Proof of* $\sigma_{pp}(\mathcal{L}_{D,eq}) = \{0\}$. Let us first show that the only eigenvalue of $\mathcal{L}_{D,eq}$ is $\lambda = 0$. First, $\lambda = 0$ is indeed an eigenvalue of $\mathcal{L}_{D,eq}$, since constant solutions are in $\ker \mathcal{L}_{D,eq}$, in particular in L^2_{eq}. Second, $\mathcal{L}_{D,eq}$ has no eigenvalue in $\mathbb{R} \setminus \mathbb{R}^+$ because it is a positive, self-adjoint linear differential operator of order 2 [CL55]. Finally, we claim that there is no eigenvalue in $\mathbb{R}^+_*$. Let us show this with the associated Schrödinger form of the

eigenproblem stated in (4.4.2). Equation (4.4.2) has a set of two linearly independent and complex conjugate solutions g_+, g_- [Olv74] verifying, if $\lambda \in \mathbb{R}_*^+$, that

$$g_\pm(s) \sim e^{\pm i\sqrt{\lambda}\, s}\,, \qquad s \to +\infty\,. \tag{4.A.1}$$

Therefore, any nonzero real solution of (4.4.2) behaves as

$$A\,\cos(\sqrt{\lambda}\, s - \theta) + o(1)\,, \qquad \text{when } s \to +\infty\,,$$

for some $A \in \mathbb{R}^*$, $\theta \in \mathbb{R}$. Such a real solution thus cannot be in $L^2(\mathbb{R})$. Therefore, using the Liouville transformation, we have proven that for all $\lambda > 0$ there is no solution $h \in L^2_{eq}$ of

$$\mathcal{L}_{D,eq}(h) = \lambda\, h\,,$$

thus $\sigma_{pp}(\mathcal{L}_{D,eq}) = \{0\}$.

— *Proof of* (4.4.16). As we can see, in each of the cases (II)-(IV), the potential Q is such that $s \to \partial_s(Q(v(s)))$ is bounded on $\mathbb{R}$ and $\lim_{s\to\pm\infty} Q(v(s)) = 0$. Therefore the following equality holds ([CR21] chapter 6):

$$\sigma_{ess}(\mathcal{L}_{D,eq}) = [0, +\infty)\,. \tag{4.A.2}$$

To prove (4.4.16), it therefore remains to show that the standard decomposition

$$\sigma(\mathcal{L}_{D,eq}) = \sigma_{Fred}(\mathcal{L}_{D,eq}) \cup \sigma_{ess}(\mathcal{L}_{D,eq})\,, \tag{4.A.3}$$

features no Fredholm spectrum $\sigma_{Fred}(\mathcal{L}_{D,eq})$. Since the union in (4.A.3) is disjoint (and since $\sigma(\mathcal{L}_{D,eq}) \subset \mathbb{R}$), from (4.A.2) one deduces that

$$\sigma_{Fred}(\mathcal{L}_{D,eq}) \subset \mathbb{R}_*^-\,.$$

Additionally, using Lemmas 6.15 and 6.16 from [CR21], we know that every element of $\sigma_{Fred}(\mathcal{L}_{D,eq})$ must be an eigenvalue. But as we have shown, there is no eigenvalue in $\mathbb{R}_*^-$, thus leading to

$$\sigma_{Fred}(\mathcal{L}_{D,eq}) = \emptyset\,, \qquad \sigma(\mathcal{L}_{D,eq}) = \sigma_{Fred}(\mathcal{L}_{D,eq}) \cup \sigma_{ess}(\mathcal{L}_{D,eq}) = \sigma_{ess}(\mathcal{L}_{D,eq})\,. \tag{4.A.4}$$

— *Proof of* (4.4.17). Let us remark first that Q is *vanishing with little oscillation* [Lav73]. This means that

— its derivative decays fast enough as $s \to \pm\infty$, namely:

$$\partial_s(Q(v(s))) = o(|s|^{-1-\varepsilon})\,, \qquad \text{as } s \to \pm\infty\,,$$

for some $\varepsilon > 0$,

— and

$$\lim_{s\to\pm\infty} Q(v(s)) = 0\,.$$

Therefore ([Lav73] Theorem 1 (a)), one can show that there is no singular continuous spectrum, such that the following usual decomposition of the spectrum [RS72]

$$\sigma(\mathcal{L}_{D,eq}) = \overline{\sigma_{pp}(\mathcal{L}_{D,eq})} \cup \sigma_{ac}(\mathcal{L}_{D,eq}) \cup \sigma_{sc}(\mathcal{L}_{D,eq}), \tag{4.A.5}$$

reduces to

$$\sigma(\mathcal{L}_{D,eq}) = \sigma_{pp}(\mathcal{L}_{D,eq}) \cup \sigma_{ac}(\mathcal{L}_{D,eq}).$$

□

BIBLIOGRAPHY

[Add+21] L. Addala, J. Dolbeault, X. Li, and M. L. Tayeb. "L^2-Hypocoercivity and Large Time Asymptotics of the Linearized Vlasov-Poisson-Fokker-Planck System". In: *Journal of Statistical Physics* 184.4 (2021). ISSN: 1572-9613. DOI: 10.1007/s10955-021-02784-4.

[AFL01] D. Anderson, R. Fedele, and M. Lisak. " A tutorial presentation of the two stream instability and Landau damping". In: *American Journal of Physics* 69.12 (2001), pp. 1262–1266. ISSN: 0002-9505. DOI: 10.1119/1.1407252.

[AH08] N. Ben Abdallah and R. El Hajj. "Diffusion and guiding center approximation for particle transport in strong magnetic fields". In: *Kinetic and Related Models* 1.3 (2008), pp. 331–354. ISSN: 1937-5093. DOI: 10.3934/krm.2008.1.331.

[Alb+19] D. Albritton, S. Armstrong, J. -C. Mourrat, and M. Novack. "Variational methods for the kinetic Fokker-Planck equation". Working paper or preprint. 2019. DOI: 10.48550/ARXIV.1902.04037.

[Arm67] T. P. Armstrong. "Numerical Studies of the Nonlinear Vlasov Equation". In: *The Physics of Fluids* 10.6 (1967), pp. 1269–1280. DOI: 10.1063/1.1762272.

[Arn+01] A. Arnold, J. A. Carrillo, I. M. Gamba, and C.-W. Shu. "Low and high field scaling limits for the Vlasov- and Wigner-Poisson-Fokker-Planck systems". In: *Transport Theory and Statistical Physics* 30 (2001), pp. 121–153. DOI: 10.1081/TT-100105365.

[Ars75] A. A. Arsen'ev. "Existence in the large of a weak solution of Vlasov's system of equations". Russian. In: *Zh. Vychisl. Mat. Mat. Fiz.* 15 (1975), pp. 136–147. ISSN: 0044-4669.

[AT04] N. Ben Abdallah and M. L. Tayeb. "Diffusion approximation for the one dimensional Boltzmann-Poisson system". In: *Discrete and Continuous Dynamical Systems - B* 4.4 (2004), pp. 1129–1142. ISSN: 1531-3492. DOI: 10.3934/dcdsb.2004.4.1129.

[Bak+08] D. Bakry, F. Barthe, P. Cattiaux, and A. Guillin. "A simple proof of the Poincaré inequality for a large class of probability measures". In: *Electronic Communications in Probability* 13 (2008), pp. 60–66. ISSN: 1083-589X. DOI: 10.1214/ECP.v13-1352.

[Bar+13] C. Bardos, E. Bernard, F. Golse, and R. Sentis. "The Diffusion Approximation for the Linear Boltzmann Equation with Vanishing Scattering Coefficient". In: *Communications in Mathematical Sciences* 13 (2013), pp. 641–671. ISSN: 1539-6746. DOI: 10.4310/CMS.2015.v13.n3.a3.

[BAW68] D. R. Baker, N. R. Ahern, and A. Y. Wong. "Ion-Wave Echoes". In: *Phys. Rev. Lett.* 20 (7 1968), pp. 318–321. ISSN: 0031-9007. DOI: 10.1103/PhysRevLett.20.318.

[BD95] F. Bouchut and J. Dolbeault. "On long time asymptotics of the Vlasov-Fokker-Planck equation and of the Vlasov-Poisson-Fokker-Planck system with Coulombic and Newtonian potentials". In: *Differential and Integral Equations* 8.3 (1995), pp. 487–514. ISSN: 0893-4983. DOI: 10.57262/die/1369316501.

[BDZ23] E. Bouin, J. Dolbeault, and L. Ziviani. "L^2 Hypocoercivity methods for kinetic Fokker-Planck equations with factorised Gibbs states". Working paper or preprint. 2023. arXiv: 2304.12040 [math.AP].

[Bed17] J. Bedrossian. "Suppression of Plasma Echoes and Landau Damping in Sobolev Spaces by Weak Collisions in a Vlasov-Fokker-Planck Equation". In: *Annals of PDE* 3.19 (2017), pp. 1–66. ISSN: 2199-2576. DOI: 10.1007/s40818-017-0036-6.

[Bed20] J. Bedrossian. "Nonlinear echoes and Landau damping with insufficient regularity". In: *Tunisian Journal of Mathematics* 3.1 (2020), pp. 121–205. ISSN: 2576-7658. DOI: 10.2140/tunis.2021.3.121.

[Ben21] S. Benzoni-Gavage. *Calcul différentiel et équations différentielles*. Sciences Sup. Dunod, 2021. 368 pp. ISBN: 978-2-10-083323-8.

[BF22] M. Bessemoulin-Chatard and F. Filbet. "On the stability of conservative discontinuous Galerkin/Hermite spectral methods for the Vlasov-Poisson system". In: *Journal of Computational Physics* 451 (2022), p. 110881. ISSN: 0021-9991. DOI: 10.1016/j.jcp.2021.110881.

[BG06] A. V. Bobylev and I. M. Gamba. "Boltzmann Equations For Mixtures of Maxwell Gases: Exact Solutions and Power Like Tails". In: *Journal of Statistical Physics* 124.2 (2006), pp. 497–516. ISSN: 1572-9613. DOI: 10.1007/s10955-006-9044-8.

[BG12] M. Bostan and I. M. Gamba. "Impact of Strong Magnetic Fields on Collision Mechanism for Transport of Charged Particles". In: *Journal of Statistical Physics* 148.5 (2012), pp. 856–895. ISSN: 1572-9613. DOI: 10.1007/s10955-012-0560-4.

[BGL91] C. Bardos, F. Golse, and D. Levermore. "Fluid dynamic limits of kinetic equations. I. Formal derivations". In: *Journal of Statistical Physics* 63.1 (1991), pp. 323–344. ISSN: 1572-9613. DOI: 10.1007/BF01026608.

[BH07] A.J. Brizard and T.S. Hahm. "Foundations of nonlinear gyrokinetic theory". In: *Rev. Mod. Phys.* 79 (2007), pp. 421–468. ISSN: 0034-6861. DOI: 10.1103/RevModPhys.79.421.

[Bia+14] N. H. Bian, A. G. Emslie, D. J. Stackhouse, and E. P. Kontar. "The formation of kappa-distribution accelerated electron populations in solar flares". In: *The Astrophysical Journal* 796.2 (2014), pp. 142–153. ISSN: 1538-4357. DOI: 10.1088/0004-637X/796/2/142.

[Bla+09] A. Blanchet, M. Bonforte, J. Dolbeault, G. Grillo, and Juan Luis Vázquez. "Asymptotics of the Fast Diffusion Equation via Entropy Estimates". In: *Archive for Rational Mechanics and Analysis* 191.2 (2009), pp. 347–385. ISSN: 1432-0673. DOI: 10.1007/s00205-008-0155-z.

[BMP11] N. Ben Abdallah, A. Mellet, and M. Puel. "Fractional diffusion limit for collisional kinetic equations: A Hilbert expansion approach". In: *Kinetic and Related Models* 4.4 (2011), pp. 873–900. ISSN: 1937-5093. DOI: 10.3934/krm.2011.4.873.

[Bob+18] A. V. Bobylev, M. Bisi, M. Groppi, G. Spiga, and I. F. Potapenko. "A general consistent BGK model for gas mixtures". In: *Kinetic and Related Models* 11.6 (2018), pp. 1377–1393. ISSN: 1937-5093. DOI: 10.3934/krm.2018054.

[Bob18] A. V. Bobylev. "Boltzmann equation and hydrodynamics beyond Navier–Stokes". In: *Philosophical Transactions of the Royal Society A: Mathematical, Physical and Engineering Sciences* 376.2118 (2018), p. 20170227. DOI: 10.1098/rsta.2017.0227.

[Bob95] A. V. Bobylev. "Quasistationary hydrodynamics for the Boltzmann equation". In: *Journal of Statistical Physics* 80.5 (1995), pp. 1063–1083. ISSN: 1572-9613. DOI: 10.1007/BF02179864.

[Bog98] V. I. Bogachev. *Gaussian measures*. Vol. 62. Mathematical Surveys and Monographs. American Mathematical Society, Providence, RI, 1998, pp. xii+433. ISBN: 0-8218-1054-5. DOI: 10.1090/surv/062.

[Bos07] M. Bostan. "The Vlasov–Maxwell System with Strong Initial Magnetic Field: Guiding-Center Approximation". In: *Multiscale Modeling & Simulation* 6.3 (2007), pp. 1026–1058. ISSN: 1540-3459. DOI: 10.1137/070689383.

[Bou93] F. Bouchut. "Existence and Uniqueness of a Global Smooth Solution for the Vlasov-Poisson-Fokker-Planck System in Three Dimensions". In: *Journal of Functional Analysis* 111.1 (1993), pp. 239–258. ISSN: 0022-1236. DOI: 10.1006/jfan.1993.1011.

[Bra65] S. I. Braginskii. "Transport processes in a plasma". In: *Reviews of plasma physics* 1 (1965), p. 205.

[Bré20] H. Brézis. *Analyse fonctionnelle: théorie et applications*. Sciences Sup. Dunod, 2020. 248 pp. ISBN: 978-2-10-082028-3.

[Bri23] G. Brigati. "Time averages for kinetic Fokker-Planck equations". In: *Kinetic and Related Models* 16.4 (2023), pp. 524–539. ISSN: 1937-5093. DOI: 10.3934/krm.2022037.

[BS01] L. L. Bonilla and J. S. Soler. "High-field limit of the Vlasov-Poisson-Fokker-Planck system: a comparison of different perturbation methods". In: *Mathematical Models and Methods in Applied Sciences* 11.08 (2001), pp. 1457–1468. ISSN: 0218-2025. DOI: 10.1142/S0218202501001410.

[BS82] A. R. Barakat and R. W. Schunk. "Transport equations for multicomponent anisotropic space plasmas: a review". In: *Plasma Physics* 24.4 (1982), p. 389. ISSN: 0032-1028. DOI: 10.1088/0032-1028/24/4/004.

[Bur35] D. Burnett. "The Distribution of Velocities in a Slightly Non-Uniform Gas". In: *Proceedings of the London Mathematical Society* s2-39.1 (1935), pp. 385–430. DOI: 10.1112/plms/s2-39.1.385.

[BZZ24] J. Bedrossian, W. Zhao, and R. Zi. "Landau damping, collisionless limit, and stability threshold for the Vlasov-Poisson equation with nonlinear Fokker-Planck collisions". Working paper or preprint. 2024. arXiv: 2402.14082 [math.AP].

[CC21] J. A. Carrillo and Y.-P. Choi. "Mean-Field Limits: From Particle Descriptions to Macroscopic Equations". In: *Archive for Rational Mechanics and Analysis* 241.3 (2021), pp. 1529–1573. ISSN: 1432-0673. DOI: 10.1007/s00205-021-01676-x.

[CG00] S. Cordier and E. Grenier. "Quasineutral limit of an Euler-Poisson system arising from plasma physics". In: *Communications in Partial Differential Equations* 25.5-6 (2000), pp. 1099–1113. DOI: 10.1080/03605300008821542.

[CGL56] G.F. Chew, M.L. Goldberger, and F.E. Low. "The Boltzmann equation and the one-fluid hydromagnetic equations in the absence of particle collisions". In: *Proceedings of the Royal Society of London. Series A. Mathematical and Physical Sciences* 236.1204 (1956), pp. 112–118. ISSN: 0080-4630.

[Che12] F.F. Chen. *Introduction to Plasma Physics*. Springer US, 2012. 330 pp. ISBN: 9781475704594. DOI: 10.1007/978-1-4757-0459-4.

[CHM16] D. Coulette, S. Hirstoaga, and G. Manfredi. "Effect of collisional temperature isotropisation on ELM parallel transport in a tokamak scrape-off layer". In: *Plasma Physics and Controlled Fusion* 58.8 (2016), p. 085004. ISSN: 0741-3335. DOI: 10.1088/0741-3335/58/8/085004.

[CL55] E. A. Coddington and N. Levinson. *Theory of ordinary differential equations*. New York, McGraw-Hill, 1955. 458 pp. ISBN: 978-0898747553.

[Cle97] D. P. Clemence. "On the Singular Behaviour of the Titchmarsh-Weyl m-Function for the Perturbed Hill's Equation on the Line". In: *Canadian Mathematical Bulletin* 40.4 (1997). Edition: 2018/11/20 Publisher: Cambridge University Press, pp. 416–421. ISSN: 0008-4395. DOI: 10.4153/CMB-1997-049-x.

[CMT12] L. Cesbron, A. Mellet, and K. Trivisa. "Anomalous transport of particles in plasma physics". In: *Applied Mathematics Letters* 25.12 (2012), pp. 2344–2348. ISSN: 0893-9659. DOI: 10.1016/j.aml.2012.06.029.

[CN] N. Crouseilles and C. Negulescu. "Hybrid modelling of energetic particles and bulk plasma". In preparation.

[CP01] Y. Chen and S. Parker. "A gyrokinetic ion zero electron inertia fluid electron model for turbulence simulations". In: *Physics of Plasmas* 8.2 (2001), pp. 441–446. ISSN: 1070-664X, 1089-7674. DOI: 10.1063/1.1335584.

[CR21] C. Cheverry and N. Raymond. *A Guide to Spectral Theory: Applications and Exercises*. Birkhäuser Advanced Texts Basler Lehrbücher. Cham: Springer International Publishing, 2021. 258 pp. ISBN: 978-3-030-67461-8. DOI: 10.1007/978-3-030-67462-5.

[CVB00] K. L. Cartwright, J. P. Verboncoeur, and C. K. Birdsall. "Nonlinear hybrid Boltzmann–particle-in-cell acceleration algorithm". In: *Physics of Plasmas* 7.8 (2000), pp. 3252–3264. ISSN: 1089-7674. DOI: 10.1063/1.874191.

[Dav+72] R. C. Davidson, D. A. Hammer, I. Haber, and C. E. Wagner. "Nonlinear development of electromagnetic instabilities in anisotropic plasmas". In: *The Physics of Fluids* 15.2 (1972), pp. 317–333. ISSN: 0031-9171. DOI: 10.1063/1.1693910.

[Deg04] P. Degond. "Macroscopic limits of the Boltzmann equation: a review". In: *Modeling and Computational Methods for Kinetic Equations*. Birkhäuser Boston, 2004, pp. 3–57. ISBN: 978-0-8176-8200-2. DOI: 10.1007/978-0-8176-8200-21.

[Deg86] P. Degond. "Global existence of smooth solutions for the Vlasov-Fokker-Planck equation in 1 and 2 space dimensions". In: *Annales Scientifiques De L'Ecole Normale Superieure* 19 (1986), pp. 519–542. ISSN: 0012-9593. DOI: 10.24033/ASENS.1516.

[Des04] L. Desvillettes. "Plasma kinetic models: the Fokker-Planck-Landau equation". In: *Modeling and Computational Methods for Kinetic Equations*. Boston, MA: Birkhäuser Boston, 2004, pp. 171–193. ISBN: 978-0-8176-8200-2. DOI: 10.1007/978-0-8176-8200-26.

[DL89] R. J. Diperna and P. L. Lions. "Global weak solutions of Vlasov-Maxwell systems". In: *Communications on Pure and Applied Mathematics* 42.6 (1989), pp. 729–757. DOI: 10.1002/cpa.3160420603.

[DMS15] J. Dolbeault, C. Mouhot, and C. Schmeiser. "Hypocoercivity for linear kinetic equations conserving mass". In: *Transactions of the American Mathematical Society*. 367th ser. (2015), pp. 3807–3828. ISSN: 1088-6850. DOI: 10.1090/S0002-9947-2015-06012-7.

[Dom+12] J. Dominski, S. Brunner, S. K. Aghdam, T. Görler, F. Jenko, and D. Told. "Identifying the role of non-adiabatic passing electrons in ITG/TEM microturbulence by comparing fully kinetic and hybrid electron simulations". In: *Journal of Physics: Conference Series* 401 (2012), p. 012006. ISSN: 1742-6588, 1742-6596. DOI: 10.1088/1742-6596/401/1/012006.

[DT07] B. Düring and G. Toscani. "Hydrodynamics from kinetic models of conservative economies". In: *Physica A: Statistical Mechanics and its Applications* 384.2 (2007), pp. 493–506. ISSN: 0378-4371. DOI: 10.1016/j.physa.2007.05.062.

[DT11] J. Dolbeault and G. Toscani. "Fast diffusion equations: Matching large time asymptotics by relative entropy methods". In: *Kinetic and Related Models* 4.3 (2011), pp. 701–716. ISSN: 1937-5093. DOI: 10.3934/krm.2011.4.701.

[EM00] N. El Ghani and N. Masmoudi. "Diffusion limit of the Vlasov-Poisson-Fokker-Planck system". In: *Models Methods Appl. Sci. Math. Models Methods Appl. Sci* 8 (2000), pp. 463–479. ISSN: 1539-6746. DOI: 10.4310/CMS.2010.v8.n2.a9.

[FN22] F. Filbet and C. Negulescu. "Fokker-Planck Multi-Species Equations in the Adiabatic Asymptotics". In: *J. Comput. Phys.* 471 (2022), p. 111642. ISSN: 0021-9991. DOI: 10.1016/j.jcp.2022.111642.

[Fur+22] G. Furioli, A. Pulvirenti, E. Terraneo, and G. Toscani. "One-Dimensional Fokker–Planck Equations and Functional Inequalities for Heavy Tailed Densities". In: *Milan Journal of Mathematics* 90.1 (2022), pp. 177–208. ISSN: 1424-9294. DOI: 10.1007/s00032-022-00352-3.

[FX20] F. Filbet and T. Xiong. "Conservative Discontinuous Galerkin/Hermite Spectral Method for the Vlasov–Poisson System". In: *Communications on Applied Mathematics and Computation* 4.1 (2020), pp. 34–59. ISSN: 2661-8893. DOI: 10.1007/s42967-020-00089-z.

[Gar+01] X. Garbet, C. Bourdelle, G. T. Hoang, P. Maget, S. Benkadda, P. Beyer, C. Figarella, I. Voitsekovitch, O. Agullo, and N. Bian. "Global simulations of ion turbulence with magnetic shear reversal". In: *Physics of Plasmas* 8.6 (2001), pp. 2793–2803. ISSN: 1089-7674. DOI: 10.1063/1.1367320.

[Gar92] S. P. Gary. "The mirror and ion cyclotron anisotropy instabilities". In: *Journal of Geophysical Research: Space Physics* 97.A6 (1992), pp. 8519–8529. ISSN: 0148-0227. DOI: 10.1029/92JA00299.

[GF67] F. C. Grant and M. R. Feix. "Fourier-Hermite Solutions of the Vlasov Equations in the Linearized Limit". In: *The Physics of Fluids* 10.4 (1967), pp. 696–702. ISSN: 0031-9171. DOI: 10.1063/1.1762177.

[GHN09] P. Ghendrih, M. Hauray, and A. Nouri. "Derivation of a gyrokinetic model. Existence and uniqueness of specific stationary solution". In: *Kinetic and Related Models* 2.4 (2009), pp. 707–725. ISSN: 1937-5093. DOI: 10.3934/krm.2009.2.707.

[Gol03] F. Golse. "The mean-field limit for the dynamics of large particle systems". In: Journées équations aux dérivées partielles, 9 (2003), pp. 1–47. ISSN: 0752-0360. DOI: 10.5802/jedp.623.

[Gol05] F. Golse. "Chapter 3 - The Boltzmann Equation and Its Hydrodynamic Limits". In: *Handbook of Differential Equations Evolutionary Equations*. Vol. 2. Handbook of Differential Equations: Evolutionary Equations. North-Holland, 2005, pp. 159–301. DOI: 10.1016/S1874-5717(06)80006-X.

[Gra49] H. Grad. "On the kinetic theory of rarefied gases". In: *Communications on Pure and Applied Mathematics* 2.4 (1949), pp. 331–407. ISSN: 0010-3640. DOI: 10.1002/cpa.3160020403.

[Gre96] E. Grenier. "Oscillations in quasineutral plasmas". In: *Communications in Partial Differential Equations* 21.3-4 (1996). ISSN: 0360-5302. DOI: 10.1080/03605309608821189.

[GS99] F. Golse and L. Saint-Raymond. "The Vlasov–Poisson System with Strong Magnetic Field". In: *Journal de Mathématiques Pures et Appliquées* 78.8 (1999), pp. 791–817. ISSN: 0021-7824. DOI: 10.1016/S0021-7824(99)00021-5.

[Hér07] F. Hérau. "Short and long time behavior of the Fokker–Planck equation in a confining potential and applications". In: *Journal of Functional Analysis* 244.1 (2007), pp. 95–118. ISSN: 0022-1236. DOI: 10.1016/j.jfa.2006.11.013.

[Hér17] F. Hérau. "Introduction to hypocoercive methods and applications for simple linear inhomogeneous kinetic models". In: *Lectures on the Analysis of Nonlinear Partial Differential Equations*. Vol. 5. Morning Side Lectures in Mathematics Series MLM 5. 2017, pp. 119–147. ISBN: 9781571463579.

[HH15] D. Han-Kwan and M. Hauray. "Stability Issues in the Quasineutral Limit of the One-Dimensional Vlasov-Poisson Equation". In: *Communications in Mathematical Physics* 334.2 (2015), pp. 1101–1152. ISSN: 1432-0916. DOI: 10.1007/s00220-014-2217-4.

[HHM17] J. R. Haack, C. D. Hauck, and M. S. Murillo. "A Conservative, Entropic Multispecies BGK Model". In: *Journal of Statistical Physics* 168.4 (2017), pp. 826–856. ISSN: 1572-9613. DOI: 10.1007/s10955-017-1824-9.

[HJ07] M. Hauray and P.-E. Jabin. "N-particles Approximation of the Vlasov Equations with Singular Potential". In: *Archive for Rational Mechanics and Analysis* 183.3 (2007), pp. 489–524. ISSN: 1432-0673. DOI: 10.1007/s00205-006-0021-9.

[HJ12] H. J. Hwang and J. Jang. "On the Vlasov-Poisson-Fokker-Planck equation near Maxwellian". In: *Discrete and Continuous Dynamical Systems - B* 18.3 (2012), pp. 681–691. ISSN: 1531-3492. DOI: 10.3934/dcdsb.2013.18.681.

[HJZ24] J. Hu, A. Jüngel, and N. Zamponi. "Global weak solutions for a nonlocal multispecies Fokker-Planck-Landau system". Working paper or preprint. 2024.

[HM03] R. D. Hazeltine and J. D. Meiss. *Plasma confinement*. Inc. Mineola, New York: Dover Publications, 2003, p. 412. ISBN: 9780201503944.

[HM19] M. Herda and L. Miguel Rodrigues. "Anisotropic Boltzmann-Gibbs dynamics of strongly magnetized Vlasov-Fokker-Planck equations". In: *Kinetic & Related Models* 12.3 (2019), pp. 593–636. ISSN: 1937-5077. DOI: 10.3934/krm.2019024.

[HMD85] A. Hasegawa, K. Mima, and M. Duong-van. "Plasma Distribution Function in a Superthermal Radiation Field". In: *Physical Review Letters* 54.24 (1985), pp. 2608–2610. ISSN: 0031-9007. DOI: 10.1103/PhysRevLett.54.2608.

[Jab14] P.-E. Jabin. "A review of the mean field limits for Vlasov equations". In: *Kinetic and Related Models* 7 (2014), pp. 661–711. ISSN: 1937-5077. DOI: 10.3934/krm.2014.7.661.

[Jin22] S. Jin. "Asymptotic-preserving schemes for multiscale physical problems". In: *Acta Numerica* 31 (2022), pp. 415–489. ISSN: 0962-4929. DOI: 10.1017/S0962492922000010.

[Kla87] M. Klaus. "On the variation-diminishing property of Schrödinger operators". In: *Oscillation, Bifurcation and Chaos: Proceedings of the 1986 Annual Seminar Held July 13-25, 1986*. CMS Conference Proceedings. American Mathematical Society, 1987, pp. 199–211. ISBN: 9780821860137.

[Kro12] J. A. Krommes. "The Gyrokinetic Description of Microturbulence in Magnetized Plasmas". In: *Annual Review of Fluid Mechanics* 44.Volume 44, 2012 (2012), pp. 175–201. ISSN: 1545-4479. DOI: 10.1146/annurev-fluid-120710-101223.

[KT14] H. Kovařík and F. Truc. "Schrödinger Operators on a Half-Line with Inverse Square Potentials". In: *Mathematical Modelling of Natural Phenomena* 9.5 (2014). Edition: 2014/07/17 Publisher: EDP Sciences, pp. 170–176. ISSN: 0973-5348. DOI: 10.1051/mmnp/20149511.

[KTT16] A. Kostenko, G. Teschl, and J. H. Toloza. "Dispersion Estimates for Spherical Schrödinger Equations". In: *Annales Henri Poincaré* 17.11 (2016), pp. 3147–3176. ISSN: 1424-0661. DOI: 10.1007/s00023-016-0474-9.

[Kwo08] D. T. K. Kwok. "A hybrid Boltzmann electrons and PIC ions model for simulating transient state of partially ionized plasma". In: *Journal of Computational Physics* 227.11 (2008), pp. 5758–5777.

[KY21] K. Kormann and A. Yurova. "A Generalized Fourier–Hermite Method for the Vlasov–Poisson System". In: *BIT Numerical Mathematics* 61.3 (2021), pp. 881–909. ISSN: 0006-3835. DOI: 10.1007/s10543-021-00853-4.

[Lan65] L. D. Landau. "On the vibrations of the electronic plasma". In: *Collected Papers of L.D. Landau*. Pergamon, 1965, pp. 445–460. ISBN: 978-0-08-010586-4. DOI: 10.1016/B978-0-08-010586-4.50066-3.

[Lav73] R. Lavine. "Absolute continuity of positive spectrum for Schrödinger operators with long-range potentials". In: *Journal of Functional Analysis* 12.1 (1973), pp. 30–54. ISSN: 0022-1236. DOI: 10.1016/0022-1236(73)90088-8.

[Liv14] G. Livadiotis. *Kappa Distributions : Theory and Applications in Plasmas*. 2014. 724 pp. ISBN: 978-0-12-804638-8.

[LN24a] E. Lehman and C. Negulescu. "Fokker-Planck equation for energetic particles. The κ-distribution function". Working paper or preprint. 2024.

[LN24b] E. Lehman and C. Negulescu. "Vlasov-Poisson-Fokker-Planck equation in the adiabatic asymptotics". To appear in *Communications in Mathematical Sciences*. 2024.

[LNP24] E. Lehman, C. Negulescu, and S. Possanner. "Asymptotic study of an anisotropic Fokker-Planck collision operator in a strong magnetic field". In: *Kinetic and Related Models* (2024). ISSN: 1937-5093. DOI: 10.3934/krm.2024004.

[Loe06] G. Loeper. "Uniqueness of the solution to the Vlasov–Poisson system with bounded density". In: *Journal de Mathématiques Pures et Appliquées* 86.1 (2006), pp. 68–79. ISSN: 0021-7824. DOI: 10.1016/j.matpur.2006.01.005.

[LRW21] R. Li, Y. Ren, and Y. Wang. "Hermite spectral method for Fokker-Planck-Landau equation modeling collisional plasma". In: *Journal of Computational Physics* 434 (2021), p. 110235. ISSN: 0021-9991. DOI: 10.1016/j.jcp.2021.110235.

[Mal+68] J. H. Malmberg, C. B. Wharton, R. W. Gould, and T. M. O'Neil. "Plasma Wave Echo Experiment". In: *Phys. Rev. Lett.* 20 (3 1968), pp. 95–97. ISSN: 0031-9007. DOI: 10.1103/PhysRevLett.20.95.

[Mel02] A. Mellet. "Diffusion Limit of a Non-Linear Kinetic Model without the Detailed Balance Principle". In: *Monatshefte für Mathematik* 134.4 (2002), pp. 305–329. ISSN: 1436-5081. DOI: 10.1007/s605-002-8265-1.

[MHD10] G. Manfredi, S. Hirstoaga, and S. Devaux. "Vlasov modelling of parallel transport in a tokamak scrape-off layer". In: *Plasma Physics and Controlled Fusion* 53.1 (2010), p. 015012. ISSN: 0741-3335. DOI: 10.1088/0741-3335/53/1/015012.

[Miy08] T. Miyazawa. "Low-energy asymptotic expansion of the Green function for one-dimensional Fokker–Planck and Schrödinger equations". In: *Journal of Physics A: Mathematical and Theoretical* 41.31 (2008), p. 315304. ISSN: 1751-8121. DOI: 10.1088/1751-8113/41/31/315304.

[MMM11] A. Mellet, S. Mischler, and C. Mouhot. "Fractional Diffusion Limit for Collisional Kinetic Equations". In: *Archive for Rational Mechanics and Analysis* 199.2 (2011), pp. 493–525. ISSN: 1432-0673. DOI: 10.1007/s00205-010-0354-2.

[Mou+13] D. Moulton, W. Fundamenski, G. Manfredi, S. Hirstoaga, and D. Tskhakaya. "Comparison of free-streaming ELM formulae to a Vlasov simulation". In: *Journal of Nuclear Materials* 438 (2013), S633–S637. ISSN: 0022-3115. DOI: 10.1016/j.jnucmat.2013.01.133.

[MRS12] P.A. Markowich, C.A. Ringhofer, and C. Schmeiser. *Semiconductor equations*. Springer Vienna, 2012. 248 pp. ISBN: 9783709169612. DOI: 10.1007/978-3-7091-6961-2.

[MV11] C. Mouhot and C. Villani. "On Landau damping". In: *Acta Mathematica* 207.1 (2011), pp. 29–201. ISSN: 1871-2509. DOI: 10.1007/s11511-011-0068-9.

[MW64] J. H. Malmberg and C. B. Wharton. "Collisionless Damping of Electrostatic Plasma Waves". In: *Physical Review Letters* 13.6 (1964), pp. 184–186. ISSN: 0031-9007. DOI: 10.1103/PhysRevLett.13.184.

[Neg13] C. Negulescu. "Asymptotic-preserving schemes. Modeling, simulation and mathematical analysis of magnetically confined plasmas". In: *Rivista di Matematica della Università di Parma* 4.2 (2013), pp. 265–343. ISSN: 0035-6298.

[Neg18] C. Negulescu. "Kinetic Modelling of Strongly Magnetized Tokamak Plasmas with Mass Disparate Particles. The Electron Boltzmann Relation". In: *Multiscale Modeling and Simulation: A SIAM Interdisciplinary Journal* 16.4 (2018), pp. 1732–1755. ISSN: 1540-3459. DOI: 10.1137/17M113109X.

[NH05] F. Nier and B. Helffer. *Hypoelliptic Estimates and Spectral Theory for Fokker-Planck Operators and Witten Laplacians*. Lecture Notes in Mathematics. Springer Berlin Heidelberg, 2005. 215 pp. ISBN: 9783540315537. DOI: 10.1007/b104762.

[Nis78] T. Nishida. "Fluid dynamical limit of the nonlinear Boltzmann equation to the level of the compressible Euler equation". In: *Communications in Mathematical Physics* 61 (1978), pp. 119–148. ISSN: 1432-0916. DOI: 10.1007/BF01609490.

[NP16] C. Negulescu and S. Possanner. "Closure of the Strongly Magnetized Electron Fluid Equations in the Adiabatic Regime". In: *Multiscale Modeling & Simulation* 14.2 (2016), pp. 839–873. ISSN: 1540-3459. DOI: 10.1137/15M1027309.

[NPS01] J. Nieto, F. Poupaud, and J. Soler. "High-Field Limit for the Vlasov-Poisson-Fokker-Planck System". In: *Archive for Rational Mechanics and Analysis* 158 (2001), pp. 29–59. ISSN: 1432-0673. DOI: 10.1007/s002050100139.

[OHO72] S. L. Ossakow, I. Haber, and E. Ott. "Simulation of Whistler Instabilities in Anisotropic Plasmas". In: *The Physics of Fluids* 15.8 (1972), pp. 1538–1540. ISSN: 0031-9171. DOI: 10.1063/1.1694123.

[Olv74] F. W. J. Olver. *Asymptotics and special functions*. Computer science and applied mathematics. New York: Academic Press, 1974. 572 pp. ISBN: 978-0-12-525850-0. DOI: 10.1016/C2013-0-11254-8.

[ONe83] T. M. O'Neil. "Collision operator for a strongly magnetized pure electron plasma". In: *The Physics of Fluids* 26.8 (1983), pp. 2128–2135. ISSN: 0031-9171. DOI: 10.1063/1.864394.

[PD15] J. T. Parker and P. J. Dellar. "Fourier–Hermite spectral representation for the Vlasov–Poisson system in the weakly collisional limit". In: *Journal of Plasma Physics* 81.2 (2015), p. 305810203. ISSN: 0022-3778. DOI: 10.1017/S0022377814001287.

[Pea88] D. B. Pearson. *Quantum scattering and spectral theory*. Techniques of physics 9. London: Academic Pr, 1988. 519 pp. ISBN: 978-0-12-548260-8.

[PF93] S. Pruess and C. T. Fulton. "Mathematical software for Sturm-Liouville problems". In: *ACM Transactions on Mathematical Software* 19.3 (1993), pp. 360–376. ISSN: 0098-3500. DOI: 10.1145/155743.155791.

[PS00] F. Poupaud and J. Soler. "Parabolic limit and stability of the Vlasov-Fokker-Planck system". In: *Mathematical Models and Methods in Applied Sciences* 10.07 (2000), pp. 1027–1045. ISSN: 0218-2025. DOI: 10.1142/S0218202500000525.

[Ric19] A. S. Richardson. *NRL (Naval Research Laboratory) Plasma Formulary*. 2019.

[RS72] M. Reed and B. Simon. *Methods of modern mathematical physics : Volume I, Functional analysis*. New York: Academic Press, 1972. 325 pp. ISBN: 978-0-12-585001-8. DOI: 10.1016/B978-0-12-585001-8.X5001-6.

[RW01] M. Röckner and F.-Y. Wang. "Weak Poincaré Inequalities and $L2$-Convergence Rates of Markov Semigroups". In: *Journal of Functional Analysis* 185.2 (2001), pp. 564–603. ISSN: 0022-1236. DOI: 10.1006/jfan.2001.3776.

[SA14] D. Stürzer and A. Arnold. "Spectral analysis and long-time behaviour of a Fokker-Planck equation with a non-local perturbation". In: *Rendiconti Lincei* 25.1 (2014), pp. 53–89. ISSN: 1120-6330. DOI: 10.4171/rlm/668.

[Sai02] L. Saint-Raymond. "Control of large velocities in the two-dimensional gyrokinetic approximation". In: *Journal de Mathématiques Pures et Appliquées* 81.4 (2002), pp. 379–399. ISSN: 0021-7824. DOI: 10.1016/S0021-7824(01)01245-4.

[Sch07] W. Schlag. "Dispersive Estimates for Schrödinger operators: A survey". In: *Mathematical Aspects of Nonlinear Dispersive Equations (AM-163)*. Princeton University Press, 2007, pp. 255–286. ISBN: 9780691129556.

[Sco21] B. Scott. *Turbulence and instabilities in magnetised plasmas, Volume 1*. IOP Series in plasma physics. IOP Publishing, 2021. 531 pp. ISBN: 978-0-7503-2504-2. DOI: 10.1088/978-0-7503-2504-2.

[SH98] J. W. Schumer and J. P. Holloway. "Vlasov Simulations Using Velocity-Scaled Hermite Representations". In: *Journal of Computational Physics* 144.2 (1998), pp. 626–661. ISSN: 0021-9991. DOI: 10.1006/jcph.1998.5925.

[ST91] D. Summers and R. M. Thorne. "The modified plasma dispersion function". In: *Physics of Fluids B: Plasma Physics* 3.8 (1991), pp. 1835–1847. ISSN: 0899-8221. DOI: 10.1063/1.859653.

[Sta00] P. C. Stangeby. *The plasma boundary of magnetic fusion devices*. Vol. 224. Institute of Physics Pub. Philadelphia, Pennsylvania, 2000. 738 pp. ISBN: 9780367801489. DOI: 10.1201/9780367801489.

[Tan93] T. Tang. "The Hermite Spectral Method for Gaussian-Type Functions". In: *SIAM Journal on Scientific Computing* 14.3 (1993), pp. 594–606. ISSN: 1064-8275. DOI: 10.1137/0914038.

[Vil09] C. Villani. "Hypocoercivity". In: *Mem. Amer. Math. Soc* 202.950 (2009). ISSN: 1947–6221. DOI: 10.1090/S0065-9266-09-00567-5.

[Vil10] C. Villani. "Landau Damping". CEMRACS Lecture Notes. 2010.

[Vil96] C. Villani. "On the Cauchy problem for Landau equation: sequential stability, global existence". In: *Advances in Differential Equations* 1.5 (1996), pp. 793–816. ISSN: 1079-9389. DOI: 10.57262/ade/1366896020.

[WC15] J. Wilkening and A. Cerfon. "A spectral transform method for singular sturm-liouville problems with applications to energy diffusion in plasma physics". In: *SIAM Journal on Applied Mathematics* 75 (2015), pp. 350–392. ISSN: 0036-1399. DOI: 10.1137/130941948.

[Yaf82] D. R. Yafaev. "The low energy scattering for slowly decreasing potentials". In: *Communications in Mathematical Physics* 85.2 (1982), pp. 177–196. ISSN: 1432-0916. DOI: 10.1007/BF01254456.

Descriptions cinétiques et limites asymptotiques des plasmas de fusion thermonucléaire

Résumé: Cette thèse de doctorat porte sur l'analyse mathématique et la résolution numérique d'équations modélisant les plasmas de fusion nucléaire. Les plasmas d'un tokamak peuvent être décrits par des modèles s'appuyant sur des postulats de la physique. Cependant, ces modèles seraient trop coûteux à simuler numériquement. Pour concevoir des machines permettant d'exploiter la fusion nucléaire à des fins civiles, il est nécessaire d'utiliser des modèles peu coûteux d'un point de vue numérique. De tels modèles peuvent être dérivés à l'aide de l'analyse asymptotique, à partir de descriptions cinétiques du plasma. Des arguments d'adimensionnement permettent d'identifier des petits paramètres qui rendent le modèle de départ singulier. Faire tendre ces paramètres vers 0 (formellement ou rigoureusement), permet d'obtenir des modèles limites moins coûteux qui doivent ensuite être étudiés mathématiquement et numériquement.

Le premier chapitre de cette thèse s'intéresse à une équation cinétique modélisant le comportement des électrons dans le cœur d'un tokamak. Les électrons y sont beaucoup plus légers que les ions. L'adimensionnement du modèle fait apparaître le ratio de masse entre électrons et ions, et l'objectif de ce chapitre est d'analyser rigoureusement ce problème singulièrement perturbé à l'aide de techniques d'hypocoercivité. Nous réalisons ensuite des simulations numériques qui confirment nos résultats théoriques. Nous présentons enfin un schéma préservant l'asymptotique du petit ratio de masse entre électrons et ions, ce qui permet de calculer efficacement la solution de ce problème.

Le deuxième chapitre de cette thèse s'intéresse à l'étude mathématique formelle d'une équation cinétique fortement anisotrope. Les ions présents dans le plasma de la couche extérieure d'un tokamak (SOL - scrape-off layer) est soumis à une faible collisionnalité dans la direction parallèle au champ magnétique, contrairement à la direction perpendiculaire. Nous analysons alors une équation singulièrement perturbée du point de vue cinétique, et nous dérivons un modèle hybride cinétique-fluide utilisé par les physiciens étudiant la SOL. Dériver ce modèle réduit à partir de l'échelle cinétique nous permet de proposer des termes correctifs, enrichissant ainsi les propriétés physiques du modèle utilisé dans la littérature.

Le troisième chapitre porte sur l'analyse mathématique et numérique de certaines équations de Fokker-Planck présentes en astrophysique et dans la physique du tokamak. Ces opérateurs de Fokker-Planck n'ont pas de trou spectral, et relaxent donc lentement la distribution d'espèces chargées vers l'équilibre. Nous le montrons rigoureusement, puis proposons une méthode numérique qui préserve la structure spectrale de ces opérateurs, ce qui permet de simuler avec précision les solutions de ces équations, même sur de longues périodes.

Kinetic descriptions and asymptotic limits of thermonuclear fusion plasmas

Abstract: This thesis focuses on the mathematical analysis and numerical resolution of nuclear fusion plasma models. Plasma in a tokamak can be described by models based on first principles. However, these models would be too costly for numerical computations, even in the near future. Thus, to design machines for civil nuclear fusion exploitation, computationally inexpensive models are necessary. Such models can be derived using asymptotic techniques from kinetic plasma descriptions. Scaling arguments allow to identify small parameters that render the starting model singularly perturbed. Letting these parameters tend towards 0, formally or rigorously, yields reduced, limit models, which must then be studied from mathematical and numerical perspectives.

The first chapter of this thesis focuses on a kinetic equation modeling the behavior of electrons in the core of a tokamak. In this case, electrons are much lighter than ions. Dimensional analysis of the model brings into play the mass ratio between electrons and ions. The objective of this chapter is to rigorously analyse this singularly perturbed problem using hypocoercivity techniques. We then perform numerical simulations to confirm our theoretical results. Finally, we present a scheme preserving the asymptotic behavior of a small electron-to-ion mass ratio, enabling efficient computation of the solution to this problem.

The second chapter of this thesis focuses on the formal mathematical study of a highly anisotropic kinetic equation. Ions present in the plasma scrape-off layer (SOL) of a tokamak experience low collisionality in the direction parallel to the magnetic field, contrary to what happens in the perpendicular direction. Hence, we analyse a singularly perturbed kinetic equation and derive a hybrid kinetic-fluid model used by physicists studying the SOL. Deriving this reduced model from the kinetic scale enables us to propose corrective terms, thus enriching the physical properties of the model used in the literature.

The third chapter centers on the mathematical and numerical analysis of Fokker-Planck equations appearing in tokamak physics as well as in astrophysics. These Fokker-Planck operators feature no spectral gap, and thus slowly relax the distribution of charged species towards equilibrium. We rigorously demonstrate this, and then propose a spectral numerical method allowing precise simulation of these equations even over long periods of time.

RÉPUBLIQUE FRANÇAISE
Liberté
Égalité
Fraternité

Université de Toulouse

Titre : Descriptions cinétiques et limites asymptotiques des plasmas de fusion thermonucléaire

Mots clés : physique des plasmas, modèles cinétiques, équation de Vlasov, équation de Fokker-Planck

Résumé : Cette thèse de doctorat porte sur l'analyse mathématique et la résolution numérique d'équations modélisant les plasmas de fusion nucléaire. Les plasmas d'un tokamak peuvent être décrits par des modèles s'appuyant sur des postulats de la physique. Cependant, ces modèles seraient trop coûteux à simuler numériquement. Pour concevoir des machines permettant d'exploiter la fusion nucléaire à des fins civiles, il est nécessaire d'utiliser des modèles peu coûteux d'un point de vue numérique. De tels modèles peuvent être dérivés à l'aide de l'analyse asymptotique, à partir de descriptions cinétiques du plasma. Des arguments d'adimensionnement permettent d'identifier des petits paramètres qui rendent le modèle de départ singulier. Faire tendre ces paramètres vers 0 (formellement ou rigoureusement), permet d'obtenir des modèles limites moins coûteux qui doivent ensuite être étudiés mathématiquement et numériquement.

Le premier chapitre de cette thèse s'intéresse à une équation cinétique modélisant le comportement des électrons dans le cœur d'un tokamak. Les électrons y sont beaucoup plus légers que les ions. L'adimensionnement du modèle fait apparaître le ratio de masse entre électrons et ions, et l'objectif de ce chapitre est d'analyser rigoureusement ce problème singulièrement perturbé à l'aide de techniques d'hypocoercivité. Nous réalisons ensuite des simulations numériques qui confirment nos résultats théoriques. Nous présentons enfin un schéma préservant l'asymptotique du petit ratio de masse entre électrons et ions, ce qui permet de calculer efficacement la solution de ce problème.

Le deuxième chapitre de cette thèse s'intéresse à l'étude mathématique formelle d'une équation cinétique fortement anisotrope. Les ions présents dans le plasma de la couche extérieure d'un tokamak (SOL - scrape-off layer) est soumis à une faible collisionnalité dans la direction parallèle au champ magnétique, contrairement à la direction perpendiculaire. Nous analysons alors une équation singulièrement perturbée du point de vue cinétique, et nous dérivons un modèle hybride cinétique-fluide utilisé par les physiciens étudiant la SOL. Dériver ce modèle réduit à partir de l'échelle cinétique nous permet de proposer des termes correctifs, enrichissant ainsi les propriétés physiques du modèle utilisé dans la littérature.

Le troisième chapitre porte sur l'analyse mathématique et numérique de certaines équations de Fokker-Planck présentes en astrophysique et dans la physique du tokamak. Ces opérateurs de Fokker-Planck n'ont pas de trou spectral, et relaxent donc lentement la distribution d'espèces chargées vers l'équilibre. Nous le montrons rigoureusement, puis proposons une méthode numérique qui préserve la structure spectrale de ces opérateurs, ce qui permet de simuler avec précision les solutions de ces équations, même sur de longues périodes.

Title: Kinetic descriptions and asymptotic limits of thermonuclear plasmas

Key words: plasma physics, kinetic models, Vlasov equation, Fokker-Planck equation

Abstract: This thesis focuses on the mathematical analysis and numerical resolution of nuclear fusion plasma models. Plasma in a tokamak can be described by models based on first principles. However, these models would be too costly for numerical computations, even in the near future. Thus, to design machines for civil nuclear fusion exploitation, computationally inexpensive models are necessary. Such models can be derived using asymptotic techniques from kinetic plasma descriptions. Scaling arguments allow to identify small parameters that render the starting model singularly perturbed. Letting these parameters tend towards 0, formally or rigorously, yields reduced, limit models, which must then be studied from mathematical and numerical perspectives.

The first chapter of this thesis focuses on a kinetic equation modeling the behavior of electrons in the core of a tokamak. In this case, electrons are much lighter than ions. Dimensional analysis of the model brings into play the mass ratio between electrons and ions. The objective of this chapter is to rigorously analyse this singularly perturbed problem using hypocoercivity techniques. We then perform numerical simulations to confirm our theoretical results. Finally, we present a scheme preserving the asymptotic behavior of a small electron-to-ion mass ratio, enabling efficient computation of the solution to this problem.

The second chapter of this thesis focuses on the formal mathematical study of a highly anisotropic kinetic equation. Ions present in the plasma scrape-off layer (SOL) of a tokamak experience low collisionality in the direction parallel to the magnetic field, contrary to what happens in the perpendicular direction. Hence, we analyse a singularly perturbed kinetic equation and derive a hybrid kinetic-fluid model used by physicists studying the SOL. Deriving this reduced model from the kinetic scale enables us to propose corrective terms, thus enriching the physical properties of the model used in the literature.

The third chapter centers on the mathematical and numerical analysis of Fokker-Planck equations appearing in tokamak physics as well as in astrophysics. These Fokker-Planck operators feature no spectral gap, and thus slowly relax the distribution of charged species towards equilibrium. We rigorously demonstrate this, and then propose a spectral numerical method allowing precise simulation of these equations even over long periods of time.